Competitive Adsorption of Iron and Natural Organic Matter in Groundwater using Granular Activated Carbon

Omar Al-Attas

Under the supervision of
Dr. Roberto M. Narbaitz

Thesis submitted to the
Faculty of Graduate and Postdoctoral Studies
In partial fulfillment of the requirements
For the PhD degree in Environmental Engineering

The Ottawa-Carleton Institute for Environmental Engineering
Department of Civil Engineering
University of Ottawa

ABSTRACT

The treatment of potable water in Vars, ON is accomplished by filtering the colored, iron-laden groundwater through granular activated carbon (GAC) filters. When first installed, these filters unexpectedly experienced chromatographic displacements of iron into the produced water which resulted in orange-brown water at consumers' taps. The treatment plant was later modified by adding potassium permanganate oxidation and a greensand filter prior to the GAC adsorption columns. Consequently, iron was almost completely removed and no longer caused operational problems. The main objective of this dissertation is to study the interactions between natural organic matter (NOM) and iron that caused the observed chromatographic effect. This study was divided into three main stages: a) characterization study on Vars groundwater and its treatment system; b) study of the competitive adsorption of iron with NOM in Vars groundwater; and c) evaluation of the rapid small-scale column test (RSSCT) for predicting the full-scale GAC column breakthroughs.

The characterization of Vars groundwater showed that ferrous iron was found to be the dominant iron species, representing 90% of the total iron, and that 15 - 35% of the iron was complexed with NOM. It was hypothesized that the chromatographic displacement of iron from the GAC columns was caused by NOM-iron complexes; however, field mini-column experiments showed this was not the case. Thus, competitive adsorption between iron and NOM was seen as the more likely cause of the chromatographic effect. The adsorption capacity of ferrous iron in Vars raw water was less than that in organic-free water by a factor of 7 due to the competition with NOM over the GAC adsorbing sites. However, the NOM adsorption capacity was not reduced due to the presence of ferrous iron.

It was hypothesized that ideal adsorption solution theory (IAST) models, which have been successful in describing competitive adsorption between target organic compounds and NOM, could model the competition between an inorganic compound such as ferrous iron and NOM. The hypothesis was proved to be correct, and the adsorption isotherm of iron in competition with NOM in Vars groundwater was simulated very well by several versions of the IAST model. However, none of the models were capable of simulating the competitive adsorption of NOM and ferrous iron simultaneously. Since the presence of iron did not

significantly reduce the adsorption capacity of NOM, a simplified approach of using the single-solute NOM isotherm to represent the competitive NOM isotherm was recommended.

The performance of the rapid small-scale column test (RSSCT) was evaluated in order to simulate the iron chromatographic effect observed at Vars' full-scale GAC column. The RSSCT was not capable of predicting the iron phenomenon and the test proved to be problematic due to the oxidation and precipitation of iron within the small voids between the small-scale column's GAC particles. The RSSCT, using constant and linear diffusivities, were applied to simulate the NOM adsorption after greensand treatment. Integrating both diffusivities, the tests predicted the onset and slope of the NOM breakthrough up to 10-L water treated/g GAC, which is equivalent to 250 days of operation time for the full-scale column. However, the NOM breakthroughs deviated beyond that point and the RSSCT using constant diffusivity underestimated the column performance greatly. On the other hand, the linear diffusivity RSSCT underestimated the performance to a lesser degree and its NOM breakthrough was quite parallel to the full-scale performance with lower NOM removals of 15%. The higher long-term NOM removal in the full-scale system may be explained by biodegradation, a phenomenon that was not considered by the short duration of RSSCT.

ACKNOWLEDGMENTS

First and above all, I praise Allah the almighty for providing me this opportunity and granting me the capability to proceed successfully.

Completing a PhD is truly a challenging endeavor, and I would not have been able to complete this journey without the assistance, guidance and support of several people. I would like to thank my esteemed supervisor, Dr. Roberto Narbaitz, for his thoughtful support during the whole period of the study, and especially for his patience and guidance during the writing process. I would like to thank the members of my PhD thesis committee, Dr. Handan Tezel, Dr. Onita Basu, Dr. Majid Sartaj and Dr. Graham Gagnon for their advises and detailed review of this thesis. I also would like to thank Dr. Danielle Fortin for allowing me to use the facilities at her lab in the department of Earth Science and for her useful suggestions. I owe sincere thankfulness to the City of Ottawa for giving me an access to Vars Treatment Plant, and the cooperation of Ian Douglas, Penny Wilson and Mark Silas of the City of Ottawa is greatly appreciated. I thank Mr. Louis Tremblay for his advices and his friendly assistance with various problems related to my experimental work. I also appreciate the financial support from the government of Saudi Arabia during my PhD study.

In my daily work I have been blessed with a friendly and cheerful group of friends and fellow students. Thanks to all my close friends and the Saudi Arabian community in Ottawa for the joyful gatherings and all their supports. Although I have lived far from my home country, their company provided a supportive atmosphere in Canada. I would like to thank my good friends, Mohamed Abdallah, Mustafa El-Khedr, Antoun El-Khoury and Eqab Al-Majali for always willing to help and give their best suggestions throughout the writing of this thesis. Many thanks to Huyen Dang and Lara Gallo for helping me in some of my experimental work.

I cannot finish without thanking my family. I warmly thank and appreciate my father, Ghazi Al-Attas, for instilling in me confidence and a drive for pursuing my PhD and my deepest appreciations go to my dear mother, Amani Saab, for her moral support and undying love that made me accomplish many of my goals in life. I also would like to thank my uncle, Hani Saab, for his continuous support and assistance in numerous ways. I would like to show my

gratitude to my dear sisters, Rana, Reem, Alyaa and Lamya for their encouragements and best wishes. I want to express my deepest appreciation to my lovely and sweet kids, Amani, Lina, Tala and Khalid, for their sweet company that cheered me up and gave me the strength to continue my journey until the end. And finally, My lovely wife, Dear Noran, who always stood by my side through the good and bad times, without your support and encouragements, I could not have finished this work, it was you who kept the fundamental of our family, I can just say thanks for everything and may Allah give you all the best in return.

TABLE OF CONTENTS

LIST OF FIGURES

LIST OF TABLES

NOMENCLATURE

A	Surface area of the adsorbent (m^2/g)
b	Energy constant (cm^3/g)
b_1	Energy constant of component 1 from the corresponding Langmuir single solute isotherms (L/mol)
b_2	Energy constant of component 2 from the corresponding Langmuir single solute isotherms (L/mol)
C_0	Initial concentration of the NOM in the solution (mgTOC/L)
C_1	Liquid phase at equilibrium of component 1 within the bisolute mixture (mol/L)
C_2	Liquid phase at equilibrium of component 2 within the bisolute mixture (mol/L)
C_c	GAC dose used in the kinetics experiment (gGAC/L)
C_e	Equilibrium liquid phase concentration of the contaminant (mol/L)
$C_{e\text{-}Fe\text{-}comp}$	Equilibrium liquid phase concentration of the competitive fractions of ferrous iron (mol/L)
$C_{e\text{-}i}$	Liquid phase concentration of component (i) (mol/L)
$C_{e\text{-}i}^{o}$	Liquid phase concentration (mol/L) in equilibrium with the single solute system (mol/L)
$C_{e\text{-}TC}$	Equilibrium liquid phase concentration of the competitive fractions of the competing compound (mol/L)
$C_{Fe\text{-}initial\text{-}comp}$	Initial concentration of the competitive fractions of ferrous iron (mol/L)
$C_{Fe\text{-}initial\text{-}Total}$	Total initial concentration of ferrous iron obtained from the isotherm experiments (mol/L)
C_{io}	Initial concentration of component i (mol/L)
C_i	Equilibrium liquid phase concentration of component i (mol/L)
C_{non}	Concentration of the non-adsorbable NOM fraction (mg/L)
C_o	Initial liquid phase concentration of the contaminant (mg/L)
$C(t)$	Concentration of the NOM in the solution at time elapsed during the kinetics experiment (mgTOC/L)
C_{TCo}	Initial concentration of the competitive fractions of the target compound (mol/L)
$C_{TC\text{-}Total}$	Initial concentration of the target compound obtained from the isotherm experiments (mol/L)
$d_{larger\text{-}particle}$	GAC particle size retained in the mesh size (μm)
d_{LC}	Mean particle diameter of the GAC in the full-scale columns (μm)

DOF	Degree of freedom
d_p	Mean GAC particle size diameter (μm)
$d_{p(SC)}$	Activated carbon particle size of small column (μm)
$d_{p(LC)}$	Activated carbon particle size of large column (μm)
D_s	Surface diffusion coefficient (cm^2/min)
D_L	Liquid diffusion coefficient (cm^2/min)
D_P	Pore diffusion coefficient (cm^2/min)
d_{SC}	Mean particle diameter of the GAC in the small-scale columns (μm)
$d_{smaller\text{-}particle}$	GAC particle size passing through the mesh size (μm)
$EBCT_{SC}$	Empty bed contact time of small column (min)
$EBCT_{LC}$	Empty bed contact time of large column (min)
K	Freundlich regressed constant $((mg/g)\cdot(L/mg)^n)$
k_f	Film mass transfer coefficients (cm^2/s)
K_F	Freundlich regressed constant $((mg/g)\cdot(L/mg)^n)$
$K_{F\text{-}1}$	Regressed parameter of the Freundlich single isotherm of component 1 $((mg/g)\cdot(L/mg)^n)$
$K_{F\text{-}2}$	Regressed parameter of the Freundlich single isotherm of component 2 $((mg/g)\cdot(L/mg)^n)$
K_{Fi}	Single solute Freundlich model parameter of component i $((mg/g)\cdot(L/mg)^n)$
$K_{F\text{-}i}$	Regressed parameter of the Freundlich single isotherm of component i in the mixture $((mg/g)\cdot(L/mg)^n)$
$K_{F\text{-}TC}$	Single solute Freundlich model parameter of the competitive fractions of the target compound $((mg/g)\cdot(L/mg)^n)$
K_{SR}	Single solute Summer-Roberts model parameter $((mg/g)\cdot(mg/g)^n)$
K_{SRi}	Single solute Summer-Roberts model parameter of component i $((mg/g)\cdot(mg/g)^n)$
$K_{SR\text{-}Fe\text{-}comp}$	Single solute Summers-Roberts model parameter of the competitive fractions of ferrous iron $((mg/g)\cdot(mg/g)^n)$
K_{QS}	Single solute Qi-Schideman model parameter $((mg/g)\cdot(mg/g)^n)$
M	Mass of carbon (g)
N	Number of components
NC	Number of components

n_F	Freundlich regressed constants
n_{F-1}	Regressed parameter of the Freundlich single isotherm of component 1
n_{F-2}	Regressed parameter of the Freundlich single isotherm of component 2
n_{Fi}	Single solute Freundlich model parameter of component i
n_{F-i}	Regressed parameter of the Freundlich single isotherm of component i in the mixture
n_{Fj}	Freundlich regressed parameter of component j
n_{F-TC}	Single solute Freundlich model parameter of the competitive fractions of the target compound
n_i	Single solute Freundlich exponent of component i
n_{SR}	Summers-Roberts model regressed constants
n_{SRi}	Single solute Summers-Roberts model parameter of component i
$n_{SR-Fe-comp}$	Single solute Summers-Roberts model parameter of the competitive fractions of ferrous iron
n_{SR-NOM}	Single solute Summers-Roberts model parameter of the NOM
O_i	Experimental value
P_i	Predicted value
q	Solid phase loading of the NOM in the solution into the GAC particles (mgTOC/gGAC)
q_0	Initial amount of the NOM adsorbed into the GAC (mgTOC/gGAC)
q_1	Solid phase concentration of component 1 in equilibrium with C_1 and C_2 (mol/gGAC)
q_2	Solid phase concentration of component 2 in equilibrium with C_1 and C_2 (mol/gGAC)
q_e	Equilibrium solid phase concentration of the contaminant (mol/gGAC)
$q_{e-Fe-comp}$	Equilibrium solid phase concentration of the competitive fractions of ferrous iron (mol/gGAC)
q_{e-i}	Solid phase concentration of component (i) (mol/gGAC)
q_{e-i}^{o}	Equilibrium solute solid phase concentration (mol/gGAC) predicted by the single solute isotherm of component (i) for the liquid concentration C_{e-i}^{o}
q_{e-j}	Equilibrium solid phase concentration of component j (mol/gGAC)
q_{e-NOM}	Equilibrium solid phase concentration of the NOM (mol/gGAC)
q_{e-TC}	Equilibrium solid phase concentration of the competitive fractions of the competing compound (mol/gGAC)

$q_{Fe\text{-}noncomp}$	Equilibrium solid phase concentration of the non-competitive fractions of ferrous iron (mol/gGAC)
q_{lim}	Limiting adsorption capacity (mgTOC/gGAC)
q_s	Monolayer adsorption capacity (mgTOC/gGAC)
q_{s1}	Monolayer adsorption capacity of component 1 from the corresponding Langmuir single solute isotherms (mol/gGAC)
q_{s2}	Monolayer adsorption capacity of component 2 from the corresponding Langmuir single solute isotherms (mol/gGAC)
q_T	Total solid phase concentration on the activated carbon (mol/gGAC)
Q_i	Equilibrium solid phase concentration of component i (mol/g GAC)
Q_j	Equilibrium solid phase concentration of component j (mol/g GAC)
R	Universal gas constant (J/mol/K)
r	GAC particle radius (cm)
Re_{LC}	Reynolds number of the full-scale column
T	Absolute temperature (K)
t	Time elapsed during the kinetics experiment (min)
t_{SC}	Elapsed time of small column (min)
t_{LC}	Elapsed time of large column (min)
V	Volume of solution (L)
v_{LC}	Hydraulic loading of the full-scale columns (cm/min)
V_{lim}	Limiting GAC pore volume (cm^3/g)
v_{SC}	Hydraulic loading of the small-scale columns (cm/min)
V_b	Molar volume of the adsorbate at the normal boiling point (cm^3/mol)
w_1	Fraction of the adsorptive capacity of ferrous iron and NOM
w_2	Fraction of the adsorptive capacity of ferrous iron and NOM
w_i	Fraction of the total capacity of component i within the mixture that is involved in competition
X	Diffusivity factor that is obtained from the relationship between the adsorbent particle diameter (d_p) and the surface diffusion coefficient (D_s)
y_i	Adsorbed phase fraction of solute i

π_i	Spreading pressure of solute i (N/mol/m)
ρ_a	Apparent adsorbent density (g/L)
ρ	Density of influent water (kg/m^3)
ρ_{NOM}	NOM adsorbed phase mass density (g/cm^3)
α_{NOM}	NOM elemental carbon fraction of adsorbed phase
ε	GAC void fraction
τ_p	Adsorbent tortuosity
μ	Viscosity of the influent water (kg/(s.m))
$(1- \theta)$	Fraction of the GAC surface area on which there are competitive effects

ABBREVIATIONS

AAPE	Absolute average percentage errors
AC	Activated carbon
AWWA	American water works association
BV	Bed volume
CMBR	Carberry mixed batch reactor
CV(RMSE)	Coefficient of variation of the root mean square error
DBP	Disinfection by-product
DCE	Dichloroethylene
DO	Dissolved oxygen
DOC	Dissolved organic carbon
DOF	Degree of freedom
EBC	Equivalent background compound
EBCT	Empty bed contact time
FCS	Fluorescence correlation spectroscopy
Fe-II	Ferrous iron
Fe-III	Ferric iron
GAC	Granular activated carbon
HPSEC	High-performance size exclusion chromatography
HSDM	Homogeneous surface diffusion adsorption model
IAST	Ideal adsorbed solution theory
ICP	Inductive coupled plasma
ICP-AES	Inductively coupled plasma atomic emission spectrometry
IMSL	International mathematics and statistics library
LC	Large-scale column
MALLS	Multi-angle laser light scattering
MIB	Methylisoborneol

MW	Molecular weight
NMWCO	Nominal molecular weight cut-off
NOM	Natural organic matter
OFW	Organic free water
ORP	Oxidation-reduction potential
PAC	Powder activated carbon
PB	Pore blocking fractions
RSSCT	Rapid small scale column test
SC	Site competing fractions
SOC	Synthetic organic chemical
SPDFR	Surface to pore diffusion flux ratio
SSE	Sum of squared errors
SUVA	Specific ultraviolet absorption
TCE	Trichloroethylene
TDS	Total dissolved solids
TOC	Total organic carbon
UF	Ultra filtration
USEPA	United states environment protection agency
UV	Ultraviolet
VOC	Volatile organic compound
WHO	World health organization

CHAPTER 1 INTRODUCTION

1.1 Background

Groundwater is the primary source of potable water for almost 8.9 million Canadians, which represent 30.3% of the Canadian population (Statistics Canada, 1996). Approximately two thirds of groundwater consumers reside in rural areas where groundwater is the only source of water (Environment Canada, 1990). Groundwater is generally a preferred source of water due to its consistent good quality. One of the most common inorganic constituent in groundwater is iron (the second most abundant metal in the earth's crust), a result of the dissolution of iron from rocks and minerals (WHO, 1996). In nature, iron usually exists in two oxidation states, reduced soluble divalent ferrous iron (Fe^{+2} or Fe(II)) and oxidized insoluble trivalent ferric iron (Fe^{+3} or Fe(III)). Under the anaerobic conditions generally prevalent in groundwater, ferrous iron is the predominant iron species because of the absence of an electron acceptor such as oxygen (Faust and Aly, 1987).

Most groundwaters also contain natural organic matter (NOM) which is a complex mixture of organic compounds resulting from the biodegradation of vegetation within the watersheds. The presence of NOM in groundwater is expected to adversely impact activated carbon's adsorption capacity and adsorption kinetics of other groundwater constituents, such as iron. Such an expectation is based on the findings of many studies that proved a reduction in GAC adsorptive capacity when NOM was present with other organic compounds due to the competition over the GAC adsorbing sites (Weber and Smith, 1989). Most of these studies were concerned with the competitive adsorption between trace compounds (i.e., synthetic organic compounds) and NOM, and they showed 50% or more reduction in the target compound's adsorption capacity. They have also shown that the extent of competitive adsorption between trace compounds and NOM was dependent on the initial concentration of trace compounds, the initial concentration of NOM, the molecular size of trace compounds, the molecular size distribution of NOM molecules, and the type of GAC. Although the fundamental understanding of the direct competition between NOM and synthetic organic

compounds has progressed in recent years, there is a lack of detailed studies on the competitive adsorption of NOM with inorganic compounds, such as iron.

1.2 Statement of the Problem

In 1996, the Ontario Ministry of Environment commissioned a new well field and water treatment system in the town of Vars, ON (population of 700 capita), to replace the communal town well that had bacterial contamination problems (City of Ottawa, 1996). The new well field consisted of two wells approximately 22-m deep. This well water had a substantial NOM content (4 - 5 mg TOC/L) and color (≈ 20 color units). The consultant engineers involved in the project decided to incorporate granular activated carbon (GAC) filters for color removal. Although the well water had significant concentration of iron (≈ 2 mg/L), the system design did not incorporate an iron removal strategy. The Vars GAC treatment system shown in Figure 1-1 consisted of: 1) two 22-m deep production wells feeding the water treatment facility with groundwater; 2) two cloth pre-filters; 3) two granular activated carbon (GAC) filter columns (A and B); 4) a post chlorination mechanism; and 5) an underground water reservoir to store the treated water before delivery to the distribution system. The cloth pre-filters proved to be ineffective and their use was discontinued.

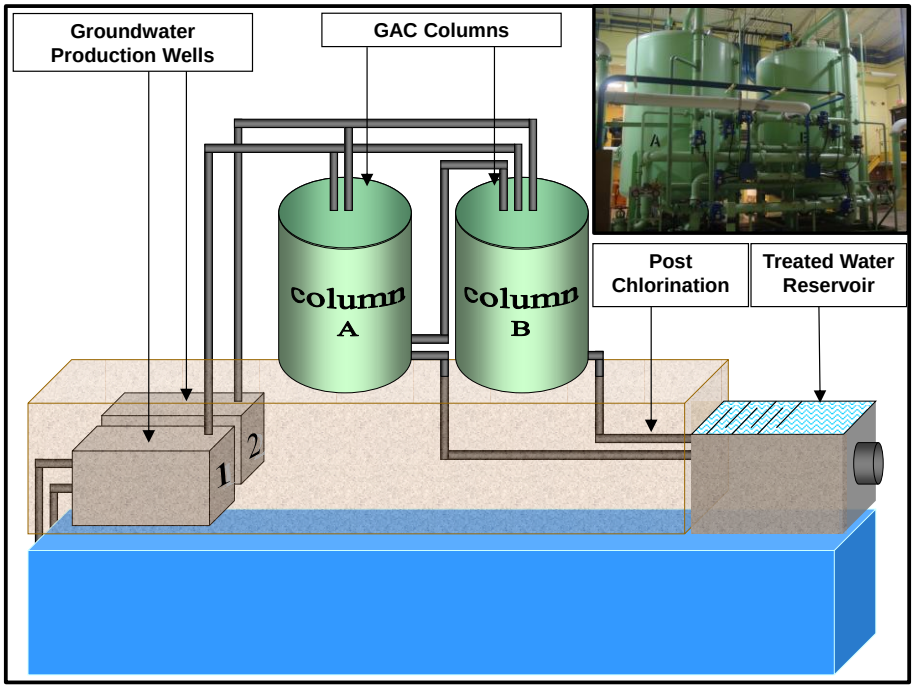

Figure 1-1: Vars groundwater treatment system

The treatment system started operation during the beginning of 1996; however, the volume of treated water was initially very low and it was increased gradually over the years to meet the demand of the Vars community. The GAC columns were initially operated in series where column "A" was fed groundwater and column "B" was fed by the effluent from column "A". After 204 days of operation and 1621 bed volumes of water treated, the effluent iron concentration from the lead GAC column (column A) increased to levels greater than the feed (a phenomenon called chromatographic effect). Therefore, it was decided to take column "A" out of operation, in order to avoid any leaching of iron from it, and only operate column "B", that was still achieving full iron removal (Narbaitz, 1997). After 400 days (i.e., 3187 bed volumes treated), the iron concentration from column "B" started to increase until the full breakthrough was reached and then the iron effluent concentration exceeded the influent concentration. The iron in the GAC column effluent was oxidized through chlorination and the exposure to air in the plant's reservoir. Consequently, the oxidized iron precipitated onto the reservoir floor and the surface of the pipes connecting the treatment facility to the consumers. Eventually, some of Vars' residents had colored water (orange and brown) coming out of their faucets as the precipitate was transported out to the distribution

system. Accordingly, the city had to perform a number of distribution system flushings and line piggings to reduce the water color problems.

During the period from 1996 to 2002, the activated carbon in columns A and B was replaced several times with different brands of activated carbon (NORIT, PICA and Filtrasorb F-400). Different types of activated carbons used in the system behaved somewhat differently in terms of iron removal. As an example, Figure 1-2 shows the performance of the Vars GAC column for treatment cycles using the three GAC brands for the removal of iron and NOM. Table 1-1 summarizes the performance of each carbon brand used in the years 1996 – 1997, 1997 – 1998 and 2001 – 2002. Figure 1-2.a shows that the iron chromatographic effect occurred in the three GAC brands treatment cycles. However, the starting times of the iron breakthrough were different. The F-400 GAC started the iron breakthrough after 42 days, which was earlier than the other two GAC brands (204 and 176 days for NORIT and PICA GACs, respectively). However, Figure 1-3 shows that the starting points of the iron breakthroughs were closer when the bed volumes (BV) of water treated were considered (1620, 1394 and 1026 for NORIT, PICA and F-400, respectively). This similarity is due to the fact that the flowrate of the groundwater treated increased over time in order to accommodate the increased domestic, commercial, and institutional water demand in Vars.

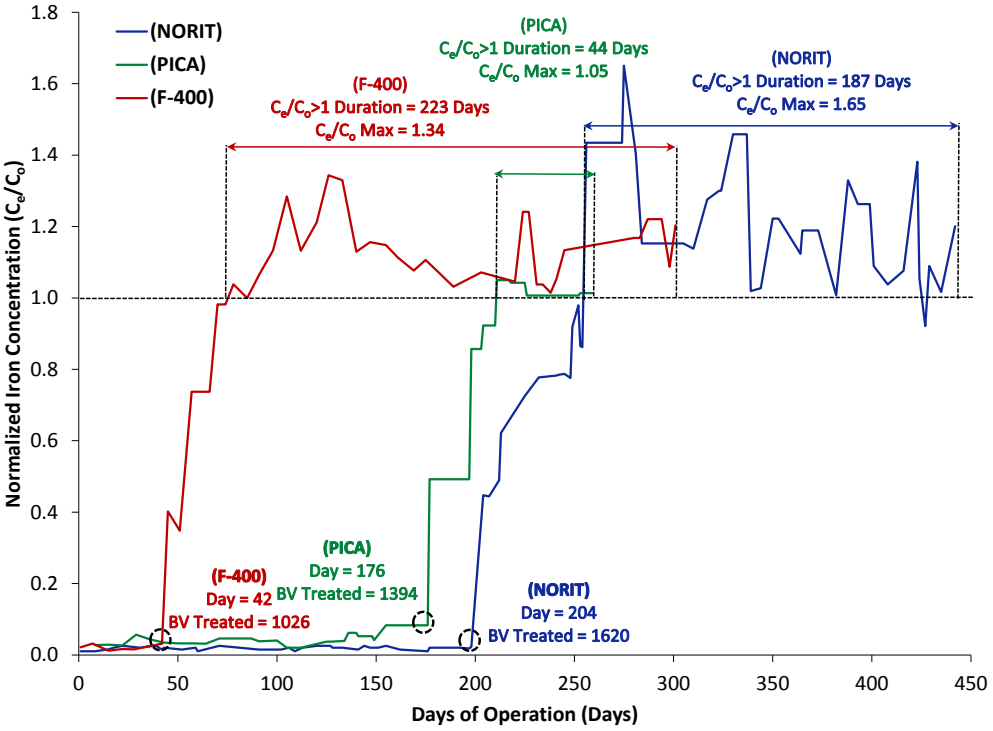

(a)

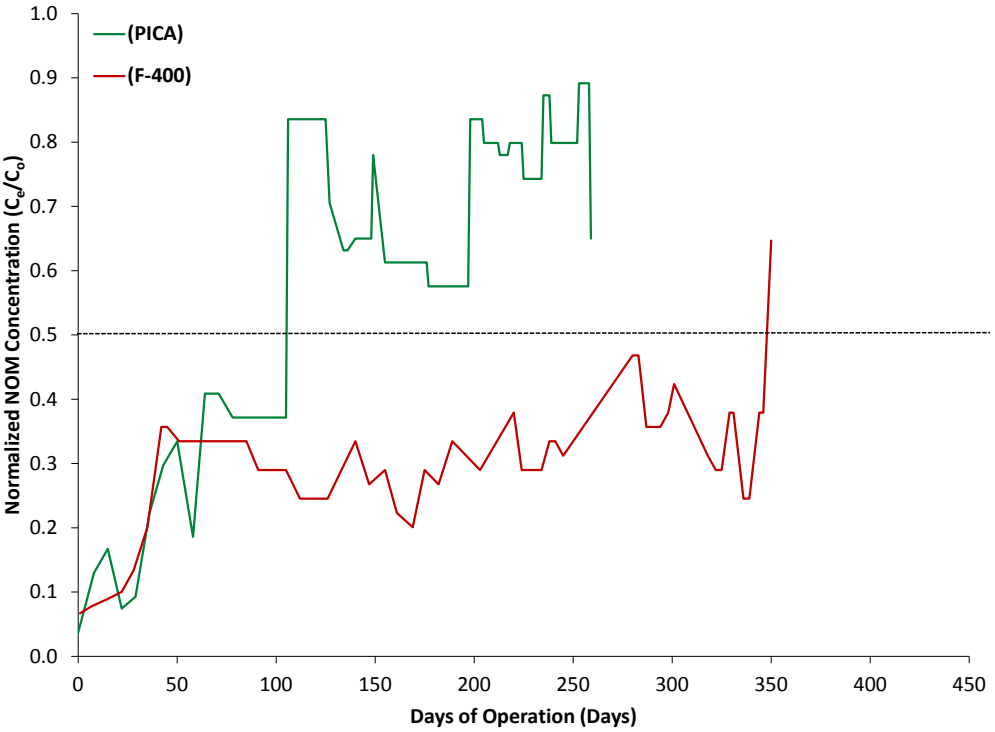

(b)

Figure 1-2: GAC columns performance using different types of GAC for the removal of: (a) iron and (b) NOM in Vars raw water

Table 1-1: GAC columns performance using different brands of activated carbon in Vars treatment plant

	NORIT	PICA	Filtrasorb (F-400)
Start of the run	January 1996	December 1997	June 2001
End of the run	November 1997	November 1998	May 2002
Bed volume of water treated at C/C_o (TOC) = 0.5	1120	840	4253
Start of iron breakthrough in days	204	176	42
Bed volume of water treated at the start of iron breakthrough	1620	1394	1026
(C/C_o) of TOC concentration at the start of iron breakthrough	0.67	0.80	0.33

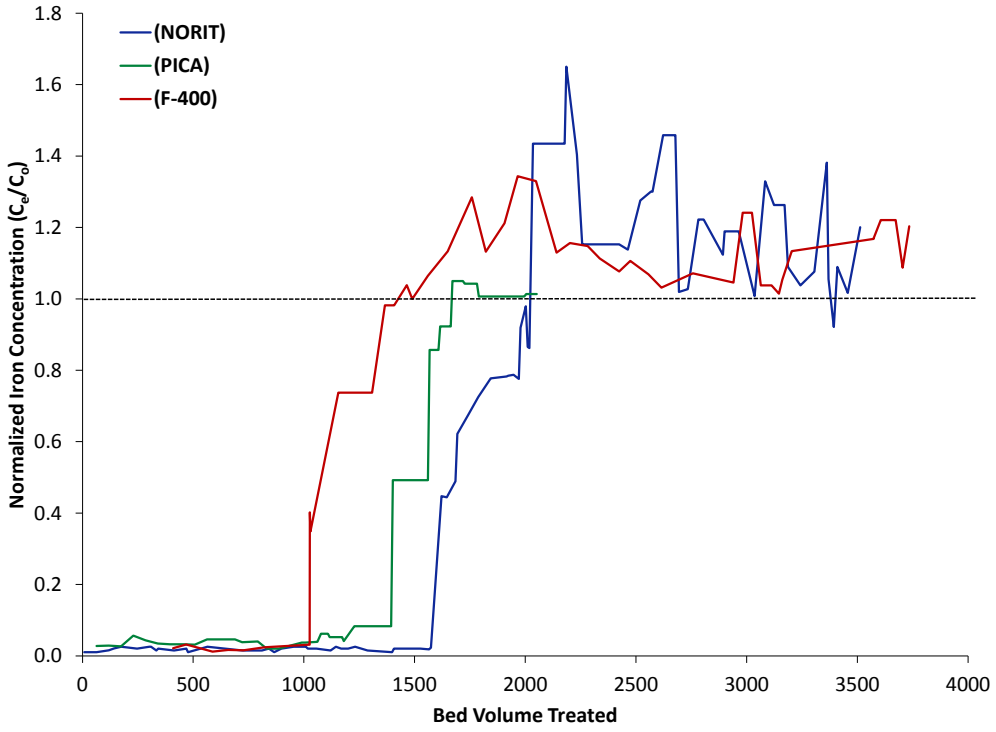

Figure 1-3: GAC column performance using different types of GAC for the removal of iron in Vars raw water considering the bed volume of water treated

While under these operating conditions, the iron became the target compound, NOM removal was nevertheless important due to the fact that residual NOM are disinfection by-product precursors. Figure 1-2.b shows a comparison of the NOM removal using the F-400 and PICA GACs. Unfortunately, only limited NOM data for the NORIT column run was available for comparison, so it was not included. The figure shows that PICA carbon reached the NOM $C/C_o > 0.5$ breakthrough level before the start of the iron breakthrough. Table 1-1 shows that the values of C/C_o of NOM at the start of the iron breakthrough were 0.67 and 0.80 using PICA and NORIT, respectively. However, F-400 GAC was capable of removing more NOM even after reaching iron breakthrough (C/C_o (TOC) ≈ 0.3). The high value of bed volume of water treated by F-400 GAC (4253 bed volumes) at C/C_o (TOC) = 0.5 was much higher than that of the other GAC brands (1120 and 840 bed volumes for NORIT and PICA, respectively), which indicates that F-400 carbon was superior in terms of removal of NOM even in the presence of iron in the water to be treated (Table 1-1). However, F-400 was not capable of solving the iron problem.

The frequent GAC replacements made the operating cost of the Vars systems much higher than the other water treatment systems operated by the City of Ottawa. Accordingly, in June 2002, the City of Ottawa implemented a modification to the treatment facility system by the addition of a greensand filter prior to the GAC adsorption columns. The greensand system included the oxidation of the reduced iron through the addition of potassium permanganate ($KMnO_4$) in a mixing tank followed by a greensand filter (Figure 1-4). The greensand filter was used to trap the oxidized iron formed, which improved the system removal of iron. Figure 1-5 shows the performance of the Vars GAC column using F-400 in the removal of NOM after the use of the greensand treatment. The bed volume of water treated increased to 9000 in terms of the $C/C_o = 0.5$ NOM breakthrough compared to 4000 before the use of greensand treatment.

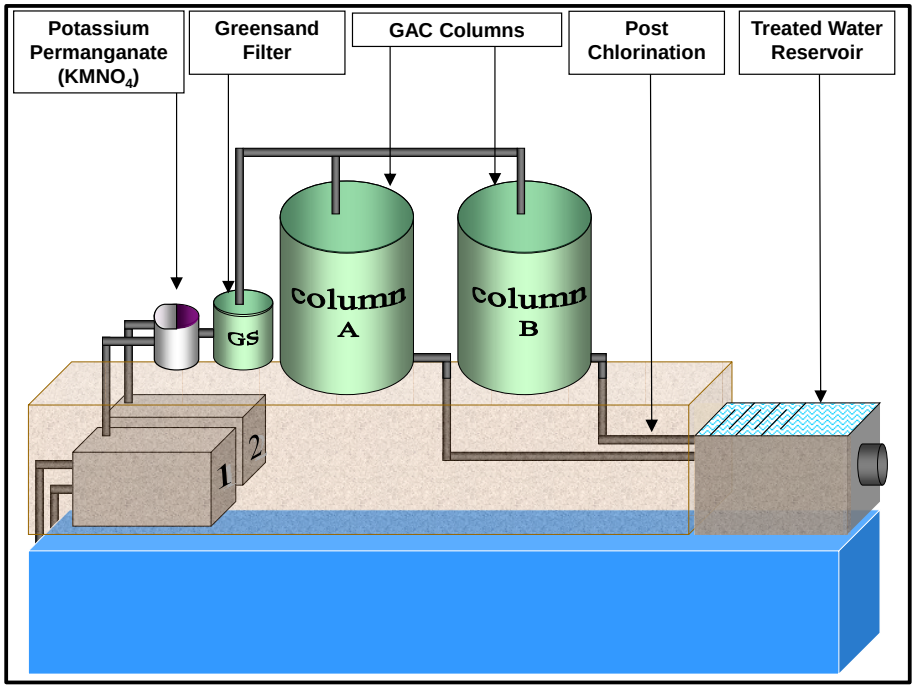

Figure 1-4: Vars groundwater treatment after the implementation of greensand treatment system

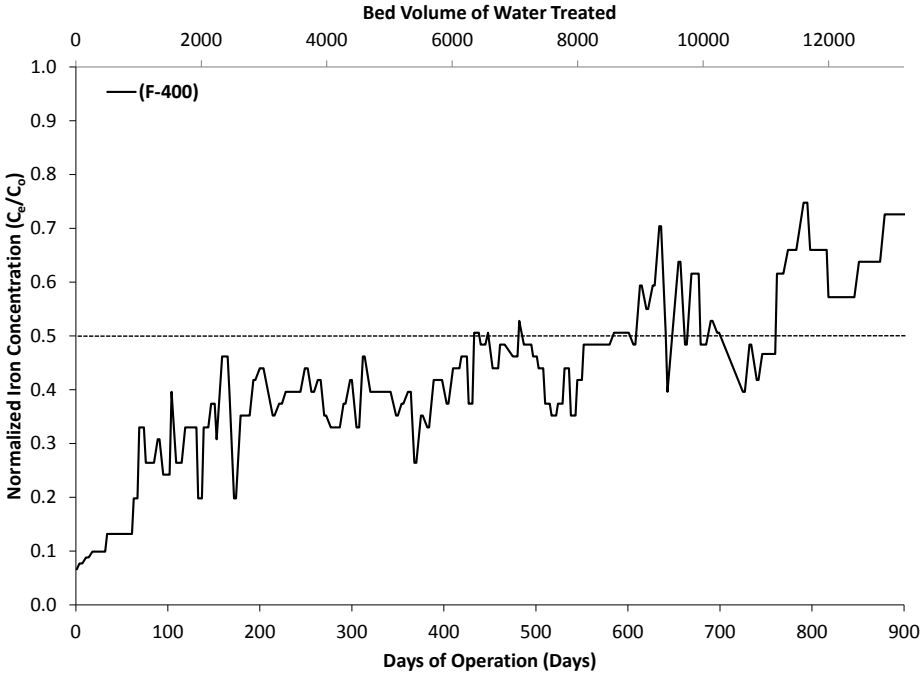

Figure 1-5: GAC columns performance using Filtrasorb F-400 GAC for the removal of NOM in Vars raw water after the implementation of greensand treatment system

1.3 Research Rationale

The originality of this work arises from the fact that there are very few applications of GAC systems to treat iron-laden groundwater and that there are no studies on the complex competitive adsorption interactions between NOM and iron.

1.4 Objectives

The main objective of this thesis is to gain an understanding of the interaction between NOM and iron in groundwater when treated with GAC. This will be achieved by an extensive characterization study of Vars' groundwater and treatment system, activated carbon adsorption isotherm, and column experiments. The specific objectives of this research are to accomplish the following:

- Characterization of NOM and iron as well as their interactions in Vars groundwater, after GAC treatment and after greensand treatment;
- Quantification of NOM and iron competitive adsorption on GAC using isotherm experiments;
- Assessment of the most popular competitive adsorption isotherm models such as IAST models for the simulation of NOM and iron in Vars groundwater;
- Evaluation of the rapid small scale test (RSSCT) ability to simulate the iron chromatographic effect observed in the full-scale GAC column;
- Simulation of NOM adsorption after greensand treatment using the small-scale columns.

1.5 Hypotheses

- The iron chromatographic effect was caused by NOM-iron complexes in groundwater.
- The competitive adsorption between iron and NOM could be described by the ideal adsorbed solution theory (IAST) based models, which were developed and successfully tested for competitive adsorption between organic solutes.

- The performance of the Vars treatment system before and after the implementation of greensand treatment can be successfully simulated using the rapid small-scale column test (RSSCT) with the appropriate scaling.

1.6 Thesis Organization

The thesis is composed of eight chapters; it was prepared in the conventional thesis format except Chapter 4 which was prepared in a paper format.

CHAPTER 2 LITERATURE REVIEW

This chapter reviews the pertinent literature to the iron and NOM adsorption phenomena observed at the Vars plant. They include discussion of the presence of iron in groundwater, the characteristics of NOM in water, iron-NOM interactions, iron removal at water treatment plants, activated carbon adsorption equilibrium and dynamic modeling.

2.1 Iron in Groundwater

Iron is a common constituent of groundwater. The presence of iron in groundwater is attributed to the dissolution of iron bearing rocks and minerals, mainly oxides (magnetite and hematite), sulphides (pyrite), carbonates (siderite), and silicates (pyroxene, biotites and olivines) under anaerobic conditions in the presence of reducing agents such as organic matter (Hem, 1989; O'Connor, 1971). Iron usually exists in two oxidation states, reduced soluble divalent ferrous ion (Fe(II)) and oxidized trivalent ferric ion (Fe(III)). Groundwater is generally anaerobic and in those situations, iron primarily exists in the soluble Fe(II) form. Although there are no detrimental human health consequences to the consumption of drinking water containing iron, it is a nuisance for domestic and industrial users, causing various aesthetic and operational problems. Some of these problems include: the formation of insoluble rusty oxide-red stains on laundry and plumbing fixtures, the attribution of color and bitter taste to water resulting in the rejection of well water, and the promotion of the growth of micro-organisms in distribution systems. Therefore, for many water supply companies using groundwater as their source, iron removal is an important concern. Various regulatory agencies have put forward standards to control iron concentrations in water supplies. The American Water Works Association (AWWA) suggested limits of 0.05 mg/L for public use (Bean, 1974). However, the current US and Canadian regulation have an aesthetic standard for iron of 0.3 mg/L. Also, the World Health Organization (WHO) recommends that the iron concentration in drinking water should be less than 0.3 mg/L (WHO, 1996).

2.2 Iron Removal from Water

There are several established methods for iron removal from water, such as oxidation, sequestering, and iron exchange softening (MWH, 2005). Of these methods, oxidation followed by filtration is the most common method of removal (Sung and Forbes, 1984). The oxidation processes include aeration, chlorination, ozonation, or potassium permanganate. These are variable methods to oxidize the iron and transfer the components from soluble substances to insoluble substances that may be filtered or sedimented in the following step. Chlorine and permanganate are the most commonly used oxidants. One of the main factors affecting the success of the process is sufficient oxidation with sufficient detention time to allow for complete removal (MWH, 2005).

Within the oxidation filtration approach, the filtration is generally carried out in pressure filters operating at loading rates of 240 to 480 $m^3/m^2/d$. Examples of filters include anthracite and greensand media. Greensand is a filter medium processed from glauconite sand that has a distinctive green color. This type of filter medium is commonly known as manganese greensand because the glauconite's surface is saturated with manganous ions (Mn(II)). The effective size of greensand particles is 0.30 – 0.35 mm, and they are characterized by an approximate specific gravity of 2.4 (Sommerfeld, 1999). Greensand has to be conditioned before use by soaking it in a potassium permanganate ($KMnO_4$) solution in order to convert the Mn(II) surface coating into MnO_2 (s) that adsorbs and catalyzes the oxidation of iron.

The typical operating mode of greensand filters (continuous regeneration mode) involves pre-oxidation followed by filtration. Pre-oxidation is done by the addition of a strong oxidant, such as $KMnO_4$, ahead of the greensand filter. This step would oxidize the iron into insoluble particulate form as shown in Equation (2-1).

$$3Fe^{2+} + KMnO_4 + 7H_2O \rightarrow 3Fe(OH)_3\,(s) + MnO_2\,(s) + K^+ + 5H^+ \qquad (2\text{-}1)$$

The insoluble forms are then removed by filtration through the greensand media. One of the advantages of this system is that if there is unoxidized iron (as a reason of underfeeding of the oxidant), it will be removed through adsorption onto the MnO_2 layer coating the greensand particles. This last step ensures that most of the soluble iron is converted into an

insoluble form and removed from water (Weber, 1972; Sommerfeld, 1999). In the regeneration step, potassium permanganate is used to remove the adsorbed iron from the greensand surface and to regenerate the MnO_2 coating of the filter medium.

Although, there are many studies on the oxidation of NOM by potassium permanganate (Matsuda and Schnitzer, 1971; Knocke *et al.*, 1991; Bryant *et al.*, 1992; Matsubara and Nakayama, 1992; Siegrist, 2001; Urynowicz *et al.*, 2008) (the pre-oxidation step before passing the water through the greensand filter), there is no study on the effect of greensand filtration on the removal of NOM in water. All studies have found that many constituents of NOM are oxidized by potassium permanganate. However, fractions of NOM are known to resist complete oxidation even at high concentrations of chemical oxidation over long periods of time. Matsuda and Schnitzer (1971) and Matsubara and Nakayama (1992) studied the reaction between the functional groups associated with humic substances and potassium permanganate and found that some of these functional groups may react with permanganate while others may not. They found that phenolic hydroxyls, which are found in abundance in humic substances, are readily susceptible to oxidation.

Few studies were performed to investigate methods of removing iron from water with NOM. MWH (2005) concluded that the oxidation of iron complexed with NOM requires a long reaction time (greater than 1 hour) and a large oxidant dosage. Accordingly, the oxidation of iron complexed with NOM using potassium permanganate was found to be a non-practical removal process. Potgieter *et al.* (2005) investigated iron removal technologies from water with a highly dissolved organic carbon (DOC) loading. They studied the use of ferric chloride as coagulant along with hydrogen peroxide as an oxidant. They also investigated different physical treatment processes such as adsorption and nanofiltration. The results of the research reveal that nanofiltration using H_2O_2 is capable of producing water with drinking-quality standards by removing both DOC and iron. However, the use of fly ash as adsorbents was found to result in low percentage removal of DOC. In general, all the treatment methods combined resulted in high removal levels of iron. A recommendation was made by the study to use staggered treatment in order to remove iron and DOC from water. This can be done by using fly ash, $FeCl_3$, and polyelectrolyte coagulant aid at the pre-treatment stage at the plant, and then nano-filtration is used as a final step.

2.3 Natural Organic Matter (NOM) in Water

NOM is a complex, heterogeneous mixture of organic compounds that can be found in almost all water sources with varying concentrations from one location to another. Aquatic NOM has a high percentage of humic substances, which are the decomposition products of plant and animal residues. NOM is very stable and has a long half-life since it has already been naturally degraded. The reason NOM is significant in water treatment is that it can participate in many interactions in an environmental setting. Water utilities may encounter several problems associated with the presence of NOM in raw water supplies such as: (Hayes *et al.*, 1989; Leenheer and Croue, 2003)

- Causing color, taste, and/or odor to drinking water;
- Facilitating the transportation of organic and inorganic contaminants;
- Interfering with the removal of other compounds by an adsorption process
- Serving as a substrate for biological growth;
- Forming carcinogenic by-products through a disinfection process.

Although NOM is common in nature and has been studied by many scientists, the specific structure, properties and interactions of NOM in environmental systems are not certain. It is an amorphous mixture of organic compounds with a wide range of molecular weights and different chemical structures. Due to the difficulty of characterizing it, NOM is often classified by fractions of similar characteristics such as molecular weight and hydrophobicity. There are three major categories based on NOM's solubility at different pH ranges; these categories are: humins, fulvic and humic acids. Humins are insoluble in water at any pH, fulvic acids are soluble at all pHs, and humic acids are soluble in water with pH greater than 2 and insoluble at pH less than 2. These fractions can be isolated from the bulk NOM using a methylmethacrylate resin called XAD-8. (Aiken, 1985; Suffet and MacCarthy, 1989)

The humic portion is most prevalent in NOM and is the key fraction in water treatment (Nissinen *et al.*, 2001; Owen *et al.*, 1995; Thurman, 1985). Humic substances (another name given to NOM by researchers) contain carbonyl, carboxyl, methoxyl, hydroxyl, phenolic,

aromatic, and aliphatic units. The percentage of humic fraction of NOM in groundwater varies from one location to another depending on the type of the aquifer and the quality of the aquifer's recharge. In a study by Thurman (1985) on different groundwaters, it was found that humic acid content of deep groundwaters (greater than 150 meters) ranged from 12 to 33%, while highly colored groundwaters contain 65% or more. In groundwater, the humic substances contain more carbon and less oxygen than in surface water. NOM with carboxylic and phenolic groups may play an important role in groundwater since they both are capable of forming complexes with metals (Drever, 1997). In a highly colored groundwater, humics are expected to have more phenolic groups since they serve as color centers in humic substances. The presence of phenolic and carbonyl groups in humics can readily reduce ferric iron to ferrous iron (Huang and Blankenship, 1984; Uchida *et al.*, 2000). The hydrogen content of groundwater humics is greater than in surface water indicating that aliphatic carbon may be more abundant in groundwater humics. (Thurman, 1985)

NOM concentrations are usually measured as total organic carbon (TOC), or dissolved organic carbon (DOC), which is the TOC of filtered samples. The DOC in groundwater is generally low since the filtration occurs during the migration of water through the ground layers. Typical concentrations of DOC in groundwater range from 0.1 to 4 mg/L (Leenheer *et al.*, 1974; Junk *et al.*, 1980). Occasionally, there are groundwaters with very high DOC concentrations. Groundwaters recharged through saturated soils, such as bogs, typically have high DOC. Also, groundwaters contaminated with high dissolved organics from landfill sites or septic tanks are another example. In such cases, DOC concentrations can exceed 10 mg/L. In a study by Wassenaar *et al.* (1990) on different groundwaters in Canada, few locations were found with substantial DOC concentrations. Rodney (ON), Taber (AB) and Oldman River (AB) have groundwaters with DOC concentrations of 12, 14 and 19 mg/L, respectively.

A large number of studies for the determination of the molecular size of NOM in water have been conducted. The principles and methods for the determination of the molecular size and weight measurements of humic substances were summarized by Aiken (1985). According to these studies, the NOM in natural water may have molecular weights from few hundred to over 5000 g/mol (Li *et al.*, 2003b; Moore *et al.*, 2001; Yoon *et al.*, 2005; Stumm and

Morgan, 1996; Newcombe *et al.*, 1997). The different methods used to determine the size distribution of NOM include ultrafiltration (UF), HPSEC (high-performance size exclusion chromatography), FCS (fluorescence correlation spectroscopy) and MALLS (multi-angle laser light scattering). However, their review clearly demonstrated that different methods might give strongly diverging results and no single method is sufficient to provide a complete understanding of these molecular characteristics. Since no standard method to determine the size distribution of NOM was presented in literature, many differences in the results were found in literature using different techniques. Accordingly, no exact value of the NOM's molecular weight can be obtained from the different fractionation techniques. In spite of the fact that none of those methods can give an exact value for the NOM's molecular weight, they can be used to identify a range of either low or high molecular weights.

2.4 Iron and NOM Interaction in Water

Many literature sources have investigated the complexation of iron by organic matter and how it affected the oxidation of iron (Hem, 1989; Morgan and Stumm, 1964; Jobin and Gosh, 1972; Theis and Singer, 1974; Knocke *et al.*, 1994; Pham *et al.*, 2004). They all concluded that organic matter was capable of forming insoluble and soluble complexes with Fe(II) and Fe(III). The focus in this study will be on the complexation with ferrous iron since it is the most abundant type of iron found in groundwaters. All these researchers found that humics were able to form complexes with ferrous iron and thereby retard its oxygenation even in the presence of dissolved oxygen. Theis and Singer (1974) showed that Fe(II) complexation by humic matter increases with the increase of organic matter concentration. Also, their study showed that humic substances are capable of reducing Fe(III) to Fe(II). Morgan and Stumm (1964) suggested that the oxidation of Fe(II) by organic species involved the cyclic oxidation of Fe(II) followed by the reduction of Fe(III) by the organic substances as described by the following equations:

$$\mathrm{Fe(II)} + \mathrm{O_2} \rightarrow \mathrm{Fe(III)} \qquad (2\text{-}2)$$

$$\mathrm{Fe(III)} + \mathrm{organic} \rightarrow \mathrm{Fe(II)} + \mathrm{oxidized\ organic} \qquad (2\text{-}3)$$

$$\mathrm{Fe(II)} + \mathrm{O_2} \rightarrow \mathrm{Fe(III)} \qquad (2\text{-}4)$$

It is generally assumed that organic complexes with ferrous iron are weaker and thermodynamically less stable than those with ferric iron and much slower to form (Emmenegger *et al.*, 2001; Rose and Waite, 2003).

2.5 Granular Activated Carbon (GAC) Adsorption

Adsorption processes are commonly used for drinking water production. Adsorption is defined as the accumulation of a material at the interface between two phases (MWH, 2005). During the adsorption process, contaminants (or adsorbates) diffuse into the adsorbent and then adsorb onto the inner surface. There are two different types of processes that can be used to describe the adsorption phenomenon: physical adsorption and chemisorption. In physical adsorption, the adsorbate is adsorbed without any change in its chemical composition and the process is considered to be reversible. On the other hand, chemisorption involves the transfer of electrons between adsorbent and adsorbate, causing changes in the molecular structures of the adsorbate (Sontheimer *et al.*, 1988). Some adsorbates are removed by both physical and chemical adsorption on the same activated carbon. There are two types of activated carbon used in water treatment; powdered activated carbon (PAC) and granular activated carbon (GAC).

PAC is typically of a small particle size diameter (i.e., 44 μm) which passes through a 325 U.S. mesh sieve. The smaller particle size distribution adsorbs organic compounds more rapidly than larger particles. PAC is usually applied for the removal of contaminants present on a seasonal or temporary basis and to treat spills. PAC can be added to various locations in the water treatment processes (i.e., raw water intake, rapid-mix tank, filter inlet and/ or slurry contactors preceding rapid mix) in order to provide time for adsorption to take place, and then removed by sedimentation and/ or filtration (MWH, 2005). Due to the completely mixed nature of the PAC contact processes, it provides partial removal of the adsorbate, and PAC tends to equilibrate with effluent adsorbate concentration. The use of PAC in water treatment includes the removal of taste and odor causing compounds, such as geosmin-2, 4-dichloropheno and 2-methylisoborneol (MIB) (Lalezary *et al.*, 1986; Gillogly *et al.*, 1998), and the removal of herbicides (Qi *et al.*, 1994; Knappe, 1996; Adams and Watson, 1996).

GAC has typical particle size diameters of 0.6 – 2.36 mm (8×30 U.S. mesh) and 0.42 – 1.70 (12×40 U.S. mesh) (MWH, 2005). GAC can be used in separated contractors (i.e., gravity feed contractors, pressure contractors and/ or fluidized-bed contactors). Also, it can be used as part of filter media replacing anthracite media in filtration operations. GAC has been used for removing synthetic organic compounds (SOCs), VOCs, and NOM from drinking water supplies. One of the key features of the GAC column systems is their ability to achieve full adsorbate removal for an extended period of time especially if the adsorbate is present at low concentrations.

Due to the nature of PAC contact systems and GAC column systems, the GAC systems use the activated carbon's adsorption capacity much more effectively. This is because of the nature of the completely mixed PAC systems where the contaminant levels within the system tend to equilibrate with contaminant concentration of the effluent. On the other hand, the GAC column systems tend to come into equilibrium with the influent contaminant concentration. As the influent concentration is higher than the effluent concentration, the mass of contaminant removed per unit mass of carbon is higher for GAC column systems.

The extent of adsorption in both PAC and GAC systems is modeled by quantifying the equilibrium adsorption capacity and the kinetics of adsorption. The equilibrium (or maximum) adsorption capacity is quantified by isotherms (i.e., constant temperature equilibrium tests). The kinetic or rate of adsorption tests are modeled through batch kinetics or column tests. Both these types of tests will be discussed below.

2.5.1 Adsorption Equilibria

Equilibrium tests between the adsorbent and the adsorbate are conducted at constant temperature and they are referred to as isotherm tests or isotherms. The use of isotherms can help quantify the maximum mass of contaminant that can be adsorbed at a given fluid phase concentration. The results of these tests are generally plotted as the solid phase equilibrium concentration (ordinate) versus the liquid phase equilibrium concentration (abscissa), and they are often referred to as isotherm plots or isotherms. Isotherms are often used to estimate the carbon capacity in an adsorber in order to optimize carbon selection (Lalezary *et al.*, 1986; Oxenford and Lykins, 1991). The most common technique used to generate the

isotherm data is the batch test, which is generally conducted via the bottle-point method. Each data point is a result of contacting a known quantity of adsorbate with a given mass of adsorbent in a bottle or flask until equilibrium is achieved. Then the solution is separated from the adsorbent and the adsorbate's (equilibrium) concentration in the liquid is measured. The solid phase equilibrium concentration of each isotherm data point is calculated using the following mass balance:

$$q_e = \frac{V}{M} (C_o - C_e) \qquad (2\text{-}5)$$

Where: q_e = the equilibrium solid phase concentration of the contaminant (mg contaminant /gGAC); V = volume of the adsorbate solution (L); M = mass of the adsorbent (gGAC); C_o = the initial liquid phase concentration of the contaminant (mg contaminant /L) and C_e = the equilibrium liquid phase concentration of the contaminant (mg contaminant /L).

Isotherms can follow three common trends as shown in Figure 2-1. They are linear, favourable, and unfavourable isotherms. Favourable isotherms will occur in columns with constant sized mass transfer zones while unfavourable isotherms have mass transfer zones that increase in depth over time (Sontheimer *et al.*, 1988). Linear isotherms are considered to be the broad line between the favourable and unfavourable isotherms.

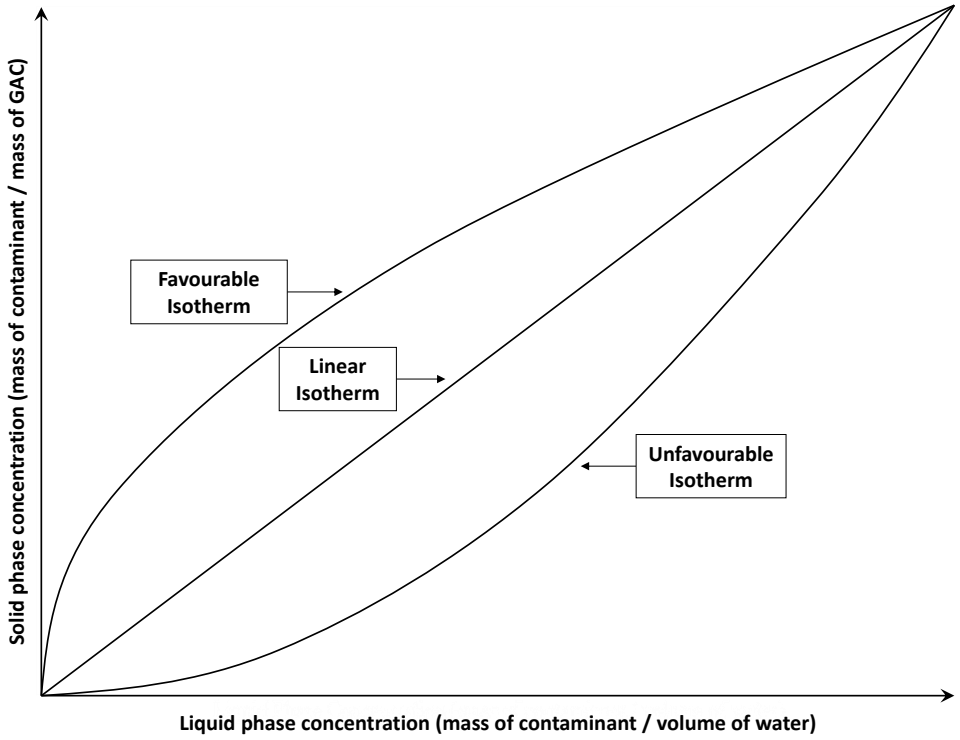

Figure 2-1: Traditional isotherm types

There are factors that affect the quantity of a compound or group of compounds that can be adsorbed by activated carbon. This is determined by the balance between the forces that keep the compound in solution and those that attract the compound to the carbon surface. These factors are grouped into three main types: 1) adsorbate properties, 2) adsorbent (i.e., activated carbon) properties, and 3) environmental and testing conditions (Weber, 1972; Faust and Aly, 1987; Sontheimer *et al.*, 1988). The adsorbate properties include the solubility and molecular weights. In general, the adsorbability of a compound decreases with increasing solubility. Also, a compound's solubility increases with decreasing molecular weights. Such a correlation is partially responsible for the relationship between adsorption capacity and the molecular weight of a compound. Traube's rule states that the adsorption capacity increases as the molecular weight of a compound increases. Such a rule only applies to compounds with the same structure that also belong to the same homologue group.

One of the adsorbent properties that affect adsorption is particle size. The particle size of activated carbon (GAC and PAC) does not have an impact on the adsorption capacity since there is no difference in the surface area per unit mass of different particle sizes. However,

the rate of adsorption is inversely proportional to the particle size squared. Thus, PAC adsorbs at a much faster rate than GAC.

The environmental and testing conditions that would have an impact on the adsorption process include the solution pH, temperature, and oxic/anoxic conditions, as well as the presence of other solutes and the equilibrium time (USEPA, 1973; Snoeyink, 1990; Stover and Thomas, 1992). The pH strongly influences the adsorption of other ions in the solution as the hydrogen and hydroxide ions are adsorbed quite strongly. Thus, the adsorption capacity of organic acids increases with decreasing pH. However, the adsorption capacity of some organics such as phenolics were found to slightly increase or remain constant as the pH increases up to the their pKa value, then the adsorption capacity decreases as the pH increases (Zogorski *et al.*, 1976). The physical adsorption process is usually expected to be exothermic (Weber, 1972). Thus, the adsorption capacity in most cases increases with decreasing temperature. However, this relationship is reversed in the case of chemisorption and the extent of chemisorption increases with the rise in temperature up to a certain limit, and then after that it starts decreasing (Zogorski *et al.*, 1976; Faust and Aly, 1987). Vidic and Suidan (1991) investigated the adsorptive capacity of different organic compounds (i.e., phenol, o-chlorophenol and 3-ethylphenol) and natural organic matter under oxic and anoxic conditions using GAC. Their experimental results proved that the presence of molecular oxygen significantly increases the adsorptive capacity of these organic compounds. Most water sources commonly contain several different compounds which will adsorb differently and may interfere with each other's adsorption. The compounds being adsorbed compete for the adsorption sites and reduce the adsorption capacity of the individual components. The quality of the isotherm results depends, among other factors, on the assumed equilibrium time. According to Peel and Benedek (1980), Randke and Snoeyink (1983) and Crittenden *et al.* (1987b), equilibrium is not achieved in some laboratory tests because the assumed equilibrium time is too short leading to the underestimation of the adsorption capacities. McCreary and Snoeyink (1980) studied the adsorptive capacity of carbon for various humic materials from aqueous solutions and noticed a difference in the adsorptive capacity for humic and fulvic materials. This was justified to be due to the incomplete achievement of equilibrium in 7 days. In a study by Randtke and Snoeyink (1983) on the adsorptive capacity

of GAC, it was concluded that humic material would take months to reach equilibrium with GAC.

The equations used to describe the isotherm data are frequently called isotherm models, or simply isotherms. There are two main types of isotherms: the first involves a single solute and is modeled using a single component model, while the second involves multi solutes and is accordingly modeled using a multicomponent model. These models help conduct comparison of carbon usage requirements as well as help calibrate dynamic adsorption models.

2.5.1.1 Single Solute Isotherm Models

The Langmuir and Freundlich models are most commonly used in single component isotherm modeling due to their simplicity and strong theoretical reasoning. The Langmuir model is based on the fact that binding sites are homogeneously distributed over the adsorbent surface. The model also assumes that there is no interaction between adsorbed molecules and all the binding sites have the same affinity for adsorption of a single molecular layer. The Langmuir mathematical model is shown in the following equation:

$$q_e = \frac{q_s\ b\ C_e}{1 + b\ C_e} \qquad (2\text{-}6)$$

Where: q_e = the solid phase concentration in equilibrium with C_e (mg contaminant /gGAC); C_e = the liquid phase at equilibrium (mg contaminant /L); q_s = the monolayer adsorption capacity (mg contaminant /gGAC); b = the energy constant (cm^3/g). The Langmuir isotherm has two limiting conditions; they are at low and high concentrations. At low concentrations, the model reduces to a linear isotherm. At high concentrations, the solid phase concentration approaches the expression $q_e = q_s$ and thus becomes independent of the solution concentration (Sontheimer *et al.*, 1988).

The Freundlich isotherm is the most widely used mathematical description of adsorption of most contaminants from water. It is an empirical model based on the assumption of heterogeneous adsorption surface comprising of different classes of adsorption sites and energies following an exponential relationship. It is described as:

$$q_e = K_F \, C_e^{\,n_F} \tag{2-7}$$

Where: K_F = Freundlich constant ((mg/g)·(L/mg)^n) and n_F = the Freundlich exponent (unitless). They are both regressed constants.

The adsorption of most synthetic organic compounds can be described well by the Freundlich and Langmuir isotherms as they are single solutes. NOM on the other hand consists of a wide range of compounds, so its adsorption isotherms are more difficult to model. Some researchers obtained satisfying results modifying Freundlich isotherm by plotting the uptake (solid phase concentration) as a function of the equilibrium NOM liquid phase concentration (i.e., the non-adsorbed NOM) divided by the GAC dose instead of just the liquid phase-phase equilibrium concentration (Summers and Roberts, 1988). Accordingly, Equation (2-7) after modification would be called the Summer-Roberts model and it is described as:

$$q_e = K_{SR} \left(\frac{C_e}{M/V} \right)^{n_{SR}} \tag{2-8}$$

Where: M = mass of GAC (g); V = volume of solution (L); K_{SR} = the Summers-Roberts constant ((mg/g)·(mg/g)^n) and n_{SR} = the Summers-Roberts exponent (unitless). Both of these constants are obtained by regressing the isotherm data. It should be noted that the K_{SR} value of the modified model is different from the K_F value obtained from the Freundlich isotherm model. The K_F value of the Freundlich isotherm model has the unit of (mg/g)·(L/g)^n, whereas the K_{SR} has the unit of (mg/g)·(mg/g)^n. Also, the exponent of the modified model (n_{SR}) is not the same as the exponent of the Freundlich model (n_F).

The Summers-Roberts model was further modified by Qi and Schideman (2008) in which the adsorbent dose (D) of their equation was eliminated as an intermediate variable, and the initial concentration effect is described explicitly by:

$$q_e = K_{QS}\left(\frac{C_e - C_{non}}{C_o - C_e}\right)^{\left(\frac{n_{QS}}{1-n_{QS}}\right)} \quad (q < q_{lim}) \tag{2-9}$$

Where: q_e = the adsorption capacity parameter (mgTOC/gGAC); K_{QS} = ((mg/g)·(mg/g)^n) and n_{QS} = the model regressed constants; C_e and C_o = the equilibrium and the initial NOM concentrations (mg/L), respectively; C_{non} = the concentration of the non-adsorbable NOM fraction (mg/L) and q_{lim} = the limiting adsorption capacity (mgTOC/gGAC). In order to ensure an attainable prediction of Equation (2-9), the restriction of $q \leq q_{lim}$ was imposed where q_{lim} is the maximum amount of NOM that can be held in adsorbent pores and it is estimated using the following equation:

$$q_{lim} = 740\ \rho_{NOM}\ \alpha_{NOM} V_{lim} \tag{2-10}$$

Where: V_{lim} = the limiting GAC pore volume (i.e., 0.30 cm^3/g for F-400 GAC (Moore *et al.*, 2001)), ρ_{NOM} = the NOM adsorbed phase mass density (g/cm^3) (i.e., 1.62 g/cm^3 (Newcombe *et al.*, 1997; Lead *et al.*, 1999), α_{NOM} = the NOM elemental carbon fraction of adsorbed phase (i.e., typically in the range of 0.45-0.6 with a corresponding average of 0.52 (VanLoon and Duffy, 2005)). Qi and Schideman (2008) demonstrated that the isotherm equation derived gave good predictions for NOM adsorption from various natural sources over a range of initial concentrations.

Figure 2-2 represents a typical NOM adsorption isotherm that is divided into three classes: nonadsorbing, moderately adsorbing, and strongly adsorbing fractions (Snoeyink, 1990; Snoeyink and Summers, 1999). Since the NOM is known to be heterogeneous and considered to be a mixture of complex organic materials, portions of the isotherm at low or high carbon doses may not be linear. The strongly adsorbable fractions of NOM (i.e., the high liquid phase concentrations in the upper right part of Figure 2-2) are adsorbed readily, and they only require small doses of activated carbon. The increase in the solid phase concentration with the increase in the liquid phase concentration reflects the high adsorbability of these fractions. However, it is very hard to obtain accurate points for this part of the isotherm because of the errors associated with the very low activated carbon

dosages and the small reduction in the liquid phase concentration. Accordingly, some researchers avoid very low activated carbon dosages and their isotherms do not include this convex upper part of the isotherm. As the carbon dose is increased, the adsorbent removes the moderately adsorbable fraction of the NOM in a fairly uniform fashion. Increasing the activated carbon doses to very large doses (i.e., the low liquid phase concentrations in the lower left part of Figure 2-2), the remaining NOM adsorbs very poorly causing the isotherm line to decrease drastically. These organics are referred to as the non-adsorbable fractions of NOM.

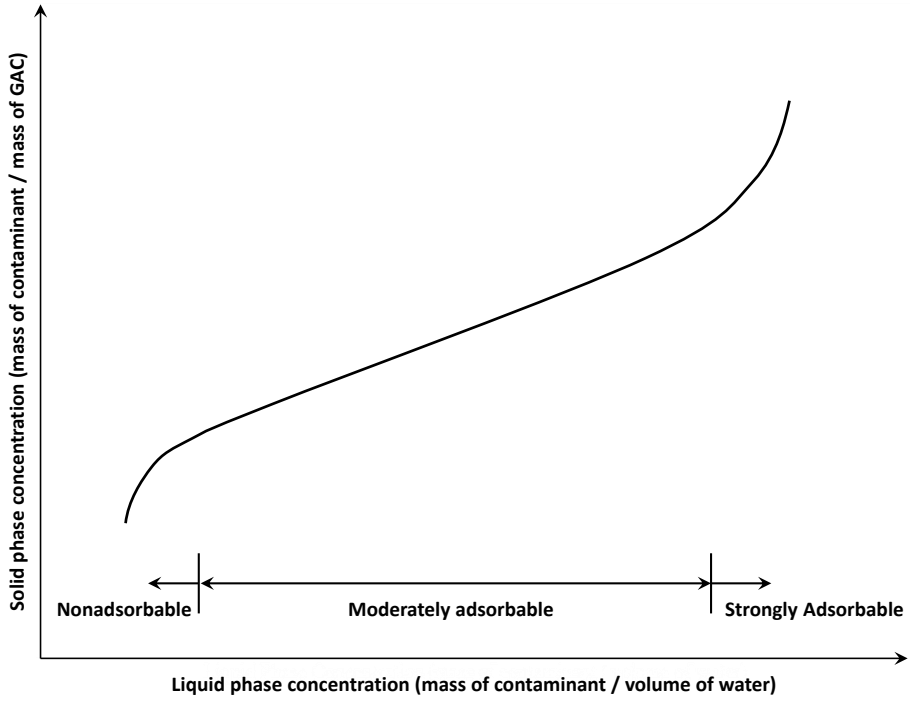

Figure 2-2: Typical NOM adsorption isotherm

To simplify the isotherm analysis, NOM adsorption has been modeled by some researchers as a single solute (Summers, 1986; Summers and Roberts, 1988; Harrington and DiGiano, 1989; Karanfil *et al.*, 1999; Karanfil *et al.*, 1999). In their approach, they expressed the NOM isotherms as a lumped concentration parameter (TOC or DOC) and used an established isotherm such as the Freundlich and Summers-Roberts models directly. The Langmuir model does not describe the shape of the NOM adsorption isotherm as well as the Freundlich and Summer-Roberts models, especially at high liquid phase concentrations, since the model

allows for saturation to occur at these high concentrations. Most of the single solute models that were capable of modeling the NOM worked well over a limited concentrations range that includes the nonadsorbable and moderately adsorbable fractions of NOM (Sontheimer *et al.*, 1988). In some situations, the above two-parameter models are incapable of describing experimental results well, so researchers have resorted to model with three or more adjustable parameters, such as Toth isotherm (Sontheimer *et al.*, 1988); Mayers isotherm (Sontheimer *et al.*, 1988) and Radke and Praustnitz isotherm (Radke and Prausnitz, 1972). Of the NOM single isotherm models found in the literature, the Summers-Roberts model (Summers and Roberts, 1988) appears to be most suitable for practical use. It requires the fewest parameters and has the capability of describing the adsorbent dose effect (Karanfil *et al.*, 1999; Kilduff *et al.*, 1996; Li *et al.*, 2002; Summers and Roberts, 1988).

The adsorption of iron onto activated carbon as a single solute has been studied by many researchers (Onganer and Temur, 1998; Uchida *et al.*, 2000; Uzun and Guzel, 2000; Mohan and Chander, 2001; Sirichote *et al.*, 2002; Kim, 2004; Üçer *et al.*, 2005). Table 2-1 summarizes the isotherm studies results presented in the literature. Some of their work was conducted on the adsorption of ferric iron Fe (III), and others on ferrous iron Fe(II). The equilibrium adsorption time for iron onto activated carbon used in the isotherm tests was found to be as follows: 30 minutes (Onganer and Temur, 1998; Kim, 2004); 1 hour (Sirichote *et al.*, 2002); 6 hours (Jusoh *et al.*, 2005); 24 hours (Uzun and Guzel, 2000), and 48 hours (Uchida *et al.*, 2000; Mohan and Chander, 2001). This difference in equilibrium times could be attributed to the different conditions in which these isotherms were conducted. Although there is a variation in equilibrium times among researchers, it can be concluded that the kinetics of iron adsorption are relatively fast. In modeling equilibrium tests, the Langmuir and Freundlich equations were the most frequently used models. Onganer and Temur (1998), Mohan and Chander (2001), Sirichote *et al.* (2002), Jusoh et *al.* (2005) and Üçer *et al.* (2005) used Langmuir isotherm to model their isotherm data whereas Uzun and Guzel (2000), and Kim (2004) found that the Freundlich model described their isotherm data points best. Most researchers tried and tested both models before deciding on which to use. According to these findings, iron isotherms can be modeled by either one of these models.

Table 2-1: Summary of isotherm studies presented in the literature on the adsorption of iron using GAC

Reference	Iron Type	GAC Type	Isotherm Equilibrium Time	Single Isotherm Model Selected	Isotherm Model Coefficients		Iron Concentration Range (mg/L)
Onganer and Temur (1998)	Ferric Iron	Merck carbon (no. 2514)	30 min	Langmuir Model	q_s = 0.92	(mg/g)	3.5 – 6.0
Uchida *et al.* (1999)	Ferric Iron	ACF-10 ACF-20	15 hr	Freundlich Model	K_F = 8.0 n_F = 0.48	$(mg/g)\cdot(L/mg)^n$	0.0 – 0.0004
				Freundlich Model	K_F = 18.5 n_F = 0.65	$(mg/g)\cdot(L/mg)^n$	0.05 – 0.5
Mohan and Chander (2001)	Ferrous Iron	F-400 PAC (325 mesh)	48 h	Langmuir Model	q_s = 14.6 b = 0.047	(mg/g) (L/mg)	0.0 – 223.2
				Freundlich Model	K_F = 3.5 n_F = 0.25	$(mg/g)\cdot(L/mg)^n$	0.0 – 223.2
Sirichote *et al.* (2002)	Ferric Iron	Bagasse GAC (325 mesh)	1 hr	Langmuir Model	q_s = 36.83 b = 0.71	(mg/g) (L/mg)	0.0 – 334.8
		Rubber Fruit GAC (325 mesh)	1 hr	Langmuir Model	q_s = 22.88 b = 1.52	(mg/g) (L/mg)	0.0 – 167.4
		Coconut Shell GAC (325 mesh)	1 hr	Langmuir Model	q_s = 10.60 b = 8.90	(mg/g) (L/mg)	0.0 – 111.6
Kim (2004)	Ferric Iron	Samchulli Co. GAC (24–16 mesh)	120 min	Freundlich Model	K_F = 0.11 n_F = 2.36	$(mg/g)\cdot(L/mg)^n$	7.4 – 20.1

2.5.1.2 Multisolute Isotherm Models

Most of the waters commonly contain several different compounds which will adsorb differently and may interfere with each other's adsorption. Multisolute or multicomponent adsorption is frequently called competitive adsorption and it can occur simultaneously or through preloading. In simultaneous adsorption, both adsorbates are exposed to the adsorbent (activated carbon). In preloading, the carbon is exposed to the natural water for some time before contacting the target compound. In competitive adsorption, the compounds being adsorbed compete for the adsorption sites and reduce the adsorption capacity of the individual components. Therefore, there is a need to account for this phenomenon in the modeling of isotherms. Multicomponent isotherm modeling generally requires the knowledge of the single solute adsorption coefficients for each solute in the mixture, as well as the competitive isotherm data. In order to model multicomponent isotherms, the use of either predictive or regression based models is needed. The use of predictive models requires only single solute isotherm data to predict competitive isotherms whereas regression based models require both single and competitive isotherm data to regress the parameters.

One of the first competitive adsorption models was developed by Butler and Ockrent (1930). The model was conducted in bi-solute solutions and it was derived from the Langmuir model (Sontheimer *et al.*,1988). The Butler and Ockrent model led to unsatisfactory results when some parts of the adsorption were non-competitive. Accordingly, Jain-Snoeyink developed a model to overcome this difficulty after taking into consideration the non-competitive adsorption on the adsorbent surface (Jain and Snoeyink, 1973). Other models for competitive adsorption in multicomponent systems were developed on the base of empirical data, such as the Fritz and Schlunder (1981) model. However, these types of empirical models require a great deal of multicomponent data to accurately define the adjustable parameters.

One of the most popular models that have been employed to predict multicomponent isotherms from single-component equilibrium data is the ideal adsorbed solution theory (IAST) isotherm model. This model was originally developed by Myers and Prausnitz (1965) for gaseous mixtures, and then modified by Radke and Prausnitz (1972) for multicomponent

adsorption in liquids. The model assumes equal competition for adsorption sites of all adsorbates. Another important assumption of the IAST model is that spreading pressures are the same for each component at equilibrium. Spreading pressure (π) is defined as the difference in interfacial tension between the pure solvent-solid interface and the solution-solid interface (Radke and Prausnitz, 1972). As summarized by Crittenden *et al.* (1985) and Sontheimer *et al.* (1988), there are five basic sets of governing equations required in the IAST model to predict multicomponent behavior from single component isotherms:

$$q_T = \sum_{i=1}^{N} q_{e\text{-}i} \qquad (2\text{-}11)$$

$$y_i = \frac{q_{e\text{-}i}}{q_T} \qquad \text{for } i = 1,\ldots,N \qquad (2\text{-}12)$$

$$\sum_{i=1}^{N} y_i = 1 \qquad (2\text{-}13)$$

$$\frac{\pi_i A}{RT} = \int_0^{C_i^\circ} q_{e\text{-}i}^\circ \frac{dC_{e\text{-}i}^\circ}{C_{e\text{-}i}^\circ} \qquad \text{for } i = 1,\ldots,N \qquad (2\text{-}14)$$

$$C_{e\text{-}i} = C_{e\text{-}i}^\circ y_i \qquad \text{for } i = 1,\ldots,N \qquad (2\text{-}15)$$

Where: $C_{e\text{-}i}$ = the liquid phase concentration of component (i) (mol/L); $q_{e\text{-}i}$ = the solid phase concentration of component (i) (mol/gGAC); y_i = the adsorbed phase fraction of solute i; q_T = the total solid phase concentration on the activated carbon (mol/gGAC); A = the surface area of the adsorbent (m^2/g); π_i = the spreading pressure of solute i (N/mol.m); R = the universal gas constant (J/mol·K); T = Absolute temperature (K); $C_{e\text{-}i}^o$ = The liquid phase concentration (mol/L) in equilibrium with the single solute system; $q_{e\text{-}i}^o$ = the equilibrium solute solid phase concentration (mol/gGAC) predicted by the single solute isotherm of component (i) for the liquid concentration $C_{e\text{-}i}^o$ and N = the number of components.

The IAST model requires one to have modeled the single solute isotherm for all components but it has the flexibility to accommodate single solute isotherm models of different forms. This makes IAST more widely applicable than other models. Several studies have successfully used the Freundlich isotherm in the IAST to model multicomponent isotherms

and found acceptable results (Crittenden *et al.*, 1985; Najm *et al.*, 1990; Knappe, 1996; Kilduff and Wigton, 1999; Yuasa *et al.*, 1997; Li *et al.*, 2003; Satoh *et al.*, 2005). When Freundlich isotherm is applied in combination with the IAST, a simpler relationship for predicting multicomponent adsorption can be derived as shown in the following equations:

$$C_{e\text{-}i} = \left[\frac{q_{e\text{-}i}}{\sum_{j=1}^{N} q_{e\text{-}j}}\right]\left[\frac{n_{Fi}\sum_{j=1}^{N}\frac{q_{e\text{-}j}}{n_{Fj}}}{K_{Fi}}\right]^{1/n_{Fi}} \tag{2-16}$$

$$q_{e\text{-}i} = \left(\frac{V}{M}\right)C_{io} - \left(\frac{V}{M}\right)\left[\frac{q_{e\text{-}i}}{\sum_{j=1}^{N} q_{e\text{-}j}}\right]\left[\frac{n_{Fi}\sum_{j=1}^{N}\frac{q_{e\text{-}j}}{n_{Fj}}}{K_{Fi}}\right]^{1/n_{Fi}} \tag{2-17}$$

Where: K_{Fi} = single solute Freundlich model coefficient of component i ($(mg/g)\cdot(L/mg)^{n}$); n_{Fi} = single solute Freundlich model exponent of component i (unitless); C_{io} = initial concentration of component i; M = mass of GAC (g); V = volume of solution (L); $C_{e\text{-}i}$ = equilibrium liquid phase concentration of component i; $q_{e\text{-}i}$ = equilibrium solid phase concentration of component i (mol/gGAC); $q_{e\text{-}j}$ = equilibrium solid phase concentration of component j (mol/gGAC) and n_{Fj} = Freundlich regressed parameter of component j.

The use of IAST in predicting the competitive adsorption of organics could be split into two categories: a) modeling of competitive adsorption of specific organic compounds in distilled water solutions; and b) modeling of competitive adsorption of specific organic compounds in water containing NOM. Most of the research that fell within the first grouping, which used the Freundlich isotherm in the IAST model, yielded good results (Najm *et al.*, 1991; Knappe *et al.*, 1998; Kilduff and Wigton, 1999; Yuasa *et al.*, 1997; Li *et al.*, 2003; Satoh *et al.*, 2005). However, the competitive modeling that incorporates NOM, particularly considering it as a single component, is difficult because NOM is a combination of many different types of compounds with different sizes and chemical characteristics. The IAST fails to adequately predict experimental data in many systems that involve NOM, especially when trying to

model both the individual organic contaminants and the NOM. Attempts to use this model with NOM have been unsuccessful due to the following reasons (Thacker *et al.*, 1981; Smith and Weber, 1988; Ebie *et al.*, 2001; Newcombe *et al.*, 2002):

- The adsorption characteristics of NOM are neither well understood nor predictable;
- The IAST does not take into account pore blockage as a potential competitive mechanism, whereas this mechanism is mostly caused by the fractions of NOM with large molecular sizes;
- The non-ideal competition between different fractions of NOM, whereas IAST assumes equal competition for adsorption sites of all adsorbates.

An alternative method to the predictive IAST model is the regression-based IAST model. One of the approaches of this type of modeling was suggested by Najm *et al.* (1991), in which the background organics are represented as a single equivalent background compound (EBC). This type of modeling describes the equilibrium NOM concentrations by the magnitude of the competitive effect of the background organic matter, instead of the actual DOC isotherms. The EBC only describe the unknown portion of the NOM which is considered as the competitive fraction. This model uses the IAST model to regress the EBC Freundlich parameters as well as the initial EBC liquid phase concentration by minimizing the error between an experimental multicomponent adsorption isotherm in the presence of NOM and the adsorption isotherm obtained by the IAST model. Then the regressed EBC isotherm can be used to predict other multicomponent isotherms of the different initial concentrations of the target compound(s) in the same NOM solution (Najm *et al.*, 1991). Many researchers have used the IAST-EBC method to model the competitive adsorption of NOM and SOCs (Newcombe *et al.*, 2002; Knappe *et al.*, 2003; Quinlivan *et al.*, 2005).

There has been another variation of the pseudocomponents procedure suggested by Frick (1980), which describes the NOM compounds as a mixture of imaginary components (pseudocomponents) according to their adsorbability. In the application of the IAST model, each of the pseudocomponents was described using a Freundlich model. Then, the molecular weight, Freundlich parameters, and the initial concentration of each pseudocomponent

needed to be regressed (Crittenden *et al.*, 1985; Sontheimer *et al.*, 1988). This approach was implemented by Crittenden *et al.* (1985) on the modeling of the adsorption capacity of volatile organic compound (VOC) mixtures containing trichloroethylene (TCE) and cis-dichloroethylene (DCE) in a sample of groundwater. However, their study was only concerned with modeling the adsorption of the VOCs and did not attempt to model the NOM results. Yuasa *et al.* (1997) also used the same approach successfully and described the competitive adsorption of different molecular weight fractions of the humic substance present in peaty water collected from an underground well.

However, the pseudocomponents approach may lead to poor predictions and many inconsistencies because of cross-correlation between the pseudocomponents coefficients (Crittenden *et al.*, 1985). There have been some suggestions to overcome the high cross-correlation among the large number of parameters in the pseudocomponent IAST models by reducing the number of parameters that needs to be regressed. Crittenden *et al.* (1985) suggested the use of three pseudocomponents with the same molecular weights. Sorial *et al.* (1993) and Yuasa *et al.* (1996) suggested using the same Freundlich exponent (n_F) value for all the pseudocomponents but different values of (K_F), so as to represent a wide range of adsorbability.

Ding *et al.* (2006) proposed a modification to the concept of the IAST pseudocomponents model that gave satisfactory simulations of the competitive adsorption between trace organic contaminants and NOM. Their approach takes into account that there is direct competition between the target compounds and NOM for some adsorption sites and there also is pore blockage that eliminates certain adsorption sites. Direct competition occurs when small NOM molecules simultaneously compete with target compound molecules for access to the adsorption sites on activated carbon. The effect of pore blockage by NOM occurs when large NOM molecules accumulate and block the openings of smaller pores, preventing target compound molecules from accessing or exiting adsorption sites. Ding *et al.* (2006) divided the NOM into two fictive fractions, site competing fractions (SC), and pore blocking fractions (PB). Additional assumptions were made by Ding *et al.* (2006) to simplify their method. The NOM that is competing with the target compounds for adsorption sites are

assumed to have the same molecular weight and the same adsorption properties as those of the target compound, including the Freundlich constants, K_F and n_F.

Most of the modifications to the IAST model include modifying the background NOM in order to simulate the competitive adsorption of the target compounds. A different approach suggested by Kilduff and Wigton (1999) is to modify the IAST procedure by assuming that the target compound could access GAC adsorption sites, while the NOM cannot. Therefore, an additional parameter was incorporated into the IAST equations of the target compound represented by (θ). This parameter represents the fraction of the GAC surface area on which there are no competitive effects. Accordingly, the solid phase adsorption capacity of the target compound was split into non-competitive and competitive fractions by multiplying the single solute isotherm models by (θ) and (1-θ), respectively. The competitive fraction is what was incorporated into the IAST calculations of the target compound (i.e., ferrous iron) as shown in Equations (2-18) and (2-19). In the proposed model, the competitive effects of NOM are modeled using the standard IAST in combination with the Freundlich model, without the incorporation of the competitive fraction (1- θ), and the NOM is represented by a single reactive component.

$$C_{e\text{-}TC} = \left[\frac{q_{e\text{-}i}}{\sum_{j=1}^{N} q_{e\text{-}j}}\right]\left[\frac{n_{F\text{-}TC}\sum_{j=1}^{N}\frac{q_{e\text{-}j}}{n_{Fj}}}{(1-\theta)\,K_{F\text{-}TC}}\right]^{1/n_{F\text{-}TC}} \tag{2-18}$$

$$q_{e\text{-}TC} = \left(\frac{V}{M}\right)C_{TCo} - \left(\frac{V}{M}\right)\left[\frac{q_{e\text{-}TC}}{\sum_{j=1}^{N} q_{e\text{-}j}}\right]\left[\frac{n_{F\text{-}TC}\sum_{j=1}^{N}\frac{q_{e\text{-}j}}{n_{Fj}}}{(1-\theta)\,K_{F\text{-}TC}}\right]^{1/n_{F\text{-}TC}} \tag{2-19}$$

Where: $K_{F\text{-}TC}$ = single solute Freundlich model coefficient of the competitive fractions of the target compound $((mg/g)\cdot(L/mg)^n)$; $n_{F\text{-}TC}$ = single solute Freundlich model exponent of the competitive fractions of the target compound (unitless); M = mass of GAC (g); V = volume of solution (L); $C_{e\text{-}TC}$ = equilibrium liquid phase concentration of the competitive fractions of

the competing compound (mol/L); $q_{e\text{-}TC}$ = equilibrium solid phase concentration of the competitive fractions of the competing compound (mol/gGAC); $q_{e\text{-}j}$ = equilibrium solid phase concentration of compound j (mol/gGAC); n_{Fj} = single solute Freundlich parameter of compound j and (1- θ) = the fraction of the GAC surface area on which there are competitive effects. The mass of target compound adsorbed by surfaces with competition is not included in the initial concentration of iron used in the IAST calculation. Accordingly, the corrected values representing the competitive fraction of the target compound initial concentration (C_{TCo}) have to be incorporated into the IAST calculations using the following equation.

$$C_{TCo} = C_{TC\text{-}Total} - \left(\frac{M}{V}\right) q_{e\text{-}TC} \qquad (2\text{-}20)$$

Where: C_{TCo} = initial concentration of the competitive fractions of the target compound (mol/L); $C_{TC\text{-}Total}$ = Total initial concentration of the target compound obtained from the isotherm experiments (mol/L) and $q_{e\text{-}TC}$ = equilibrium solid phase concentration of the non-competitive fractions of the target compound (mol/gGAC).

Most studies used the regression based IAST to model the target compounds without attempting to model the NOM adsorption (Kilduff and Wigton, 1999; Najm *et al.*, 1990; Crittenden *et al.*, 1985; Knappe *et al.*, 1998; Andrews, 1990). The only studies that attempted to simultaneously model the adsorption of a target compound and NOM were Narbaitz and Benedek (1994), and Simpson and Narbaitz (1997). The former researchers used a simplified version of the IAST model in which fractions of the solutes adsorbed without competition. Simpson and Narbaitz (1997) evaluated the same competitive adsorption isotherms for 1,1,2-trichloroethane (TCEA) in competition with NOM from a river water, using the pseudocomponent IAST, and found that the simultaneous regression of both components provided reliable results which described both isotherms well. Presumably other IAST model users have not reported on the quality of their NOM adsorption simulations because their NOM behaved differently, making their simulations inaccurate.

2.5.2 Adsorption Kinetics

The kinetics, or the rate of adsorption, depends on how fast the contaminant can be transferred from the bulk liquid phase to the external surface of the GAC, and how fast it can migrate into the pores until reaching an adsorption site. In addition, different solutes adsorb at different rates. Predicting the adsorption by GAC columns using kinetic studies can be achieved by several methodologies such as pilot-scale columns and rapid small-scale column tests (RSSCT). The use of a pilot plant is inherently expensive and time consuming. This makes the dynamic testing with the selected GAC and the site water using RSSCT particularly attractive. This type of testing incorporates competitive interactions between adsorbing compounds under dynamic conditions similar to those in large-scale system.

2.5.2.1 The Rapid Small Scale Column Test (RSSCT)

The RSSCT method was developed by Frick (1982) to predict the behavior of full-scale columns based on the performance of small-scale columns. This method was extensively applied by Crittenden and his research group (Crittenden *et al.*, 1986a; 1987; 1989; 1991). The RSSCT uses fixed-bed mass transfer models to scale down the full-scale design to a much smaller column. The RSSCT method uses significantly smaller GAC granules than those used in full-scale adsorbers, in order to take advantage of the fact that the rate of adsorption is proportional to the inverse of the particle diameter squared, and thus the breakthrough in the small columns occur in a matter of days. The appropriate scale-up equations are used to: a) design the small-scale columns based on the characteristics of the full-scale column; and b) transform the small-scale column breakthrough data into a prediction of the full-scale column breakthrough. The method does not require extensive isotherm or kinetic studies to obtain the full-scale performance prediction, and the amount of water required is small enough so that the small-scale column tests can be conducted in a laboratory (i.e., they do not have to be conducted on site to have a continuous supply of raw water).

The three parameters required for proper design of the RSSCT include: empty bed contact time (EBCT), the hydraulic loading, and the GAC bed length inside the small-scale column.

The proper EBCT scaling between the small-scale column (SC) and the full-scale (or "large") column (LC) can be determined using the following equation (Crittenden *et al.*, 1991):

$$\frac{EBCT_{SC}}{EBCT_{LC}} = \left(\frac{d_{SC}}{d_{LC}}\right)^{2-X} = \frac{t_{SC}}{t_{LC}} \qquad (2\text{-}21)$$

Where: d_{LC} and d_{SC} = mean particle diameters of the GAC in the full-scale and small-scale columns (μm), respectively; t_{LC} and t_{SC} = the operation times of the full-scale and small-scale columns (min), respectively; $EBCT_{LC}$ and $EBCT_{SC}$ = empty bed contact time of the full-scale and small-scale columns (min), respectively; and X = the diffusivity factor that is obtained from the relationship between the adsorbent particle diameter (d_P) and the surface diffusion coefficient (D_s), which is the HSDM's mass transfer coefficient describing the resistance to mass transfer within the adsorbent particles. This relationship can be quantified experimentally through batch kinetic experiments with different GAC particle sizes. These two standard relationships have been frequently used: 1) the constant diffusivity RSSCT (i.e., X = 0), which assumes that the rate controlling the interparticle diffusivity does not depend on the GAC particle radius, and 2) the linear (proportional) diffusivity RSSCT (i.e., X = 1), which assumes that the rate controlling the interparticle diffusivity depends linearly on the GAC particle radius. (Crittenden *et al.*, 1991; Crittenden *et al.*, 1987; Crittenden *et al.*, 1986a; Summers *et al.*, 1995; Snoeyink and Summers, 1999).

The equivalent hydraulic loading in the RSSCT is directly related to the hydraulic loading in the full-scale column by the following relationship:

$$\frac{v_{SC}}{v_{LC}} = \frac{d_{LC}}{d_{SC}} \qquad (2\text{-}22)$$

Where: v_{SC} and v_{LC} = the hydraulic loading of the small-scale and full-scale columns, respectively. The depth of GAC within the RSSCT column (l_{SC}) can be calculated by multiplying the hydraulic loading by the EBCT of the small-scale column:

$$l_{SC} = v_{SC} \cdot EBCT_{SC} \quad (2\text{-}23)$$

By combining Equations (2-21), (2-22) and (2-23) and using the linear diffusivity assumption, it is clear that the small-scale GAC bed length is identical to the full-scale length:

$$l_{SC} = \left(v_{LC} \frac{d_{LC}}{d_{SC}} \right) . \left(EBCT_{LC} \frac{d_{SC}}{d_{LC}} \right) = v_{LC} \cdot EBCT_{LC} = l_{LC} \quad (2\text{-}24)$$

It would be impractical to use such a long column and it may present operational problems in the form of large head losses and high operating pressures. Therefore, another equation can be used to minimize these effects and help shorten the length of the GAC bed length inside the small-scale column. Equation (2-25) can be used to lower the hydraulic loading of the small-scale column, provided that the intraparticle mass transfer remains the dominant transfer mechanism. $Re_{SC\text{-}min}$ represents the smallest possible value at which the Reynolds number for the small-scale column can be set, so that the effects of external mass transfer and dispersion do not exceed those of the full size column. Studies have shown that adjustments brought to the RSSCT's Reynolds number so it would be equal to values between 0.1 and 1.0 have negligible impact on results (Crittenden *et al.*, 1991; Summers *et al.*, 1995).

$$\frac{v_{SC}}{v_{LC}} = \frac{d_{LC}}{d_{SC}} . \frac{Re_{SC\text{-}min}}{Re_{LC}} \quad (2\text{-}25)$$

Where: Re_{LC} = Reynolds number of the full-scale column:

$$Re_{LC} = \frac{V_{LC} \cdot d_{LC} \cdot \rho}{\mu} \quad (2\text{-}26)$$

Where: ρ = density of influent water (kg/m^3) and μ = viscosity of the influent water ($kg/(s.m)$).

By combining Equations (2-25) and (2-26), the hydraulic loading rate and the GAC bed length of the small-scale column can be calculated by the following equations:

$$v_{SC} = \frac{Re_{SC\text{-}min} \cdot \mu}{d_{SC} \cdot \rho} \qquad (2\text{-}27)$$

$$l_{SC} = \frac{Re_{SC\text{-}min} \cdot \mu}{\rho} \cdot EBCT_{LC} \qquad (2\text{-}28)$$

The RSSCT has been successfully used to predict the full or pilot-scale breakthrough curves and a survey of past comparisons of the RSSCT to full-scale data for many waters and for several different adsorbates (including NOM) was prepared by Summers *et al.* (1995). Some researchers successfully predicted pilot-scale column breakthrough profiles of SOCs and VOCs in the presence of background NOM by using the linear diffusivity scale-up systems (Crittenden *et al.*, 1991; Summers *et al.*, 1994), while others found the constant diffusivity scale-up more appropriate for their tests (Vidic *et al.*, 1992; Matsui *et al.*, 1994). Unfortunately, the scaling relationships are usually not known beforehand, requiring researchers to: 1) test both scaling equations in order to choose the more appropriate relationship for the field situation; or 2) conduct batch kinetic tests using different sizes of carbon particles to establish a relationship between the particle size and the surface diffusivity.

Although the RSSCT method provides great cost and time savings over pilot-plant studies, careful consideration must be taken when applying the findings as the approach has its limitations. First, the RSSCT tests are conducted with a single sample, which may not be representative of the seasonal water quality variations at the full-scale facility. Second, the short duration of the RSSCT tests precludes the development of sufficient biomass and related contaminant biodegradation that is observed in full-scale adsorbers, which may cause differences in the breakthroughs (Crittenden *et al.*, 1991; Knappe *et al.*, 1997). Third, RSSCT scaling method for predicting the performance of adsorption systems experiencing significant preloading was found inadequate because of the inability to accurately scale the preloading effect (Summers *et al.*, 1989; Speth and Miltner, 1989; Septh, 1991). Summers *et al.* (1989) proposed preloading of the small GAC particles, and then performing a small-scale column test in order to increase the precision in predicting the large-scale columns. One

drawback of initial preloading of the GAC particles for column tests is determining the appropriate preloading time.

Therefore, implementing such an experiment requires multiple elements to ensure that similarity between the small-scale column and full-scale adsorber is maintained. First, data from a full-scale or larger scale adsorber must be readily available to adequately compare the results from the RSSCTs. Information regarding the large-scale column carbon with regard to its type, capacities, bulk densities, and void fraction is necessary to ensure adequate similarity. Proper scaling of the small-scale column and amount of carbon used as well as the type of pump and piping to build the system and limit dead zones are needed. Additional precautions are required to prevent change in the characteristics of the water. Furthermore, proper analysis is fundamental in the success of such experiments.

With the proper set-up, and if the RSSCT is capable of predicting the performance of the large-scale adsorber, then different experiments could be undertaken to help determine how Vars GAC columns should be used in the future.

2.6 Summary

It is clear that there is a lack of knowledge in the process of competitive adsorption between NOM and iron in groundwater using activated carbon due to the fact that there are very few applications of GAC systems to treat iron in groundwater. However, based on the literature reviewed, it is evident that an understanding of the interaction between NOM and iron in groundwater when treated with GAC can be achieved by extensive characterization of NOM and iron in groundwater, activated carbon adsorption isotherms, and column experiments. It is also hypothesized that the IAST competitive isotherm models that were successfully tested for competitive adsorption between organic solutes can be used to simulate the competition between the NOM and iron. RSSCT is a very powerful tool, and it is of great interest to determine if the NOM and iron breakthrough curves obtained from the Vars treatment plant before and after the implementation of the greensand treatment process could be well simulated by the RSSCT scaling procedures. The following chapters present the research work that targets the application of these prospective ideas.

CHAPTER 3 EXPERIMENTAL METHODS

This chapter discusses the materials, analytical methods and procedures of the experimental work conducted throughout the thesis. The three main types of experiments that were designed to achieve the research objectives are: 1) Characterization of the groundwater, GAC treated water and greensand treated water to gain an understanding of the role of the various NOM and iron fractions on the GAC column performance. 2) Isotherm experiments that would quantify the competitive adsorption of NOM and iron in a natural water source on activated carbon. Also, the competitive isotherm results would be used to determine if the competitive adsorption of NOM and iron in Vars raw water can be described by the different variations of the IAST model. 3) Adsorption kinetics and mini-column tests that would be used to simulate the performance of Vars treatment system before and after the implementation of greensand treatment.

3.1 Materials

3.1.1 Adsorbates

Organic free water (OFW) processed by a Millipore Milli-Q ultrapure water system (Millipore Corporation, Billerica, MA) was used for the preparation of stock solutions, standard solutions as well as for glassware cleaning. In order to perform the kinetics and isotherm experiments of ferrous iron as a single component, stock solutions were prepared using organic free water. Ferrous iron stock solutions were prepared fresh daily from the dissolution of ferrous ammonium sulfate hexahydrate powder (ACS reagent, 99%) (Aldrich, Milwaukee, WI) in OFW. The pH of the ferrous iron stock solution was adjusted to 2.0 using HCl to prevent oxidation. The ferrous iron stock solution was then used to prepare solutions with different desired concentrations. The pH was then immediately adjusted to 6 before the solution was used in the experiments. The reason behind choosing pH of 6 is based on the findings of (Stumm and Lee, 1961), who found that the rate oxidation of ferrous iron is pH-dependent and rate of oxidation reduces at pH lower than 6. All of the stock solution preparation, as well as the transfer of the ferrous iron solutions into glass bottles, was

performed inside an anaerobic glove box at 25^{o}C to minimize oxidation of the iron. For all the experiments with ferrous iron, two controls were used in order to quantify the oxidation and precipitation of iron in the bottles.

The multicomponent isotherm experiments of this study were performed using Vars raw water and greensand treated water. Most of the experiments as well as sample preparations were performed on-site (i.e., Vars treatment facility) in order to minimize any oxidation of the ferrous iron in the groundwater. For a detailed description of the quality of Vars groundwater, see Chapter 4. Greensand treatment lowered the iron levels in the groundwater to below 0.1 mg/L. Accordingly; greensand treatment samples were used to study the effect of removing iron from Vars raw water on the adsorption of NOM.

3.1.2 Adsorbent

The GAC used for the isotherm experiments was Filtrasorb F-400 from CALGON (Pittsburgh, USA). This is the same agglomerated bituminous activated carbon currently used at the Vars facility. Before use, the GAC was sieved, cleaned with organic free water and oven dried for 24 hours at 85°C. The properties of F-400 GAC are summarized in Table 3-1.

Table 3-1: Physical properties of Calgon F-400 GAC[a]

Property	**F-400**
Original raw material	Bituminous coal
BET surface area (m^2/g)	1050 – 1200
Total pore volume (m^3/g)	0.84
Iodine number (mg/g)	1000
Ash (%)	5.4
Moisture as packed (%)	2
Apparent density (kg/m^3)	270

[a] Data obtained from manufacturer.

Sieving of GAC was used for separating the GAC particles into different size fractions. The oversized materials are trapped above a screen, while undersized materials can pass through a screen. The mesh number system is a measure of how many openings there are per linear

inch in a screen. So, the size of these openings correspond the GAC particle size diameters (Table 3-2). The GAC mean particle size diameter is calculated using the following equation

$$d_p = \sqrt{d_{smaller\text{-}particle} * d_{larger\text{-}particle}} \quad (3\text{-}1)$$

Where: d_p= mean GAC particle size diameter, $d_{smaller\text{-}particle}$ = maximum GAC particle size passing through a given mesh size sieve and $d_{larger\text{-}particle}$ = maximum GAC particle size retained in the same mesh size sieve. The GAC mesh size used for the isotherm experiments throughout this work was 40×50 mesh with a mean particle diameter of 0.35 mm. The GAC mesh size ranges used in the kinetics experiments were 20×30, 30×40, 40×50 and 80×100 and their mean particle diameters were 0.70, 0.50, 0.35 and 0.16 mm, respectively.

Table 3-2: GAC US sieve size numbers and the corresponding particle size diameters

US Sieve Size (Mesh Number)	GAC Particle Size Diameter (mm)
20	0.841
30	0.595
40	0.420
50	0.297
80	0.177
100	0.149

3.1.3 Isolation Resins

Fractionation of the natural organic matter into hydrophobic and hydrophilic fractions was performed using a methyl methacrylate resin (XAD-8, Fisher Scientific, Hampton, NH). The preparative cleaning of the resin is described by Thurman and Malcolm (1981).

CHELEX-100 (Analytical Grade Chelating Resin, 50–100 mesh, sodium form, Hercules, CA, USA) is a non-NOM-adsorbing cation-exchange resin used to separate the free iron from the organically-bound iron present in Vars groundwater. Researchers have found that CHELEX-100 was a strong complexing resin and it was preferred for metal removal from water (Pesavento *et al.*, 2001; Soylak, 2004; Alberti *et al.*, 2005; Biesuz *et al.*, 2006). Moreover, other researchers have confirmed the high preference of CHELEX-100 resin for

iron (Patrick and Verloo, 1998; Jensen *et al.*, 1998). Although, it was confirmed that the CHELEX-100 resin has a high preference for iron, Schmitt *et al.* (2003) found that the resin was neither capable of holding the iron bound to NOM nor capable of dissociating the bond between them at pH values higher than 6.

3.2 Analytical Methods

3.2.1 Basic Analytical Methods

The natural organic matter was measured in terms of TOC concentrations by a UV-persulfate oxidation based TOC analyzer (Tekmar-Dohrmann, Phoenix 8000, Cincinnati, OH). The analyzer adds a small amount of 20% phosphoric acid to the liquid sample to decrease the pH and convert all of the inorganic carbon species (i.e., dissolved carbon dioxide, carbonate, and bicarbonate) to carbon dioxide and then strips it from the solution by sparging with carrier gas (i.e. nitrogen gas). Then, the liquid sample with a volume of 20 mL is simultaneously exposed to persulfate reagent and UV radiation. The oxidation converts the organics to carbon dioxide and a non-dispersive infrared (NDIR) detector measures the amount of carbon dioxide. The internal computer integrates the data and relates it to the stored calibration curve to produce the TOC concentration of the sample. One of the features of this analyzer is showing if the oxidation is not complete through a warning. Given that there were no such warnings during the analysis; the reaction time of 4 minutes appeared to be sufficient to insure that all available organic carbon is oxidized.

In addition, UV absorbance at 254 nm was determined using a UV spectrophotometer (DU-40, Beckman Inc., Fullerton, CA). A 100-mm path-length quartz cell was used instead of 10-mm cell in order to accurately measure the UV_{254} absorbance of the samples with low TOC concentrations (Figure 3-1). The UV absorbance measurements are fast and require no sample preparations which would save time and analysis cost. So, UV-TOC correlations for both types of water (Vars raw water and greensand treated water) were established from measuring the TOC and UV_{254} of many water samples throughout the research study. MacCraith *et al.* (1993) and Amy *et al.* (1986) confirmed that the correlation between the UV absorption measurements and the chemically determined TOC values can be used as a

method of measuring TOC. Accordingly, the established correlations (Figure 3-2) were used to reduce the number of TOC analyses, especially for the kinetics and RSSCT experiments, that require more frequent samplings. The Specific UV-absorption (SUVA) of Vars groundwater was calculated by dividing the UV_{254} absorbance of the sample in (1/m) by the TOC of the sample in (mg/L). To obtain the above absorption units the absorption measured using a 10-mm path-length quartz cell needs to be multiplied by 100.

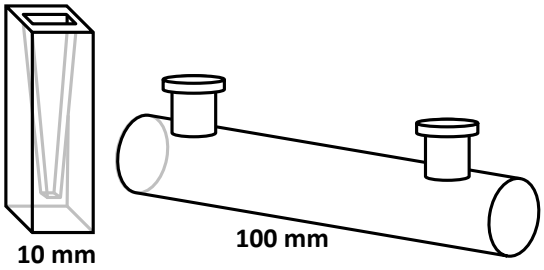

Figure 3-1: UV spectrophotometer cells

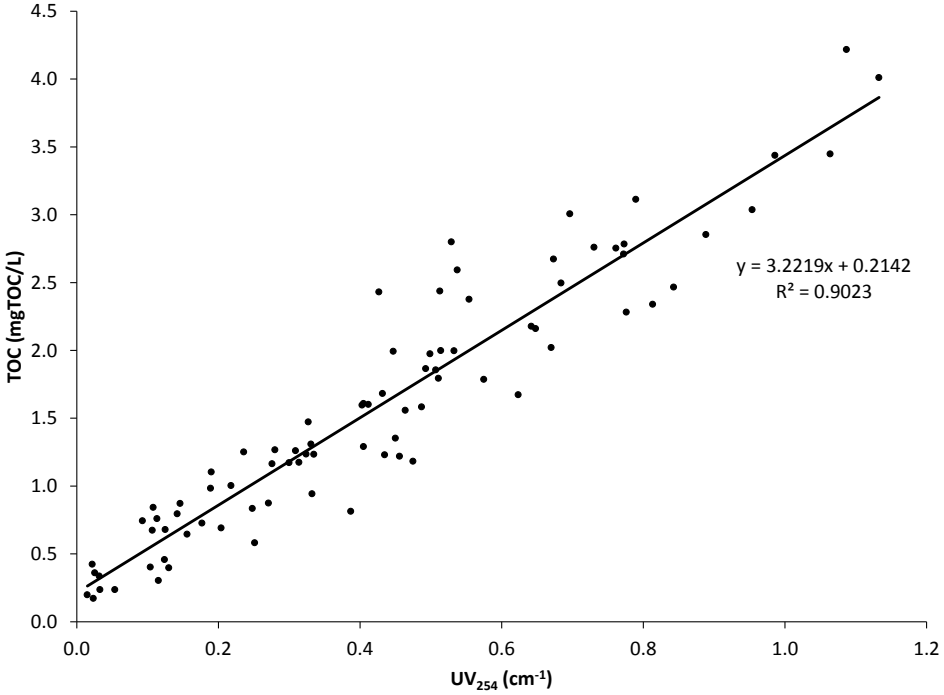

(a)

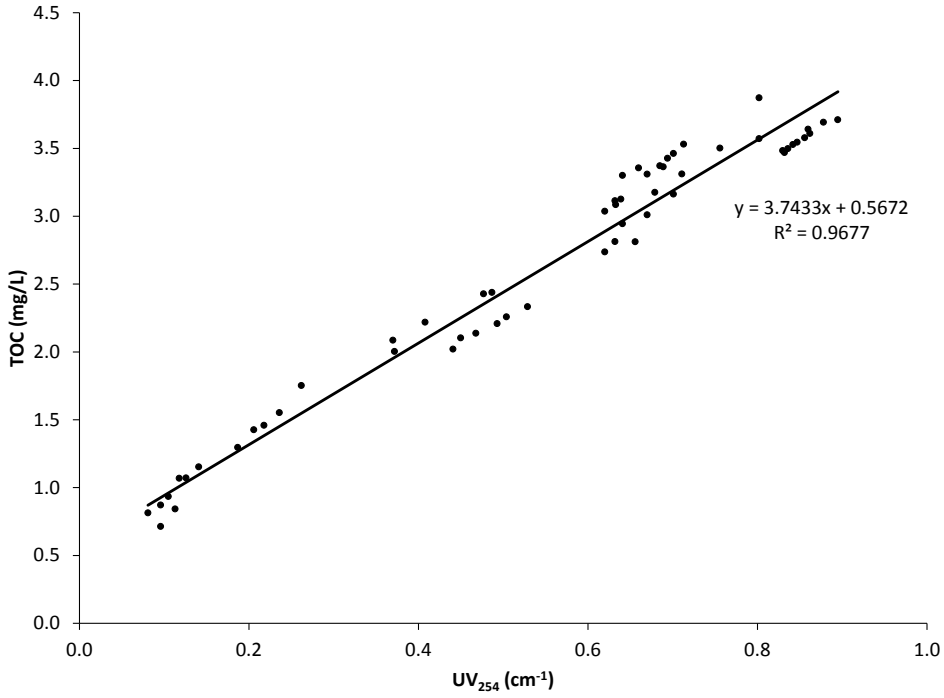

(b)

Figure 3-2: TOC-UV correlations using 100-mm path-length quartz cell for: a) Vars raw water and b) greensand treated water

Ferric and ferrous iron concentrations were measured via a two-step procedure. Axially inductively coupled plasma atomic emission spectroscopy (ICP-AES) (Varian Vista-Pro, Melbourne, Australia) with a detection limit of 0.0003 mgFe/L was used to determine the total iron concentration present in the water samples. The ferrous iron concentrations were measured at the site in order to avoid any type of oxidation that may occur during sample transportation. These measurements were performed by the phenanthroline method using a portable spectrophotometer (HACH DR-2800, Loveland, CO). Before each use, the HACH DR-2800 spectrophotometer was calibrated using different ferrous iron concentrations (0.03 – 3 mg/L) standards prepared from a ferrous ammonium sulfate hexahydrate stock solution. The ferric iron concentration was calculated by subtracting the ferrous concentration from the total iron concentration.

The pH and Eh values were measured using a pH meter (Accumet model 910, Fisher Scientific, Hampton, NH). The measurements of color of the water samples were performed via a spectrophotometer (HACH DR-2800, Loveland, CO) using the built-in color scale. Analysis of turbidity, alkalinity and hardness were performed in accordance with Standard Methods (APHA, 1998).

3.2.2 Water Characterization Methods

The quality of Vars groundwater was characterized before and after treatment. Water characterization was performed on water collected from different locations along the treatment line: untreated well water (i.e., Vars raw water), prior to entering the greensand filter (but subjected to potassium permanganate oxidation), and immediately after greensand filtration (i.e., greensand treated water). Water samples collected from these three sampling locations were characterized using step (I) and only the untreated well water was characterized using step (II) as shown Figure 3-3. The fraction methods utilized are described in detail in the next subsections.

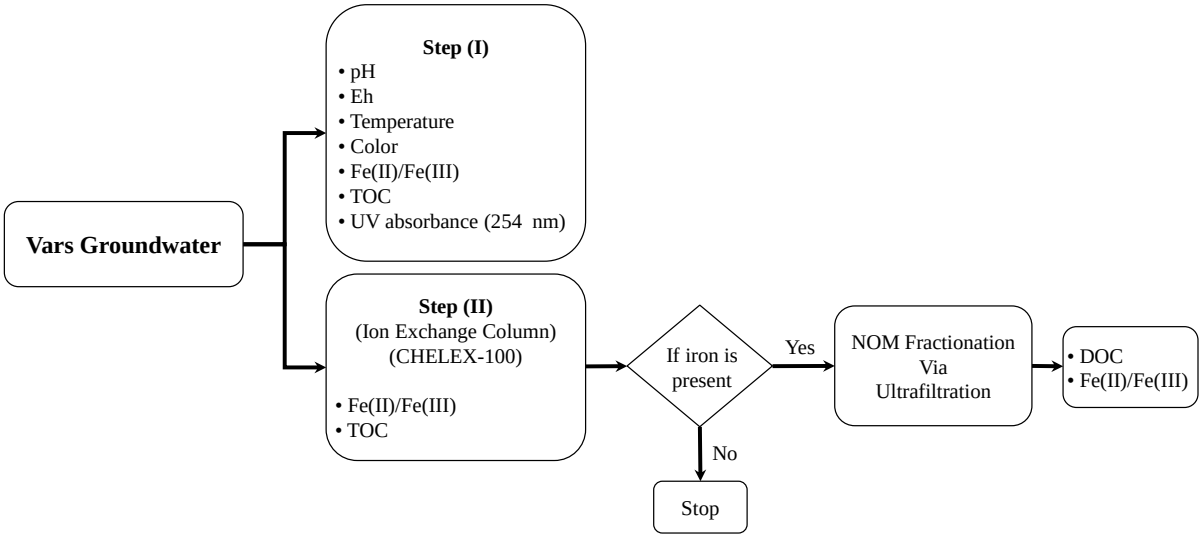

Figure 3-3: Steps of water characterization analysis

3.2.3 Organic-bound Iron Analysis

The water sample extracted from Vars groundwater was filtered through a glass column packed with 150 mg of CHELEX-100 resin using a peristaltic pump at a flowrate of 5 mL/min. Glass wool was placed at the bottom of the column to prevent the loss of resin. The free iron in the water samples was adsorbed onto the CHELEX-100 resin, whereas the organically-bound iron flowed through the CHELEX-100 column. The tests were conducted until the breakthrough was reached and then the resin was replaced before starting the next run.

3.2.4 XAD-8 Fractionation

Fractionation of the natural organic matter into hydrophobic and hydrophilic fractions was performed using a methyl methacrylate resin (XAD-8, Fisher Scientific, Hampton, NH). This test quantifies the hydrophobic fractions of NOM in water samples. These fractions are known to have the capability of forming soluble complexes with inorganic species such as iron. A 200 mL of Vars groundwater sample was adjusted to a pH level of 2 (± 0.1) using 10% 0.1M HCl (ACS Grade, Fisher Scientific, Hampton, NH) and was passed three times through a column filled with XAD-8 resin. The hydrophilic fraction passed through the column, while the hydrophobic fraction is adsorbed onto the resin. The hydrophobic fraction

was later eluted off the column with a 0.1N NaOH (ACS Grade, Fisher Scientific, Hampton, NH) solution. After analyzing the samples using the TOC analyzer, a mass balance was conducted to calculate the hydrophobic fractions in the groundwater.

3.2.5 Ultrafiltration Fractionation (UF)

NOM was fractionated using ultrafiltration membranes in a pressure-driven dead-end filtration system to determine the molecular size distribution of the NOM. In this method, the sample was sequentially filtered using a 400-mL stirred ultrafiltration cell (Amicon Corp., MA, USA) with different nominal molecular weight cut-offs (NMWCO) ultrafiltration membranes. These UF membranes (Millipore Corp., Billerica, MA) had a nominal molecular weight cut-off (NMWCO) of 500, 1000, 3000, 5000, 10000 and 30000 Da. The water was driven through the membranes by high purity nitrogen gas in order to limit the oxidation of iron present in the samples. The fractionation was performed by the in-series ultrafiltration fractionation method, which has been extensively used in the literature (Kilduff *et al.*, 1996; Pelekani *et al.,* 1999; Tadanier, 2000; Kitis *et al.,* 2002). The samples were sequentially filtered through membranes with decreasing NMWCO. The mass fractions of NOM and iron of a particular molecular weight were obtained by subtracting the TOC and total iron concentration values of the filtrate of one membrane from the filtrate of the next larger NMWCO membrane. UF fractionation was used to characterize the raw water as well as the CHELEX-100 treated water (i.e., the organically bound iron in the raw water).

3.3 Experimental Procedures

3.3.1 Mini-column Experiment for NOM-Iron Complex Removal

Since the current Vars treatment system no longer uses GAC filters to treat the raw well water directly, it was not possible to assess the impact of NOM complexed iron on the breakthroughs with chromatographic overshoots in the full-scale columns. Therefore, a mini-column experiment was used to assess the removal of complexed iron at different points within the iron breakthrough. This experiment would identify if the GAC has the capability to dissociate the bond between the NOM and iron during the adsorption process and thus

contributed to the chromatographic effect. The column experimental setup (Figure 3-4) consisted of two peristaltic pumps, two glass mini-columns (height of 40 cm and 1.1 cm internal diameter). The design parameters of the GAC mini-column (flowrate, GAC particle size, and depth) were selected to decrease the iron breakthrough time and to avoid any wall effect (column diameter to GAC particle median diameter ratio equal to 69). The GAC column was packed with 7 g of 80×100 mesh size GAC particles to accelerate the kinetics. The GAC used was bituminous coal-based Calgon Filtrasorb F-400, the same type currently used at the Vars plant. The carbon depth inside the column was 13 cm, providing an empty bed contact time (EBCT) of approximately 1.2 minutes and a hydraulic loading rate of 6.3 m/hr (corresponding to a flowrate of 10 mL/min). To maintain anaerobic raw water conditions and minimize iron oxidation in these experiments, the mini-column system was operated using water directly from one of Vars raw groundwater pumps that was operated on a continuous basis. Because of the particulars of the piping and operational constraints, it is difficult to have a continuous supply of raw water for long periods of time. The small EBCT of the mini-column (EBCT = 1.2 min) was chosen to limit the length of the run to approximately one week. However, the small EBCT in this test was not very critical since the objective of the tests was to be able to quantify the NOM-iron complexes removal at different points along the iron breakthrough and not to use it for scale-up. GAC column effluent samples were collected regularly and their iron (both ferrous and total iron) concentrations were measured. Upon reaching one of the chosen points on the iron breakthrough curve the NOM-iron complexation in the GAC effluent was quantified by passing part of the GAC column effluent through a CHELEX-100 column. The CHELEX-100 column was filled with 150 mg of the resin and the hydraulic loading rate supplied to the column was maintained at 3.2 m/hr (flowrate of 5 mL/min). The CHELEX-100 effluent was tested for TOC, ferrous and total iron.

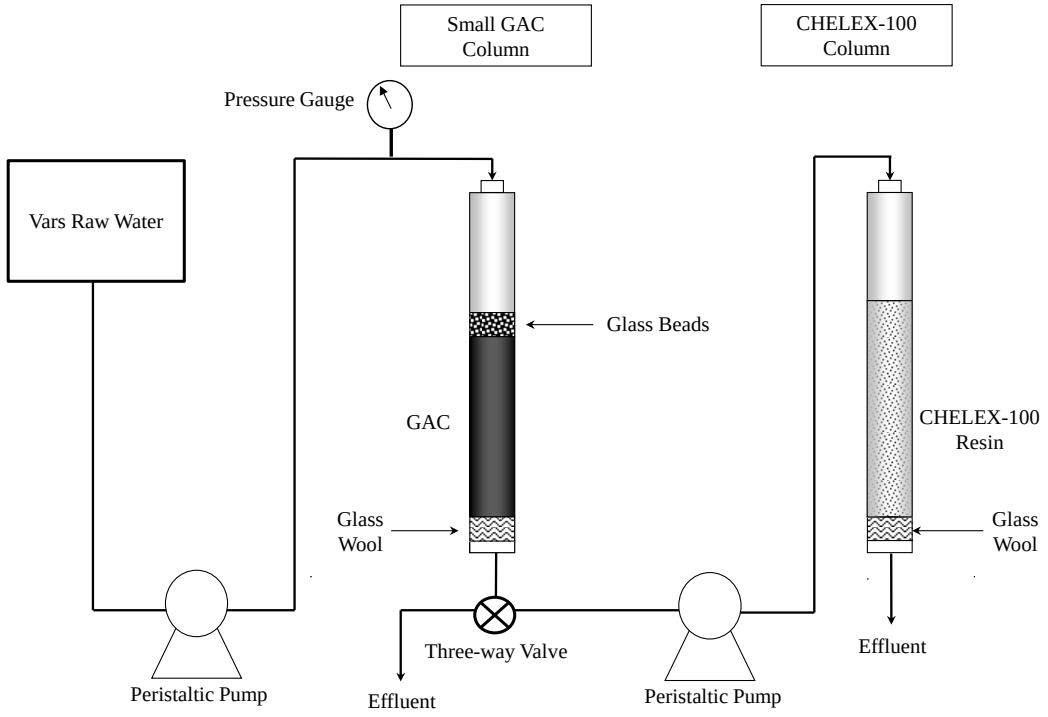

Figure 3-4: Setup of the mini-column experiment

3.3.2 Isotherm Experiments

Adsorption isotherms were performed using the bottle-point method using the same adsorbate solution and different carbon doses for all the bottles. Filling the isotherm bottles with Vars water proved to cause the ferrous iron to be oxidized. So another strategy for filling these bottles had to be used. The strategy involved the following steps. First, the GAC carbon in the lab was weighed using an analytical scale (Model#R200D, Sartorius, Goettingen, Germany) and transferred into 160 mL glass bottles. The GAC dosage ranged from 0.004 to 4 gGAC/L. Second, these bottles were covered with PTFE/SIL septa and sealed with aluminum crimp tops. Nitrogen gas was injected and released a few times in each bottle in order to remove any oxygen present. Third, the bottles were taken to the Vars site and each bottle was filled with water directly from the groundwater source by injection through the septa making sure that air bubbles were not trapped in the isotherm bottles. Two of the samples were controls with no GAC in order to check if the iron concentration changed through oxidation, precipitation or adsorption on the surface of the bottles during

the equilibration time. Also, two samples were blanks with OFW and GAC in order to check if there is any leaching from the GAC. Then, the glass bottles were placed in the end-over-end tumbler and rotated for 30 days. At the end of this period, each sample was analyzed for ferrous iron, total iron and TOC, UV absorbance at 254nm. Each isotherm bottle was opened inside the anaerobic glove box after allowing the GAC particles to settle for 5 min, and then the supernatant was collected and analyzed for ferrous iron by the phenanthroline method and total iron by ICP-AES. The remaining water sample was filtered with vacuum filtrations using glass Millipore filter holder and 47 mm diameter membrane with nominal pore size of 1.2 μm (Millipore corp., Billerica, MA) for TOC and UV_{254} analysis.

3.3.3 Iron Adsorption Kinetics Experiments

Adsorption kinetic experiments were performed on ferrous iron solution prepared with organic free water in order to obtain the equilibrium time needed for the isotherm experiment. The experiment was performed using the bottle-point technique. The preparation of the samples for the kinetics experiment started by weighing the 160 mL empty glass bottles using a laboratory scale (PC4400, Mettler-Toledo Inc., Columbus, OH). Then, the bottles were filled with the water to be analyzed and weighed again to calculate the volume of water in each bottle again. The calculated volume of water was then multiplied by the required GAC dose of 0.1 g/L to calculate the weight of GAC needed in each bottle. The GAC was weighed on an analytic balance (Model#R200D, Sartorius, Goettingen, Germany). The carbon was then carefully transferred into the bottle using a clean soft brush. For each bottle that contained GAC, a matching control bottle was prepared with no GAC in order to monitor any oxidation or precipitation of iron that may occur during the same length of the experiment. Then, the bottles were covered with PTFE/SIL septa, sealed with aluminum crimp top and injected with the water to be analyzed to remove any air gap that may cause an oxidation of the iron in the water. The bottles were then placed in an end-over-end tumbler for mixing for different lengths of time. The tumbler was located in a lab where the temperature was 21°C. Two bottles, one with GAC and a matching control bottle were collected at different time intervals and analyzed for total and ferrous iron. In order to limit the oxidation of ferrous iron in the water samples, each bottle was opened inside an

anaerobic glove box after allowing the GAC particles to settle for 5 min, and then the supernatant was collected and analyzed for ferrous iron by the phenanthroline method. As for the total iron, the samples were analyzed using ICP-AES.

3.3.4 NOM Batch Kinetics Experiments

NOM batch kinetics tests were performed to obtain the relationship between the adsorbent particle diameter (d_P) and the surface diffusion coefficient (D_s), which is the HSDM's mass transfer coefficient describing the resistance to mass transfer within the adsorbent particles. This relationship is not known a priori and once obtained it would be used in the scaling of the RSSCT (described in the next section) (Crittenden *et al.*, 1986a; 1987; 1991; Summers *et al.*, 1995; Snoeyink and Summers, 1999).

The kinetics experiments of NOM using Vars raw water and the greensand treated water were performed using a 20-L liquid-phase Carberry reactor that was specially constructed for this study after the design of Carberry (1964) (Figure 3-5). The dose of GAC used in this study (i.e., 0.06 gGAC/L) was contained in stainless steel screen baskets that are rotated at low rotational speed (10 rpm). A dual range laboratory scale mixer (KA-Werke GmbH, Staufen, Germany) with digital speed display was used to rotate the impeller. Four baffles were used to promote the mixing inside the reactor. The body of the reactor was built of clear PVC plastics and was covered with commercial aluminum foil in order to prevent any possible NOM degradation by ultraviolet radiation resulting from the exposure to direct sunlight. The reactor was sealed with O-rings on the lid and shafts. Nitrogen gas was supplied into the system and the free-space within the reactor in order to limit the oxidation of ferrous iron in Vars raw water. A pressure release valve was used to lower the build-up of pressure inside the reactor caused by the continuous supply of nitrogen gas. All sampling was conducted through a sampling port on the side of the reactor. In each experiment, the reactor was filled with the water in study (Vars raw water or greensand treated water). Then, an accurately weighed quantity of GAC with a specific particle size was placed in the basket and the apparatus assembled. Subsequent measurements of TOC concentrations were monitored at ever increasing intervals until the run was terminated.

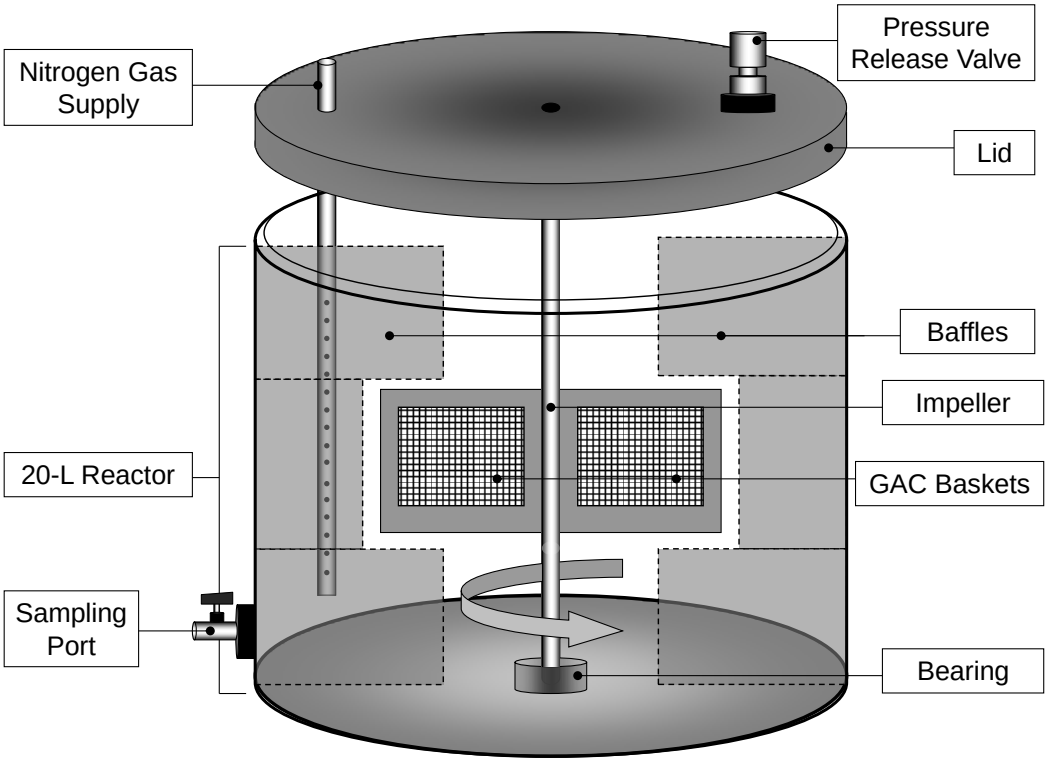

Figure 3-5: Liquid phase Carberry reactor

3.3.5 Rapid Small Scale Column Test (RSSCT)

The design, construction, and operation of the RSSCTs were in accordance with the methods outlined in the ICR Manual for Bench- and Pilot-Scale Treatment Studies (EPA, 1996). The RSSCT setup assembled in the lab is shown Figure 3-6. The GAC used for the RSSCT was Calgon F-400 (Bituminous coal) activated carbon with an 80×100 mesh size. The GAC was thoroughly washed with organic free water and dried in an oven at 85^{o}C for 24 hours before use. The GAC was packed into a glass chromatography column with 2.6 cm inner-diameter (Pharmacia, Uppsala, Sweden). All materials in contact with the water were glass, Teflon, or stainless steel. Effluent samples were collected from a sampling port directly after the column and the influent samples were periodically taken from the sealed container. Stainless steel screens, glass beads, and glass wool provided support for the column bed. A Varian 9010 HPLC pump (Varian Associates) Palo Alto, California was used as the feed pump. When the experiment was performed in the lab, the water was fed from a 20-L carboy, which was refilled with the batch influent water, as needed. The effluent from the RSSCT was

analyzed for TOC and total iron. The samples were taken at intervals throughout each run to fully capture the breakthrough curves. In addition, the influent samples were taken throughout the duration of each RSSCT to ensure that the influent TOC and iron concentrations remained constant. The ferrous iron concentration in Vars raw water was measured at the site in order to avoid any type of oxidation that may occur during sample transportation.

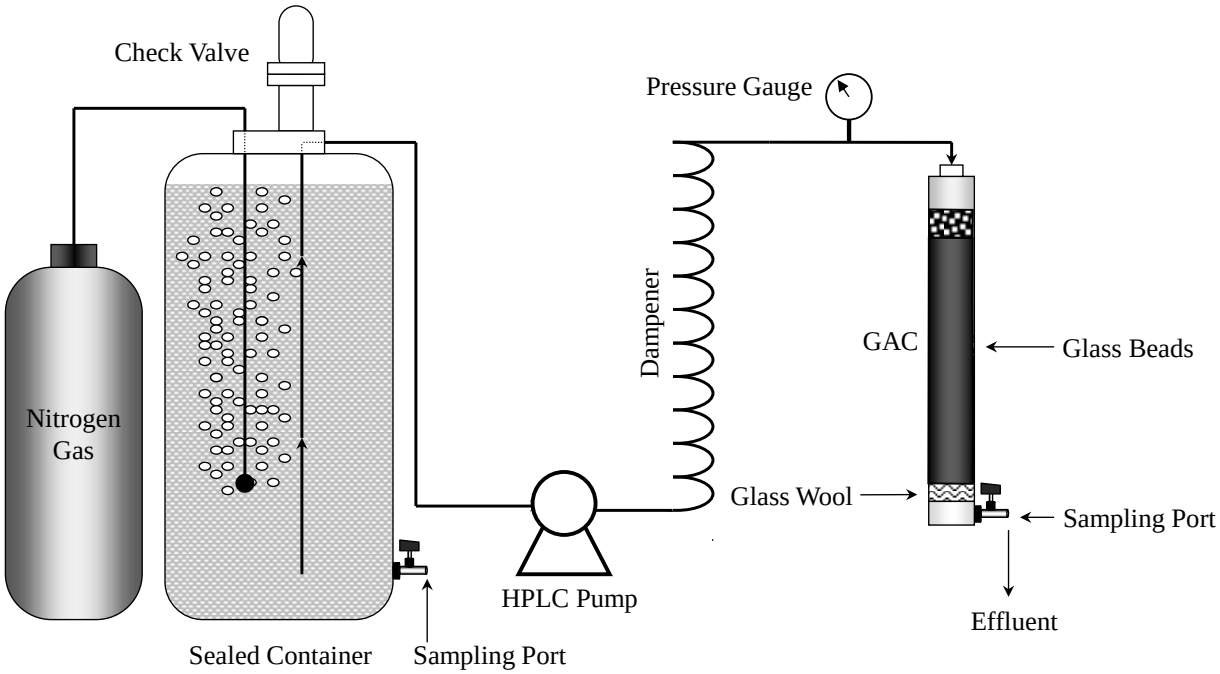

Figure 3-6: The rapid small-scale column test (RSSCT) setup

CHAPTER 4 IRON AND NOM INTERACTIONS IN GAC GROUNDWATER TREATMENT

Omar Al-Attas [a], Roberto Narbaitz [a], Ian Douglas [b]
[a] *Department of Civil Engineering, University of Ottawa, 161 Louis-Pasteur, Ottawa, ON K1N 6N5*
[b] *Drinking Water Services, City of Ottawa, 2731 Cassels St, Ottawa, ON K2B 1A8*

4.1 Abstract

The town of Vars, Ontario suffered from iron related problems when a system of granular activated carbon (GAC) columns was used to treat its groundwater. The iron concentration from the GAC columns started to increase until the iron concentration of the effluent exceeded the influent causing a phenomenon called the chromatographic effect. It was speculated that the chromatographic displacement of iron from the GAC columns may be caused by complexes of natural organic matter (NOM) and iron. The Vars water treatment plant was later modified by the addition of a potassium permanganate ($KMnO_4$) oxidation and a greensand filter prior to the GAC adsorption columns, which improved their performance by removing the iron. The objective of this research article is to investigate the GAC chromatographic displacements that occurred in the past by: 1) characterizing the quality of Vars groundwater as well as the greensand treated water; and 2) quantifying the role of NOM-complexed iron fractions on the operation of the adsorption system. NOM fractionation using XAD-8 resin showed that 30% of the NOM in Vars groundwater were hydrophobic with the capability of forming complexes with the iron present in the groundwater. CHELEX-100 isolation indicated that between 32 and 37% of the iron in Vars groundwater was organically bound and the rest was in the form of free iron. The quantification of complexed iron performed on the GAC mini-column effluent at the point of iron exhaustion showed that complexed iron was neither adsorbed nor split from NOM. Such a finding indicated that NOM-iron complexes were not the cause of the chromatographic displacement of iron observed at Vars. Another potential reason for the chromatographic displacement of iron was that the competitive adsorption between iron and NOM could force the iron to be desorbed from the GAC adsorbing sites causing the iron chromatographic displacement observed at Vars in the past. The full removal of iron during the greensand

treatment indicates that NOM-iron complexes must be either broken by the potassium permanganate oxidation or adsorbed by the greensand filter.

Keywords: Activated carbon, Iron, Natural Organic Matter, Adsorption, Groundwater

4.2 Background

In 1996, the City of Ottawa commissioned a new well field and water treatment system in the town of Vars, Ontario (population of 700) to replace the numerous local private wells that had bacterial contamination problems (City of Ottawa, 1996). The well water had a substantial natural organic matter (NOM) concentration (4 - 6 mg TOC/L) and color (≈ 20 color units). Based on these two parameters, the consultant engineers involved in the project decided to incorporate granular activated carbon (GAC) filters to treat the groundwater in Vars. Although the well water had significant concentrations of iron (≈ 2 mg/L), the final water treatment system design did not incorporate an iron removal strategy because it was considered to be an aesthetic issue rather than a health concern. The treatment system consisted of two 22-m deep production wells, two particle cloth pre-filters, two granular activated carbon (GAC) columns (A and B), post chlorination and a water reservoir to store the treated water before delivery to the distribution system. The GAC system was designed with an empty bed contact time (EBCT) of 33 minutes per column at an average design flowrate of 10.6 L/s.

The treatment system started production on January 1st, 1996. The GAC columns were initially operated in series where column "B" was fed by the effluent from column "A". The removal of total organic carbon (TOC) by the GAC columns was nearly complete and gradually decreased with time. After 204 days of operation and 1620 bed volumes of water treated, the effluent concentration of iron from the lead GAC column increased to levels greater than those of the feed. This phenomenon is called the chromatographic effect. Given that the GAC was intended for TOC removal and the effluent of the second column still contained no iron and very little NOM, the GAC column in the series system was kept in operation. After 443 days and 3520 bed volumes of water treated, it was decided to bypass column "A" due to the chromatographic displacement of iron, and operate only column "B" that was still achieving full iron removal (Narbaitz, 1997). After 507 days (i.e., 4030 bed

volumes treated), the iron concentration from column "B" started to increase until the iron concentration of the effluent exceeded that of the influent. After GAC treatment, the iron in water was oxidized through chlorination and the exposure to air in the plant's reservoir. Consequently, oxidized iron precipitated onto the reservoir floor and the pipes' inner surface connecting the treatment facility to the consumers. Eventually, some of Vars' residents had discolored water (orange and brown) coming out of their faucets as the iron precipitate was transported out to the distribution system. Accordingly, the city had to perform a number of distribution system flushings and line pigging to solve the colored water problems.

Over the years (1996 - 2002), the activated carbon was replaced several times with different brands of activated carbon (NORIT, PICA and Filtrasorb F-400). However, the iron chromatographic effect occurred in all the GAC types used. As an example, Figure 4-1 shows the performance of the Vars GAC column for a typical run. It presents the treatment cycle with Filtrasorb F-400 activated carbon in which the iron breakthrough started after 42 days, the effluent iron concentration exceeded that of the raw water after approximately 70 days, and thereafter the GAC column eluted rather than removed the iron.

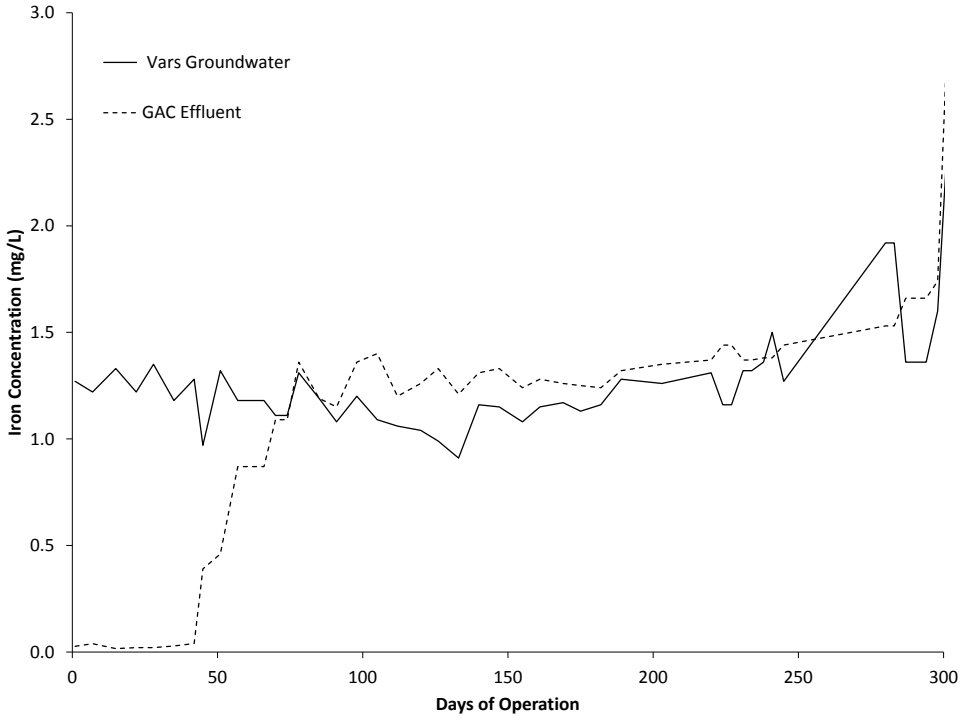

Figure 4-1: Performance of Vars GAC column using Filtrasorb F-400 for iron removal (June 2001 - May 2002)

Table 4-1 summarizes the performance of each carbon type used in Vars in the years 1996, 1998 and 2001. In 1996 when NORIT carbon was used, both GAC columns (A and B) were run in series, whereas only one GAC column was run at a time when PICA and F-400 GACs were used. Although F-400 GAC started the iron breakthrough after 42 days, which was earlier than the other two GAC brands (204 and 176 days for NORIT and PICA, respectively); the bed volumes (BV) of water treated at the start of the iron breakthrough were close (1620, 1394 and 1026 for NORIT, PICA and F-400, respectively). This similarity is due to the fact that the flowrate of the groundwater to be treated increased when the F-400 GAC was used. Also, PICA and NORIT carbons were exhausted in terms of NOM (C/C_o > 0.5) before the start of the iron breakthrough. Table shows that the values of C/C_o of TOC at the start of iron breakthrough were 0.67 and 0.8 using PICA and NORIT GAC, respectively. However, F-400 GAC was capable of removing more NOM even after reaching iron breakthrough (C/C_o (TOC) ≈ 0.33). The high value of bed volume of water treated by F-400 GAC (BV = 4253) at C/C_o (TOC) = 0.5 compared to the other GAC brands (BV = 1120 and 840 for NORIT and PICA, respectively) indicates that F-400 carbon was superior in terms of removal of NOM even in the presence of iron in the water to be treated. However, F-400 was not capable of solving the iron problem.

Table 4-1: GAC columns performance using different brands of activated carbon in Vars treatment plant

	NORIT	**PICA**	**Filtrasorb (F-400)**
Start of the run	January 1996	December 1997	June 2001
End of the run	November 1997	November 1998	May 2002
Bed volume of water treated at C/C_o (TOC) = 0.5	1120	840	4253
Start of iron breakthrough in days	204	176	42
Bed volume of water treated at the start of iron breakthrough	1620	1394	1026
(C/C_o) of TOC concentration at the start of iron breakthrough	0.67	0.80	0.33

The GAC replacements for such a small size treatment plant made the operating cost per cubic meters of Vars systems much higher than other water treatment systems operated by the City of Ottawa. Accordingly, in June 2002, the City of Ottawa modified the treatment system by the addition of a potassium permanganate ($KMnO_4$) oxidation system and greensand filtration prior to the GAC adsorption columns. The oxidation system consisted of a pump which introduced $KMnO_4$ solution into a mixing tank to oxidize the iron. The greensand filter removed the iron from the water by trapping the ferric hydroxide flocs formed and by adsorbing iron onto the surface of greensand that is coated with manganese oxide. This process significantly improved the performance of the GAC columns. For runs using F-400, the bed volume of water treated to reach 50% TOC removal increased from approximately 4000 to 9000.

The objective of this research is to gain a better understanding of both NOM and iron removals at Vars treatment facility. This type of groundwater is complex as it contains free ferrous iron (Fe-II), ferric iron (Fe-III), NOM-complexed iron, and NOM. The chromatographic displacement of iron from the GAC columns may be associated with the dissociation and leaching of NOM-iron complexes, or possibly with competitive adsorption. The specific objectives of this research are to gain a better understanding of the GAC treatment system by: 1) characterizing the quality of Vars groundwater; 2) quantifying the role of NOM-complexed iron fraction and other fractions on the operation of the adsorption system; and 3) characterizing the greensand treated water and the effect of this treatment process on the NOM present in water.

4.3 Materials and Methods

4.3.1 Groundwater Quality Characterization

Vars groundwater quality was characterized before and after treatment. Water characterization was performed on water collected from different locations along the treatment line: untreated well water, prior to entering the greensand filter (but subjected to potassium permanganate oxidation), and immediately after greensand filtration. Water

samples collected from these three sampling locations were characterized using step (I) and only the untreated well water was characterized using step (II) as shown in Figure 4-2.

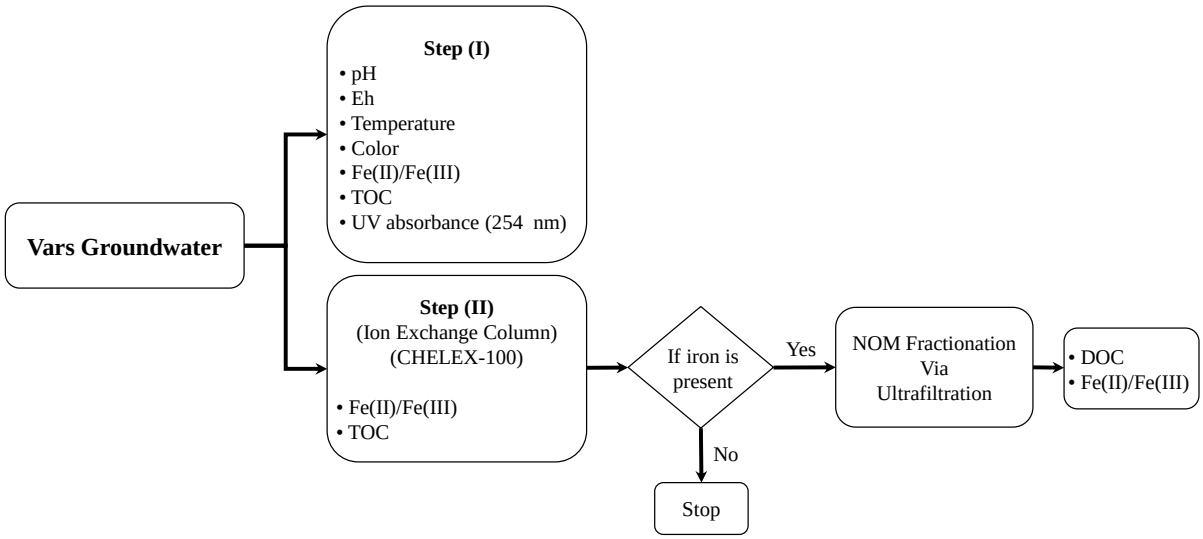

Figure 4-2: Steps of water characterization analysis

Organic free water processed by a Millipore Milli-Q ultrapure water system (Millipore Corporation, Billerica, MA) was used for the preparation of the standard solutions as well as for glassware cleaning. The natural organic matter was measured in terms of TOC concentrations, which were determined using a UV-persulfate oxidation based TOC analyzer (Tekmar-Dohrmann, Phoenix 8000, Cincinnati, OH). In addition, UV absorbance at 254nm was determined using a UV spectrophotometer (DU-40, Beckman Inc., Fullerton, CA). A 100-mm path-length quartz cell was used instead of a 10-mm cell in order to accurately measure the UV_{254} absorbance of the samples with low TOC concentrations. The Specific UV-absorption (SUVA) of Vars groundwater was calculated by multiplying the UV_{254} absorbance of the sample using a 10-mm cell by 100 (to convert the units to m^{-1}) and then dividing the product by the TOC concentration of the sample. Ferric and ferrous iron concentrations were measured via a two-step procedure. An axially inductively coupled plasma atomic emission spectrometer (ICP-AES) (Varian Vista-Pro, Melbourne, Australia) was used to determine the total iron concentration present in the water samples. The ferrous iron concentrations were measured at the site in order to avoid any type of oxidation that may occur during sample transportation. These measurements were performed by the phenanthroline method using a portable spectrophotometer (HACH DR-2800, Loveland,

CO). The ferric iron concentration was calculated by subtracting the ferrous concentration from the total iron concentration. The pH and Eh values were measured using a pH meter (Accumet model 910, Fisher Scientific, Hampton, NH). The measurements of color of the water samples were performed via a spectrophotometer (HACH DR-2800, Loveland, CO) using the built-in color scale. Analysis of turbidity, alkalinity and hardness were performed in accordance with Standard Methods (APHA, 1998).

4.3.2 Organic-bound Iron Analysis

CHELEX-100 is a non-NOM-adsorbing cation-exchange resin used to separate the free iron from the organically-bound iron present in Vars groundwater. Researchers have found that CHELEX-100 was a strong complexing resin and it was preferred for metal removal from water (Pesavento *et al.*, 2001; Soylak, 2004; Alberti *et al.*, 2005; Biesuz *et al.*, 2006). Moreover, other researchers have confirmed the high preference of CHELEX-100 resin for iron (Patrick and Verloo, 1998; Jensen *et al.*, 1998). Although, it was confirmed that the CHELEX-100 resin has a high preference for iron, Schmitt *et al.* (2003) found that the resin was neither capable of holding the iron bound to NOM nor capable of dissociating the bond between them at pH values higher than 6. The water sample extracted from Vars groundwater was filtered through a column packed with 150 mg of CHELEX-100 resin using a peristaltic pump at a flowrate of 5 mL/min. Glass wool was placed at the bottom of the column to prevent the loss of resin. The free iron in the water samples was adsorbed onto the CHELEX-100 resin, whereas the organically bound iron flowed through the CHELEX-100 column. The tests were conducted until the breakthrough was reached and then the resin was replaced before starting the next run.

4.3.3 XAD-8 Fractionation

Fractionation of the natural organic matter into hydrophobic and hydrophilic fractions was performed using a methyl methacrylate resin (XAD-8, Fisher Scientific, Hampton, NH) following the procedure outlined by Thurman and Malcolm (1981). This test quantifies the hydrophobic fractions of NOM in water samples. These fractions are known to have the capability of forming soluble complexes with inorganic species such as iron. A 200 mL of

Vars groundwater sample was adjusted to a pH level of 2 (± 0.1) using 10% 0.1M HCl (ACS Grade, Fisher Scientific, Hampton, NH) and was passed three times through a column filled with XAD-8 resin. The hydrophilic fraction passed through the column, while the hydrophobic fraction is adsorbed onto the resin. The hydrophobic fraction was later eluted off the column with a 0.1N NaOH (ACS Grade, Fisher Scientific, Hampton, NH) solution. After analyzing the samples using the TOC analyzer, a mass balance was conducted to calculate the fractions in the groundwater.

4.3.4 Ultrafiltration Fractionation (UF)

NOM was fractionated using ultrafiltration membranes in a pressure-driven dead-end filtration system. In this method, the sample was sequentially filtered using a 400-mL stirred ultrafiltration cell (Amicon Corp., MA, USA) with different nominal molecular weight cut-offs (NMWCO) ultrafiltration membranes. These UF membranes (Millipore Corporation, Billerica, MA) had NMWCO of 500, 1000, 3000, 5000, 10000 and 30000 Da. The water was driven through the membranes by high purity nitrogen gas in order to limit the oxidation of iron present in the samples. The fractionation was performed by the in-series ultrafiltration fractionation method, which has been extensively used in the consulted literature (Kilduff *et al.,* 1996; Pelekani *et al.,* 1999; Tadanier, 2000; Kitis *et al.,* 2002). The mass fractions of NOM and iron of a particular molecular weight were obtained by subtracting the TOC and total iron concentration values of the filtrate of one membrane from the filtrate of the next, larger NMWCO membrane. UF fractionation was used to characterize the raw water as well as the CHELEX-100 treated water (i.e., the organically bound iron in the raw water).

4.3.5 Mini-column Experiment

Since the current Vars treatment system no longer uses GAC filters to treat the raw well water directly, it was not possible to assess the impact of NOM complexed iron on the breakthroughs with chromatographic overshoots. Therefore, mini-column experiments were used to assess the removal of complexed iron at different points within the iron breakthrough. This experiment would identify if the GAC has the capability to dissociate the bond between the NOM and iron during the adsorption process.

The column experiments shown in Figure 4-3 consisted of two peristaltic pumps, two glass mini-columns (height of 40 cm and diameter of 1.1 cm). Small particle sized GAC was used to accelerate the kinetics. The design parameters of the GAC mini-column (flowrate, GAC particle size, and depth) satisfied the criteria to decrease the iron breakthrough time and to avoid any wall effect (column diameter to GAC particle median diameter ratio equal to 69). The GAC column was packed with 7 g of 80×100 mesh size, Calgon F-400 (Bituminous coal) activated carbon. The carbon depth inside the column was 13 cm, providing an EBCT of approximately 1.2 minutes and a hydraulic loading rate of 6.3 m/hr (corresponding to a flowrate of 10 mL/min). To minimize iron oxidation in these experiments and maintain anaerobic raw water conditions, the mini-column system was operated using water from one of Vars' raw groundwater pumps. Because of the particulars of the piping and operational constraints, it is difficult to have a continuous supply of raw water for long periods of time. The small EBCT of the mini-column (EBCT = 1.2min) was chosen to limit the length of the run to approximately one week. However, the size of the EBCT was not critical since the objective of the tests was to sample the NOM-iron complexes removal at different points along the iron breakthrough and not to use it for scale-up. The effluent from the GAC was collected regularly and its iron (both ferrous and total iron) concentrations were measured. Upon reaching one of the chosen points on the iron breakthrough curve, the NOM-iron complexation in the GAC effluent was quantified by passing the GAC column effluent through a CHELEX-100 column. The CHELEX-100 column was filled with 150 mg of the resin and the hydraulic loading rate supplied to the column was maintained at 3.2 m/hr (flowrate of 5 mL/min). The CHELEX-100 effluent was tested for TOC, ferrous and total iron.

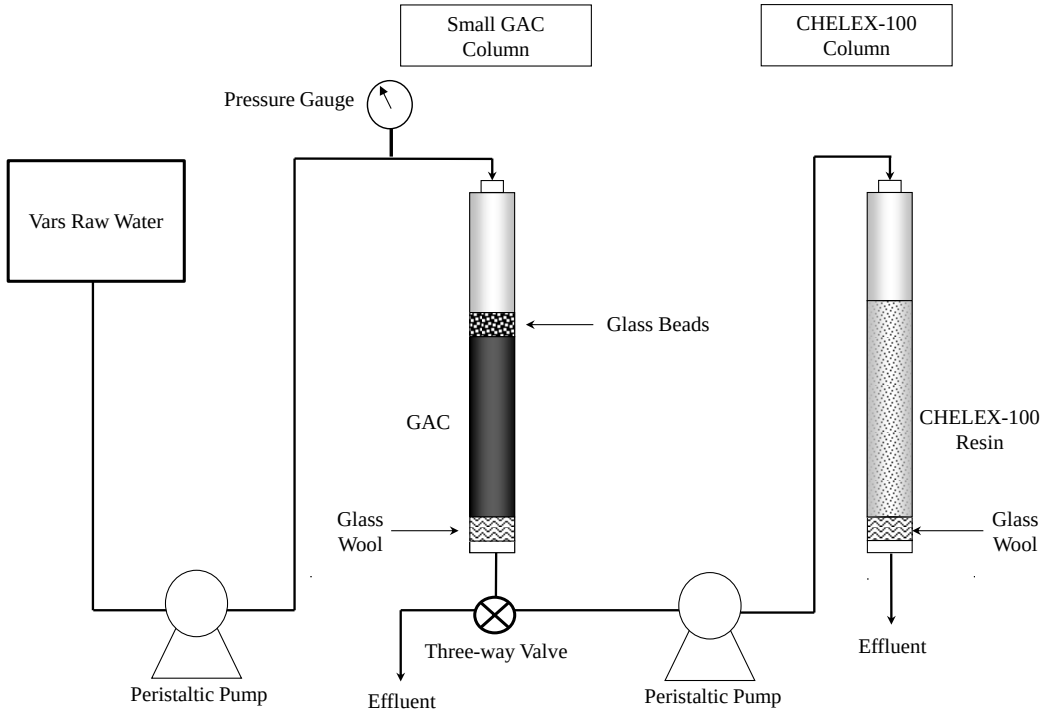

Figure 4-3: Setup of the mini-column experiment

4.4 Results and Discussion

4.4.1 Water Quality Characteristics

The quality of Vars groundwater was characterized during two visits in the winter of 2008 (January 10th and February 14th, 2008) and a third visit in the spring of the same year (April 25th, 2008). Table 4-2 summarizes the characteristics on one of the three visits (February 14th, 2008); the results obtained from all the visits were very similar. The iron concentrations from the two wells were slightly different, which was somewhat surprising given that the two wells have the same depth and are about 30 meters apart. However, the TOC concentration of Vars groundwater was approximately 3.9 mg/L, which is relatively high for a groundwater. This is possibly because the well is adjacent to a wetland. According to the results of the temperature, pH and redox potential values obtained from the preliminary analysis of Vars groundwater and the values on the potential-pH diagram of iron (known as Pourbaix diagram) presented by Brookins (1988), the iron present in this groundwater falls

around the boundary line between the soluble divalent ferrous iron Fe (II) and the precipitate ferric hydroxide $Fe(OH)_{3(s)}$. However, the analysis of ferrous iron in the groundwater from the three preliminary visits concluded that most of the iron in Vars groundwater was in the form of Fe (II). Vars groundwater has a relatively steady temperature of 8 - 9°C. The water from both wells had an average value of 13 color units with the values not changing over a span of the three visits to Vars. The SUVA values found from the three visits were in the range of 2.01 and 2.02 L/mg.m for both wells 1 and 2. According to Edzwald and Tobiason (1999), for raw waters with SUVA ≤ 2 L/mg.m, NOM is normally dominated by mostly low molecular weight and substances with low hydrophobicity. Thus, much of the organic content of Vars well water appears to be hydrophilic in nature. Such a hypothesis would be tested later using XAD-8 and ultrafiltration fractionation.

Table 4-2: Characteristics of Vars groundwater (February 14th, 2008)

Parameters		**Well # 1**	**Well # 2**
pH		7.5	7.6
Eh	(Volts)	0.21	0.21
pe		3.6	3.6
Temperature	(°C)	8.5	8.7
Turbidity	(N.T.U)	0.22	0.23
Total Alkalinity	mg/L (as CaCO3)	218	196
Total Hardness	mg/L (as CaCO3)	231	204
Total Fe	(mg/L)	1.07	1.37
Fe (II)	(mg/L)	1.04	1.36
Fe (III)	(mg/L)	0.03	0.01
TOC	(mg C/L)	3.96	3.87
UV_{254}	(cm^{-1})	0.08	0.08
SUVA	(L/mg.m)	2.02	2.01

4.4.2 Identification of Organically-bound Iron using CHELEX-100

As shown in Figure 4-4, the CHELEX-100 fractionations showed that the percentage of the organically-bound iron in Vars raw water was 37%. The same experiment was repeated in the spring of 2008 (April 25th, 2008) and the percentage of the organically-bound iron was found to be 32% for well #2. The TOC of the CHELEX-100 column effluent was measured throughout the time of the experiments. As expected there were no changes in the concentrations of the groundwater TOC levels after passing through the column indicating that none of the organics were removed by the CHELEX-100 resin. For the groundwater samples, the percentage of free iron removal started to decrease after 50 minutes indicating the decreasing ability of the resins to hold more of the free iron. Based on these results, only samples of the water passing through the columns that were collected during the first 30 minutes of the experiment were used in the ultrafiltration fractionation in order to identify which NOM fractions were bound to the iron.

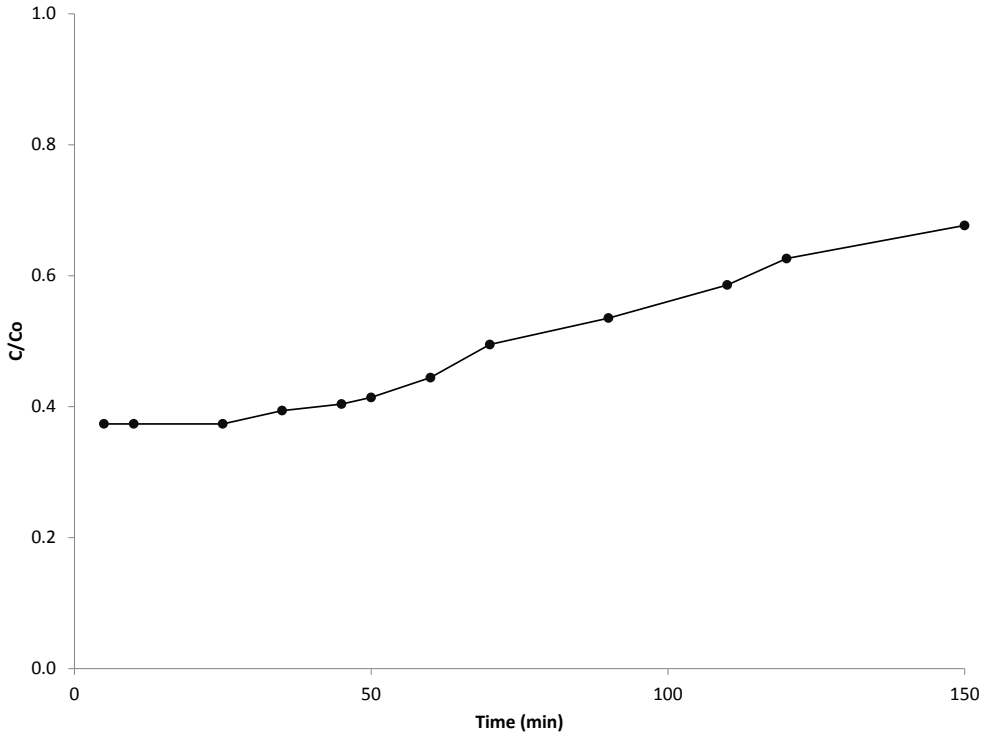

Figure 4-4: Iron concentration of Vars groundwater passing through CHELEX-100 column (mass of CHELEX-100 used = 150 mg, flowrate = 5 mL/min)

The organically-bound iron found in the groundwater collected from the CHELEX-100 column effluent was fractionated using the ultrafiltration fractionation method in order to identify which NOM fractions were bound to the iron. Figure 4-5 shows the results of the UF fractionation of CHELEX-100 filtered Vars groundwater which contains both Fe-NOM complexes as well as uncomplexed NOM. Samples collected from each molecular weight cut-off ultrafiltration were analyzed for TOC and Total Iron. The results presented in Figure 4-5 illustrate that most of the (organically-bound) iron was in NOM fractions that are larger than 5-kDal, indicating that only large molecular weight fractions of NOM were capable of forming complexes with the iron present in Vars groundwater. This coincides with the findings of Gu *et al.* (1995), who found that the NOM bound with iron was predominantly a high molecular weight fraction that is hydrophobic in nature.

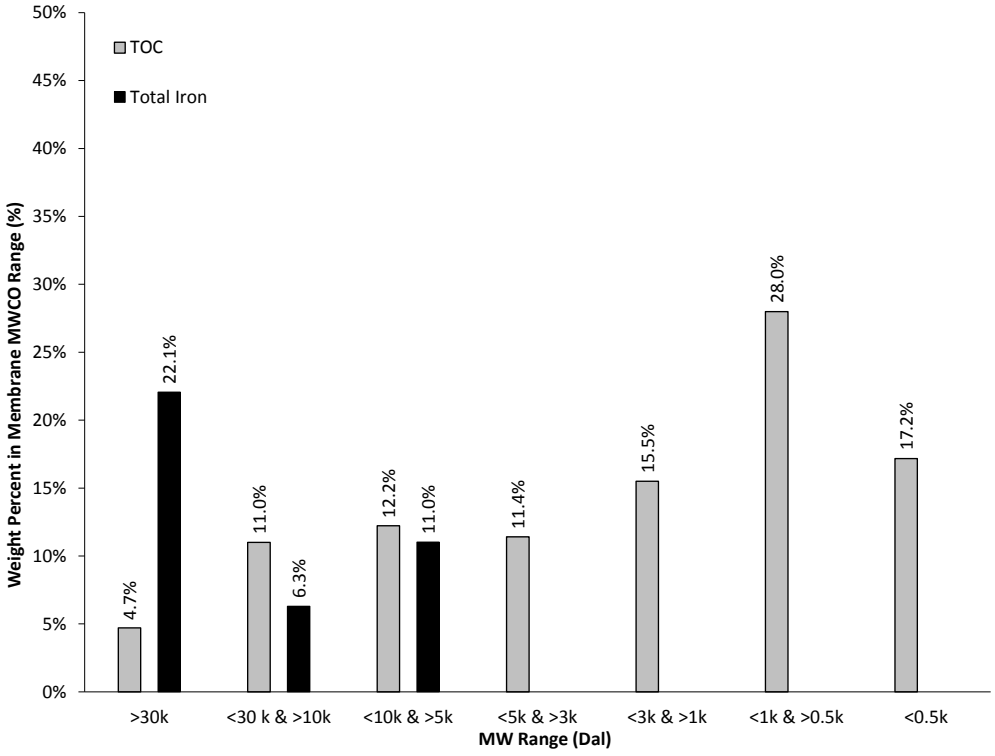

Figure 4-5: UF fractionation of the complexed iron in Vars groundwater passing through the CHELEX-100 column

4.4.3 Identification of Complexed Organics through XAD-8 Isolation

The XAD-8 fractionation was conducted on water samples collected on three different sampling days. The hydrophilic NOM in the Vars groundwater was found to be 75%, 73%, and 78% for the samples collected on January, February and April 2008, respectively. This signifies that less than 30% of the NOM was hydrophobic (including humic and fulvic acids). Such a finding confirms the SUVA results of the preliminary analysis of Vars groundwater, which revealed that NOM is dominated by mostly low molecular weight and substances with low hydrophobicity. This is consistent with the findings of Thurman (1985), who found that different deep groundwaters contained 12-33% hydrophobic (humic and fulvic) acids. Thurman (1985) hypothesized that the long residence time of natural organic matter in groundwater causes the hydrophobic fractions to be either adsorbed onto the aquifer solids or degraded by bacteria into simpler organic acids. The hydrophobic fractions were found to have the capability of forming soluble complexes with inorganic species, such as iron, through the phenolic and carboxylic functional groups (Stevenson, 1982; Christman *et al.,* 1989; Perdue, 1985; Gjessing, 1976). Accordingly, the maximum amount of NOM that could be complexed with iron is 30% which represents the hydrophobic fraction of Vars groundwater.

4.4.4 Mini-column Experiment

Mini-column experiments were conducted to investigate the potential relationship between NOM-iron complexes and GAC column performance, particularly the chromatographic displacement of iron. Figure 4-6 shows the breakthrough of both NOM and iron represented by the left and right y-axes respectively. The TOC of the influent ranged between 4.23 and 4.74 mg/L and the iron ranged from 0.95 to 1.10 mg/L. The column experiment lasted for 8 days. At the end of the breakthrough, the iron in the effluent was 92% of the influent whereas the TOC was 60%.

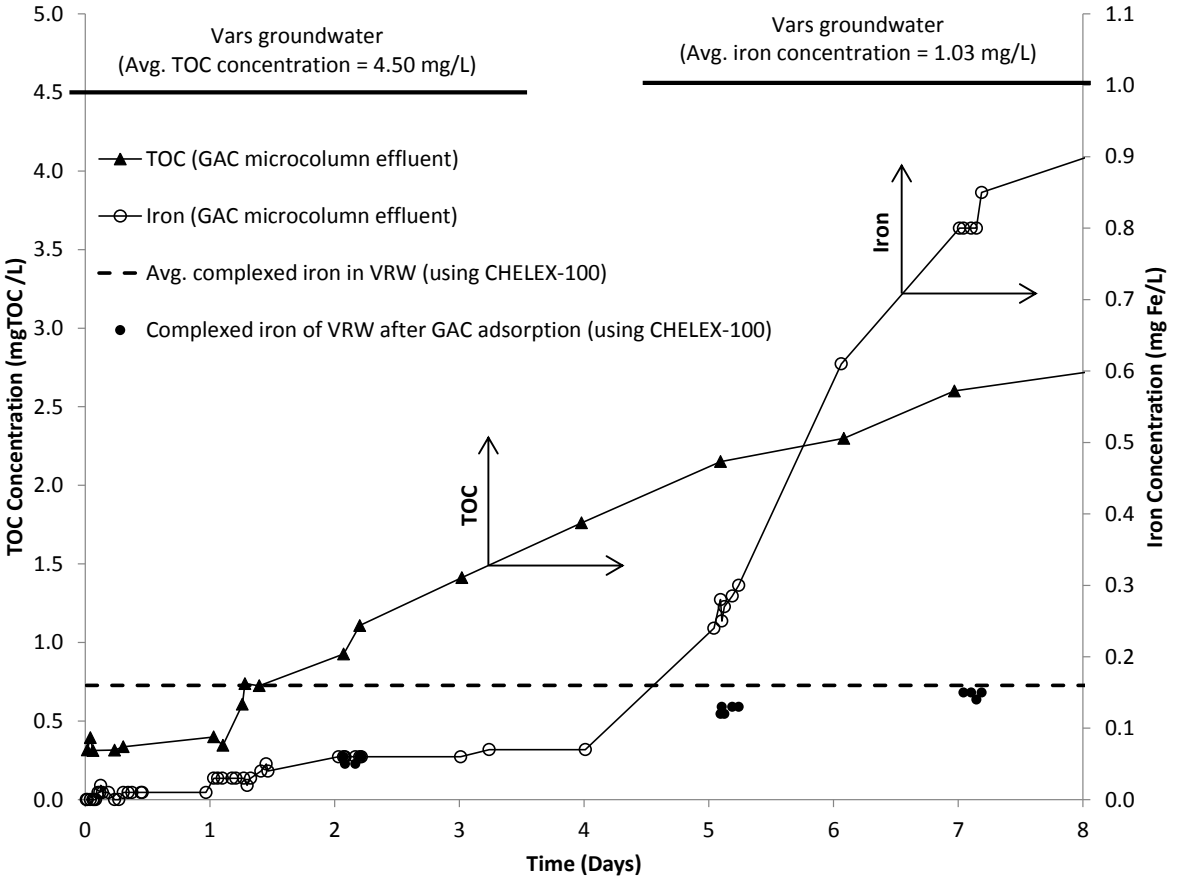

Figure 4-6: Adsorption results of Vars groundwater using mini-columns

The quantification of the NOM-iron complex removals was carried out on days 2, 5 and 7 on the breakthrough curve shown in Figure 4-6**.** These times represent sampling before the iron breakthrough (day 2), early in the iron breakthrough (day 5), and near exhaustion (day 7). The dashed line in the figure represents the average value of 15% (± 2%) for the complexed iron in the raw water based on multiple samplings. The results of the first two samplings (before the breakthrough and early in the breakthrough) indicated that complexed iron was either adsorbed into the activated carbon or split from NOM, and both components were adsorbed separately. The results from the last sampling on the 7th day show that complexed iron was neither adsorbed nor split from the NOM since the concentrations of complexed iron in the raw water and the GAC effluent were almost the same. Such a finding indicates that chromatographic displacement of iron from the GAC observed at Vars was not related to NOM-iron complexes. Another potential reason for the chromatographic displacement of

iron could be the competitive adsorption between iron and NOM that forces the iron to be desorbed from the GAC adsorbing sites. Such a hypothesis will be studied in another paper investigating the adsorption behavior of Vars groundwater.

The mini-column was operated for few additional days after reaching the iron's point of exhaustion (after the 8^{th} day) but the chromatographic displacement of iron was not observed. Instead, there was a clear visible accumulation of iron within the top section of the mini-column, which impacted its operation and the test had to be terminated. Given the smaller GAC granule sizes (80×100 mesh size), this phenomenon of iron accumulation is more significant in a mini-column test than in full-scale facilities. This also indicates that the mini-column tests are not a good tool for simulating adsorption of iron-laden waters.

The difference between the values of 15% iron complexed with NOM and the 32 – 37% measured during the 2008 characterization stage was due to the fact that the mini-column experiment was performed three years later (September, 2011). This was nonetheless rather surprising given that in these three years the iron concentrations, the NOM concentrations, and the hydrophilic fraction of the NOM remained fairly constant.

4.4.5 Impact of Greensand Treatment

As expected, the greensand pretreatment (permanganate oxidation) was successful in removing the iron from the groundwater. The dark bars in Figure 4-7 show that the permanganate treatment was effective in oxidizing the ferrous iron in the well groundwater into ferric iron. The clear bars show that the greensand filter removed the oxidized iron to levels below the 0.3 mg/L drinking water standard (WHO, 2004).

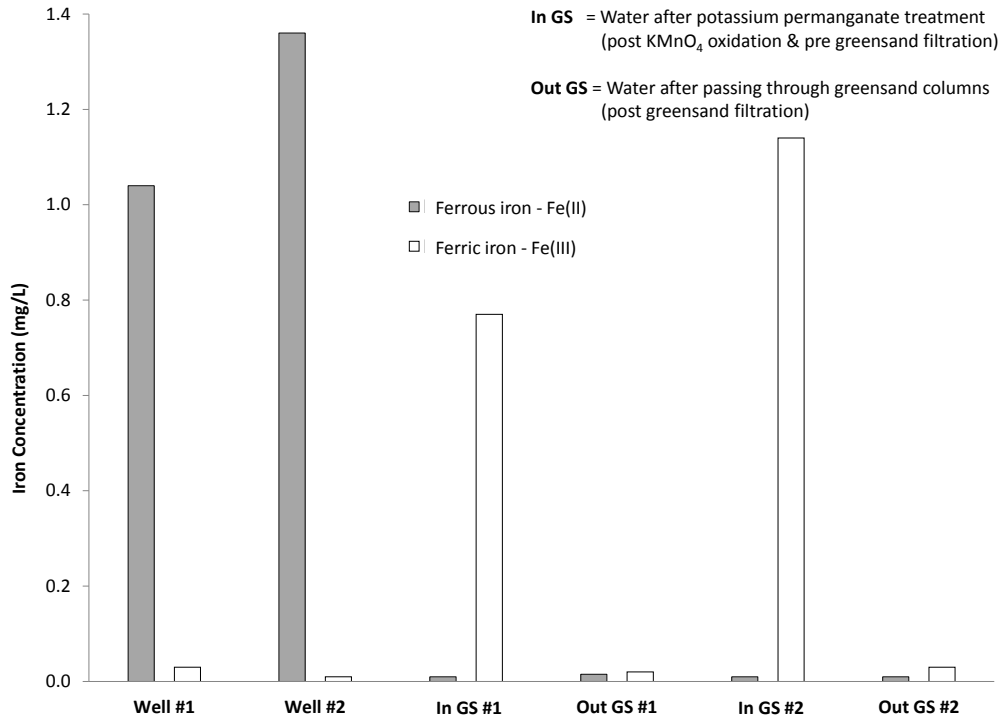

Figure 4-7: Iron concentrations at different locations along the greensand pretreatment (February 14th, 2008)

The TOC concentrations indicate that the greensand treatment removed only 9 to 13 % of the NOM (Table 4-3). This is consistent with the work of Li *et al.* (2003) who found negligible TOC removals by greensand treatment of a central Illinois groundwater (TOC = 2.17 mg/L). They hypothesized that the potassium permanganate oxidation reaction of the organically-bound iron would form iron-NOM particulate matter that would be removed consequently through greensand filtration.

Table 4-3: TOC removal due to greensand pretreatment

	TOC Removal (%)	
	Greensand# 1	**Greensand# 2**
1st Visit (January 10th, 2008)	11.93	10.61
2nd Visit (February 14th, 2008)	10.33	11.79
3rd Visit (April 25th, 2008)	12.85	9.05

The results of the UF fractionation of Vars groundwater and the greensand treated water (Figure 4-8) indicate that most of the NOM fractions that were removed by the greensand pretreatment were with a molecular weight of less than 1 kDal. Another effect of the $KMnO_4$ treatment on the NOM was the agglomeration of certain fractions (between 1 and 5 kDal) after the removal of most of the iron present in Vars groundwater. Since the greensand filter removed all of the iron, the NOM-iron complexes must have been either broken by the potassium permanganate oxidation or were adsorbed by the greensand filter. Unfortunately, due to the high permanganate concentrations in the greensand column influent, it was impossible to determine the NOM complexed iron at this point.

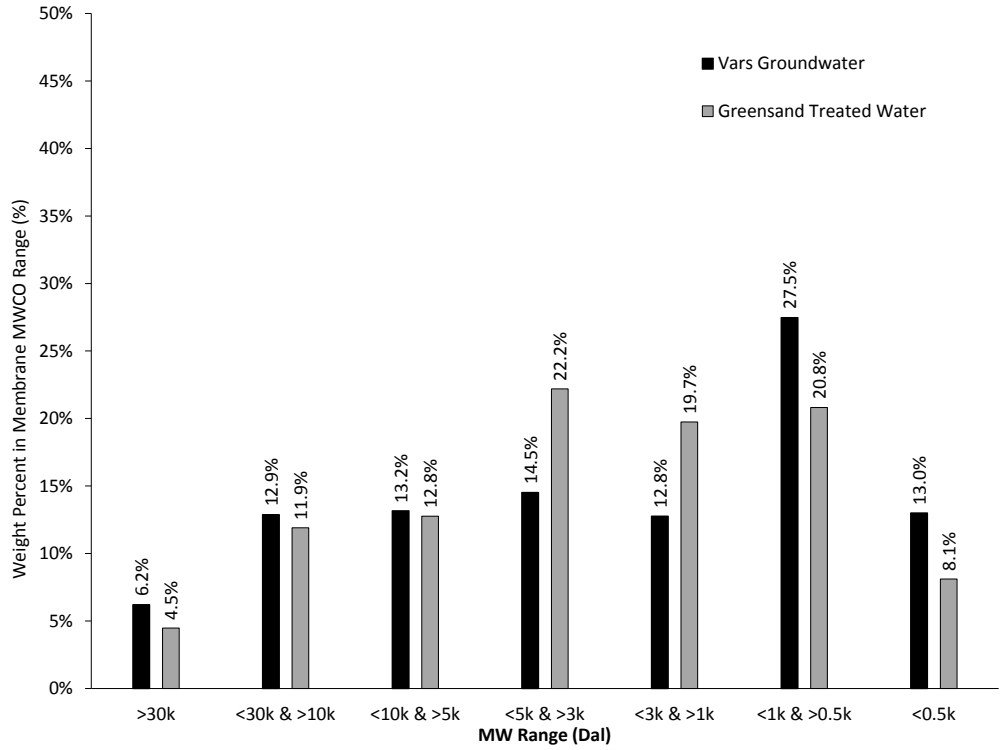

Figure 4-8: UF fractionation of NOM in Vars groundwater and the greensand treated water (February 14th, 2008)

4.5 Conclusions

Based on the results obtained from the XAD-8 fractionation, it was found that 30% of the NOM in Vars groundwater in both wells were hydrophobic with the capability of forming complexes with the iron present in the groundwater. During the initial sampling campaign,

between 32 and 37% of the iron in Vars groundwaters was organically-bound to NOM and the rest was in the form of free iron. The UF fractionation of the CHELEX-100 filtered water showed that most of the organically bound iron was attached to the NOM fractions larger than 5 kDal.

The mini-column experiment using GAC was used to test for the possibility of NOM-iron complexes to be dissociated due to adsorption causing the observed chromatographic displacement of iron. However, the percentage of the NOM-iron complexes from the GAC mini-column at the point of near exhaustion on the iron breakthrough was found to be almost the same as the percentage of the raw water. Such a finding indicated that NOM-iron complexes were not the cause of the chromatographic displacement of iron observed in Vars. Also, the results of the mini-column experiment showed that GAC adsorption did not have the capability of dissociating the complexation bond between NOM and iron at the point of near exhaustion. Based on these findings, another potential cause of the chromatographic displacement of iron was suggested. The competitive adsorption between NOM and iron could cause the iron to be desorbed from the GAC adsorbing sites.

Greensand treatment is generally considered to only remove the inorganic compounds (i.e., iron). However, in this application it also removed between 9 to 13% of the NOM. In addition, the UF fractionation showed that the NOM fractions that were removed by the greensand treatment process were with a molecular weight of less than 1 kDal. The full removal of iron during the greensand treatment indicates that either NOM-iron complexes were broken by the potassium permanganate oxidation or were adsorbed by the greensand filter.

CHAPTER 5 ADSORPTION ISOTHERMS OF IRON AND NATURAL ORGANIC MATTER AS SINGLE COMPONENTS

5.1 Introduction

One of the hypotheses of this dissertation is that competitive adsorption of NOM (i.e., a mixture of organic compounds characterized by its TOC content) and iron in Vars raw water on activated carbon can be described by existing mathematical models. Competitive or multicomponent isotherm modeling is generally based on the isotherms of each individual solute in distilled water (i.e., as a single solute), as well as the multisolute isotherm data. This chapter describes the modeling of the single solute isotherms of NOM and iron.

5.2 NOM Isotherms

NOM is widely recognized to be a complex mixture of organic matter with different characteristics. In spite of this, for convenience and simplicity, many have attempted to model NOM adsorption as a single component (Brown *et al.*, 1999; Gu *et al.*, 1995; Hansen *et al.*, 1990; Summers, 1986; Summers and Roberts, 1988; Harrington and DiGiano, 1989; Karanfil *et al.*, 1999). In some situations this assumption has worked satisfactorily, and in others it has not. The most common simulations of NOM as a multi-solute mixture have been conducted using pseudocomponent IAST modeling when modeling the competitive adsorption of NOM with other solutes (Li *et al.*, 2005; Qi and Schideman, 2008; Simpson and Narbaitz, 1997; Kilduff and Wigton, 1999; Najm *et al.*, 1990; Crittenden *et al.*, 1985; Knappe *et al.*, 1998; Andrews, 1990). This approach has been fairly successful in simulating the adsorption of the other competing solutes but not the NOM. Accordingly, modeling the NOM in this thesis will be initially considered as a single solute and then, if necessary, it will be modeled as a multi-solute mixture. Adsorption of Vars groundwater consists of the competitive adsorption of the principal solutes within it (i.e., NOM and ferrous iron). As discussed above, to model competitive adsorption, many models require the isotherms for each individual solute. Unfortunately, it was impossible to isolate the NOM present in Vars raw water from the other components and particularly because a fraction of the NOM that

was found to be complexed with iron. As the greensand treatment used in the Vars water treatment system removes most of the iron in the groundwater and only 9 – 13% of the NOM (see Chapter 4), the greensand treatment effluent was considered as a candidate to represent the single solute isotherm of NOM. Figure 5-1 shows the NOM adsorption isotherms of Vars raw water and greensand treated water. The figure shows the data of NOM isotherm results accompanied with their Freundlich isotherms. Like all isotherms presented in this chapter, the horizontal axis represents the equilibrium liquid phase concentration (C_e) and the vertical axis presents the equilibrium solid phase concentrations (q_e). TOC was used to quantify the NOM and the organic carbon was assumed to account for 50% of the NOM's molecular weight. The solid and dashed lines are the Freundlich isotherm model simulations of the Vars raw water and the greensand treated water isotherms, respectively. They were generated by the non-linear regression of the isotherm data performed using the statistical software GraphPad Prism 5.03 (GraphPad Software, San Diego, CA, USA). The regression was performed by minimizing the sum of squares of the difference between the isotherm data and the Freundlich isotherm model simulations. This software also calculates the 95% confidence intervals (95% CI) for each regressed Freundlich model parameter (i.e., K_F and n_F). The concave upward shape of the NOM isotherms (Figure 5-1) indicates that some of the NOM is more strongly adsorbable than the rest. The strongly adsorbable NOM was removed with small doses of the GAC (i.e., the higher values of C_e) and yielded large values of q_e which results in a substantial increase in the isotherm slope. In contrast, the more weakly adsorbable NOM was removed with larger GAC doses (i.e., smaller values of C_e) and yielded relatively low values of q_e. Many studies have obtained the same shape of the NOM isotherms shown in Figure 5-1 (Karanfil *et al.*, 1999; Kilduff *et al.*, 1996; Li *et al.*, 2002; Summers and Roberts, 1988).

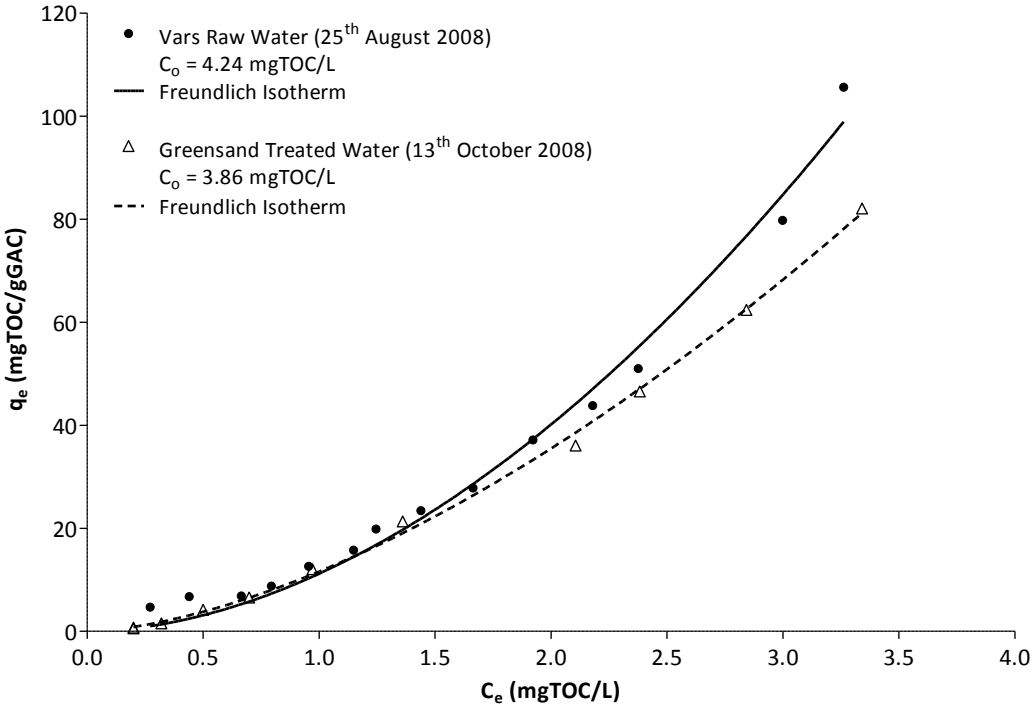

Figure 5-1: NOM adsorption isotherms of Vars raw water and greensand treated water (F-400 GAC 40×50 mesh size)

Based on the lack of competing compounds in the greensand treated water, the NOM adsorption capacity of the post-greensand treatment was expected to be slightly higher than that of the Vars raw water. However, the isotherm experiments for the greensand treated water showed a slight reduction in the NOM adsorption capacity compared to that of Vars raw water for liquid phase concentrations greater than 2 mg/L. It appears that the difference is attributed to the removal of some of the most adsorbing NOM by the greensand treatment. Also, this reduction may be associated with the fact that the water samples were collected on different dates (i.e., August 25th, 2008 and October 13th, 2008). Given that groundwater quality is generally constant, the differences between these two days are not expected to be due to changes in the groundwater quality. It seems more likely that the differences in the isotherms were caused by the greensand treatment.

To eliminate the possibility that the differences in the isotherms was caused by changes in the groundwater quality, the isotherm experiments of Vars raw water and the greensand treated water were repeated using water samples collected on the same day. The results of

these isotherm experiments are shown in Figure 5-2. The data shows very similar behavior of the isotherms for both waters over the entire concentration range, including the higher range in which the earlier isotherms had shown some differences. In spite of this similar behavior between the two isotherms in Figure 5-2, the adsorption capacity of the greensand treated water isotherm was still slightly less than that of the Vars raw water. It is hypothesized that the slight decrease in adsorption capacity observed between Vars raw water and the greensand treated water was due to the higher adsorbability of the NOM fraction (9 – 13%) removed by the greensand filter.

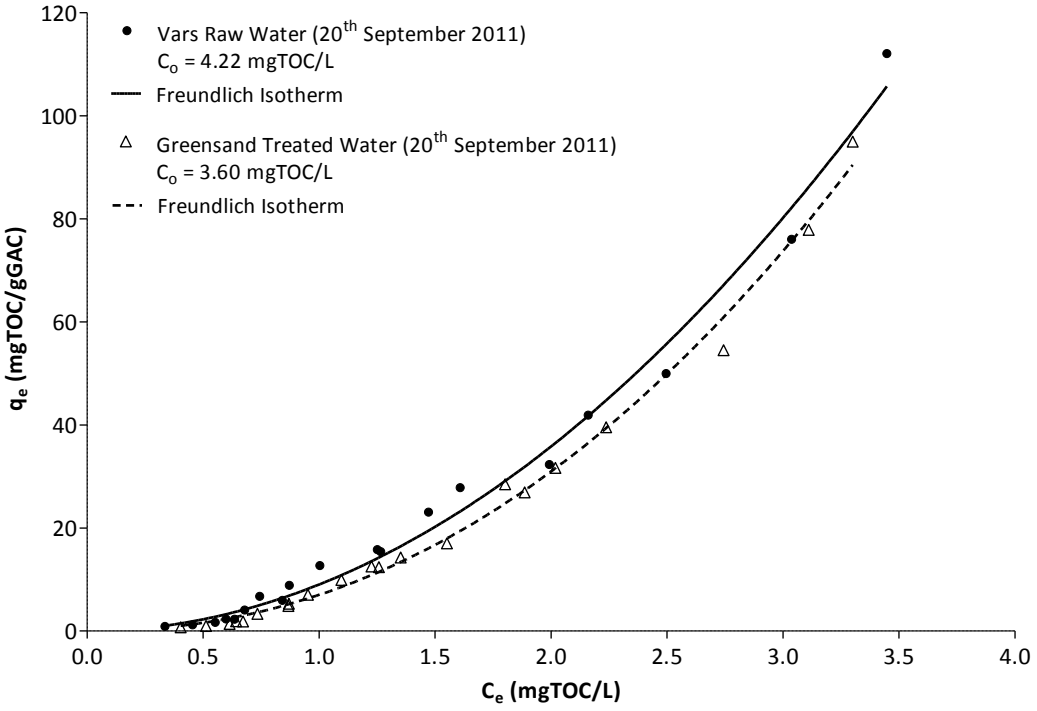

Figure 5-2: NOM adsorption isotherms of Vars raw water and greensand treated water (F-400 GAC 40×50 mesh size) performed on samples collected on the same day

Comparing the Freundlich isotherm fitted parameters of Vars raw water performed on different days, as shown in Table 5-1, indicates that the data for the two Vars raw water adsorption isotherms overlap. The Freundlich parameters values of the Vars raw water performed on September 20th, 2011 (K_F = 9.05 (mg/g)·(L/mg)^n and n_F = 1.99) fall within the 95% confidence intervals of the same experiment performed on August 25th, 2008 (shown as shaded entries in the last column of Table 5-1). Thus, statistically, one cannot differentiate

one of the isotherms from the other; it appears that they are the same. Also, the characteristics of Vars raw water were found to be the same for the two dates (summarized in Appendix A). Such a finding is consistent with the fact that groundwater quality is not expected to change significantly with time. The differences between the isotherms data of the greensand treated water performed on different dates suggests that the greensand treatment process was performing differently when the two samples were collected. Such differences caused a slight change in the TOC (from 3.86 mgTOC/L on October 13th, 2008 to 3.60 mgTOC/L on September 20th, 2011), possibly small changes in the NOM characteristics, and consequently caused the difference in the isotherm for the greensand treated water samples collected at different times.

Table 5-1: Fitted parameter of Freundlich isotherm models used to model the NOM in Vars raw water and greensand treated water on different days

Water Sampling Location	Day of the Isotherm Experiment	NOM Initial Concentration (mgTOC/L)	Parameter	Parameter Value	95% Confidence Interval
Vars Raw Water	August 25th, 2008	4.24	K_F (mg/g)·(L/mg)^n	11.18	9.03 – 13.34
			n_F	1.84	1.66 – 2.03
	September 20th, 2011	4.22	K_F (mg/g)·(L/mg)^n	9.05	7.44 – 10.63
			n_F	1.99	1.82 – 2.15
Greensand Treated Water	October 13th, 2008	3.86	K_F (mg/g)·(L/mg)^n	11.59	10.42 – 12.77
			n_F	1.61	1.52 – 1.71
	September 20th, 2011	3.60	K_F (mg/g)·(L/mg)^n	7.02	6.10 – 7.94
			n_F	2.14	2.02 – 2.26

Kilduff *et al.* (1996) studied the GAC adsorption of commercially available humic and fulvic acids and found that smaller molecular size humic and fulvic acids were preferentially adsorbed. Accordingly, further investigations of the NOM's characteristics before and after

greensand treatment was carried out. Figure 5-3 shows the results of the ultrafiltration fractionation of Vars raw water and the greensand treated water. The results show that 11% of NOM fraction with a molecular size of less than 1 kDa was removed by the greensand treatment (i.e., 6% difference for <1kDa – >0.5 kDa fractions and 5% difference for <0.5 kDa fractions). These fractions are presumed to be strongly absorbable onto GAC and their removal by the greensand treatment could cause the slight reduction in the adsorption capacity that was observed in the isotherm results shown in Figure 5-2.

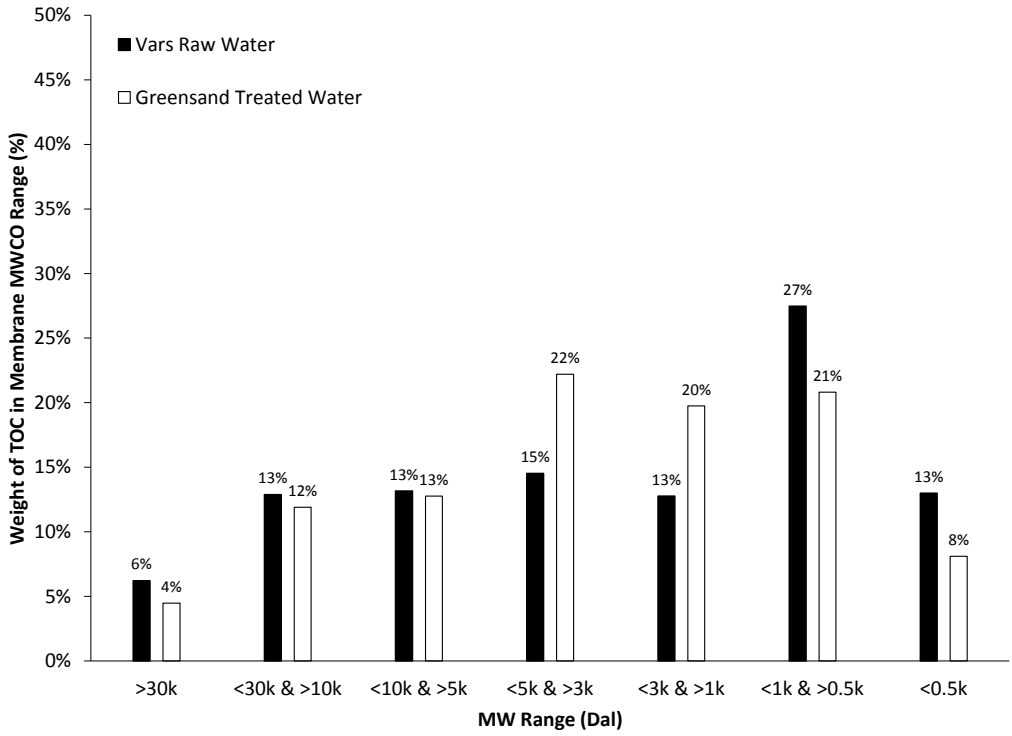

Figure 5-3: Ultrafiltration fractionation of NOM in Vars raw water and greensand treated water (February 14th, 2008)

Although single solute isotherms are expected to be higher than competitive isotherms for the same solute, it was decided to use the Vars raw water NOM isotherm as the NOM single solute isotherm for the competitive adsorption modeling. The decision was based on the fact that Freundlich isotherms of NOM obtained from Vars raw water and greensand treated water, that does not contain competing iron, were statistically the same. Therefore, the presence of iron did not significantly decrease the adsorption capacity of NOM in Vars raw water. In a study by Narbaitz and Benedek (1994) on the competitive adsorption isotherms

between river water NOM and 1,1,2-trichloroethane (TCEA), they found that the adsorption capacity of background organics was almost unaffected by the presence of TCEA.

5.2.1 NOM Isotherm Modeling

In the attempt to model the single adsorption of NOM in Vars raw water, the NOM isotherm data was initially modeled using the most common isotherm models applied in solid/liquid systems such as Freundlich isotherm model. Additionally, the Summers-Roberts model and a modified form of their model, the Qi-Schideman model, were tested to check if these newer models would improve the simulations. The parameters of the isotherm models were obtained by nonlinear regression of the isotherm data. The nonlinear regression analysis was performed by minimizing the squares of the difference between the isotherm data and the isotherm model simulations using the statistical software GraphPad Prism 5.03. This software also calculates the 95% confidence intervals (95% CI) for simulations and the 95% CI for each regressed parameter of the isotherm model. As a method to assess the fit of the models, the calculated values of the equilibrium solid phase concentrations (q_e) were compared with the isotherm experimental data points visually, as well as by computing the absolute average percentage errors (AAPE) and coefficient of variation of the root mean square error CV(RMSE) using Microsoft Excel according to the following equations:

$$\text{AAPE}(\%)=\frac{100}{N}\sum_{i=1}^{N}\frac{\left|P_i-O_i\right|}{O_i} \tag{5-1}$$

$$\text{CV(RMSE)}\ (\%)=\frac{100}{\sum_{i=1}^{N}O_i}\sqrt{\frac{1}{\text{DOF}}\sum_{i=1}^{N}(P_i-O_i)^2} \tag{5-2}$$

Where: N is the number of observations; P_i = predicted value; O_i= experimental value; DOF = degree of freedom (DOF = N – number of parameters to be regressed). The coefficient of variation of the root mean squared error, CV(RMSE) (%) is essentially the root mean squared error divided by the measured mean of the data. These criteria were chosen because it is often convenient to report a non-dimensional result (Draper and Smith, 1998). The

CV(RMSE) was used instead of the sum of squares because it incorporates the number of regressed parameters within the model (through the degrees of freedom term); thus, it permits a more equitable comparison between models with different numbers of parameters. CV(RMSE) allows one to determine how well a model fits the data; the lower the CV(RMSE), the better the model fit. AAPE was used because it gives a direct assessment on the average error, which provides a more tangible assessment of the quality of the fit.

5.2.1.1 Freundlich Model

The Freundlich model showed a good fit for the Vars raw water NOM isotherm data (Figure 5-4). However, the model underpredicted the isotherm points with liquid phase concentrations less than 0.5 mgTOC/L. The CV(RMSE) and AAPE values (Table 5-2), of 11.13 and 18.7% respectively, also show that the Freundlich model describes the NOM isotherm data well. Another indication of the quality of fit is the tightness of the 95% confidence intervals for each regressed parameters. Table 5-2 shows that the regressed values of K_F = 11.18 $(mg/g)\cdot(L/mg)^n$ and n_F = 1.84 have 95% confidence intervals of ±19.3% and 15.5%, respectively. These percentages and the 18.7% AAPE indicate that the fit is relatively good but they also show room for improvement.

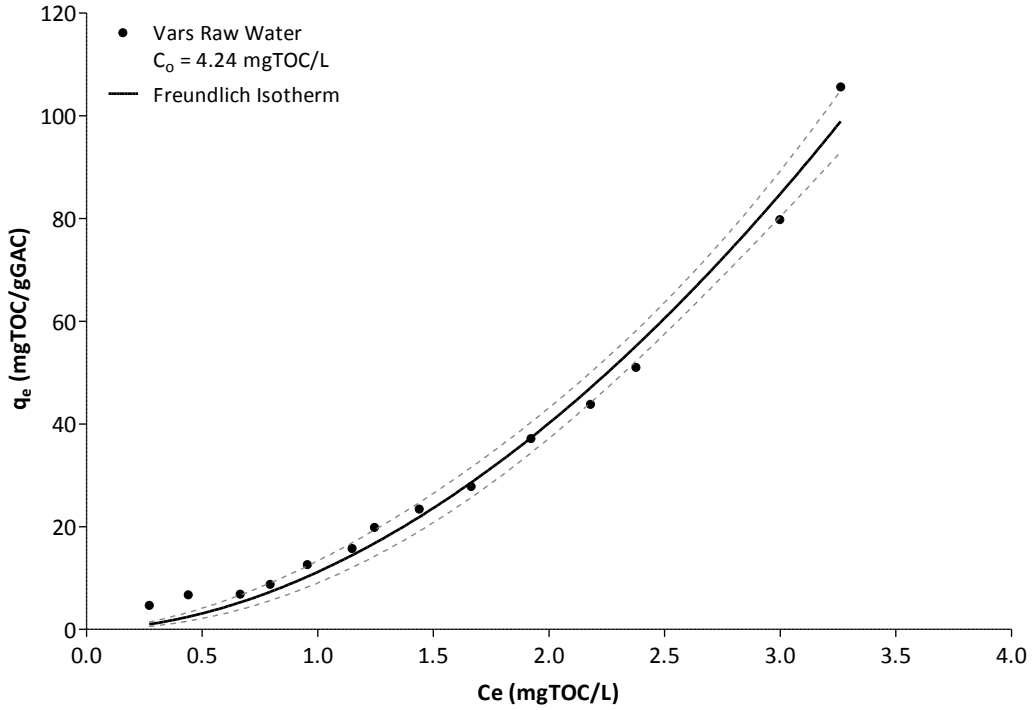

Figure 5-4: Single solute isotherms of NOM in Vars raw water using Freundlich model within 95% confidence interval (F-400 GAC (40×50 mesh size), C_o = 4.24 mg/L, pH = 7.5, Temperature = 25 ^oC)

Table 5-2: Fitted parameter for Freundlich model used to model the NOM in Vars raw water

Model	Parameter	Parameter Value	95% Confidence Interval	Model Fit Indicators	
				CV(RMSE), %	AAPE, %
Freundlich Isotherm	K_F (mg/g)·(L/mg)^n	11.18	9.03 – 13.34	11.3	18.7
	n_F	1.84	1.66 – 2.03		

Number of data points = 14

Number of regressed parameters (Freundlich Model) = 2 (K_F and n_F)

5.2.1.2 Summers-Roberts Model

The Freundlich isotherm model fit of the NOM isotherm is reasonably good but not perfect, specifically in relation to the points of low concentrations (< 0.5 mgTOC/L). Figure 5-5

shows that the Summers-Roberts model yields an excellent simulation of the Vars raw water NOM adsorption isotherm. Table 5-3 summarizes the fitted parameters of the Summers-Roberts model. It is clear that incorporating the GAC doses (M/V) within the Freundlich isotherm has improved the fit compared to the standard Freundlich isotherm. The absolute average percentage errors (AAPE) and coefficient of variation of the root mean square error CV(RMSE) of the Summers-Roberts model were found to be 1.1 and 4.5%, respectively. Also, the regressed values of K_{SR} = 7.65 (mg/g)·(g/mg)^n and n_{SR} = 0.45 have 95% confidence intervals of ± 6.4% and 2.3%, respectively, which is an indication of a very tight fit of the Summers-Roberts model.

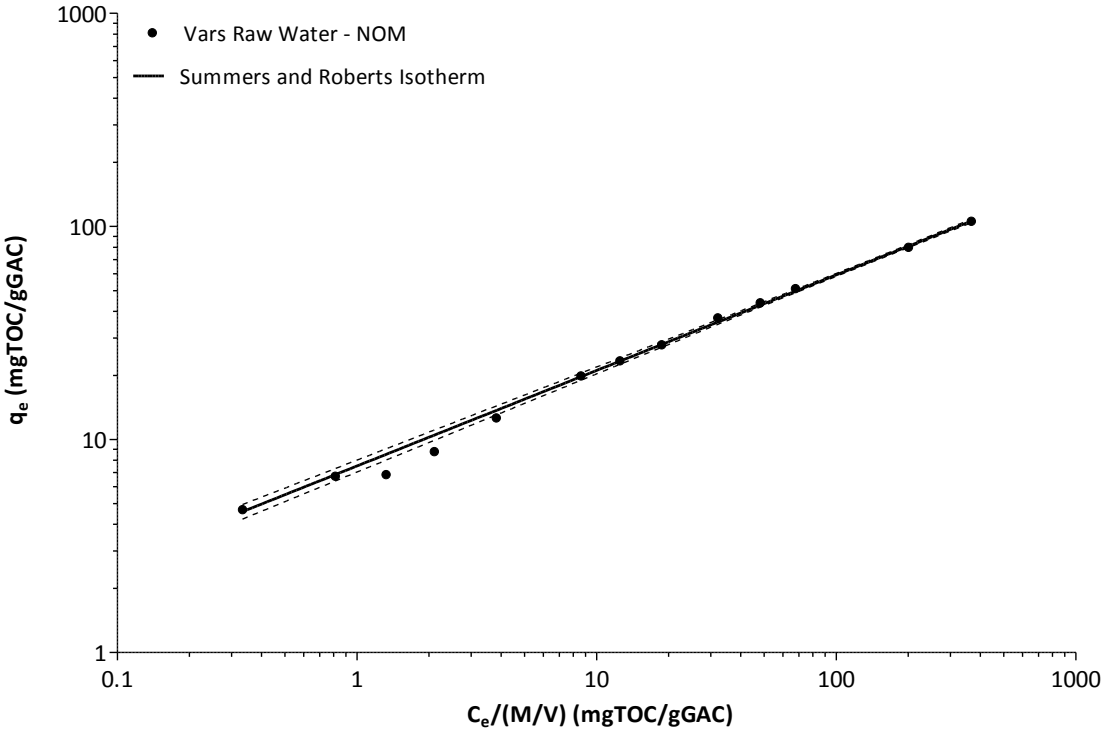

Figure 5-5: Single solute isotherms of NOM in Vars raw water using Summers-Roberts model with 95% confidence interval (F-400 GAC (40×50 mesh size), C_o = 3.99 mg/L, pH = 7.5, Temperature = 25 ^oC)

Table 5-3: Fitted parameter for Summers-Roberts model used to model the NOM in Vars raw water

Model	Parameter	Parameter Value	95% Confidence Interval	Model Fit Indicators	
				CV(RMSE), %	AAPE, %
Summers-Roberts Isotherm	K_{SR} (mg/g)·(g/mg)^n	7.65	7.16 – 8.14	1.1	4.5
	n_{SR}	0.45	0.44 – 0.46		

Number of data points = 14

Number of regressed parameters = 2 (K_{SR} and n_{SR})

5.2.1.3 Qi-Schideman Model

Although, the Summers-Roberts model showed an excellent fit of NOM isotherm data in Vars raw water, the Qi-Schideman model was also tested, as it is a potentially superior model. The three parameters (i.e., K_{QS}, n_{QS} and C_{non}) of the Qi-Schideman model can be determined simultaneously using an incremental search for non-adsorbable NOM concentration (C_{non}) and a linear regression of Log C_e versus Log q_e for the isotherm parameters K_{QS} and n_{QS}. The initial guess for C_{non} is chosen as zero or close to the value obtained from the isotherm experimental data. Since the NOM's non-adsorbable fraction in this study was negligible, the value of C_{non} used in the model was equal to zero. Table 5-4 summarizes the fitted parameters of the Qi-Schideman model as well as the fit indicators. The use of the Qi-Schideman model resulted in a good fit of the NOM in Vars raw water (Figure 5-6). The fit indicators (CV(RMSE) and AAPE) of the model were 9.3% and 10.6%, respectively. Also, the regressed values of K_{QS} = 39.03 (mg/g) and n_{QS} = 0.46 have 95% confidence intervals of ± 10.1% and 4.4%, respectively. However, the Qi-Schideman model does not describe the NOM isotherm data as well as the Summers-Roberts model.

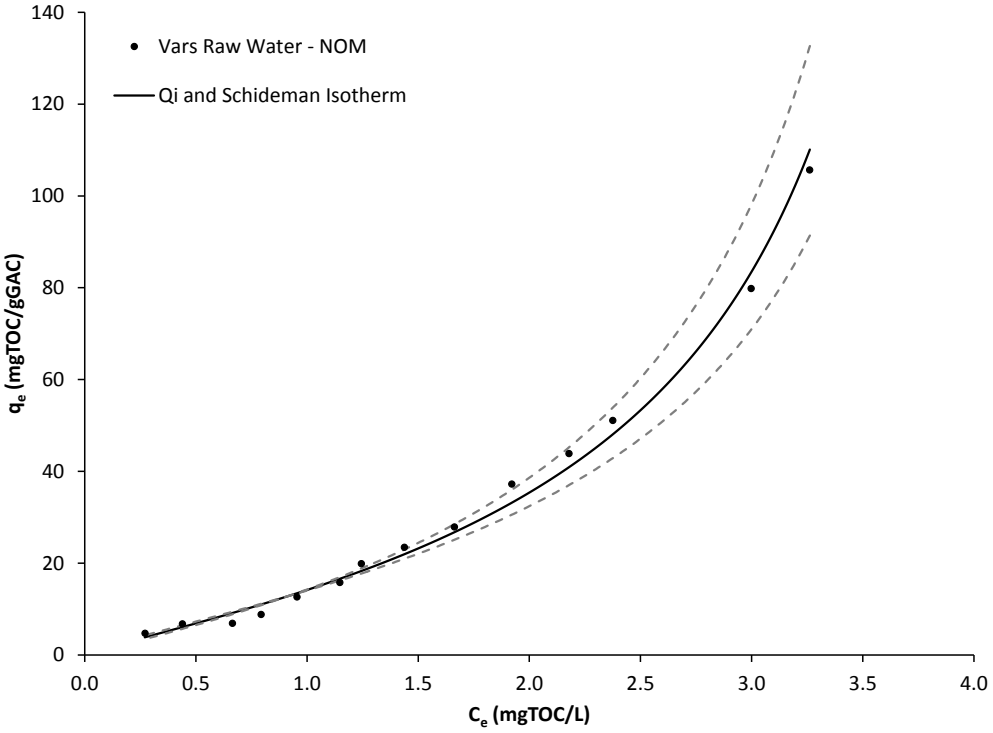

Figure 5-6: Single solute isotherms of NOM in Vars raw water using Qi-Schideman model with 95% confidence interval (F-400 GAC (40×50 mesh size), C_o = 3.99 mg/L, pH = 7.5, Temperature = 25 ^oC)

Table 5-4: Fitted parameter for Qi-Schideman model used to model the NOM in Vars raw water

Model	Parameter	Parameter Value	95% Confidence Interval	Model Fit Indicators	
				CV(RMSE) %	AAPE %
Qi-Schideman Isotherm	C_{non} (mg/L)	0.00	-	9.3	10.6
	K_{QS} (mg/g)	39.03	35.45 – 42.97		
	n_{QS}	0.46	0.44 – 0.48		

Number of data points = 14

Number of regressed parameters = 3 (C_{non}, K_{QS} and n_{QS})

5.2.2 Summary of NOM Modeling

The NOM in Vars raw water was modeled as a single component using the Freundlich, Summers-Roberts, and Qi-Schideman models. The regressed parameters of different models and their fit indicators are summarized in Table 5-5. Based on the summary of the model's fit indicators, it is clear that only the Freundlich, Summers-Roberts, and Qi-Schideman models were capable of modeling the NOM's isotherm data well and the best fit was obtained using the Summers-Roberts model. The NOM isotherm data was also modeled by the Langmuir model (Appendix C). However, the model simulation was rather poor and did not describe the data well. The IAST competitive isotherm models that will be tested in the next chapter were developed based on the Freundlich model. Accordingly, the Freundlich parameter values obtained above will be utilized in these competitive adsorption models. However, the competitive adsorption models that can accommodate the Summers-Roberts model will be modified to do so. Finally, the potential improvement of the modeling of NOM and iron in Vars raw water using these new models will be verified.

Table 5-5: Summary of the fitted parameter and fit indicators of the single isotherm models used to model the NOM in Vars raw water

Model	Parameter	Parameter Value	95% Confidence Interval	Model Fit Indicators	
				CV(RMSE) (%)	AAPE (%)
Freundlich Isotherm	K_F $(mg/g)\cdot(L/mg)^n$	11.18	9.03 – 13.34	11.3	18.7
	n_F	1.84	1.66 – 2.03		
Summers-Roberts Isotherm	K_{SR} $(mg/g)\cdot(g/mg)^n$	7.65	7.16 – 8.14	1.1	4.5
	n_{SR}	0.45	0.44 – 0.46		
Qi-Schideman Isotherm	C_{non} (mg/L)	0.00	-	9.3	10.6
	K_{QS} $(mg/g)\cdot(g/mg)^n$	39.03	35.45 – 42.97		
	n_{QS}	0.46	0.44 – 0.48		

5.3 Iron Isotherms

Many researchers have reported that the kinetics of iron adsorption is relatively fast (Uchida *et al.*, 1999; Mohan and Chander, 2001; Sirichote *et al.*, 2002; Kim, 2004; Onganer and Temur, 1998). Providing sufficient equilibration time is critical to achieving full equilibrium and generating reliable isotherm models. Thus, a kinetics experiment of ferrous iron as a single component (i.e., separate distilled water solutions to which ferrous salt was added) was conducted in order to obtain the equilibrium time needed for the isotherm experiments. Figure 5-7 shows the kinetics of ferrous iron with an initial concentration of 1.5 mg/L and a GAC dose of 0.1 g/L. The empty circles (○) represent the iron concentrations in the control bottles with water samples containing iron but no GAC. The change in iron concentrations of the controls in both experiments represented by the triangles (Δ) indicates that there was some oxidation of ferrous iron despite the precautions that were taken in order to minimize the exposure of iron to oxygen during the preparation of the kinetics experiments. The solid circles (●) represent the total decrease of iron over time due to adsorption and oxidation of ferrous iron. Subtracting the amount of iron oxidized from the total iron decrease data would result in the net decrease of iron due to adsorption. This is represented by the multiplication (X) symbols in Figure 5-7.

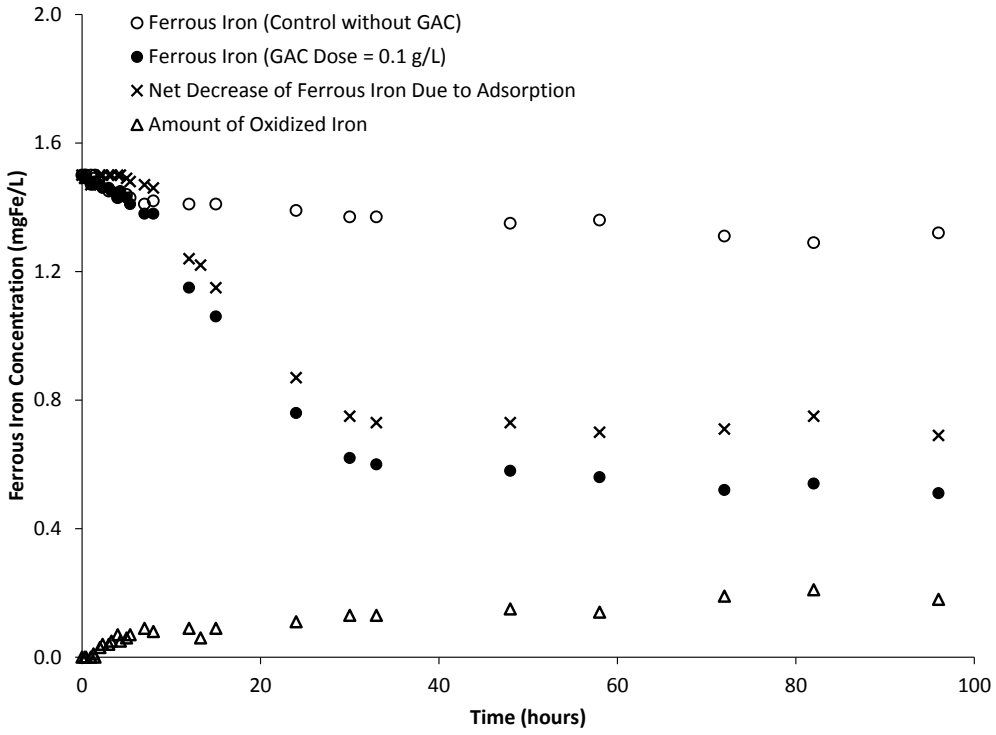

Figure 5-7: Kinetics of ferrous iron (F-400 GAC (40×50 mesh size), C_o = 1.5 mg/L, GAC dose = 0.1 g/L, pH = 6)

Based on the results of the kinetics, an equilibrium time was chosen for the single solute isotherm experiments. The final concentration for ferrous iron in the control bottles at 48 hours was 1.35 mg/L, which indicate that 10% of ferrous iron was oxidized. The value of the equilibrium liquid phase concentration of ferrous iron at 48 hours was 0.73 mg/L, meaning that the calculated solid phase concentration (q_e) of ferrous iron into the GAC was 6.2 mg/gGAC.

5.3.1 Ferrous Iron Isotherm Modeling

The single solute isotherm for the adsorption of ferrous iron was conducted using ferrous iron-distilled water buffered to pH 6. The initial concentration of ferrous iron at the start of the isotherm experiment was 0.50 mg/L; however, there was some visible iron precipitation and the concentration of ferrous iron in the control bottles dropped to 0.41 mg/L. Such results indicate that 18% of ferrous iron was oxidized during the isotherm experiments. In the first isotherm experiments, the oxidation of ferrous iron in the control bottles reached up to

50%. For this reason, the ferrous isotherm experimental procedure was modified by limiting the exposure of iron to oxygen during the preparation of the isotherm experiments as described in Chapter 3. Accordingly, the oxidation of ferrous iron was significantly reduced to approximately 18%. Figure 5-8 shows the ferrous iron isotherm results presented by the solid circles (●). The concave downward shape of the isotherm data indicates a favourable isotherm with a rapid rise in the GAC adsorption capacity for ferrous iron as the liquid phase concentration increases. Such a shape suggest that as the ferrous iron loading increases, the capacity for adsorbing iron molecules directly on the adsorbent surface increases. As shown in Table 5-6, the values of liquid and solid phase concentrations obtained from the ferrous iron isotherm experiment were close to those of Uchida *et al.* (2000). They studied the mechanisms of adsorption of ferrous iron ions onto activated carbon fibers with a surface area of 1000 m^2/g and also utilized the same 48 h equilibrium time used in this dissertation. For comparison, using an equilibrium liquid phase concentration (C_e) of 0.3 mg/L for ferrous iron, the solid phase concentrations (q_e) of ferrous iron obtained in this study and by Uchida *et al.* (2000) were 6.7 and 6.0 mg/gGAC, respectively.

The isotherm data of ferrous iron was modeled using the Freundlich and Langmuir isotherm models as shown in Figure 5-8, and the regressed parameters of both models are summarized in Table 5-7. Both isotherm models gave a good fit for the ferrous iron isotherm. However, the values of the fit indicators of the Freundlich model were lower than those of the Langmuir model; the CV(RMSE) was 6.2% versus 9.3%, and the AAPE was 4.5% versus 7.0%. Also, the 95% confidence intervals of the Freundlich model parameters were tighter than those of the Langmuir model. The Freundlich parameters K_F = 10.56 $(mg/g)\cdot(L/mg)^n$ and n_F = 0.35 have 95% confidence intervals of ± 11.0 % and 17.1%, respectively. The Langmuir parameters q_s = 8.63 (mg/g) and b = 13.43 (L/mg) have 95% confidence intervals of ± 16.6 % and 53.9%, respectively.

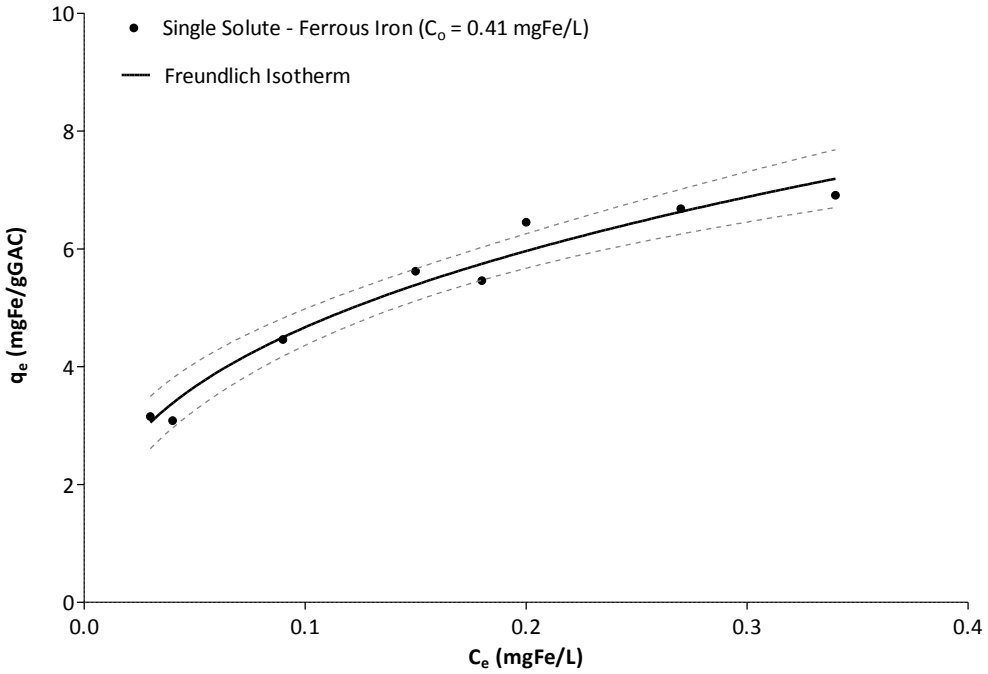

(a)

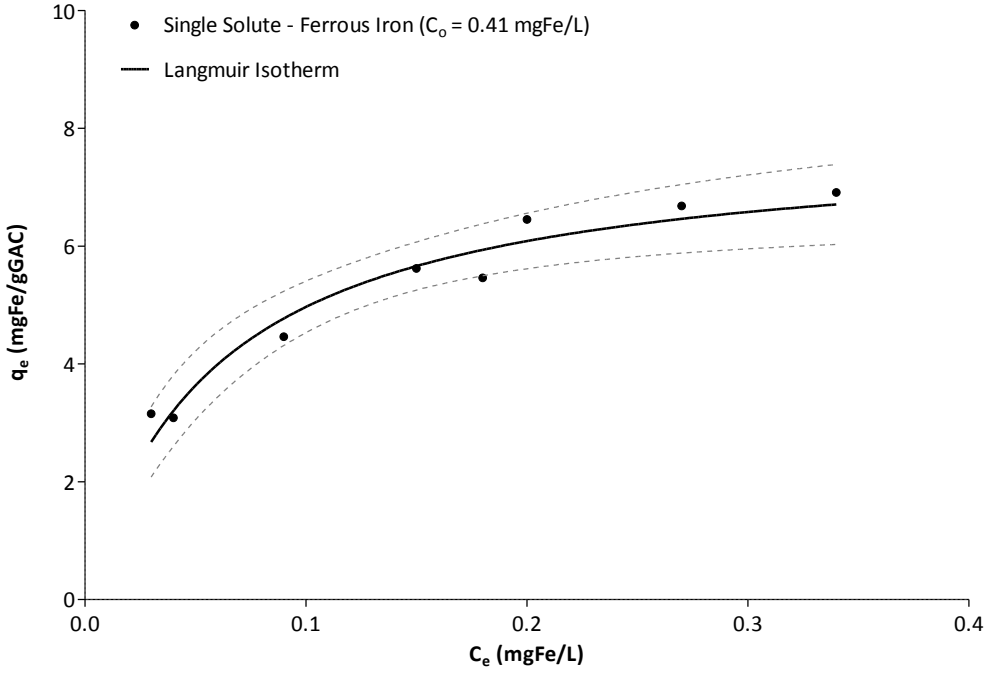

(b)

Figure 5-8: Single solute isotherms for ferrous iron using: (a) Freundlich and (b) Langmuir models within the 95% confidence interval (F-400 GAC (40×50 mesh size), C_o = 0.41 mg/L, pH= 6, Temperature = 25 ^oC)

Table 5-6: Comparison of isotherm results of ferrous iron between this study and a study by Uchida *et al.* (2000)

	Equilibrium Concentration Range (mg/L)	Amount of Ferrous Iron Adsorbed Range (mg/gGAC)
This Study	0.02 – 0.34	2.36 – 6.91
Uchida *et al.*, (2000)	0.05 – 1.20	1.90 – 7.50

In an attempt to further improve the modeling of the ferrous iron isotherm, the Summers-Roberts model was tested for the ferrous iron data. Figure 5-9 shows that the Summers-Roberts model fits the ferrous iron isotherm well. All the fitted parameters are summarized in Table 5-7, and the fit indicators show that the Summers-Roberts model and the Freundlich model are equivalent fits for ferrous iron isotherm data, and that they are tighter fit than the Langmuir model. The values of CV(RMSE) and AAPE were found to be 6.1% and 4.4%, respectively. The 95% confidence intervals of the model regressed parameters also show a tight fit. The Summers-Roberts parameters K_{SR} = 4.20 $(mg/g)\cdot(g/mg)^n$ and n_{SR} = 0.20 have 95% confidence intervals of ± 9.05 % and 20.0%, respectively which is an indication of a tight fit of the model.

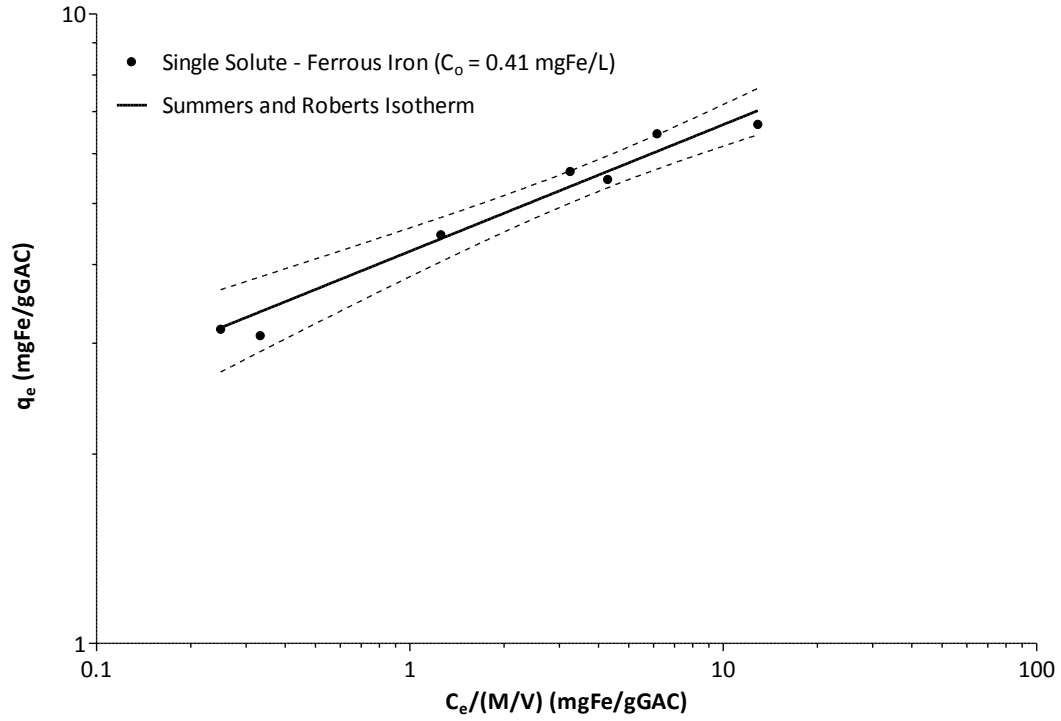

Figure 5-9: Single solute isotherms of ferrous iron using Summers-Roberts model (F-400 GAC (40×50 mesh size), C_o = 0.41 mg/L, pH= 6, Temperature = 25 ^oC)

Table 5-7: Fitted parameter for Langmuir, Freundlich and Summers-Roberts models used to model ferrous iron as single solute in organic free water

Model	Parameter	Parameter Value	95% Confidence Interval	Model Fit Indicators	
				CV(RMSE) (%)	AAPE (%)
Langmuir Isotherm	q_s (mg/g)	8.63	7.20 – 10.07	9.3	7.0
	b (L/mg)	13.43	6.19 – 20.68		
Freundlich Isotherm	K_F (mg/g)·(L/mg)^n	10.56	9.40 – 11.72	6.2	4.5
	n_F	0.35	0.29 – 0.42		
Summers-Roberts Isotherm	K_{SR} (mg/g)·(g/mg)^n	4.20	3.82 – 4.57	6.1	4.4
	n_{SR}	0.20	0.16 – 0.24		

Number of data points = 8
Number of regressed parameters (Langmuir Model) = 2 (q_s and b)
Number of regressed parameters (Freundlich Model) = 2 (K_F and n_F)
Number of regressed parameters (Summers-Roberts Model) = 2 (K_{SR} and n_{SR})

CHAPTER 6 COMPETITIVE ADSORPTION OF IRON AND NATURAL ORGANIC MATTER

6.1 Introduction

The main focus of this study is to determine if the competitive adsorption of NOM and iron in Vars raw water can be described by the different variations of the IAST competitive isotherm model. This study is the first in quantifying and modeling the competitive adsorption of NOM and iron in a natural water source on activated carbon. This chapter describes the model fitting approach and the fit achieved by different variations of the IAST models. The use of the IAST model has been widely accepted and successfully applied for simulating competitive adsorption equilibria (Crittenden *et al.*, 1985; Najm *et al.*, 1991; Knappe *et al.*, 1998; Andrews, 1990). In order to be able to perform the IAST model simulations, the single solute and competitive isotherm data of both components are needed.

6.2 Experimental Results of Competitive Isotherms

In order obtain the competitive isotherm data for iron and NOM, an isotherm experiment was performed using Vars raw water. Adsorption of Vars groundwater consists of the competitive adsorption of the two principal solutes within it (i.e., NOM and ferrous iron). The ferrous iron was considered to be the target compound competing with NOM since it was found to be the dominant iron species in Vars raw water as explained in Chapter 4 and the fact that ferrous iron is the critical solute in terms of the drinking water systems as it can potentially lead to red water problems. The main challenge associated with the isotherm experiments of Vars raw water was the oxidation of ferrous iron in the samples. Accordingly, the experimental procedure had to be modified and the experiments were repeated a few times in order to minimize the exposure of the water samples to oxygen. The key precaution was achieved by using a nitrogen-filled glove box during the preparation and final GAC separation of the isotherm bottle samples, the procedure was discussed in the materials and methods (Chapter 3). However, despite all the precautions and modifications associated with the isotherm experiment, oxidation of ferrous iron took place in the isotherm bottles and the

concentration of ferrous iron in the two control bottles (without GAC) decreased from 1.04 to 0.35 (± 0.05) mg Fe/L. Similar problems occurred with the single solute ferrous iron isotherm and the precipitation was reduced by reducing the initial ferrous iron concentration, for the Vars raw water such a manipulation is not realistic. Accordingly, the isotherm calculations of ferrous iron solid phase concentration were based on the value of 0.35 mg Fe/L. The adsorbed ferrous iron was quantified considering that the change in the control bottles accounted for the iron oxidation. The comparison between the isotherm results of ferrous iron in Vars raw water and organic-free water are shown in Figure 6-1. It indicates that the range of adsorption capacity of ferrous iron decreased from 2.36 – 6.91 mg/gGAC of the ferrous iron single solute isotherm to 0.34 – 1.07 mg/gGAC of the ferrous iron in Vars raw water. Such a decrease by approximately a factor of 7 is due to the competition with NOM over the GAC adsorbing sites.

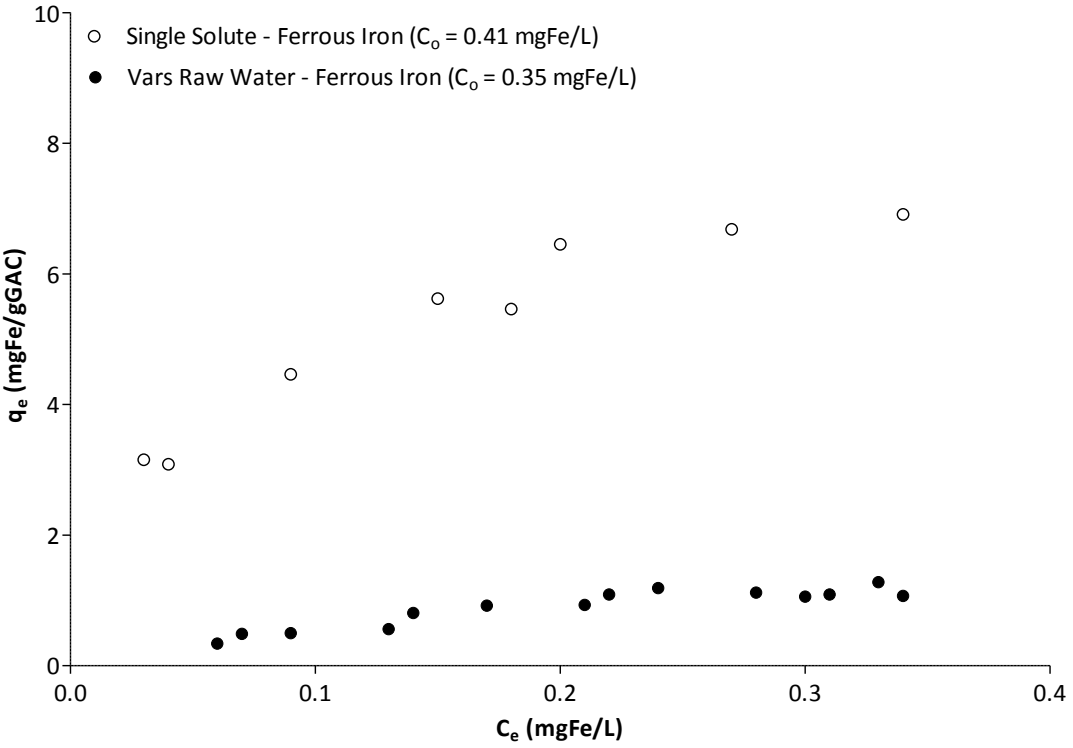

Figure 6-1: Adsorption isotherms for ferrous iron in Vars raw water and organic free water

6.3 IAST Calculation Procedures

All IAST models were developed on a molar basis and one of the problems with the use these models for NOM arises from the fact that NOM is known to be a complex mixture of organic compounds of different molecular weights, size, functionality and adsorbability. A large number of studies for the determination of molecular size of NOM have been conducted. The principles and methods for the determination of molecular size and weight measurements of humic substances were summarized by Aiken (1985). According to these studies, the NOM in natural water may have molecular weights from few hundred to over 5000 g/mol (Li *et al.*, 2003; Moore *et al.*, 2001; Yoon *et al.*, 2005; Stumm and Morgan, 1996; Newcombe *et al.*, 1997). In most of the studies that used the IAST modeling, the NOM's molecular weights were either regressed or set to low range values (i.e., 100 to 500 g/mol) in order for the IAST model to work well (Newcombe *et al.*, 2002; Newcombe and Drikas, 1997; Newcombe *et al.*, 1997; Newcombe *et al.*, 1997; Li *et al.*, 2003; Quinlivan *et al.*, 2005).

The values of the NOM molecular weights in this study were constrained to be equal to or higher than the molecular weight of 100 g/mol. Many researches that successfully used the IAST to model the competitive adsorption of specific organic compounds in water containing NOM have yielded NOM molecular weights higher than 100 g/mol (Simpson and Narbaitz, 1997; Kilduff and Wigton, 1999; Najm *et al.*, 1990; Crittenden *et al.*, 1985; Crittenden *et al.*, 1985; Knappe *et al.*, 1998). Such a constraint would prevent the regression routine from selecting unreasonably low values for the molecular weight of NOM that could be lower than the molecular weight of the target competing compound (i.e., iron molecular weight = 55.8 g/mol). The molar concentration of NOM was computed based on an organic carbon content of 50% which means that the estimated NOM molecular weight regressed by IAST model is half the value of the molecular weight (Thurman and Malcolm, 1981). Most studies used the regression based IAST to model the target compounds without attempting to model the NOM adsorption (Kilduff and Wigton, 1999; Najm *et al.*, 1990; Crittenden *et al.*, 1985; Knappe *et al.*, 1998; Andrews, 1990). Accordingly, the different variations of the

IAST model tested in this study were used to fit the ferrous iron data only. Thus, the simulations of the NOM adsorption data cannot be expected to be as good.

All IAST competitive isotherm models yield simulation values for liquid-phase (C_e) and solid-phase (q_e) concentrations for all the solutes. In this study, only the solid-phase concentrations (q_e) were used for the comparison of the goodness of each model's fit since the optimized value of (q_e) is linked to the (C_e) value by a mass balance (check Equation 2-5). As a method to assess the fit of the models, the calculated values of the equilibrium solid phase concentrations (q_e) will be compared with the isotherm experimental data points visually, as well as by computing the absolute average percentage errors (AAPE) and coefficient of variation of the root mean square error CV(RMSE) using Microsoft Excel according to the following equations:

$$\text{AAPE}(\%)=\frac{100}{N}\sum_{i=1}^{N}\frac{\left|P_i-O_i\right|}{O_i} \tag{6-1}$$

$$\text{CV(RMSE)}\ (\%) = \frac{100}{\sum_{i=1}^{N} O_i}\sqrt{\frac{1}{\text{DOF}}\sum_{i=1}^{N}(P_i-O_i)^2} \tag{6-2}$$

Where: N = the number of observations; P_i = predicted value; O_i= experimental value; DOF = degree of freedom (DOF = N – number of parameters to be regressed). The coefficient of variation of the root mean squared error, CV(RMSE) (%) is essentially the root mean squared error divided by the measured mean of the data. These criteria were chosen because it is often convenient to report a non-dimensional result (Draper and Smith, 1998). The CV(RMSE) was used instead of the sum of squares because it incorporates the number of regressed parameters within the model (through the degrees of freedom term), thus it permits a more equitable comparison between models with different number of parameters. CV(RMSE) allows one to determine how well a model fits the data; the lower the CV(RMSE), the better the model fit. AAPE was used because it gives a direct assessment on the average error, which provides a more tangible assessment of the quality of the fit.

One of the advantages of the IAST model is that the best single-solute isotherm model, regardless of its mathematical form, can be incorporated into the IAST to describe the multicomponent competition which makes it more widely applicable than other multicomponent models. The most common applications of the IAST model are those based on the Freundlich single solute isotherm models. In this study, all the different variations of the IAST models were first applied in combination with the Freundlich model, which will be called IAST-FR. The different model variations that were evaluated are IAST-FR predictive, IAST-FR one pseudocomponents, IAST-FR two pseudocomponents, Ding modified IAST-FR and Kilduff-Wigton modified IAST-FR. Then, all the modeling variations were tested with the IAST model in combination with Summers-Roberts single solute model. The Summers and Roberts isotherm form of the IAST model, which will be called IAST-SR, is represented by the following equations:

$$C_{e\text{-}i} = \left(\frac{M}{V}\right)\left[\frac{q_{e\text{-}i}}{\sum_{j=1}^{N} q_{e\text{-}j}}\right]\left[\frac{n_{SR_i}\sum_{j=1}^{N}\frac{q_{e\text{-}j}}{n_{SR_j}}}{K_{SR_i}}\right]^{1/n_{SR_i}} \tag{6-3}$$

$$q_{e\text{-}i} = \left(\frac{V}{M}\right)C_{io} - \left[\frac{q_{e\text{-}i}}{\sum_{j=1}^{N} q_{e\text{-}j}}\right]\left[\frac{n_{SR_i}\sum_{j=1}^{N}\frac{q_{e\text{-}j}}{n_{SR_j}}}{K_{SR_i}}\right]^{1/n_{SR_i}} \tag{6-4}$$

Where: K_{SRi} = the single solute Summers-Roberts model parameter of component i $((mg/g)\cdot(mg/g)^n)$; n_{SR} = the single solute Summers-Roberts exponent of component i (unitless); M = mass of GAC (g); V = volume of solution (L); $C_{e\text{-}i}$ = equilibrium liquid phase concentration of component i (mol/L); $q_{e\text{-}i}$ = equilibrium solid phase concentration of component i (mol/gGAC) and $q_{e\text{-}j}$ = equilibrium solid phase concentration of component j (mol/gGAC).

6.3.1 IAST Predictive Model Calculation Procedures

The IAST-FR and IAST-SR competitive isotherm models consist of numerous nonlinear equations that need to be solved simultaneously. These nonlinear equations were solved using the SOLVER add-in within Microsoft's spreadsheet, Microsoft Excel. For each trial value of the parameters the steps involved in solving the IAST-FR equations for each isotherm experimental data point are described below. The same approach can be followed for the IAST-SR predictive model using Equations (6-3) and (6-4):

1. First, the initial concentrations ($C_{initial}$), as well as the values of Freundlich parameter (K_F) of each component are converted to molar basis using the molecular weight of iron and the assumed molecular weight of NOM.
2. Initial guesses for the solid phase concentrations of both NOM ($q_{e\text{-}NOM\text{-}guessed}$) and iron ($q_{e\text{-}Fe\text{-}guessed}$) are chosen.
3. The values of $q_{e\text{-}NOM\text{-}calculated}$ and $q_{e\text{-}Fe\text{-}calculated}$ are calculated using the NOM initial concentration ($C_{NOM\text{-}initial}$), the iron initial concentration ($C_{Fe\text{-}initial}$), $K_{F\text{-}NOM}$, $K_{F\text{-}Fe}$, $n_{F\text{-}NOM}$, $n_{F\text{-}Fe}$, $q_{e\text{-}NOM\text{-}guessed}$, $q_{e\text{-}Fe\text{-}guessed}$ and GAC dose (M/V) for each data point. The following equation is used to calculate the values of $q_{e\text{-}NOM\text{-}calculated}$ and $q_{e\text{-}Fe\text{-}calculated}$.

$$q_{e\text{-}i\text{-}calculated} = \left(\frac{V}{M}\right) C_{i\text{-}initial} - \left(\frac{V}{M}\right) \left(\frac{q_{e\text{-}i\text{-}gussed}}{\sum_{j=1}^{N} q_{e\text{-}j\text{-}gussed}} \right) \left[\frac{\left(n_{Fi} \sum_{j=1}^{N} \frac{q_{e\text{-}j\text{-}gussed}}{n_{Fj}} \right)}{K_{Fi}} \right]^{1/n_{Fi}} \qquad (6\text{-}5)$$

4. The SOLVER add-in within Microsoft's Excel spreadsheet was used to minimize the sum of squared errors (SSE) between the values of $q_{e\text{-}guessed}$ and $q_{e\text{-}calculated}$ for both NOM and iron.
5. The concentration ($C_{e\text{-}calculated}$) of each component is calculated by substituting the values of $q_{e\text{-}NOM\text{-}calculated}$ and $q_{e\text{-}Fe\text{-}calculated}$ obtained from the previous step into the following equation.

$$C_{e\text{-}i\text{-}calculated} = \left(\frac{q_{e\text{-}i\text{-}calculated}}{\sum_{j=1}^{N} q_{e\text{-}j\text{-}calculated}} \right) \left[\frac{\left(n_{Fi} \sum_{j=1}^{N} \frac{q_{e\text{-}j\text{-}calculated}}{n_{Fj}} \right)}{K_{Fi}} \right]^{1/n_{Fi}} \quad (6\text{-}6)$$

6. Finally, the values of $q_{calculated}$ and $C_{calculated}$ for each component are converted to mg/gGAC mg/L, respectively using their molecular weights.
7. The above process is repeated for each of the data points, and finally the quality of fit parameters was evaluated using the absolute average percentage errors (AAPE) and coefficient of variation of the root mean square error CV(RMSE).

6.3.2 IAST Regression-Based Model Calculation Procedures

For the predictive IAST model calculations, the multiple nonlinear equations of the IAST competitive isotherm model were solved using the SOLVER add-in within Microsoft Excel spreadsheets for each data point. However, when the NOM parameters (C_o, NOM-MW, K or n) are regressed, SOLVER cannot be readily used to simultaneously solve the nonlinear equations and conduct the regression required for the IAST-pseudocomponents model. Accordingly, a different platform was used for the evaluation. A FORTRAN code written by Simpson (1995) and modified by the author was used to implement the IAST pseudocomponent model (presented in Appendix E). The code has two main parts, a fitting subroutine and model subroutine. The first subroutine finds the values of NOM-MW, K, n and possibly C_o that yield the minimum absolute average percent error of the solid phase concentration (q_e) of the competing compound (i.e., ferrous iron). The minimization is conducted by systematically evaluating the trial values of the above parameters using a number of loops. For each set of NOM parameters (C_o, NOM-MW, K or n), the FORTRAN code calls the model subroutine library subroutine NEQNF to solve the IAST nonlinear equations for each data point. The NEQNF routine is a part of the International Mathematics and Statistics Library (IMSL) within FORTRAN and it is based on a variation of Newton's method that uses finite difference approximations to the Jacobian.

6.4 IAST in Combination with Freundlich Model

6.4.1 IAST-FR Predictive Model

The effectiveness of the IAST-FR predictive model for simulating the competitive adsorption of NOM and ferrous iron on GAC was evaluated in this study using different molecular weights of NOM. Changing the molecular weights of NOM would vary the initial concentration and the Freundlich K-parameter of NOM used in the IAST-FR predictive model. So, based on a sensitivity analysis of the IAST model results using different NOM molecular weights, it was found that only using NOM molecular weight less than 200 g/mol would improve the results of the ferrous iron simulation. Using NOM molecular weights higher than 200 g/mol would only have an impact on the IAST-FR simulation of NOM not the ferrous iron. Given the fact that the NOM molecular weight was varied, the model cannot be considered as strictly predictive, but all the other input isotherm parameters were determined from the single solute isotherms.

Figure 6-2 shows the IAST-FR simulations of competitive adsorption isotherms of NOM and ferrous iron in Vars raw water using NOM molecular weights of 200 and 100 g/mol. The isotherm parameters used for modeling and the fit indicators are summarized in Table 6-1 and Table 6-2, respectively. The best fit for NOM was obtained using the IAST-FR with a molecular weight of 100 g/mol and the fit indicators (CV(RMSE) and AAPE) were 10.7% and 6.9%, respectively. However, the IAST model was not capable of simulating the competitive adsorption of ferrous iron in Vars raw using both NOM molecular weights. The simulations could presumably be improved using even smaller NOM molecular weights; however these molecular weights would be unrealistically small.

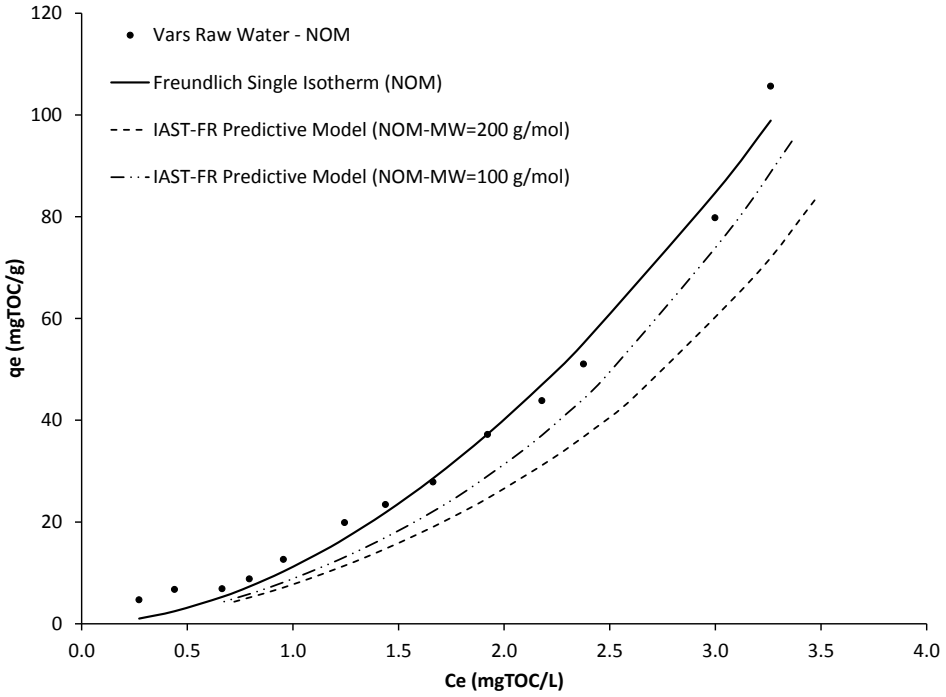

(a)

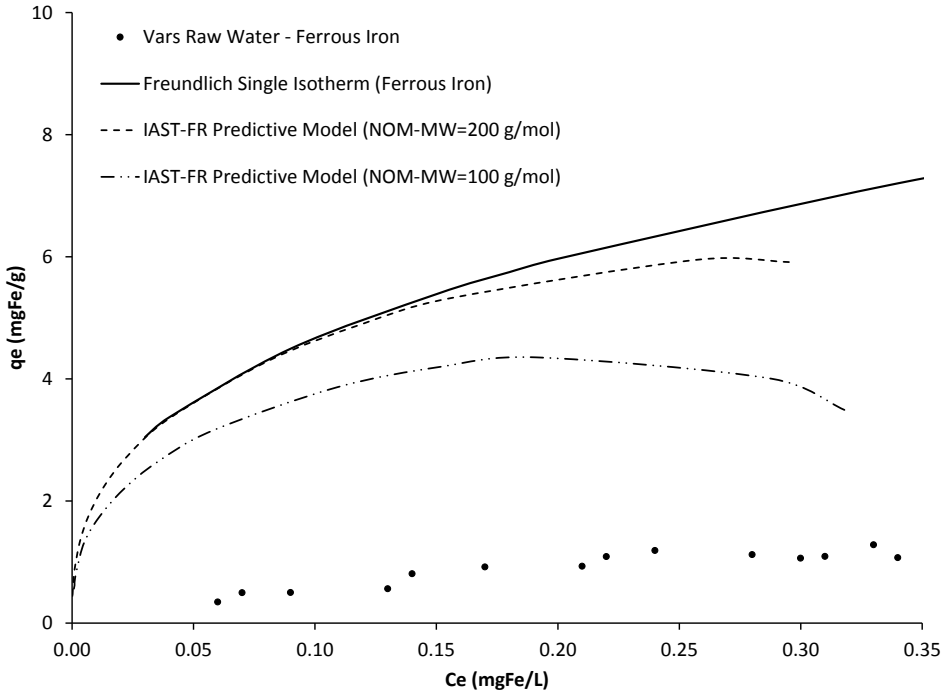

(b)

Figure 6-2: : IAST-FR predictive model simulation of: (a) NOM and (b) ferrous iron using different molecular weights for NOM

Table 6-1: Parameters for IAST-FR predictive model

	Ferrous Iron	NOM	
MW (g/mol)	55.8	200	100
Initial Concentration (µmol/L)	6.27	42.42	84.84
K_F $(\mu mol/g)\cdot(L/\mu mol)^n$	67.98	1.60	0.89
n_F	0.35	1.84	1.84

Note: Organic carbon was assumed to account for 50% of the NOM molecular weight

Table 6-2: Fit indicators for IAST-FR predictive model

Competitive Isotherm Model	NOM-MW (g/mol)	Fit Indicator	(Ferrous Iron) q_e	(NOM) q_e
IAST-FR	200	CV(RMSE) (%)	297.8	23.2
		AAPE (%)	187.0	11.4
	100	CV(RMSE) (%)	212.8	10.7
		AAPE (%)	143.6	6.9

Number of data points = 14

Number of regressed parameters (IAST-FR) = 0

6.4.2 IAST-FR One Pseudocomponent Model

The graphical representations of the results of NOM and ferrous iron simulations using IAST-FR one pseudocomponent are presented in Figure 6-3 and all regressed parameters are summarized in Table 6-3. Note that in pseudocomponent versions of IAST, the single solute Freundlich isotherm parameters for NOM were not used, instead the pseudocomponent(s) Freundlich isotherm parameter values were adjusted to yield the best possible simulation of the target solute's (i.e., ferrous iron) adsorption. The simulation in Figure 6-3.b shows a good fit for the ferrous iron data. However, the simulation was very poor for the NOM

adsorption data (Figure 6-3.a). The best fit for ferrous iron was achieved using a regressed NOM molecular weight of 111.6 g/mol. Also the best fit was achieved when the regressed value of (K_F) for NOM was almost the same as the (K_F) value of ferrous iron (i.e., 68 $(\mu mol/g)\cdot(L/\mu mol)^n$). The fit indicator of the IAST-one pseudocomponent (CV(RMSE) and AAPE) for the solid-phase concentration of ferrous iron are 10.2% and 8.0%, respectively (Table 6-4). According to these findings, the IAST using one pseudocomponent is considered as a good model that successfully describe the competitive adsorption isotherms of ferrous iron in Vars raw water. The poor simulation of the NOM is not surprising given that the fitting was based strictly on the ferrous iron adsorption.

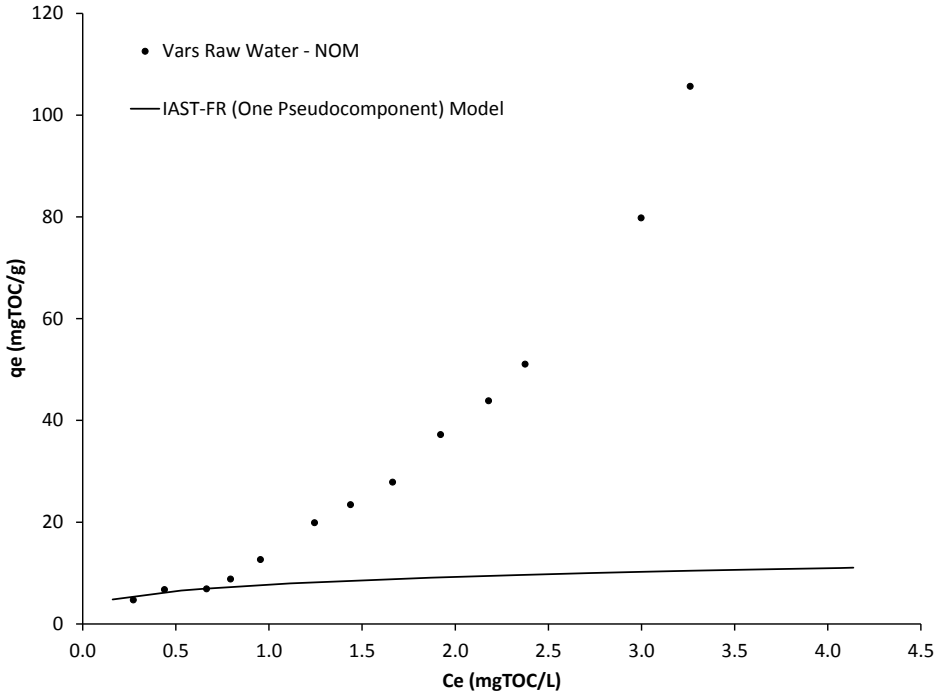

(a)

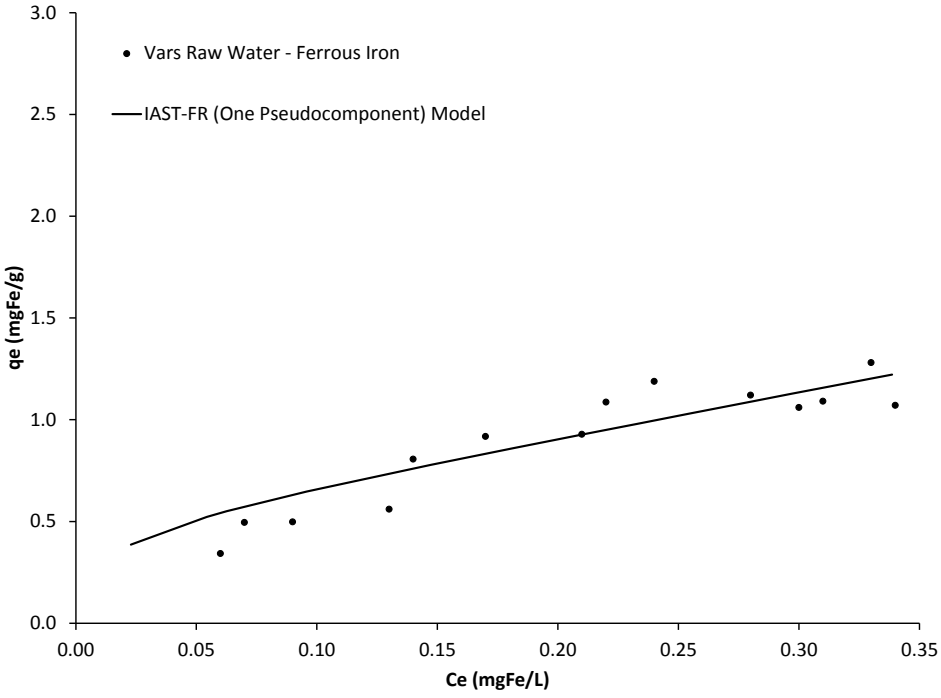

(b)

Figure 6-3: IAST-FR one pseudocomponent model simulations of: (a) NOM and (b) ferrous iron

Table 6-3: Regressed parameters used for IAST-FR one pseudocomponent model

Model	Component	Initial Concentration (mgTOC/L)	Initial Concentration (µmol/L)	Molecular Weight (g/mol)	K_F $(\mu mol/g)\cdot(L/\mu mol)^n$	n_F
IAST-FR	NOM	4.24	75.99	111.6	68.00	0.26
	Ferrous Iron	0.35	6.27	55.8	67.98	0.35

Note: Organic carbon was assumed to account for 50% of the NOM molecular weight

Table 6-4: Fit indicators for IAST-FR one pseudocomponent model

Model	Fit Indicator	Ferrous Iron q_e	NOM q_e
IAST-FR	CV(RMSE) (%)	10.2	126.5
	AAPE (%)	8.0	46.54

Number of data points = 14

Number of regressed parameters (IAST-FR) : 3 (MW_{NOM}, $K_{F\text{-}NOM}$, $n_{F\text{-}NOM}$)

Even though, the IAST-FR model using one NOM pseudocomponent showed a good fit of the ferrous iron in Vars raw water, the model overpredicted the lower concentration range of ferrous iron (< 0.15 mgFe/L) and the NOM adsorption was not predicted well. Another variation of the IAST model that consider NOM as one component such as the equivalent background compound (EBC) which incorporates the Freundlich isotherm (IAST-FR-EBC) model was tested in order to check if it would improve the simulations of ferrous iron and NOM in Vars raw water. All the simulation results as well as the regressed parameters of these models are summarized in Appendix B. The IAST-FR-EBC model simulation of ferrous iron showed a good fit for the ferrous iron data and yielded a very poor simulation of the NOM adsorption data. The regressed value of the NOM initial concentration based on the IAST-FR-EBC model was found to be 7.10 mgTOC/L which is higher than the actual Vars raw water TOC concentration of 4.24 mgTOC/L. Thus, the regressed initial EBC

concentration of NOM is unrealistic and the simulation result of IAST-FR-EBC was rejected as a reasonable simulation of Vars raw water isotherm data.

Over all, such modeling approaches treat all the NOM as a single component. This approach simplifies the modeling but ignores the fact that NOM consists of different molecular sizes that affect the adsorption of target compounds through different mechanisms (Najm *et al.*, 1991; Knappe *et al.*, 1998; Li *et al.*, 2003; Randtke and Snoeyink, 1983; Crittenden *et al.*, 1985; Qi *et al.*, 1994). Accordingly, the use of the IAST model that considers the NOM as different fractions is needed to improve the predictions of isotherm data of Vars raw water.

6.4.3 IAST-FR Two Pseudocomponents Model

As models with a larger number of pseudocomponents have an increased number of adjustable parameters in which it is expected to yield better simulations. However, the application of the IAST model with more than one pseudocomponent may lead to poor predictions and many inconsistencies as a reason of the cross correlation between the pseudocomponents (Sontheimer *et al.*, 1988; Crittenden *et al.*, 1985). Therefore, there have been some suggestions to overcome the high correlation of the large number of parameters of the pseudocomponents by reducing the number of parameters that needs to be regressed. Crittenden *et al.* (1985) suggested the use of pseudocomponents with the same molecular weights. Also, there has been another suggestion by Sorial *et al.* (1993) and Yuasa *et al.* (1997) on using the same value of (n_F) from the Freundlich single solute for all the pseudocomponents but different values of (K_F) so as to represent a wide range of adsorbabilities. All these suggestions were tested when different variations of the IAST-pseudocomponents models were used. The IAST-FR model was tested using two pseudocomponents to represent the NOM. Although Crittenden *et al.*, (1985) recommended the use of three pseudocomponents; one of these three components was the non-adsorbable fraction of NOM which had a very small value and did not impact the IAST results. For the IAST-FR model only two pseudocomponents were used because higher number of pseudocomponents led to numerical instabilities in the computations and because the NOM's non-adsorbable fraction in this study was negligible so it was not necessary to include it in the IAST modeling.

In this study, the IAST-FR (two pseudocomponents) model was fitted by regressing the NOM molecular weight (MW), initial concentrations (C_o), Freundlich isotherm parameters of each pseudocomponent representing the NOM to minimize the sum of the squares of the difference of the experimental and simulated values of the solid-phase concentration (q_e). The graphical representations of the results of NOM and ferrous iron simulations using two pseudocomponents are presented in Figure 6-4. The regressed parameters of the IAST-FR two pseudocomponents model are summarized in Table 6-5. The best fit was achieved by fixing the value of (n_F) for all NOM pseudocomponents to n_F = 0.05. The equal (n) assumption has been widely applied to model the competitive adsorption isotherms containing NOM using IAST pseudocomponents model (Sontheimer *et al.*, 1988; Crittenden *et al.*, 1993; Matsui *et al.*, 1998; Li *et al.*, 2003; Newcombe *et al.*, 2002; Sorial *et al.*, 1993; Yuasa *et al.*, 1997). Also, the regressed initial concentrations of the two NOM pseudocomponents were found to be 3.75 and 0.50 mgTOC/L for components one and two, respectively. The regressed molecular weights of both components were 500 and 450 g/mol.

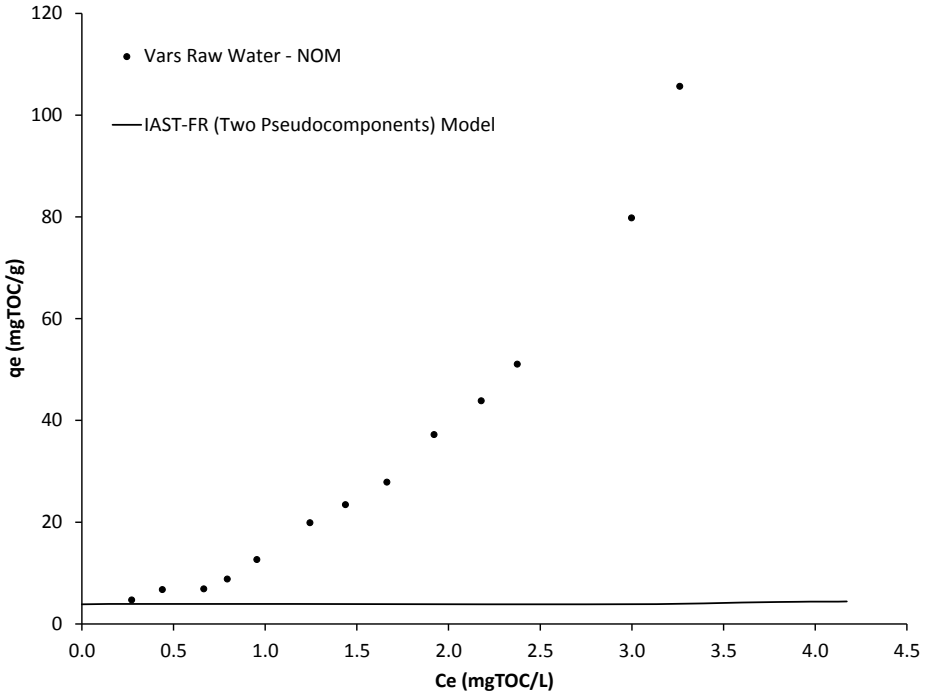

(a)

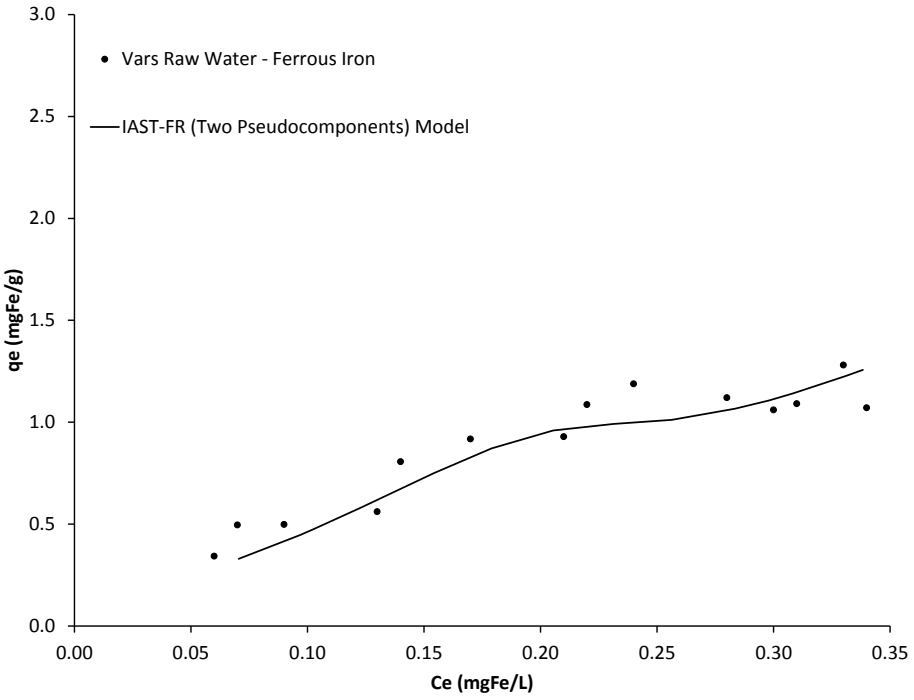

(b)

Figure 6-4: IAST-FR two pseudocomponents model simulation of: (a) NOM and (b) ferrous iron

Table 6-5: Regressed parameters used for IAST-FR two pseudocomponents model

Model	Component Number	Initial Concentration (mgTOC/L)	Initial Concentration (µmol/L)	Molecular Weight (g/mol)	K_F $(\mu mol/g)\cdot(L/\mu mol)^n$	n_F
IAST-FR	NOM – 1	3.74	14.96	500	15.00	0.05
	NOM – 2	0.50	2.22	450	21.00	0.05

Note: Organic carbon was assumed to account for 50% of the NOM molecular weight

Visually, the competitive ferrous isotherm simulations (Figure 6-4) are slightly wavy in contrast to more concave downward isotherms shown in the literature for other target compounds. The fit indicator (CV(RMSE) and AAPE) summarized in Table 6-6 for the solid-phase concentration of ferrous iron using IAST-FR with two pseudocomponent are 14.1% and 6.8%, respectively. The model was not capable of simulating the NOM and the fit indicators (CV(RMSE) and AAPE) for the solid-phase concentration of NOM are 191.8% and 72.7%, respectively. According to these findings, the IAST model using two pseudocomponents is considered as a good model that successfully describe the competitive adsorption isotherms of ferrous iron in Vars raw water.

Table 6-6: Fit indicators for IAST-FR two pseudocomponents model

Model	Fit Indicator	Ferrous Iron q_e	NOM q_e
IAST-FR	CV(RMSE) (%)	14.1	191.8
	AAPE (%)	6.8	72.2

Number of data points = 14

Number of regressed parameters (IAST-FR) :

8 ($C_{o\text{-}NOM\text{-}1}$, $C_{o\text{-}NOM\text{-}2}$, $MW_{NOM\text{-}1}$, $MW_{NOM\text{-}2}$, $K_{F\text{-}NOM\text{-}1}$, $K_{F\text{-}NOM\text{-}2}$, $n_{F\text{-}NOM\text{-}1}$, $n_{F\text{-}NOM\text{-}2}$)

6.4.4 Ding Modified IAST-FR Model

Ding *et al.* (2006) proposed a modification to the concept of IAST-FR two pseudocomponents model. Their approach takes into account that there is direct competition

between the target compounds and NOM for some adsorption sites and there also is pore blockage that eliminates certain adsorption sites. Direct competition occurs when small NOM molecules simultaneously compete with target compound molecules for access to the adsorption sites on activated carbon. The effect of pore blockage by NOM occur when large NOM molecules accumulate and block the openings of smaller pores, preventing target compound molecules from accessing or exiting adsorption sites. Ding *et al.* (2006) divided the NOM into two fictive fractions, site competing fractions (SC) and pore blocking fractions (PB). Additional assumptions were made by (Ding *et al.*, 2006) to simplify their method. The NOM that is competing with the target compounds for adsorption sites are assumed to have the same molecular weight and the same adsorption properties as those of the target compound, including the Freundlich constants, K_F and n_F.

In the case of competitive adsorption between NOM and iron in Vars raw water, the IAST-FR model was applied to calculate equilibrium concentrations for ferrous iron and the (SC) fraction of NOM as a function of carbon dose. Also, as suggested by Ding *et al.* (2006), the Freundlich constant (K_F and n_F) and the molecular weight of (SC) fraction of NOM were equated to the values of ferrous iron. The only unknown to be regressed is the initial concentration (C_o) of the (SC) fraction of NOM. The Ding modified IAST-FR model was not capable of simulating the site competing fraction of the NOM in Vars raw water (Figure 6-5.a). However, Figure 6-5.b shows that the model was capable of fitting the ferrous iron experimental data. The fit indicators of the model (CV(RMSE) and AAPE) for the solid-phase concentration of ferrous iron are 9.2% and 9.0%, respectively (Table 6-8). According to these findings, the IAST model using Ding's approach is considered as a good model that successfully describe the competitive adsorption isotherms of ferrous iron in Vars raw water. The regressed value of the initial concentration of SC fraction using IAST models (Table 6-7) was equal to 96.77 µmol/L which is equivalent to 2.70 mgTOC/L. Such a value suggest that 64% of the NOM's concentration in Vars raw water (i.e., 4.24 mgTOC/L) has a molecular weight of 55.8 g/mol and competes with the ferrous iron for the GAC adsorbing sites.

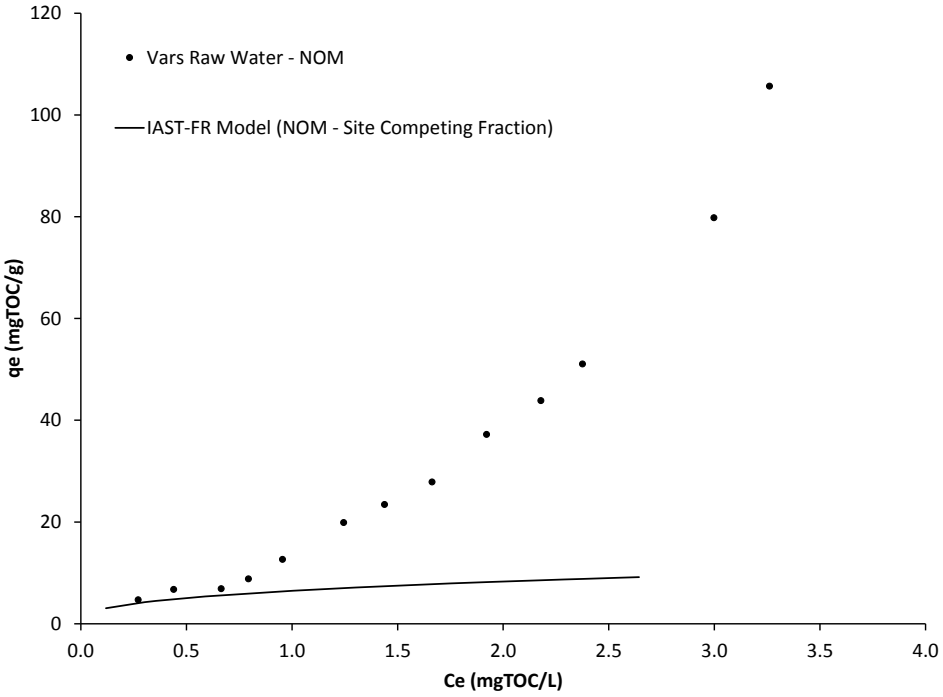

(a)

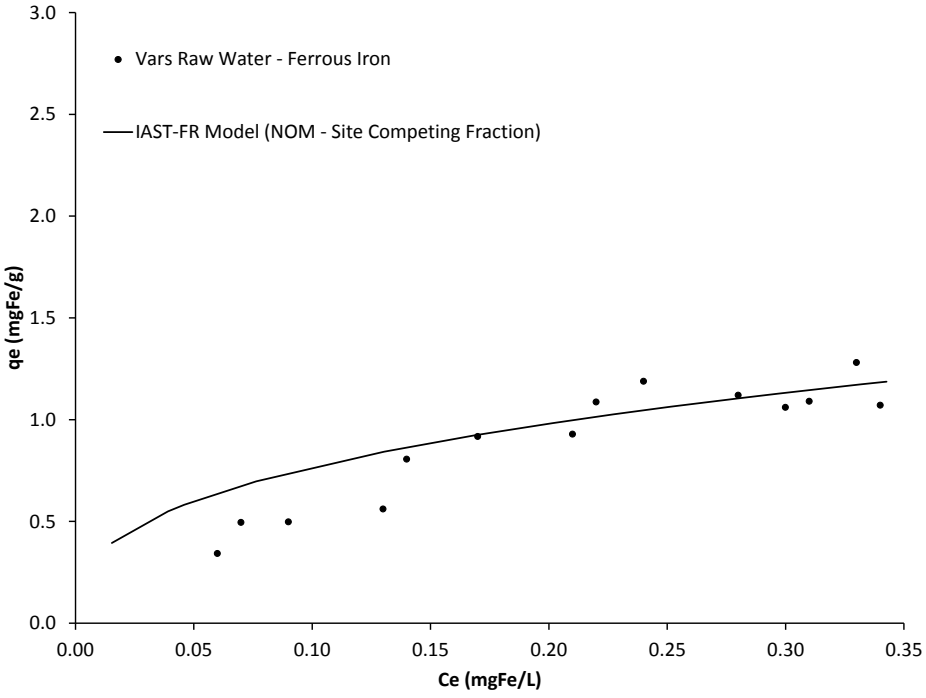

(b)

Figure 6-5: Ding modified IAST-FR simulations of: (a) site competing (SC) fraction of NOM and (b) ferrous iron

Table 6-7: Regressed parameters for Ding modified IAST-FR model of ferrous iron and the site competing (SC) fraction of NOM

Model	Component	Initial Concentration (mg/L)	Initial Concentration (μmol/L)	Molecular Weight (g/mol)	K_F $(\mu mol/g)\cdot(L/\mu mol)^n$	n_F
IAST-FR	NOM (SC Fraction)	2.70	96.77	55.8	67.98	0.35
	Ferrous Iron	0.35	6.27	55.8	67.98	0.35

Note: Organic carbon was assumed to account for 50% of the NOM molecular weight

Table 6-8: Fit indicators for Ding modified IAST-FR model of ferrous iron and the site competing (SC) fraction of NOM

Model	Fit Indicator	Ferrous Iron q_e	NOM (SC Fraction) q_e
IAST-FR	**CV(RMSE) (%)**	9.2	120.7
	AAPE (%)	9.0	61.9

Number of data points = 14

Number of regressed parameters: 1 ($C_{o\text{-}NOM}$)

6.4.5 Kilduff-Wigton Modified IAST-FR Model

The Kilduff-Wigton modified IAST-FR model was applied on the Vars raw water competitive isotherm data. In the data fitting, the value of the GAC surface area fraction on which there is no competitive effects (θ) was varied from 0.01 to 0.99 using different molecular weights for NOM. The best fit for ferrous iron was obtained when the θ-parameter was equal to 0.85 and the NOM's molecular weight was 3000 g/mol as shown in Figure 6-6.b and Table 6-9 summarizes the regressed isotherm parameters for NOM and iron obtained by the model. Even though, the NOM simulation improved greatly over the IAST-FR model using one and two pseudocomponents, the model under predicted in the NOM isotherm data by a factor of 1.2 as shown in Figure 6-6.b. The fit indicators (CV(RMSE) and AAPE) for

the solid-phase concentration of ferrous iron are 26.1% and 28.9%, respectively (Table 6-10). According to these findings, the Kilduff-Wigton modified IAST-FR model is considered as a good model that successfully described the competitive adsorption isotherms of ferrous iron in Vars raw water. The fit indicator (CV(RMSE) and AAPE) for the solid-phase concentration of NOM are 39.5% and 15.8%, respectively. According to the model, the value of $\theta = 0.85$ means that competition between NOM and ferrous iron occurs only on 15% of the GAC adsorption sites. It also implies that 85% of the total surface area can be accessed by iron only while the NOM with molecular size of 3000 g/mol cannot access these areas. As a comparison with the results of Kilduff and Wigton (1999) modeling of trichloroethylene (TCE) adsorption by humic-preloaded activated carbon, they found that θ values were equal to 0.71 and 0.41 for GAC preloaded with 45.6 and 87.0 mg humic acid/g, respectively.

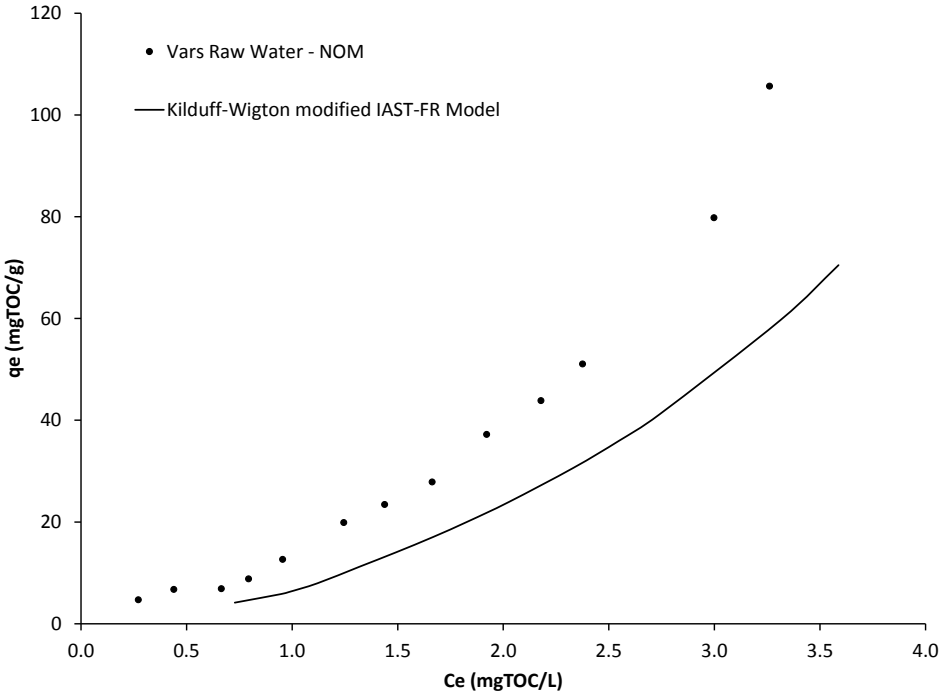

(a)

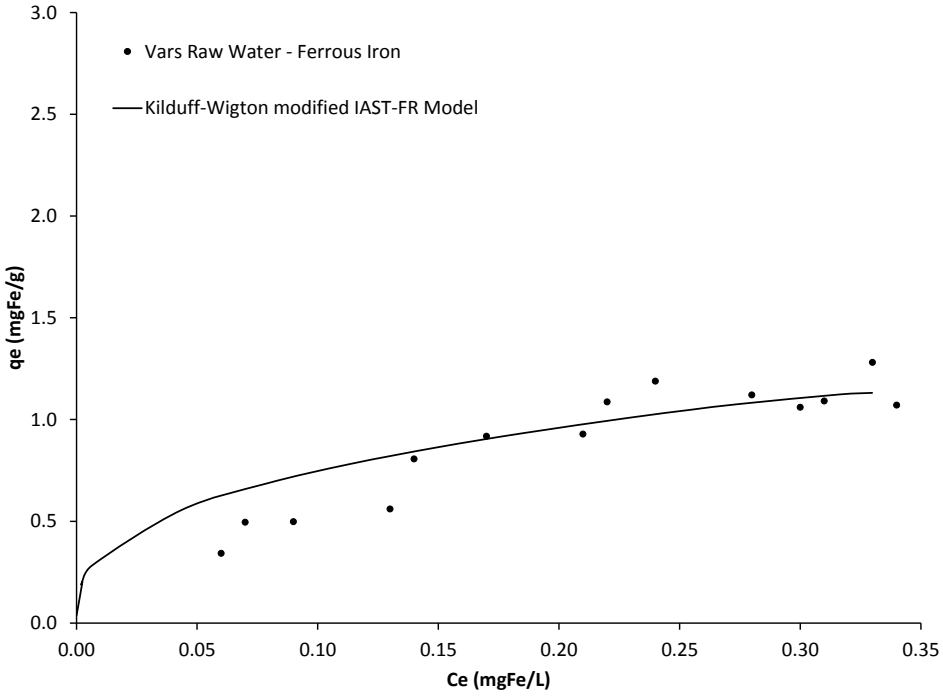

(b)

Figure 6-6: Kilduff-Wigton modified IAST-FR model of: (a) NOM and (b) competitive fraction of ferrous iron

Table 6-9: Regressed parameters for Kilduff-Wigton modified IAST-FR model of NOM and competitive fraction of ferrous iron

	Ferrous Iron	NOM
MW (g/mol)	55.8	3000
Initial Concentration (µmol/L)	6.27	2.83
θ	0.85	0.85
K_F (µmol/g)·(L/µmol)n	67.98	15.75
n_F	0.35	1.84

Note: Organic carbon was assumed to account for 50% of the NOM molecular weight

Table 6-10: Fit indicators for Kilduff-Wigton modified IAST-FR model of NOM and competitive fraction of ferrous iron

NOM - Molecular Weight (g/mol)	θ	Fit Indicator	Ferrous Iron q_e	NOM q_e
3000	0.85	CV(RMSE) (%)	26.1	39.5
		AAPE (%)	28.9	15.8

Number of data points = 14

Number of regressed parameters = 2 (θ, MW_{NOM})

All the IAST-FR models, that were tested, resulted in good simulations for the ferrous iron. However, none of them was capable of modeling the NOM. Given that the single solute isotherms of NOM and ferrous iron were modeled slightly better by the Summers-Roberts model than the Freundlich model as discussed in Chapter 5, then the Summers-Roberts IAST (i.e., IAST-SR) model should be assessed.

6.5 IAST in Combination with Summers-Roberts Model

In order to check if the simulations of the IAST-FR models could improve for both ferrous iron and NOM, all different variations of the IAST models were tested in combination with Summers-Roberts model (i.e., IAST-SR models). All the simulations of the IAST-SR models

were presented with the results of the previously tested IAST-FR models for easy comparisons.

6.5.1 IAST-SR Predictive Model

Figure 6-7 shows the IAST-SR prediction of competitive adsorption isotherms of NOM and ferrous iron in Vars raw water in comparison to the simulation of IAST-FR predictive model. The isotherm parameters used for the IAST-SR modeling are summarized in Table 6-11. The prediction results shown in Figure 6-7 were calculated using two molecular weights for NOM (200 and 100 g/mol). Based on the sensitivity analysis performed on the IAST-SR model, increasing the molecular weights for the NOM (> 200 g/mol) caused the isotherm simulations for both NOM and ferrous iron to worsen. However, the IAST-SR model simulation for NOM and ferrous iron were better than those for the IAST-FR model when both models were using a NOM's molecular weight values of 100 and 200 g/mol. Table 6-12 compares the fit indicators between the IAST-FR and the IAST-SR models. Based on the solid-phase concentration (q_e) simulations of NOM, the fit indicators (CV(RMSE) and AAPE) for NOM molecular weight of 100 gTOC/L decreased from 10.7% and 6.9% for IAST-FR to 1.9% and 1.7% for IAST-SR, respectively. The fit indicators (CV(RMSE) and AAPE) of the ferrous iron simulation for NOM molecular weight of 200 g/mol decreased from 297.8% and 187.0% for IAST-FR to 51.3% and 40.7% for IAST-SR, respectively. Thus, the IAST-SR simulation of the ferrous iron shows some improvement but the overall fit is still poor.

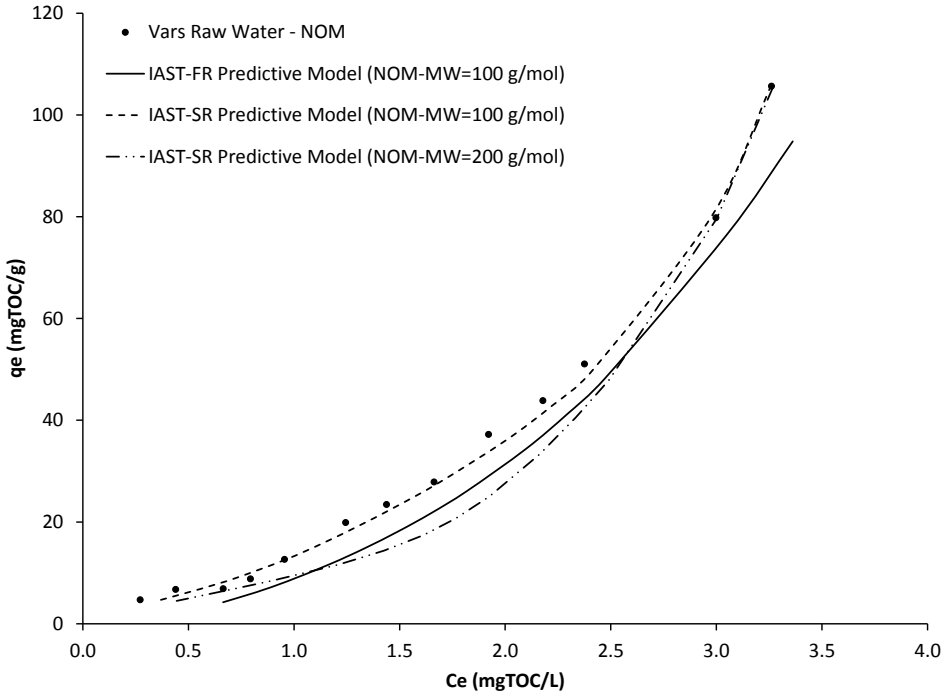

(a)

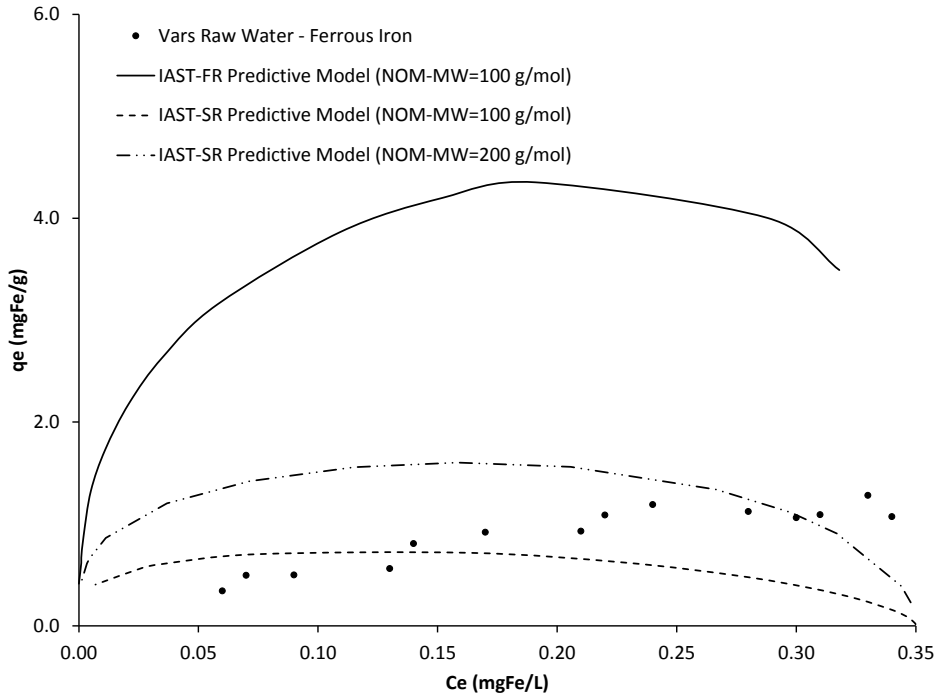

(b)

Figure 6-7: IAST-SR and IAST-FR predictive models of: (a) NOM and (b) ferrous iron using different molecular weights for NOM

Table 6-11: Parameters for IAST-SR predictive model

	Ferrous Iron	NOM	
MW (g/mol)	55.8	200	100
Initial Concentration (µmol/L)	6.27	42.42	84.84
K_{SR} (µmol/g)·(g/µmol)^n	42.09	27.23	39.92
n_{SR}	0.20	0.45	0.45

Note: Organic carbon was assumed to account for 50% of the NOM molecular weight

Table 6-12: Fit indicators for IAST-FR and IAST-SR predictive models

Competitive Isotherm Model	NOM-MW (g/mol)	Fit Indicator	(Ferrous Iron) q_e	(NOM) q_e
IAST-FR	200	CV(RMSE) (%)	297.8	23.2
		AAPE (%)	187.0	11.4
	100	CV(RMSE) (%)	212.8	10.7
		AAPE (%)	143.6	6.9
IAST-SR	200	CV(RMSE) (%)	51.3	6.5
		AAPE (%)	40.7	6.4
	100	CV(RMSE) (%)	81.0	1.9
		AAPE (%)	55.9	1.7

Number of data points = 14

Number of regressed parameters (IAST-FR) and (IAST-SR) = 0

In summary, the predictive IAST-FR model was only capable of simulating the NOM and the best prediction was found using NOM's molecular weight 100 g/mol. Modifying the IAST model using Summers-Roberts (i.e., IAST-SR) model improved the simulation of ferrous iron and resulted in a good fit for NOM using a molecular weight of 100 g/mol for NOM. However, both of the IAST-FR and IAST-SR models were not capable of simulating the ferrous iron isotherm well despite the improvement of the IAST-SR predictions for ferrous iron.

6.5.2 IAST-SR One Pseudocomponent Model

The ferrous iron simulation using the alternative approach, IAST-SR one pseudocomponents model, showed a very similar fit to the IAST-FR one pseudocomponent (Figure 6-8.b). However, a slight improvement was noticed when modeling the NOM in Vars raw water at liquid phase concentration (C_e) greater than 1.5 mgTOC/L (Figure 6-8.a). The regressed parameters of the IAST-SR model are summarized in Table 6-13. The best fit of ferrous iron adsorption data was achieved with a NOM molecular weight of 111.6 g/mol which is the same as the regressed value obtained by the IAST-FR one pseudocomponent. Table 6-14 compares the fit indicators between the IAST-FR and IAST-SR one pseudocomponent models. The difference in the fit indicators (CV(RMSE) and AAPE) for the ferrous iron solid-phase concentration (q_e) between IAST-FR and IAST-SR were found to be 1.1% and 0.8%, respectively. The fit indicators (CV(RMSE) and AAPE) for the NOM solid phase concentration (q_e) of IAST-SR model were 93.9% and 35.3% whereas the values for IAST-FR model were 125.5% and 46.5%, respectively. The IAST-FR and IAST-SR models using one pseudocomponent are considered as good models that successfully described the competitive adsorption isotherms of ferrous iron in Vars raw water. Even though, the use of the IAST-SR model improved the simulation of NOM over the IAST model, it was not able to accurately simulate the NOM in Vars raw water.

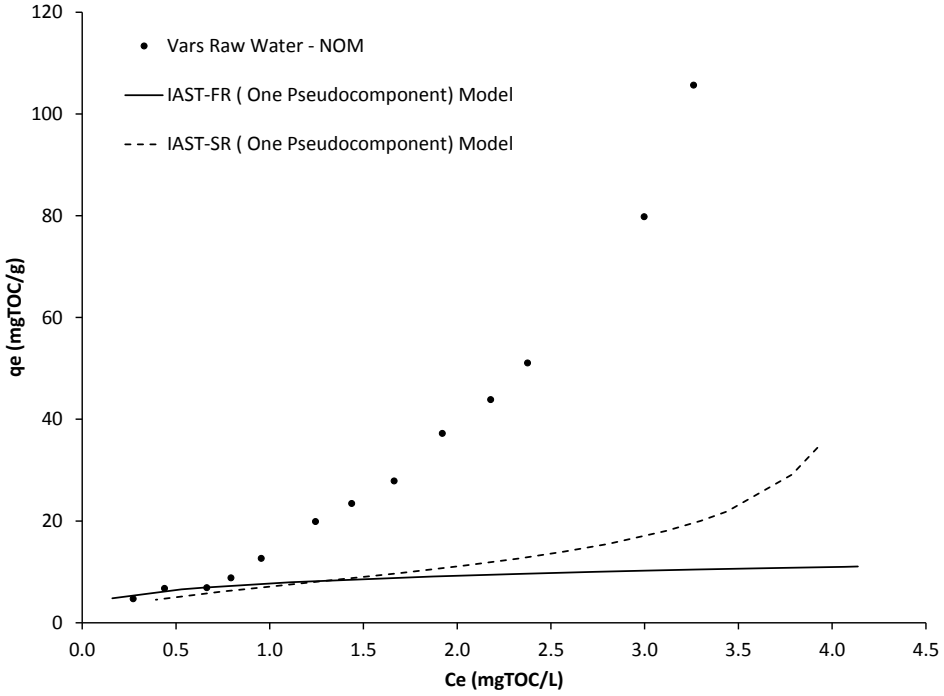

(a)

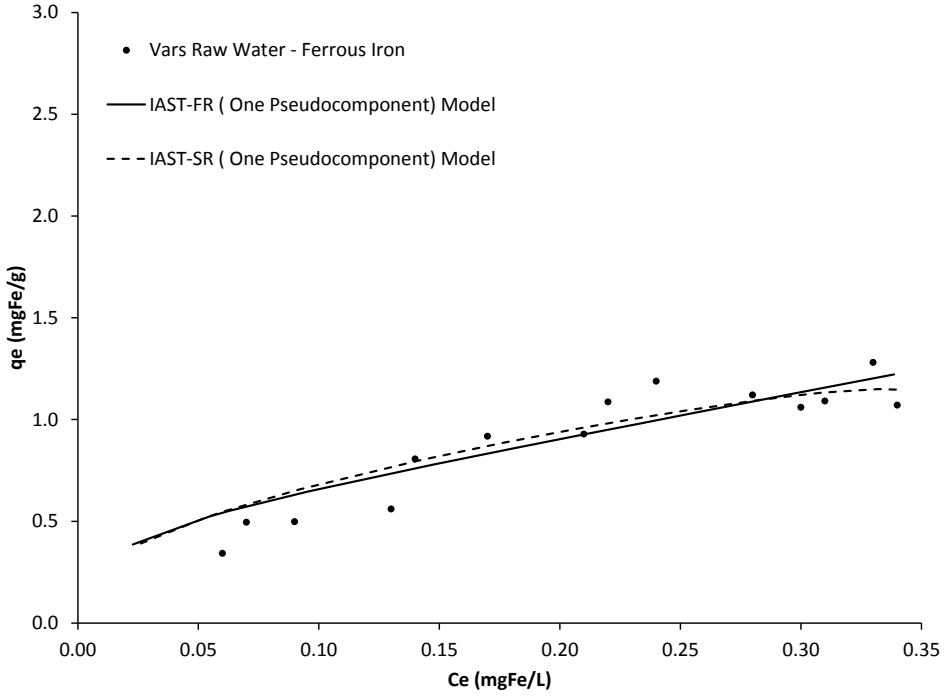

(b)

Figure 6-8: IAST-FR and IAST-SR one pseudocomponent model simulations of: (a) NOM and (b) ferrous iron

Table 6-13: Regressed parameters used for IAST-SR one pseudocomponent model

Model	Component	Initial Concentration (mgTOC/L)	Initial Concentration (µmol/L)	Molecular Weight (g/mol)	K_{SR} (µmol/g)·(g/µmol)^n	n_{SR}
IAST-SR	NOM	4.24	75.99	111.6	33.87	0.26
	Ferrous Iron	0.35	6.27	55.8	42.09	0.20

Note: Organic carbon was assumed to account for 50% of the NOM molecular weight

Table 6-14: Comparison between fit indicators for IAST-FR and IAST-SR one pseudocomponent models

Model	Fit Indicator	Ferrous Iron q_e	NOM q_e
IAST-FR	CV(RMSE) (%)	10.2	126.5
	AAPE (%)	8.0	46.5
IAST-SR	CV(RMSE) (%)	9.1	93.9
	AAPE (%)	7.2	35.3

Number of data points = 14

Number of regressed parameters (IAST-FR) : 3 (MW_{NOM}, $K_{F\text{-}NOM}$, $n_{F\text{-}NOM}$)

Number of regressed parameters (IAST-SR) :3 (MW_{NOM}, $K_{SR\text{-}NOM}$, $n_{SR\text{-}NOM}$)

6.5.3 IAST-SR Two Pseudocomponents Model

The graphical representations of the results of NOM and ferrous iron simulations using IAST-SR with two pseudocomponents are presented in Figure 6-9 and all regressed parameters are summarized in Table 6-15. The simulation shows that the model was only capable to model the ferrous iron only and was not able to simulate the NOM well. The assumption of fixing the value of (n) was tested and did not result in a good fit, so the values had to be regressed independently. The regressed values of (n) were found to be 0.15 and 0.25 for components one and two, respectively. The regressed initial concentrations of the

two NOM pseudocomponents were found to be 1.50 and 2.74 mgTOC/L for pseudocomponents one and two, respectively. Also, the regressed molecular weights of both components were 250 and 150 g/mol. As discussed in the description of the simulation of IAST-FR two pseudocomponents model (section 6.4.3), the simulation shows that the competitive ferrous isotherms were slightly wavy. However, the use of the modified IAST-SR model with two pseudocomponents improved the shape of the simulation of ferrous iron compared to the IAST simulations (Figure 6-9.b). The fit indicator (CV(RMSE) and AAPE) summarized in Table 6-16 for the solid-phase concentration of ferrous iron using IAST with two pseudocomponent are 14.1% and 6.8% whereas the values of the simulation using IAST-SR with two pseudocomponents are 12.8% and 6.5%, respectively. Even though none of the models was capable of simulating the NOM in Vars raw water as expected, using the IAST-SR has slightly improved the NOM simulation compared to the IAST-FR simulation. Such an improvement was coincidental since the model was used to fit the ferrous iron data only. The fit indicator (CV(RMSE) and AAPE) for the solid-phase concentration of NOM using IAST-FR two pseudocomponent are 191.8% and 72.7% whereas the values of the simulation using IAST-SR with two pseudocomponents are 151.1% and 45.8%, respectively. According to the results of ferrous iron simulations, the IAST-SR and IAST-FR models using two pseudocomponents were considered as good models that successfully described the competitive adsorption isotherms of ferrous iron in Vars raw water. The IAST-SR model has improved the fit of ferrous iron and the simulation shape was found to be better than that of the IAST-FR two pseudocomponents.

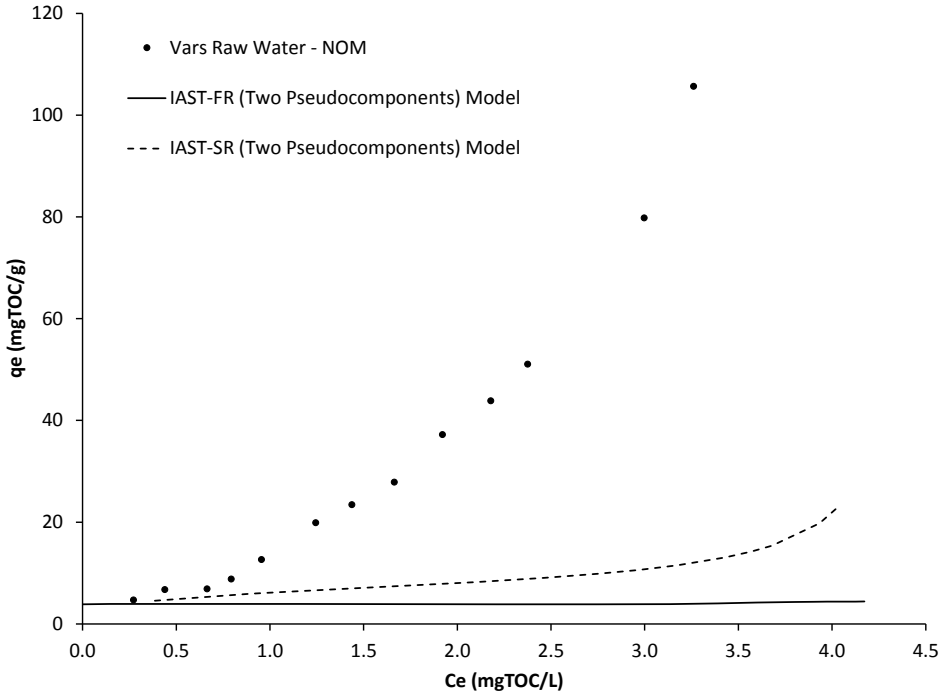

(a)

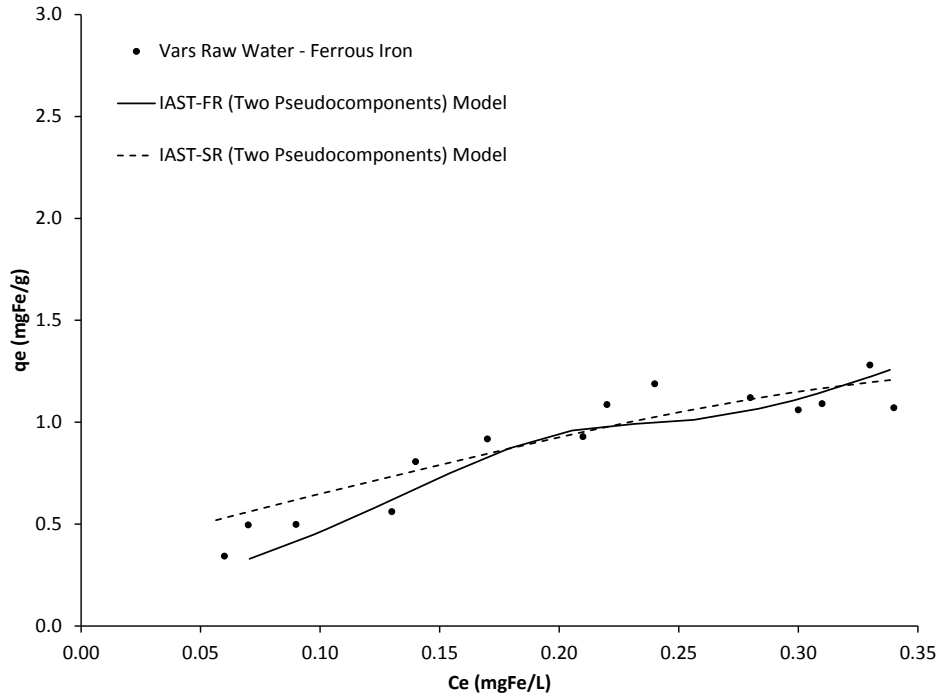

(b)

Figure 6-9: IAST-FR and IAST-SR two pseudocomponents model simulations of: (a) NOM and (b) ferrous iron

Table 6-15: Regressed parameters used for IAST-SR two pseudocomponents model

Model	Component Number	Initial Concentration (mgTOC/L)	Initial Concentration (µmol/L)	Molecular Weight (g/mol)	K_{SR} (µmol/g)·(g/µmol)^n	n_{SR}
IAST-SR	NOM – 1	1.50	12.00	250	35.14	0.15
	NOM – 2	2.74	36.53	150	41.87	0.25

Note: Organic carbon was assumed to account for 50% of the NOM molecular weight

Table 6-16: Comparison between fit indicators for IAST-FR and IAST-SR two pseudocomponents models

Model	Fit Indicator	Ferrous Iron q_e	NOM q_e
IAST-FR	CV(RMSE) (%)	14.1	191.8
	AAPE (%)	6.8	72.2
IAST-SR	CV(RMSE) (%)	12.8	151.1
	AAPE (%)	6.5	45.8

Number of data points = 14

Number of regressed parameters (IAST-FR) :

8 ($C_{o\text{-}NOM\text{-}1}$, $C_{o\text{-}NOM\text{-}2}$, $MW_{NOM\text{-}1}$, $MW_{NOM\text{-}2}$, $K_{F\text{-}NOM\text{-}1}$, $K_{F\text{-}NOM\text{-}2}$, $n_{F\text{-}NOM\text{-}1}$, $n_{F\text{-}NOM\text{-}2}$)

Number of regressed parameters (IAST-SR) :

8 ($C_{o\text{-}NOM\text{-}1}$, $C_{o\text{-}NOM\text{-}2}$, $MW_{NOM\text{-}1}$, $MW_{NOM\text{-}2}$, $K_{SR\text{-}NOM\text{-}1}$, $K_{SR\text{-}NOM\text{-}2}$, $n_{SR\text{-}NOM\text{-}1}$, $n_{SR\text{-}NOM\text{-}2}$)

6.5.4 Ding Modified IAST-SR Model

Since the variation of the IAST-FR model that was suggested by Ding *et al.* (2006) resulted in a good simulation for ferrous iron, the same approach was tested using IAST-SR model. The Summers-Roberts constants (K_{SR} and n_{SR}) as well as the molecular weight of the site competing (SC) fraction of NOM were equated to the values of ferrous iron. The only unknown to be regressed is the initial concentration of the (SC) fraction of NOM. The Ding modified IAST-FR and IAST-SR models were not capable of simulating the site competing fraction of the NOM (Figure 6-10.a). As for the ferrous iron simulation using both model

variations, Figure 6-10.b shows that only the IAST-FR model was capable of fitting the ferrous iron experimental data since the Ding modified IAST-SR simulation yielded concave upward shaped isotherms and the trend of the ferrous iron isotherm data is rather concave downward. The regressed value of the initial concentration of SC fraction using IAST-SR model (Table 6-17) was equal to 54.48 µmol/L which is equivalent to 1.52 mgTOC/L. The comparison between the fit indicators of each model variation shows deterioration in the quality of the IAST-SR simulation compared to the IAST-FR model (Table 6-18). The fit indicators (CV(RMSE) and AAPE) for the ferrous iron solid phase concentration (q_e) of IAST-SR model were 23.3% and 14.7% whereas the values for IAST-FR model were 9.2% and 9.0%, respectively. Accordingly, the model was rejected as a successful competitive adsorption model for NOM and ferrous iron in Vars raw water.

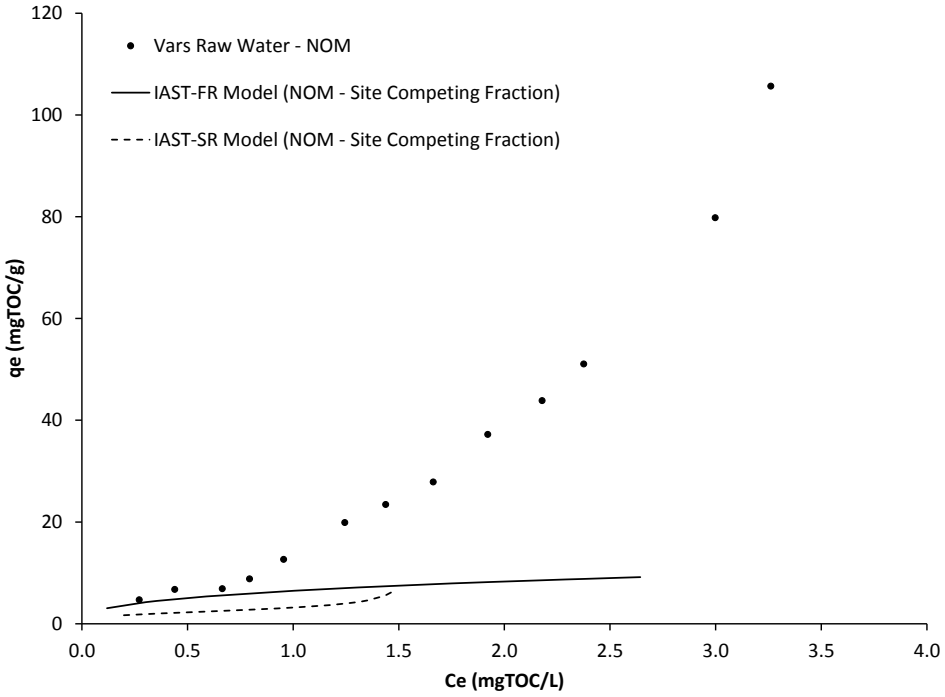

(a)

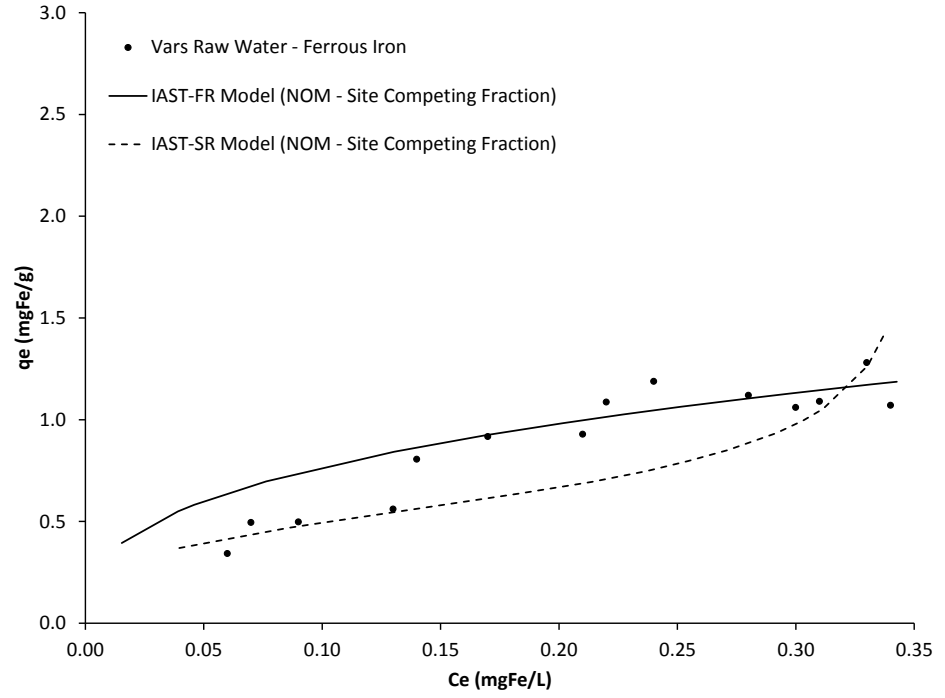

(b)

Figure 6-10: Ding modified IAST-FR and IAST-SR model simulations of: (a) the site competing (SC) fraction of NOM and (b) ferrous iron

Table 6-17: Regressed parameters for Ding modified IAST-SR model of ferrous iron and the site competing (SC) fraction of NOM.

Model	Component	Initial Concentration (mg/L)	Initial Concentration (µmol/L)	Molecular Weight (g/mol)	K_{SR} (µmol/g)·(g/µmol)^n	n_{SR}
IAST-SR	NOM (SC Fraction)	1.52	54.48	55.8	42.09	0.20
	Ferrous Iron	0.35	6.27	55.8	42.09	0.20

Note: Organic carbon was assumed to account for 50% of the NOM molecular weight

Table 6-18: Comparison between fit indicators for Ding modified IAST-FR and IAST-SR models of ferrous iron and the site competing (SC) fraction of NOM.

Model	Fit Indicator	Ferrous Iron q_e	NOM (SC Fraction) q_e
IAST-FR	**CV(RMSE) (%)**	9.2	103.0
	AAPE (%)	9.0	40.0
IAST-SR	**CV(RMSE) (%)**	23.3	101.6
	AAPE (%)	14.7	41.8

Number of data points = 14

Number of regressed parameters: 1 ($C_{o\text{-}NOM}$)

6.5.5 Kilduff-Wigton Modified IAST-SR Model

Since the Kilduff-Wigton modified IAST-FR model generated good simulations for both NOM and ferrous iron (section 6.4.5), the Summers-Roberts based version may provide even better simulations. In the proposed model, the calculations of the competitive fractions of ferrous iron using IAST-SR are calculated using the following equations:

$$q_{e\text{-}Fe\text{-}comp} = \left(\frac{V}{M}\right) C_{Fe\text{-}initial\text{-}comp} - \left(\frac{V}{M}\right)\left(\frac{q_{e\text{-}Fe\text{-}comp}}{q_{e\text{-}NOM} + q_{e\text{-}Fe\text{-}comp}}\right)\left[\frac{\left(n_{SR\text{-}Fe\text{-}comp}\frac{q_{e\text{-}NOM} + q_{e\text{-}Fe\text{-}comp}}{n_{SR\text{-}NOM} + n_{SR\text{-}Fe\text{-}comp}}\right)}{(1-\theta)K_{SR\text{-}Fe\text{-}comp}}\right]^{1/n_{SR\text{-}Fe\text{-}comp}} \quad (6\text{-}7)$$

$$C_{e\text{-}Fe\text{-}comp} = \left(\frac{q_{e\text{-}Fe\text{-}comp}}{q_{e\text{-}NOM} + q_{e\text{-}Fe\text{-}comp}}\right)\left[\frac{\left(n_{SR\text{-}Fe\text{-}comp}\frac{q_{e\text{-}NOM} + q_{e\text{-}Fe\text{-}comp}}{n_{SR\text{-}NOM} + n_{SR\text{-}Fe\text{-}comp}}\right)}{(1-\theta)K_{SR\text{-}Fe\text{-}comp}}\right]^{1/n_{SR\text{-}Fe\text{-}comp}} \quad (6\text{-}8)$$

Where: $K_{SR\text{-}Fe\text{-}comp}$ = the single solute Summers-Roberts model parameter of the competitive fractions of ferrous iron ((mg/g)·(mg/g)^n); $n_{SR\text{-}Fe\text{-}comp}$ = the single solute Summers-Roberts exponent of competitive fractions of ferrous iron; $C_{e\text{-}Fe\text{-}comp}$ = equilibrium liquid phase concentration of the competitive fractions of ferrous iron (mol/L); $q_{e\text{-}Fe\text{-}comp}$ = equilibrium solid phase concentration of the competitive fractions of ferrous iron (mol/gGAC); $q_{e\text{-}NOM}$ = equilibrium solid phase concentration of the NOM (mol/gGAC); $n_{SR\text{-}NOM}$ = single solute Summers-Roberts model parameter of the NOM and (1- θ) = the fraction of the GAC surface area on which there are competitive effects.

The mass of target compound (i.e., iron) adsorbed by surfaces with competition is not included in the initial concentration of iron used in the IAST-SR calculations. Accordingly, the corrected values representing the competitive fraction of the target compound initial concentration have to be incorporated into the IAST-SR calculations using the following equation:

$$C_{Fe\text{-}initial\text{-}comp} = C_{Fe\text{-}Total} - \left(\frac{M}{V}\right) q_{e\text{-}Fe\text{-}noncomp} \quad (6\text{-}9)$$

Where: $C_{Fe\text{-}initial\text{-}comp}$ = initial concentration of the competitive fractions of ferrous iron (mol/L); $C_{Fe\text{-}initial\text{-}Total}$ = Total initial concentration of ferrous iron obtained from the isotherm

experiments (mol/L) and $q_{Fe\text{-}noncomp}$ = equilibrium solid phase concentration of the non-competitive fractions of ferrous iron (mol/gGAC).

The model was applied on the competitive isotherm data obtained from Vars raw water and the best fit for ferrous iron was obtained when the θ-parameter was equal to 0.81 and the NOM's molecular weight was 3550 g/mol (Table 6-19). Figure 6-11 shows a comparison between the fits of Kilduff-Wigton modified IAST-FR and IAST-SR models for NOM and the competitive fraction of ferrous iron. The IAST-SR model shows a similar fit to the IAST-FR for ferrous iron (Figure 6-11.b) without distinctive improvements in the simulation. As for the simulation of the NOM, the IAST-SR shows deterioration in the quality of the fit by underpredicting the isotherm data when compared to the IAST-FR (Figure 6-11.a). The fit indicators (CV(RMSE) and AAPE) for the solid-phase concentration of ferrous iron are 30.6% and 33.9%, respectively (Table 6-20). The fit indicator (CV(RMSE) and AAPE) for the solid-phase concentration of NOM are 78.1% and 49.6%, respectively. Thus the Kilduff-Wigton modified IAST-FR model gave better simulations for both NOM and ferrous iron than Kilduff-Wigton modified IAST-SR model.

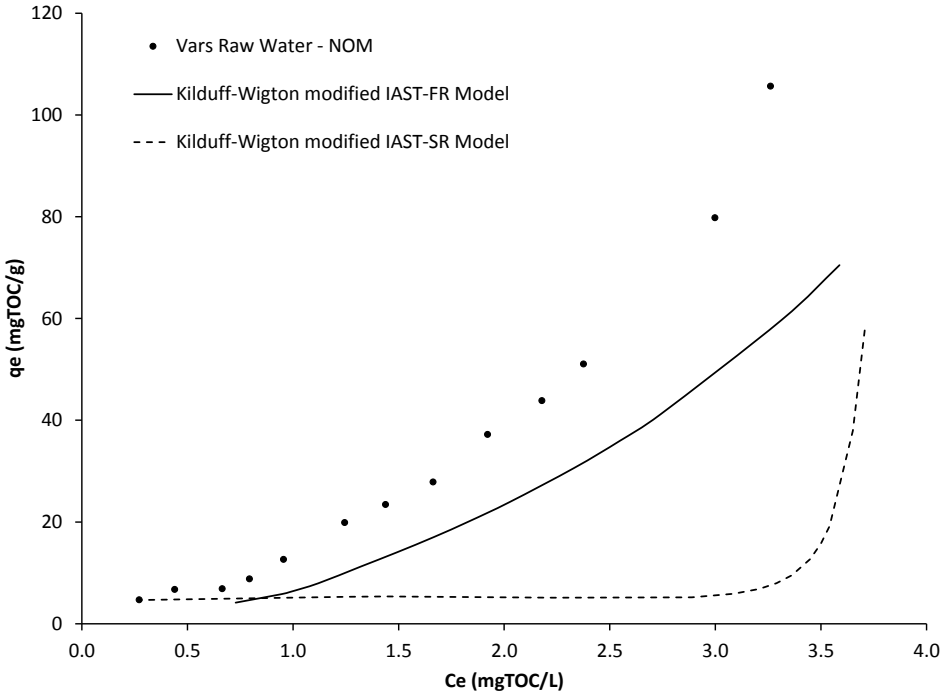

(a)

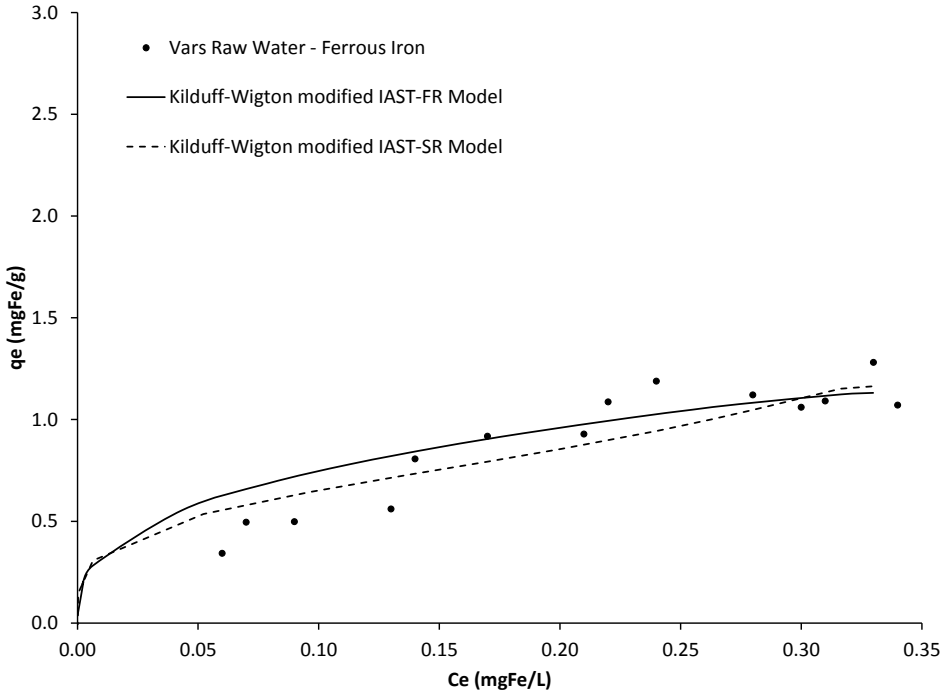

(b)

Figure 6-11: Kilduff-Wigton modified IAST-FR and IAST-SR models of: (a) NOM and (b) competitive fraction of ferrous iron

Table 6-19: Regressed parameters for Kilduff-Wigton modified IAST-FR and IAST-SR models of NOM and competitive fraction of ferrous iron

	Ferrous Iron	NOM
MW (g/mol)	55.8	3550
Initial Concentration (µmol/L)	6.27	2.39
θ	0.81	0.81
K_{SR} (µmol/g)·(g/µmol)n_{SR}	42.09	5.57
n_{SR}	0.20	0.45

Note: Organic carbon was assumed to account for 50% of the NOM molecular weight

Table 6-20: Fit indicators for Kilduff-Wigton modified IAST-FR and IAST-SR models of NOM and competitive fraction of ferrous iron

Model	NOM - Molecular Weight (g/mol)	θ	Fit Indicator	Ferrous Iron q_e	NOM q_e
IAST-FR	3000	0.85	CV(RMSE) (%)	26.1	39.5
			AAPE (%)	28.9	15.8
IAST-SR	3550	0.81	CV(RMSE) (%)	30.6	78.1
			AAPE (%)	33.9	49.6

Number of data points = 14

Number of regressed parameters = 2 (θ, MW_{NOM})

Using other types of regression based models offer an alternative to the IAST based models. Several of these models were evaluated in Appendix D. Most of these models did not fit the data well except the highly empirical Fritz and Schlunder model that was found to be capable to model both NOM and ferrous iron in Vars raw water utilizing six adjustable parameters. However, due to its empirical nature, it is unclear if the Fritz and Schlunder model would be able to simulate adsorption experiments using different iron and NOM concentrations. Due to these uncertainties, it was not used further.

Several experiments were conducted to develop another isotherm to confirm the effectiveness of the IAST models tested in this study. The isotherm experiments of Vars raw water were repeated three times prior to the implementation of the new isotherm experimental technique (discussed in Chapter 3) but none of them gave good results due to the problems of ferrous iron oxidation. An additional isotherm experiment was also performed using Vars raw water spiked with ferrous iron (by adding ferrous ammonium sulfate hexahydrate) prior to filling the isotherm bottles. The pH of the ferrous iron salt was adjusted to 6 before the solution was mixed with Vars raw water. pH 6 was chosen based on the findings of (Stumm and Lee, 1961), who found that the rate oxidation of ferrous iron is pH-dependent and rate of oxidation reduces at pH lower than 6. However, once the solution was mixed with Vars raw water, the total pH was increased from 6 to 8. Such a change in pH led to significant oxidation of ferrous iron and the initial ferrous iron concentration decreased from 2.0 mg/L to 0.42 mg/L. Also, the isotherm conducted with this solution showed a large variability. Unfortunately, these experiments restricted the ability to confirm the suitability of the best fitting models above.

6.6 Column Simulation

The competitive adsorption isotherms between iron and NOM in Vars raw water were successfully modeled using different variations of the IAST models. The ultimate benefit of this modeling effort is that they can be used in predicting the column breakthrough in Vars. This section presents the simulation of Vars GAC column data using one of the competitive isotherm models and the pore and surface diffusion GAC column model (PSDM). The PSDM is a mechanistic model of fixed bed adsorption that has been shown to successfully model multi-solute adsorption systems (Crittenden *et al.*, 1986b; Hutzler *et al.*, 1986; Hand *et al.*, 1997). The model simulation was conducted using the AdDesignS software (Michigan Technological University, Houghton, MI) (Mertz *et al.*, 1999). The software accounts for the effects of competitive adsorption using the IAST in combination with the Freundlich isotherm (i.e. IAST-FR). In order to apply the PSDM, the software requires the column system design and operating parameters including the GAC particle diameter, bed porosity, bed density and flowrate. In addition, the equilibrium adsorption and kinetic parameters of

iron and NOM are also required. The equilibrium adsorption parameters used for the simulation were determined using the IAST-FR (one pseudocomponent) model summarized in Table 6-3. The kinetics parameters needed for the simulation include the tortuosity (τ), film mass transfer coefficient (k_f), surface (D_s) and pore (D_p) diffusion coefficients. A tortuosity value of 3.0 was used as it has been found to yield a good match between the PSDM and the experimental data in typical water treatment applications (Sontheimer *et al.*, 1988; Cussler, 2009). The film mass transfer coefficients (k_f) were determined from the Gnielinski correlation (Gnielinski, 1978) using the following equation:

$$k_f = \left[2+0.644\left(\frac{\rho\, d_P\, \nu}{\mu} \right)^{1/2} \left(\frac{\mu}{\rho\, D_L} \right)^{1/3} \right] \frac{\left[1+1.5\left(1-\varepsilon\right)\right] D_L}{d_P} \qquad (6\text{-}10)$$

Where: d_p = GAC particle diameter (m); ε = GAC void fraction; ρ = water density (kg/m^3); ν = liquid phase interstitial velocity (m/s); μ = water viscosity (kg/m/s); and D_L = adsorbate liquid diffusion coefficient (m^2/s). The liquid diffusion coefficient for both components in water was estimated via the Hayduk and Laudie (1974) correlation:

$$D_L = \frac{13.26\times10^{-5}}{\mu^{1.14}\, V_b^{0.589}} \qquad (6\text{-}11)$$

Where: V_b = molar volume of the adsorbate at the normal boiling point (cm^3/mol).

The surface diffusion coefficient (D_s) was obtained by relating the surface diffusion flux to the pore diffusion flux by a correlation factor (the surface to pore diffusion flux ratio - SPDFR). This results in the following correlation which is used to calculate the surface diffusion coefficient (Sontheimer *et al.*, 1988):

$$D_S = \frac{D_L\, \varepsilon\, C_0}{\tau_P\ \rho_a\ q_0} \times \text{SPDFR} \qquad (6\text{-}12)$$

Where: C_o = initial inlet concentration (mg/L); D_s = surface diffusion coefficient (cm^2/s); q_o = solid phase concentration in equilibrium with C_o for a single-solute equilibrium (mg/g); ρ_a = apparent adsorbent density (g/L); τ_p = adsorbent tortuosity; and SPDFR = surface to pore diffusion flux ratio. For liquid phase adsorption where there is background organic matter

and single or multiple components are present, an SPDFR between 2.0 and 8.0 can be used (Hand *et al.*, 1989). The AdDesignS software defaults to a SPDFR value of 5.0.

The pore diffusion coefficients (D_p) were determined by dividing the liquid diffusion coefficient in water (D_L) of both compounds by the tortuosity (Sontheimer *et al.*, 1988):

$$D_P = \frac{D_L}{\tau_P} \qquad (6\text{-}13)$$

The following table summarizes the PSDM model inputs parameters used in the AdDesignS software to simulate the iron breakthrough at Vars GAC columns.

Table 6-21: PSDM input parameters

System Design And Operating Parameters		
GAC Particle Diameter (cm)	0.08	
GAC Bed Porosity	0.70	
GAC Apparent density (g/mL)	0.75	
Flowrate (m^3/d)	300	
GAC Bed Mass (kg)	7500	
The Equilibrium Adsorption Parameters	**NOM**	**Iron**
Initial Concentration (mg/L)	4.24	1.21
Molecular Weight (g/mol)	111.60	55.80
Freundlich Parameter, K_F $(mg/g)\cdot(L/mg)^n$	8.04	10.35
Freundlich Parameter, n_F	0.26	0.35
The Kinetic Parameters	**NOM**	**Iron**
The Molar Volume, V_b (cm^3/mol)	$1.00\times10^{+03}$	$0.71\times10^{+01}$
The Liquid Diffusion Coefficient, D_L (cm^2/s)	2.41×10^{-06}	4.43×10^{-05}
The Film Mass Transfer Coefficients, k_f (cm^2/s)	4.05×10^{-04}	3.42×10^{-03}
The Surface Diffusion Coefficient, D_S (cm^2/s)	1.36×10^{-09}	7.54×10^{-09}
The Pore Diffusion Coefficient, D_P (cm^2/s)	8.02×10^{-07}	1.48×10^{-05}
Tortuosity	3	3
SPDFR	5	5

Figure 6-12 shows the results of the PSDM simulation compared to the iron breakthrough curve obtained from Vars. The PSDM predicted an iron chromatographic effect after 100 days of operation, thus showing that the competitive isotherms could predict a chromatographic effect. However, the model did not describe the iron breakthrough at Vars accurately. The model predicted the start of the iron breakthrough to be after 61 days of operation whereas the actual breakthrough started after 42 days. This shift in prediction was likely due to the higher than actual adsorption capacity (q_{Fe}) predicted by the IAST-FR (one pseudocomponent) model. The actual iron adsorption capacity (q_{Fe}) obtained by integrating the Vars iron breakthrough was 2.1 mg/g. On the other hand, the PSDM simulations predicted a value of 3.9 mg/g. A few possible explanations for the delay in the simulated breakthrough have been identified. First, NOM preloading which was not incorporated in the isotherms may cause a reduction in the adsorption capacity for iron in the GAC column at Vars. Second, the discharge of the precipitated iron from the GAC column (similar to that observed in the isotherms) may also have a significant role in the observed behavior at Vars. Third, the low accuracy (15%) of the field flow measuring equipment may have also led to the inaccurate prediction. In order to further investigate the NOM preloading effect on the prediction of the iron breakthrough, it is recommended that isotherms with GAC preloaded with Vars NOM be conducted, model these isotherms and use these new isotherms to re-simulate the column performance for the prediction of the iron chromatographic effect.

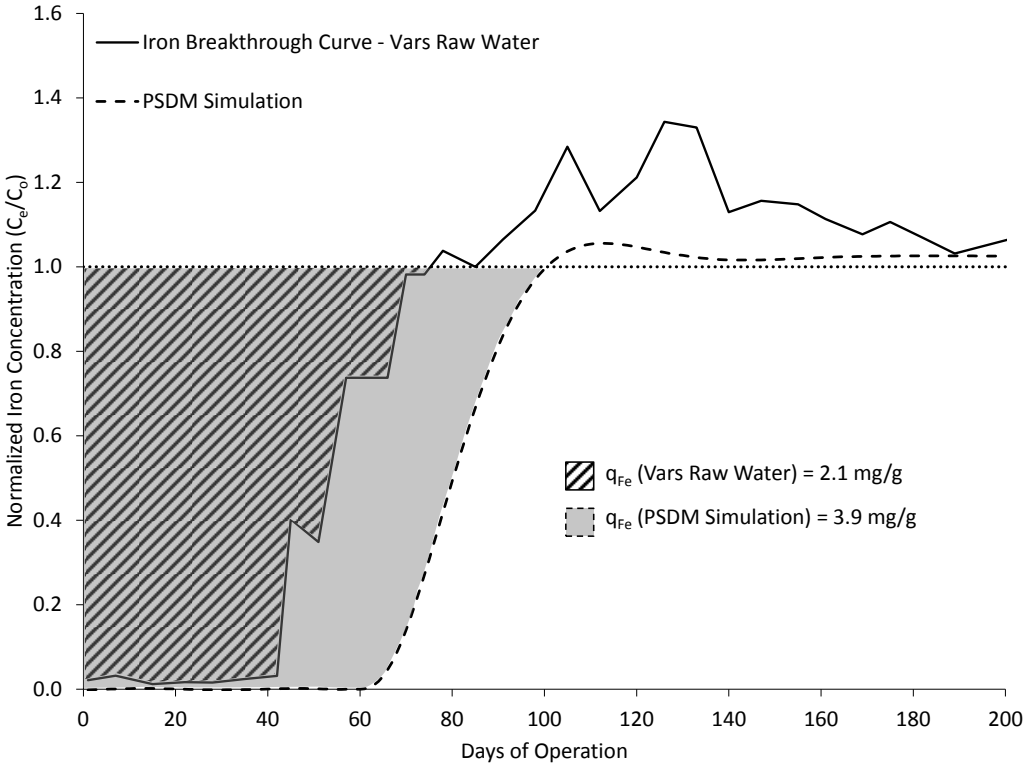

Figure 6-12: PSDM simulation of the iron breakthrough curve at Vars

6.7 Summary

The main focus of this study is to determine if the activated carbon adsorption of iron in competition with the NOM in Vars raw water can be described by different variations of the IAST models. The ferrous iron was considered to be the target compound competing with NOM since it was found to be the dominant iron species in Vars raw water. The ferrous iron adsorption capacity in Vars raw water was about $1/7^{th}$ of those of ferrous iron in organic-free water due to the competition with NOM over the GAC adsorbing sites. On the other hand, the NOM adsorption was not decreased due to the presence of ferrous iron.

In the modeling attempts, different variations of the IAST models in combination with the Freundlich and the Summers-Roberts single solute isotherms were evaluated. Most of the variations of the regression-based IAST-FR and IAST-SR models were capable of simulating the ferrous iron adsorption in competition with the NOM in Vars groundwater. Some of the simulations were good and others were excellent. Table 6-22 summarizes the fit indicator

CV(RMSE) obtained by the different variations of IAST models. The use of IAST-SR improved the fit of ferrous iron using one and two pseudocomponents over the IAST-FR model and the best fit was achieved with IAST-SR one pseudocomponent (CV(RMSE) = 9.1%). Even though the modification of IAST-SR has improved the simulation of the NOM over those by the IAST-FR models, none of the models were accurately capable of simulating the NOM and ferrous iron simultaneously. As explained earlier, this was expected as the model fitting was based just on simulating the ferrous iron loadings, not both the iron and NOM loadings. It should be noted that in the literature most regression based IAST models were used to just model the target organic target compounds without attempting to model the NOM adsorption. Given the fact that the presence of ferrous iron did not significantly decrease the adsorption capacity of NOM, a simplified approach is to use the NOM single solute isotherm to model the competitive NOM adsorption isotherm.

Table 6-22: Fit indicators CV(RMSE) of the best fits obtained by different variations of IAST-FR and IAST-SR models

Model	Variations	No. of Regressed Parameters	Ferrous Iron q_e	NOM q_e
IAST-FR (in combination with Freundlich model)	**One pseudocomponent**	3	10.2	126.5
	Two pseudocomponents	8	14.1	191.8
	Ding Modified	1	9.2	120.7
	Kilduff-Wigton Modified	2	26.1	39.5
IAST-SR (in combination with Summers-Roberts model)	**One pseudocomponent**	3	9.1	93.9
	Two pseudocomponents	8	12.8	151.1
	Ding Modified	1	23.3	101.6
	Kilduff-Wigton Modified	2	30.6	78.1

Column simulations using PSDM could not predict well the iron breakthrough at Vars. The possible explanations for the delay in the simulated breakthrough include:

- NOM preloading which was not incorporated in the isotherms may cause a reduction in the adsorption capacity for iron in the GAC column at Vars.
- The discharge of the precipitated iron from the GAC column (similar to that observed in the isotherms) may also have a significant role in the observed behavior at Vars. Breakthrough Prediction of NOM and Iron Removal by GAC using RSSCT

CHAPTER 7 BREAKTHROUGH PREDICTION OF NOM AND IRON REMOVAL BY GAC USING RSSCT

7.1 Introduction

This chapter will investigate whether the RSSCT approach can be used to simulate the adsorption of iron and NOM in the full-scale columns treating Vars raw water and to simulate the adsorption of NOM after the greensand treated Vars groundwater in the full-scale Vars GAC columns. To determine if the RSSCT approach could be used to predict the performance of the full-scale GAC column adsorbers a number of steps were taken. First, batch kinetics experiments were conducted using both water sources (i.e., Vars raw water and greensand treated water) with GAC of different particle sizes. Then, HSDM was used to calculate the NOM surface diffusivity coefficients (D_s) of each particle size in order to assess the relationship between D_s and GAC particle size. Finally, RSSCTs were performed and scaled to be able to conduct comparisons with full-scale column breakthroughs and ascertain the effectiveness of the RSSCT approach for these waters. The originality of the proposed investigation is that published literature involving RSSCT did not include studies on predicting the removal of iron and NOM by GAC.

7.2 Breakthrough Prediction of NOM and Iron using Vars Raw Water

7.2.1 Batch Kinetics of NOM using Vars Raw Water

A Carberry mixed batch reactor (CMBR) was used with Vars raw water and three different GAC particle sizes (20×30, 40×50 and 80×100 mesh sizes). In the CMBR, all the samples are exposed to the same adsorbent dose, which is difficult to achieve with the bottle-point method. Also, using this method would guarantee that the GAC particles are exposed to the same initial concentration of the compounds in the solution. Although a nitrogen gas atmosphere was maintained in the free-space within the reactor (as discussed in Chapter 3), there was oxidation of ferrous iron to ferric iron which made it impractical to conduct ferrous

iron adsorption kinetic experiments using the batch reactor. Accordingly, only the kinetics of NOM will be used in order to determine the type diffusivity relationship (linear or constant) in Vars raw water using F-400 GAC.

The surface diffusivity coefficient of NOM (i.e., D_s) was obtained by fitting the HSDM model prediction to experimental data for each kinetic data set. The numerical solution had been formulated using a MATLAB program built by Ding (2010) to solve the HSDM to get an aqueous concentration versus time profile for GAC. The program implements Rose (1952) model the adsorption kinetics for a spherical adsorbent particle assuming that it is controlled by the surface diffusion mechanism. The model consists of the partial differential describing the mass transfer within the particle (Equation 7-1) and its initial condition in Equation (7-2) and its boundary conditions described by Equations (7-3) and (7-4):

$$\frac{\partial q}{\partial t} = \frac{1}{r^2}\frac{\partial}{\partial r}\left(r^2 D_s \frac{\partial q}{\partial r}\right) \tag{7-1}$$

$$q = q_0(r) \quad \text{for } t = 0 \text{ and } 0 \le r \le R \tag{7-2}$$

$$\frac{\partial q}{\partial r} = 0 \qquad t \ge 0 \text{ and } r = 0 \tag{7-3}$$

$$q = q_s(t) \quad t \ge 0 \text{ and } r = R \tag{7-4}$$

Where: q = the solid phase loading of the NOM in the solution into the GAC particles (mgTOC/gGAC); q_s = the solid phase loading at the GAC particle surface (mg/gGAC); q_0 = initial amount of the NOM adsorbed into the GAC (mgTOC/gGAC); r and R = GAC particle radius (cm); D_s = surface diffusion coefficient (cm^2/min) and t = time elapsed during the kinetics experiment (min). Figure 7-1 shows the mass balance used in the HSDM as well as the initial and boundary conditions. The model assumes the activated carbon particles are spherical with a homogeneous structure and the adsorbate molecules diffuse along the internal surface of pores to adsorption sites. It also assumes the surface diffusion coefficient D_s is uniform. One of the assumptions used for simplifying the model was ignoring the thin film resistance and the liquid phase concentration in the bulk solution (i.e., C) was equal to the liquid phase concentration at the liquid phase before entering the GAC particle

concentration (i.e., C_s) (Figure 7-1). The HSDM can be used in conjunction with any isotherm model, which in our case is the Freundlich isotherm (Equation (7-5**)**. The HSDM requires the isotherm parameters (i.e., K_F and n_F) of the NOM in Vars raw water which had been determined earlier (Chapter 5) in order to substitute for the value of q_s in Equation (7-6):

$$q_s = K_F C^{n_F} \tag{7-5}$$

Where: q_s = the solid phase loading at the GAC particle surface (mg/gGAC) and it is related to the bulk solution concentration C (mg/L) by the isotherm equilibrium. The MATLAB code was formulated based on the Carslaw and Jaeger (1986) analytical solution of Rose's model (Equations 7-1 to 7-4) as applied to a batch reactor. This solution is:

$$\frac{C_0 - C(t)}{C_c} = \frac{6}{R^2}\sum_{i=1}^{\infty} e^{-i^2\pi^2\frac{D_s}{R^2}t}\left[\frac{R^2}{i^2\pi^2}q_0 + D_s\int_0^t e^{i^2\pi^2\frac{D_s}{R^2}(x)}q_s(x)dx\right] \tag{7-6}$$

Where: C_0= initial concentration of the NOM in the solution (mgTOC/L); C(t) = concentration of the NOM in the solution at time elapsed during the kinetics experiment (mgTOC/L); C_c = GAC dose used in the kinetics experiment (gGAC/L); R = GAC particle radius (cm); D_s = surface diffusion coefficient (cm^2/min); q_0 = initial amount of the NOM adsorbed into the GAC (i.e., q_0 = 0) (mgTOC/gGAC); t = time elapsed during the kinetics experiment (min) and q_s = the solid phase loading at the GAC particle surface (mg/gGAC) and its value is obtained by Equation (7-5). The proposed HSDM Equation (7-6) was solved numerically using MATLAB by minimizing the absolute average percentage error (AAPE) of C(t) while regressing the value of D_s. Details of the MATLAB code can be found in Ding's PhD thesis (Ding, 2010).

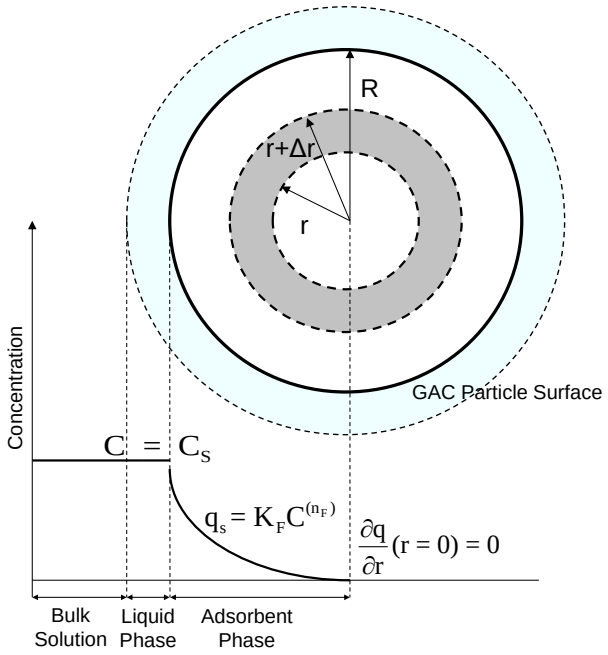

Figure 7-1: Mass balance used for the HSDM

Figure 7-2 displays the kinetics data of the NOM in Vars raw water. The lines in the graph are the results of the regression analysis using the HSDM model, for different particle sizes of GAC. The adsorption kinetics of NOM was very slow and more than 300 hours of operation was required for the plateau in the kinetic curves to be reached. The rate of adsorption was found to be affected by the GAC particle size where the 80×100 mesh size GAC adsorbs NOM more rapidly than the 40×50 particles which in turn adsorb more rapidly than the 20×30 mesh particles. The reason behind the rapid adsorption of the smaller GAC particle sizes is primarily due to the fact that the diffusion pathways inside the smaller GAC grains decrease and therefore, the intraparticle mass transfer is more rapid. Table 7-1 summarizes the regressed parameter values and fit indicators of the HSDM for NOM in Vars raw water using different GAC particle sizes. As expected the calculated effective surface diffusivities were higher for the 20×30 mesh GAC (3.36×10^{-11} cm^2/s) than for 40×50 mesh GAC (1.08×10^{-11} cm^2/s), and lowest for the 80×100 mesh GAC (0.38×10^{-11} cm^2/s). The fit indicators show that the HSDM resulted in very good fits for the NOM data. The absolute average percentage errors (AAPEs) of the HSDM using GAC with mesh sizes 20×30, 40×50 and 80×100 were found to be 1.27%, 1.95% and 1.65%, respectively. The calculated surface diffusivity value of 1.08×10^{-11} cm^2/s for 40×50 mesh GAC size was close to the 0.96×10^{-11}

cm^2/s obtained by Narbaitz (1985) for a river water and the 1.7×10^{-11} cm^2/s value obtained by Lee *et al.* (1981) using the same GAC particle size.

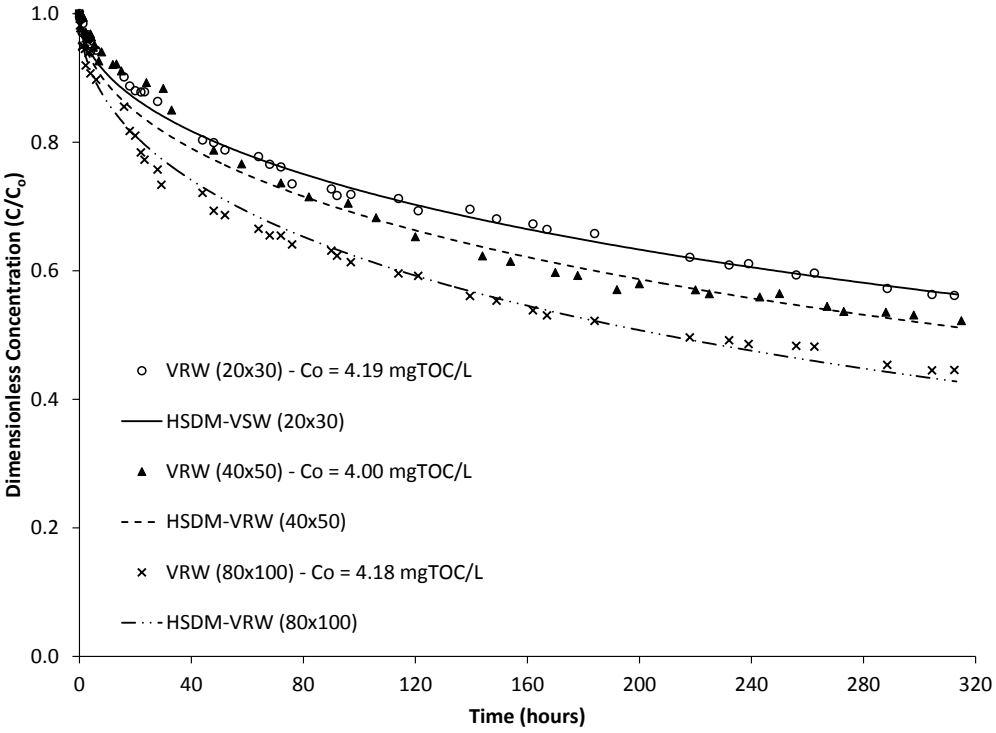

Figure 7-2: Adsorption kinetics of NOM in Vars raw water using different particle sizes of F-400 GAC with HSDM fits

Table 7-1: Parameters and fit indicators of the HSDM for NOM in Vars raw water using different GAC particle sizes

Parameters	Units	GAC Particle Sizes		
		20×30	40×50	80×100
R	(cm)	0.071	0.035	0.016
C_o	(mgTOC/L)	4.19	4.00	4.18
C_c	(gGAC/L)	0.06	0.06	0.06
K_F	$(mg/g)\cdot(L/mg)^n$	11.18	11.18	11.18
n_F		1.84	1.84	1.84
D_s	(cm^2/s)	3.36×10^{-11}	1.08×10^{-11}	0.38×10^{-11}
AAPE	(%)	1.27	1.95	1.65

According to Figure 7-3, the estimated diffusivities values for NOM on GAC are not constant, but rather vary approximately linearly with GAC particle size. These factors suggest that the linear diffusivity scaling may be more reasonable than the constant diffusivity scaling approach for the design of the RSSCT. Previous studies agree with this finding and they have shown that diffusion of NOM to the GAC adsorbing sites was proportional to the GAC particle sizes (Crittenden *et al.*, 1989; Sontheimer *et al.*, 1988).

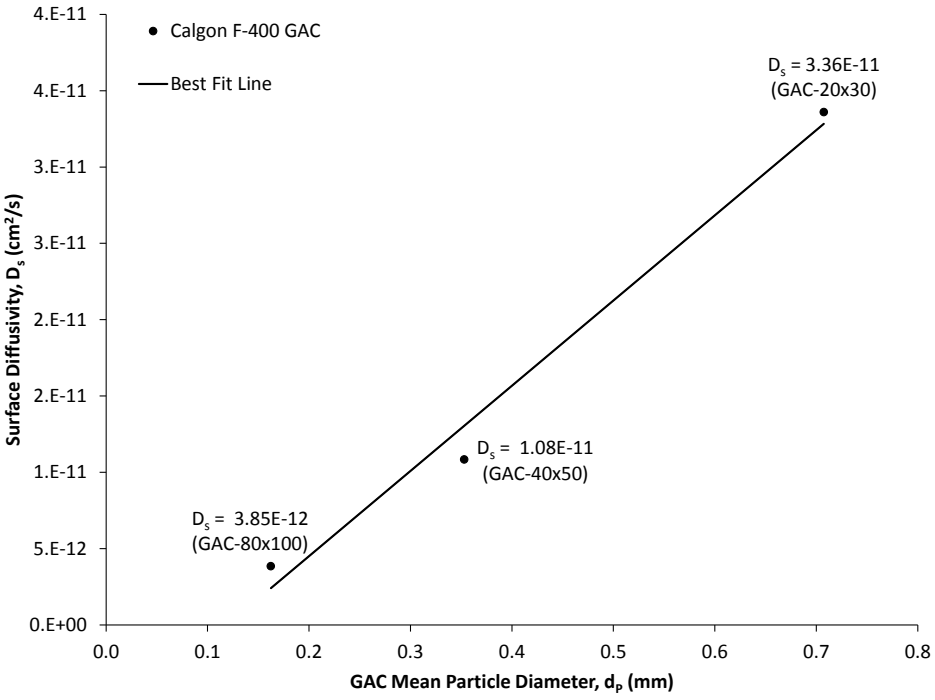

Figure 7-3: The dependence of the surface diffusivity coefficients (D_s) on GAC particle sizes for NOM in Vars raw water

7.2.2 RSSCT for Vars Raw Water

The main purpose of the RSSCT with Vars raw water was to test if it is possible to use this method to simulate the iron chromatographic problem that occurred at the Vars treatment plant. However, there were few limitations and problems observed during the operation of the RSSCT using Vars raw water. In spite of many attempts with increasing number of precautions, iron oxidation and precipitation in RSSCT feed reservoir could not be controlled which caused fluctuations in the feed iron concentrations. Accordingly, the only option was

to conduct the tests at the site (i.e., the Vars treatment plant) and continuously feed the RSSCT column with fresh groundwater. Given the plant characteristics, its distant location, its small size, its operating schedule, and access constraints made it nearly impossible to conduct such a test. Luckily, the City of Ottawa gave permission to conduct a RSSCT lasting up to five days. Such a limitation had a considerable impact on the operation of the RSSCT and which scaling design to be chosen (i.e., linear or constant diffusivity).

7.2.2.1 Breakthrough Prediction of Iron and NOM Removal using RSSCT

Table 7-2 summarizes the characteristics of Vars raw water used in the RSSCT tests, the concentration of NOM was 4.49 mgTOC/L. The concentration of total iron was found to be 1.25 mg/L and 76% of total iron in Vars raw water was in the ferrous iron form. These values were found to be comparable to the average values obtained from Vars treatment plant during the GAC full-scale run between June 11th, 2001 and May 27th, 2002, the only period during which the Vars GAC filters used F-400 to treat raw groundwater. The average values of NOM and iron concentrations obtained between these dates were 4.48 mgTOC/L and 1.33 mg/L, respectively. As for the temperature and pH of Vars raw water, the records of the City of Ottawa show that the values during that period were steady and the changes were in the range of 8.0 – 8.9 $^{\circ}$C for temperature and 7.4 – 8.0 for pH. The values of temperature and pH of Vars raw water obtained during the RSSCT were within these ranges and equal to 8.6 $^{\circ}$C and 7.9, respectively.

Table 7-2: Characteristics of Vars raw water used for the RSSCT (May 31st, 2011)

Parameters	Well # 1
pH	7.91
Temperature ($^{\circ}$C)	8.60
Total Fe (mg/L)	1.25
Fe (II) (mg/L)	0.95
Fe (III) (mg/L)	0.30
TOC (mgTOC/L)	4.49

The design and operational parameters used for the full-scale column and RSSCT using Vars raw water are summarized in Table 7-3. The full-scale column had an average flowrate of 12.5 m^3/hr (equivalent to 208,333 mL/min) during the treatment cycle between June 11th, 2001 and May 27th, 2002. Such a flowrate passing through the 7.31 m^2 cross-sectional area resulted in a hydraulic loading of 1.7 m/hr. This value is smaller than the recommended range of 5 to 15 m/hr for down-flow GAC contactors (MWH, 2005). This low value occured because the water demand was far below the design flow value. Due to the same reason, the full-scale column had an EBCT value of 89.8 min which is large than the design EBCT of 31 minutes for the GAC full-scale column at Vars. It should be noted that the design EBCT was also significantly larger than the conventional value of 10 to 20 minutes. The GAC size selected to be used in the RSSCT was 80×100 mesh size. This particle size is less that 1/5 that of the GAC particle size used in the full-scale column (i.e., 12×40 mesh size). Using such a small particle size would shorten the duration of the RSCCT and would also minimize the channeling effects (as the column diameter to GAC particle median diameter ratio equals 160) since the minimum column diameter to particle size ratio should be 50 to avoid such an effect (Martin, 1978). The design of the RSSCT resulted in a hydraulic loading of 8.8 m/hr and a flowrate of 78.3 mL/min. Using this calculated value of the hydraulic loading would result in the same Reynolds number for both full-scale and small-scale columns, which guarantees the similarities between the flows of both columns (i.e., Reynolds number = 1.1). However, the 78.3 mL/min flowrate is high and will result in a high interstitial velocity of water in the small-scale column, and hence, a high head loss. Accordingly, the suggestion of Crittenden (1991) was used where it was recommended that a lower velocity in the small-scale column be chosen, as long as the effect of dispersion in the small column does not become dominant over other mass transport processes. So, the flowrate was adjusted to a value of 10 mL/min which would result in a hydraulic loading of 1.14 m/hr (equivalent to 1.9 cm/min). Based on the RSSCT scaling equations (discussed in Chapter 2), changing the hydraulic loading would impact the mass of GAC to be used in the RSSCT. So, reducing the hydraulic loading from 8.8 to 1.14 m/hr (while keeping the same EBCT) would reduce the mass of GAC in the small column to 13.5 g. The recalculated value of Reynolds number based on this adjusted hydraulic loading was equal to 0.1 and studies have shown that the

adjustments to the RSSCT's Reynolds number to values between 0.1 and 1.0 have a negligible impact on results (Crittenden *et al.*, 1991; Summers *et al.*, 1995).

Table 7-3: Design and operational parameters used for full-scale column and RSSCT under constant and linear diffusivities using Vars raw water

Operational Parameters	**RSSCT**		**Full-Scale Column**
GAC Brand	Calgon F-400		Calgon F-400
Bulk Density (g/cm^3)	0.401		0.401
GAC Mean Particle Diameter (mm)	0.16 (80×100 mesh size)		0.84 (12×40 mesh size)
Column Diameter (cm)	2.6		305
Cross-Sectional Area (cm^2)	5.3		73100
Flowrate (mL/min)	10		208333
Hydraulic Loading (cm/min)	1.9		2.8
Reynolds Number	0.1		0.4
	RSSCT (Constant Diffusivity)	**RSSCT (Linear Diffusivity)**	
EBCT (min)	3.4	17.4	89.8
Depth of GAC (cm)	6.3	32.7	260
Mass of GAC (g)	13.5	69.6	7500×10^3
Iron Breakthrough Time (days)	1.6	8	42

Table 7-3 shows the design parameters used for the RSSCT under both the constant and linear varying diffusivity assumptions. The use of constant diffusivity to design the RSSCT results in a small column with an EBCT of 3.4 min, a GAC mass of 13.5 g, a GAC depth of 6.3 cm and a predicted start of the iron breakthrough at 1.6 days. The use of linear diffusivity would result in a small column with EBCT of 17.4 min, GAC mass of 69.6 g, GAC depth inside the small column of 32.7 cm and a predicted iron breakthrough of 8 days. The predicted iron breakthrough time for both designs (linear and constant) was calculated based on the start of the iron breakthrough of 42 days observed at Vars full-scale column. Based on the results of the kinetics experiments and the HSDM, the more appropriate design for the Vars raw water was the linear diffusivity RSSCT. However, due to operational constraints at the Vars treatment plant, the City of Ottawa could only provide us with a continuous flow of raw Vars groundwater for five consecutive days due to their operations schedule. Such a constraint did not allow us to use the linear diffusivity design since the estimated breakthrough time for iron was 8 days. So, it was decided to only use the constant diffusivity scale-up design with a calculated iron breakthrough time of 1.6 days.

The full-scale column and RSSCT iron breakthroughs are shown Figure 7-4. The influent concentrations of NOM and iron were analyzed seven times throughout the duration of each RSSCT to ensure that the influent concentrations remained constant and the average value of total iron was equal to 1.05 ± 0.07 mgFe/L. The results show that the full-scale data yielded an earlier iron breakthrough than scaled data from the RSSCT. According to the RSSCT design using constant diffusivity, the start of the iron breakthrough was expected to start after 1.6 days after 2.2 L/gGAC water were treated. However, the start of the iron breakthrough using the RSSCT was observed after 3 days and 3.4 L/gGAC water treated. The data shows that the RSSCT predicted the slope of the iron breakthrough and was not capable of predicting the onset of the full-scale breakthrough. Also, the results of the iron breakthrough obtained by the RSSCT show that an average concentration of iron of 0.05 mgFe/L started to appear in the effluent of the RSSCT after 1.0 L/gGAC water treated and before the start of the principal iron breakthrough. This 0.05 mgFe/L concentration was assumed to be in the form of NOM-iron complexes that are present in Vars raw water. It was discussed in Chapter

4 that complexed iron appeared before the start of the breakthrough was mostly in the form of NOM-iron complexes

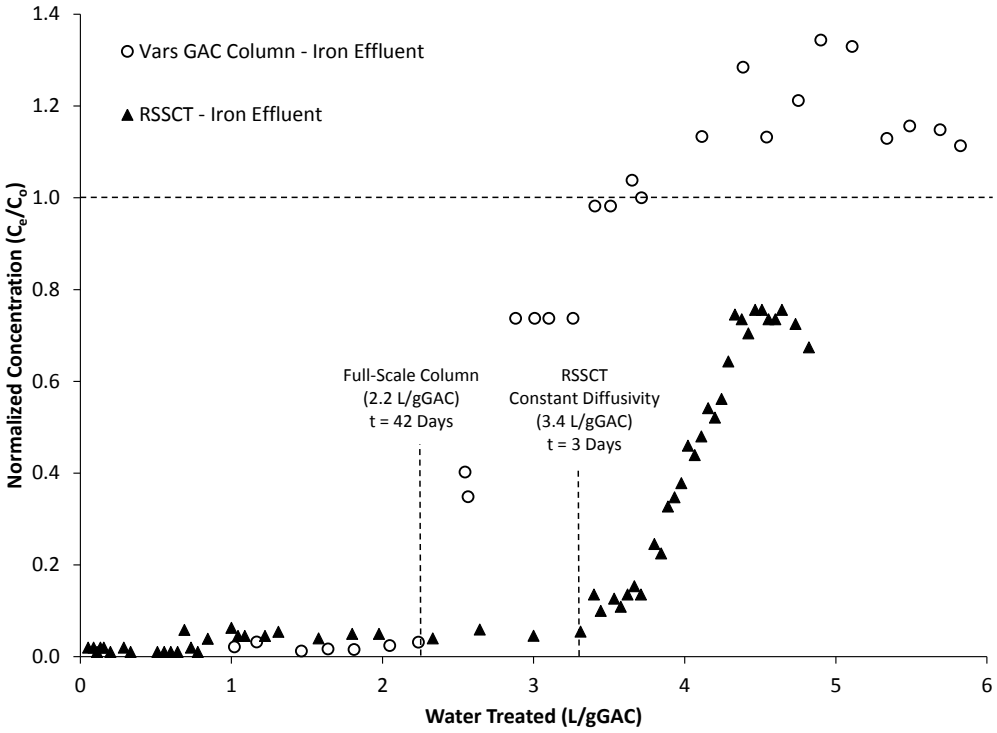

Figure 7-4: Comparison of RSSCT (constant diffusivity) and Vars GAC column for iron breakthrough using Vars raw water

Unfortunately, the RSSCT was not capable of predicting the iron chromatographic effect observed at the GAC full-scale column the run was terminated. The maximum value of C_e/C_o that was reached by the RSSCT was 0.8 at 4.64 L/gGAC (Figure 7-4). The iron concentration in the RSSCT effluent reached a plateau and then started to decrease indicating that the small column was getting plugged. Also, there was a visible accumulation of iron precipitate that started to accumulate in the top section the GAC small column. Given the smaller GAC granule sizes (80×100 mesh size) compared to those in the full-scale column (d_P 0.84 mm versus 0.16 mm), the inter-granule voids will be smaller and thus the greater impact of the iron accumulation phenomenon (and enhanced removal) in the small-scale columns than in the full-scale facility. This also indicates that the mini-column tests are not a good tool for simulating adsorption of iron-laden waters. The higher iron removal in columns

and delayed iron breakthrough are likely due to the accumulation of iron particles in the column. Since the linear diffusivity RSSCT column would have five times more GAC and EBCT than the constant diffusivity RSSCT column (69.6 g versus 13.5 g) and the constant diffusivity RSSCT model already overestimates the iron breakthrough time, the linear diffusivity RSSCT would overestimate the breakthrough time even more.

The results of the NOM breakthrough curves obtained from RSSCT (constant diffusivity) and the full-scale GAC column using Vars raw water are shown in Figure 7-5. The RSSCT using constant diffusivity shows a very gradual NOM breakthrough, which is what is normally observed at full-scale plants. The NOM breakthrough of the full-scale GAC column also starts gradually, but after treating approximately 2.2 L/g of GAC (42 days of operation) the NOM removal stabilizes at approximately 60%. This is an unusual pattern in that generally the slow breakthrough pattern continues until it reaches a constant level as the adsorption capacity is gradually exhausted and removal only occurs through biodegradation. As NOM has a long half-life and most of its readily biodegradable components have been already oxidized, only a small fraction of the NOM is generally biodegradable. While the development of biological activity with full-scale GAC columns is common and it leads to some biological NOM removal, this generally only accounts for 10 to 20% and not 60%. A possible explanation for this large long-term removal is that the NOM in Vars raw water is mostly hydrophilic (i.e., 73 – 78% of the TOC). This hydrophilic fraction is expected to be biologically active due to the presence of biodegradable compounds such as carbohydrates, amino acids, and proteins (Croue *et al.*, 2000). However, there might be some other unidentified removal mechanism involved (possibly associated with iron) which should be evaluated in the future.

The comparison between the RSSCT and full-scale breakthrough curves indicate that the RSSCT gave a reasonable prediction of the NOM breakthrough up to the point of 3.0 L/gGAC water treated and C/C_o of 0.35. Then, the full-scale breakthrough curve started to flatten whereas the RSSCT breakthrough was gradually increasing. One of the possible reasons of the flat breakthrough curve observed at the full-scale GAC column is biodegradation which may increase the NOM removal. On the other hand, the run time for the RSSCT is 5 days, which is too short for the NOM biodegradation to take effect in the

small column and thus may cause differences in the breakthroughs. Given the different breakthrough patterns observed in the RSSCT and the full-scale column, it is unlikely the RSSCT could predict well the full-scale breakthrough. Note that the inability to predict biological NOM removal within GAC beds is an acknowledged limitation of RSSCT predictions (Crittenden *et al.*, 1991; Knappe *et al.*, 1997).

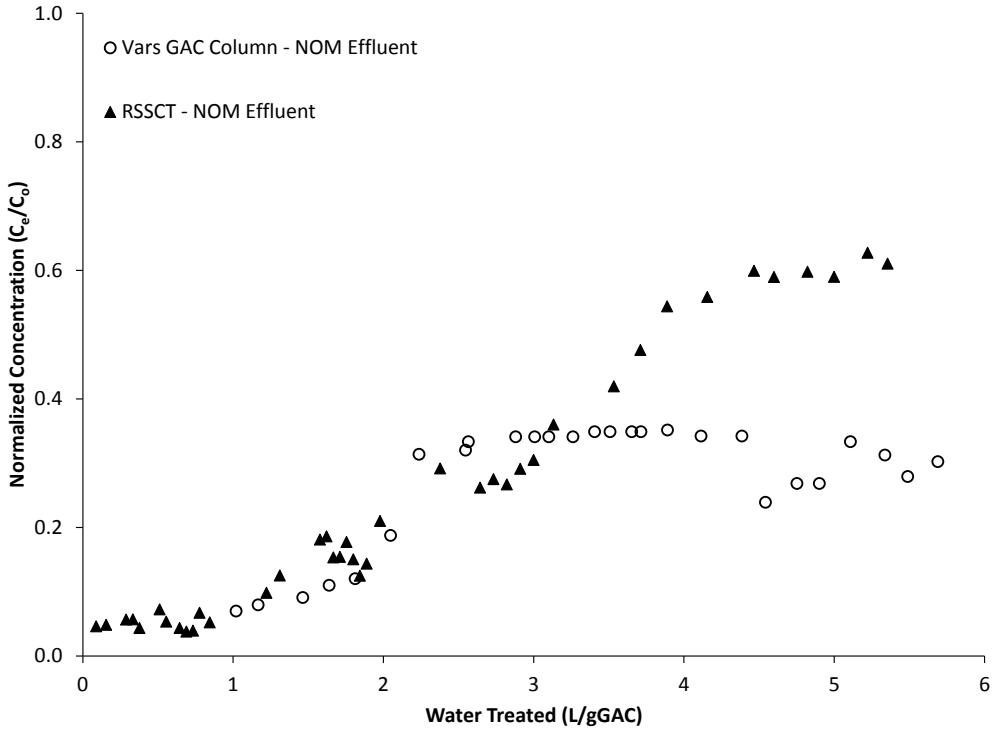

Figure 7-5: Comparison of RSSCT (constant diffusivity) using Vars raw water and Vars GAC column for NOM breakthrough

The RSSCT data also shows that NOM breakthrough started to flatten after 4 L/gGAC water treated, this may be due to the plugging caused by the iron precipitates on the top section of the GAC column or due to natural variability due to the heterogeneity of the NOM. Overall, the RSSCT was not capable of predicting the breakthrough of both NOM and iron in Vars raw water using constant diffusivity design. Also, the combination of iron precipitation and the use of small GAC particles (80×100 mesh size) plugged the small column which led to the termination of the RSSCT experiments.

7.3 Breakthrough Prediction of NOM using Greensand Treated Water

7.3.1 Batch Kinetics of NOM using Greensand Treated Water

Figure 7-6 displays the NOM kinetics data for the greensand treated water using three different GAC particle sizes (20×30, 40×50 and 80×100 mesh sizes). The lines in the graph are the results of the regression analysis using the homogeneous surface diffusion model (HSDM) for different particle sizes of GAC. The figure shows the effect of GAC particle size on the rate of adsorption of NOM in the greensand treated water and the obtained behavior was similar to the kinetics of Vars raw water, which is the rate of adsorption increases with decreasing particle size. Table 7-4 summarizes the parameters and fit indicators of the HSDM for NOM in the greensand treated water using different GAC particle sizes. The calculated effective surface diffusivities were higher for the 30×40 mesh GAC (2.46×10^{-12} cm^2/s) than for 40×50 mesh GAC (1.6×10^{-12} cm^2/s), and lowest for the 80×100 mesh GAC (4.8×10^{-13} cm^2/s). The AAPEs show that the HSDM resulted in good fits for the NOM data. The absolute average percentage errors (AAPEs) of the HSDM using GAC with mesh sizes 30×40, 40×50 and 80×100 were found to be 1.24%, 2.15% and 2.39%, respectively.

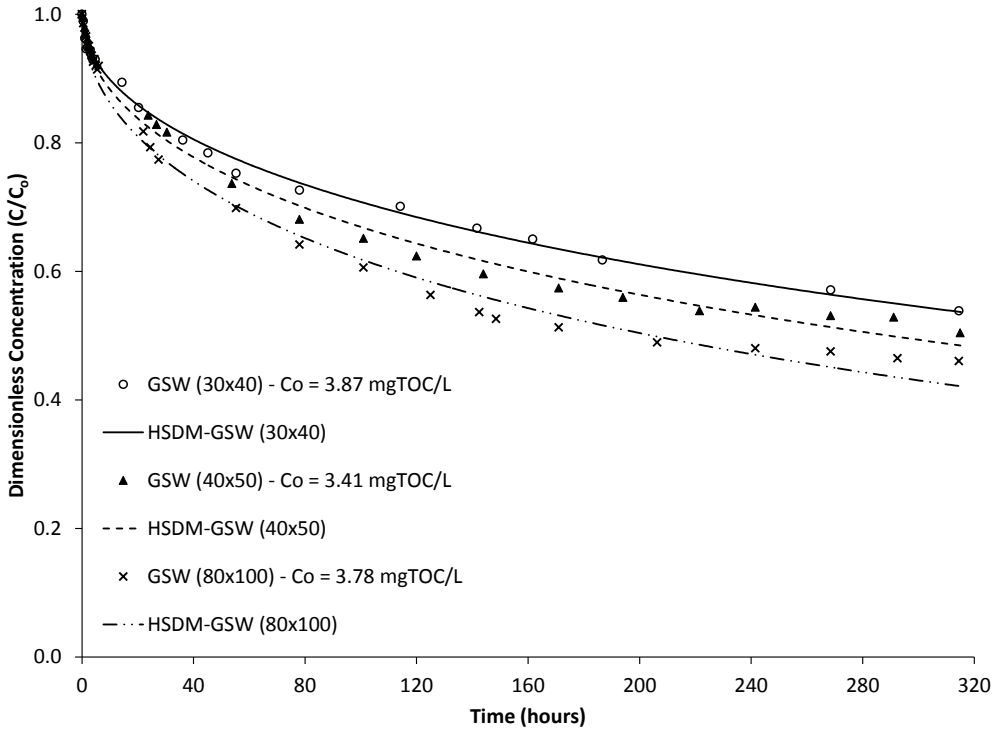

Figure 7-6: Adsorption kinetics of NOM in greensand treated water using different particle sizes of F-400 GAC with the HSDM model

Table 7-4: Parameters and fit indicators of the HSDM model for NOM in Vars raw water using different GAC particle sizes

Parameters	Units	GAC Particle Sizes		
		30×40	**40×50**	**80×100**
R	cm	0.050	0.035	0.016
C_o	mgTOC/L	3.60	3.62	3.60
C_c	gGAC/L	0.06	0.06	0.06
K_F	$(mg/g)\cdot(L/mg)^n$	7.02	7.02	7.02
n_F		2.14	2.14	2.14
D_s	cm^2/s	2.4×10^{-12}	1.6×10^{-12}	4.8×10^{-13}
AAPE	%	1.24	2.15	2.39

Although, months might be needed for the NOM to reach equilibrium, the kinetics experiments were run for 13 days since the main purpose of the experiment was to calculate the GAC surface diffusivity with respect to GAC particle sizes and not finding the equilibrium time of NOM adsorption. The same MATLAB code designed by Ding (2010) was used to solve the HSDM in order to calculate the surface diffusivity coefficients for each GAC particle size. Figure 7-7 shows the relationship between the surface diffusivities and the GAC particle sizes, they are clearly linearly related. The calculated effective surface diffusivities were highest for the 30×40 mesh GAC particles (2.40×10^{-12} cm^2/s) followed by that for the 40×50 mesh GAC particles (1.61×10^{-12} cm^2/s), and the 80×100 mesh GAC particles had the lowest values (0.48×10^{-12} cm^2/s). Accordingly, linear diffusivity scale-up approach should be more appropriate than constant diffusivity scaling for the design of the RSSCT using the greensand treated water.

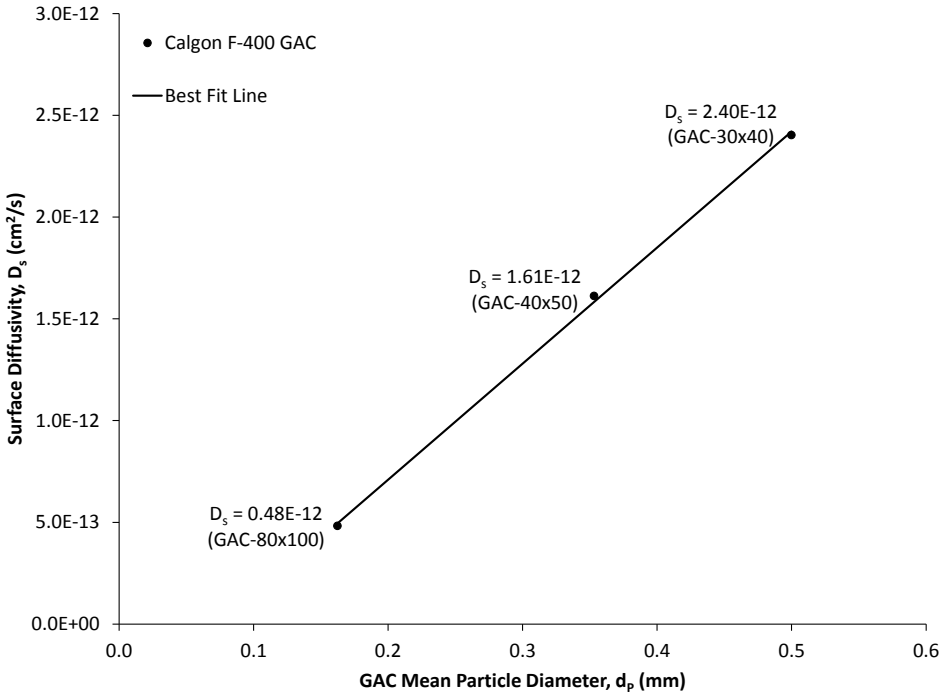

Figure 7-7: The dependence of the surface diffusivity (D_s) on GAC particle sizes for NOM in greensand treated water

A comparison between the surface diffusivity coefficients (D_s) of Vars raw water and the greensand treated water obtained at different GAC particle sizes was summarized in Table 7-

5. The data shows that the differences between the surface diffusivity coefficients of Vars raw water and the greensand treated water using GAC particle sizes of 40×50 and 80×100 mesh GAC size were reduced by approximately a factor of 7. The reduction in the surface diffusivity coefficients means slower adsorbing kinetics of NOM in the greensand treated water. These differences could be attributed to one of the previous findings that the greensand treatment removed between 9 to 13% of the NOM in Vars raw water and some of the removed NOM fractions have molecular weights less than 1 KDa (see Chapter 4). These small fractions were presumably considered as the fastest diffusing NOM molecules and removing them by the greensand treatment would cause the NOM diffusivity to be 7 times slower than Vars raw water.

Table 7-5: Comparison between the surface diffusivity coefficients (D_s) of Vars raw water and the greensand treated water obtained at different GAC particle sizes

GAC Mean Particle Size (mm)	Surface Diffusivity Coefficient (D_s) ($\times 10^{-12}$ cm^2/s)	
	Vars Raw Water	Greensand Treated Water
0.70 (20×30 mesh size)	33.6	-
0.50 (30×40 mesh size)	-	2.4
0.35 (40×50 mesh size)	10.8	1.6
0.16 (80×100 mesh size)	3.8	0.5

7.3.2 RSSCT for Greensand Treated Water

As discussed in Chapter 4, greensand treatment removed between 9 to 13% of the NOM in Vars raw water in addition to the inorganic compounds (i.e., iron). So, the same RSSCT approach was used with the greensand treated water in order to test if the NOM breakthrough using the greensand treated water can be predicted. Although the batch kinetic tests indicated that the linear diffusivity assumption is more appropriate for the scaling of RSSCT using the

greensand treated water, both linear and constant diffusivities were evaluated for completeness. Due to the limitation of performing the RSSCT experiments at Vars treatment plant, the experiments were performed in a water research lab at the University of Ottawa and the greensand treated water was collected at Vars and transported to the lab every two days. Storing the water for two days to be used in the RSSCT caused a few changes in the water characteristics (such as the water temperature) which may cause slight differences in the breakthroughs.

7.3.1.1 Breakthrough Prediction of NOM Removal using RSSCT for Greensand Treated Water

Table 7-6 summarizes the characteristics of the greensand treated water that was collected prior to the RSSCT experiments. The water quality of the two samples was almost the same. The average concentration of NOM was 4.06 mgTOC/L. This value was found to be comparable to the average value obtained from Vars treatment plant during the GAC full-scale run between June 6th, 2002 and February 21st, 2005 (i.e. 4.25 mgTOC/L). The temperature of the greensand treated water ranged from 11.3 to 11.5 °C, which is higher than the 8.0 and 8.9 °C of Vars raw water. This increase is due to the greensand treatment process which is housed within the treatment plant building. The process involves mixing Vars raw water with potassium permanganate ($KMnO_4$) in an open tank and then passing the water through the above-ground greensand filters before passing the treated water to the GAC column.

Table 7-6: Characteristics of greensand treated water used for the RSSCT (constant and linear diffusivity)

Parameters	Greensand Treated Water (Constant Diffusivity) (August 16th, 2011)	Greensand Treated Water (Linear Diffusivity) (June 13th, 2011)
pH	7.85	7.78
Temperature ($^{\circ}$C)	11.50	11.34
TOC (mgTOC/L)	4.02	4.11

The design and operational parameters used for the full-scale RSSCT columns for the treatment of the greensand treated water are summarized in Table 7-7. The greensand filter system was installed at Vars treatment facility in 2002 and the first treatment cycle started on June 6th, 2002. Comparing the operational parameters of the GAC full-scale column at Vars before (Table 7-3) and after (Table 7-7) the use of greensand treatment shows some changes in the flowrate and the mass of GAC used. The flowrate increased by a factor of three compared to the flowrate that was used prior to the use of greensand treatment in order to accommodate the increasing domestic, commercial and institutional water demand supplied to the town of Vars. The full-scale flowrate was increased to 36 m^3/hr (equivalent to 600000 mL/min) and the mass of GAC used in the full-scale column was increased from 7500 kg to 8618 kg of F-400 GAC. These changes decreased the EBCT of the full-scale facility from 89.8 to 36.0 min. Such a value is still higher than the original design EBCT of 31 minutes for the GAC full-scale column at Vars. The GAC size selected for both RSSCT tests (i.e., constant and linear diffusivity scaling) was 80×100 mesh size. The use of constant and linear diffusivities to design the RSSCT would result in small-scale columns with EBCTs of 1.3 min and 7.0 min, respectively. The design of the RSSCT resulted in a hydraulic loading of 25.5 m/hr and a flowrate of 225.5 mL/min. Such a high flowrate would result in a high interstitial velocity in the small-scale column, and hence, a high head loss. Also, using these high values of flowrate and hydraulic loading would result in a small-scale column with 57.2 cm depth of GAC (121.7 g of GAC) using the constant diffusivity approach. For the linear diffusivity approach and the same hydraulic loading and flowrate, the small-scale column would have a GAC depth of 295.6 cm (629.4 g of GAC). To avoid using these unreasonably long columns for the RSSCT tests, the flowrate was adjusted to 10 mL/min which would result in a hydraulic loading of 1.14 m/hr (equivalent to 1.9 cm/min). Changing the flowrate and hydraulic loading (while maintaining the scaled EBCT) decreased the GAC depth to 2.5 cm (5.4 g GAC) using constant diffusivity scaling and to 13.1 cm (27.9 g GAC) using linear diffusivity scaling. The recalculated value of Reynolds number based on these adjusted parameters was decreased from 1.15 to 0.1. As discussed in Section 7.2.2.1, adjustments to the RSSCT's Reynolds number so it would equal to values between 0.1 and 1.0 have negligible impact on results (Crittenden *et al.*, 1991; Summers *et al.*, 1995).

Table 7-7: Design and operational parameters used for full-scale column and RSSCT under constant and linear diffusivities using greensand treated water

Operational Parameters	RSSCT		Full-Scale Column
GAC Brand	Calgon F-400		Calgon F-400
Bulk Density (g/cm^3)	0.401		0.401
GAC Mean Particle Diameter (mm)	0.16 (80×100 mesh size)		0.84 (12×40 mesh size)
Column Diameter (cm)	2.6		305
Cross-Sectional Area (cm^2)	5.3		73100
Flowrate (mL/min)	10.0		600000
Hydraulic Loading (cm/min)	1.9		4.9
	RSSCT (Constant Diffusivity)	**RSSCT (Linear Diffusivity)**	
EBCT (min)	1.3	7.0	36.0
Depth of GAC (cm)	2.5	13.1	290
Mass of GAC (g)	5.4	27.9	8618×10^3
NOM Breakthrough Time (days)	16	85	440

Note: NOM breakthrough was decided to be when the column effluent reaches 50% of the column influent

The design of the RSSCT for the greensand treated water was based on the NOM breakthrough observed at Vars full-scale column. The reference NOM breakthrough time was based on the 50% removal level. Figure 7-8 shows the NOM breakthrough curve observed at Vars full-scale column between June 6th, 2002 and February 21st, 2005 using greensand treated water and the breakthrough time at C_e/C_o = 0.5 was equal to 440 days or 16.44 L/gGAC water treated.

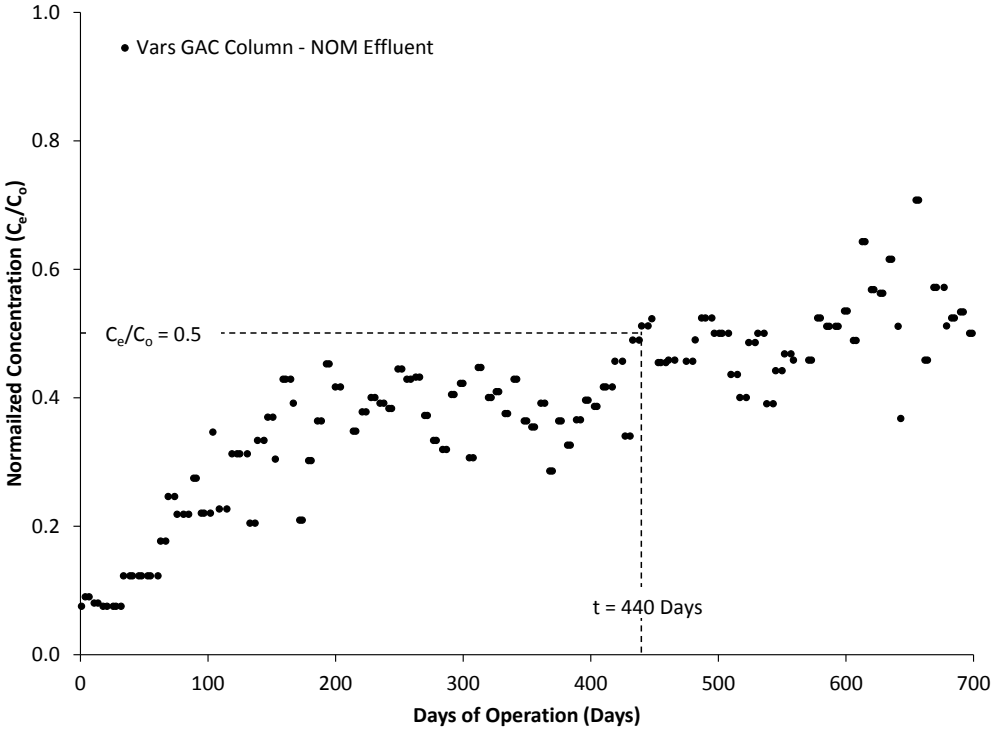

Figure 7-8: NOM breakthrough observed at Vars full-scale column using greensand treated water (June 6th, 2002 – February 21st, 2005)

The results of the NOM breakthrough curves obtained from RSSCT (constant and linear diffusivity) and the full-scale GAC column are shown in Figure 7-9. The influent concentration of NOM was analyzed nine times throughout the duration of each RSSCT run and the average value was equal to 4.15 ± 0.06 mgTOC/L. In order to compare the behavior of each breakthrough curve (constant versus linear diffusivities) with the behavior of the GAC full-scale column breakthrough curve, all figures were combined into one graph (Figure 7-10). The figure shows that the RSSCT using both scale-up assumptions were capable of predicting very well the onset of the NOM breakthrough up to the point of 10 L/gGAC water treated, that is over 250 days of operation for the full-scale column. Then, the constant diffusivity RSSCT breakthrough curve kept increasing beyond the line of C_e/C_o = 0.5 whereas the breakthrough of the RSSCT using linear diffusivity was moving parallel to the breakthrough of the GAC full-scale column. The results of the breakthrough curves of both RSSCTs (constant and linear diffusivity scaling) show that none of them was capable of

predicting the NOM breakthrough (C_e/C_o = 0.5 at 16.4 L/gGAC water treated) of the full-scale column. The breakthrough curves of the RSSCT using constant and linear diffusivity designs reached the NOM breakthrough (C_e/C_o = 0.5) at 10.0 and 14.0 L/gGAC water treated, respectively. The results indicated that the RSSCT using linear diffusivity predicted the shape of the NOM breakthrough better than the RSSCT using constant diffusivity. Such results agree with findings of Crittenden *et al.* (1991), Summers *et al.* (1995) and Corwin and Summers (2010) who found that RSSCT using linear diffusivity approach yielded good predictions of the NOM breakthrough, as measured by dissolved organic carbon (DOC).

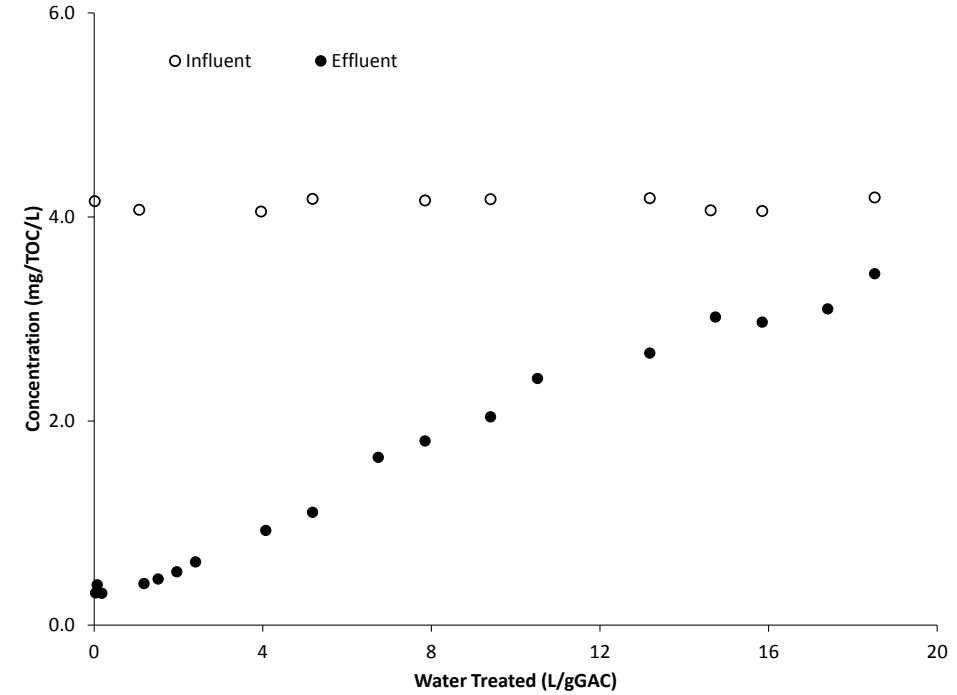

(a)

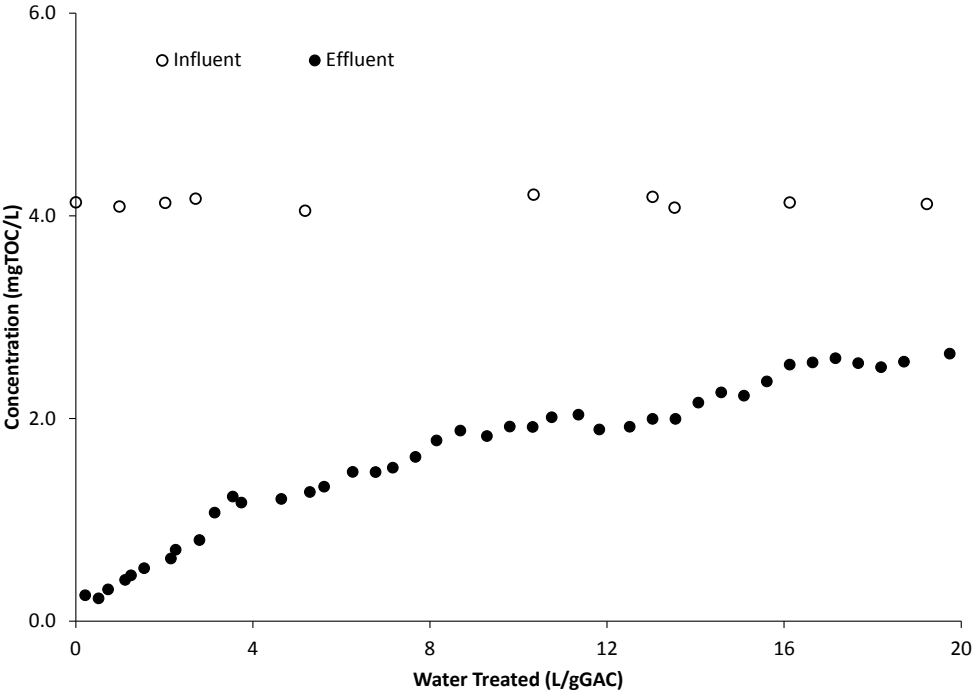

(b)

Figure 7-9: NOM breakthrough curves using greensand treated water for: (a) RSCCT (constant diffusivity) and (b) RSCCT (linear diffusivity)

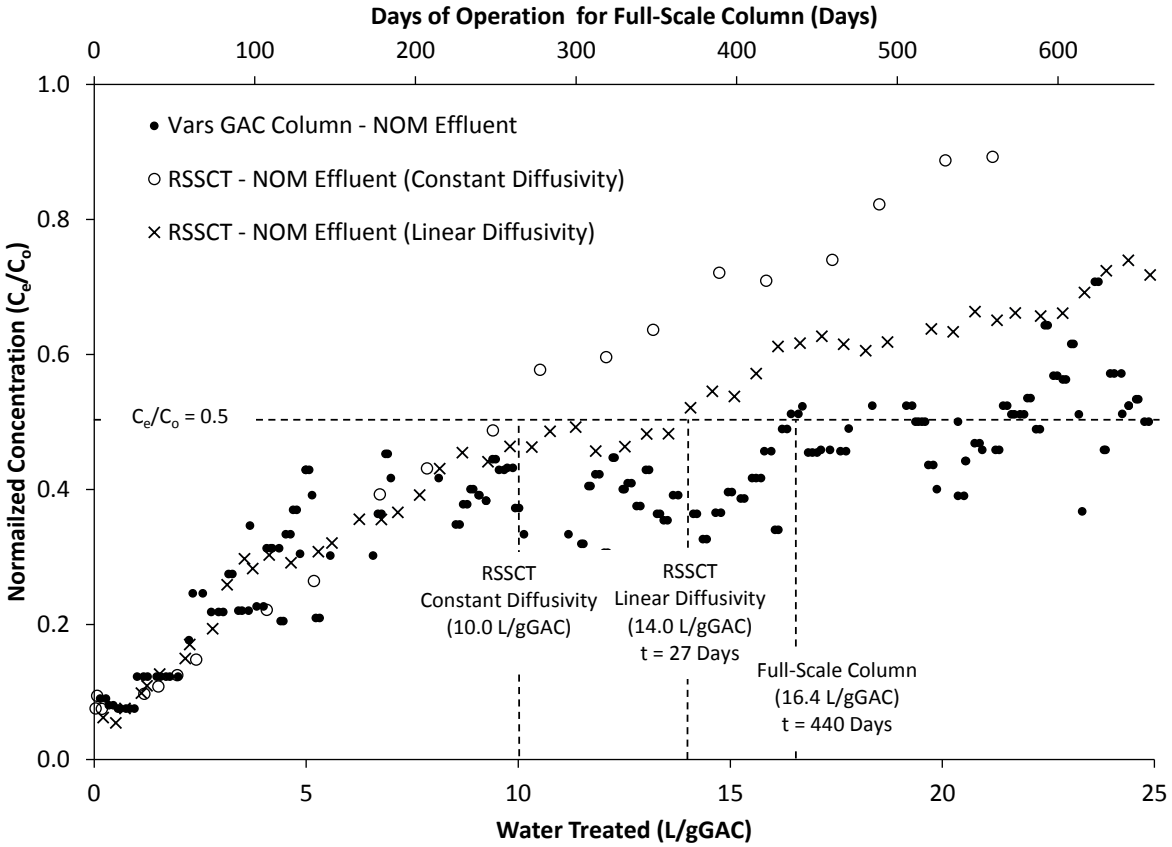

Figure 7-10: Comparison of RSSCT (constant and linear diffusivity) using greensand treated water and Vars GAC column after greensand treatment for NOM breakthrough

Even though, the results of the RSSCT breakthrough curve using linear diffusivity in Figure 7-10 were parallel to the breakthrough of the full-scale column, there was a difference in adsorption capacity between the two curves beyond the point of 12.0 L/gGAC water treated. This difference could be attributed to some of the limitations of the RSSCT that include representative sample collection, variations of influent concentrations, and biodegradable organic matter in the influent water that could affect the prediction of breakthrough characteristics (Knappe *et al.*, 1997; Snoeyink and Summers, 1999; Marhaba, 2000). The run time for the RSSCT is too short for the NOM biodegradation to take effect in the small column which may cause differences in the NOM breakthroughs (Crittenden *et al.*, 1991; Knappe *et al.*, 1997).

In the full-scale column, a TOC removal of more than 60% was observed even after 250 days of operation and the level of removal only decreased slightly over the next year. While there was likely some TOC removal via adsorption, biodegradation was presumably the main removal mechanism. Such a long time for the NOM biodegradation to take place in the GAC columns was observed by other researchers. In a study by Van der Aa *et al.* (2011) on the biodegradation of NOM in GAC filters, the observed period of time with biodegradation as the main NOM removal process was from day 194 to day 559.

7.4 Summary

Batch kinetics reactor using Vars raw water was used with three different GAC particle sizes showed that there was a linear relationship between the NOM's surface diffusivity and the GAC granule size of GAC. However, due to plant operational constraints, only the constant diffusivity RSST could be evaluated. The prediction of the full-scale iron breakthrough using constant diffusivity RSSCT for Vars raw water overestimated the iron breakthrough time and it had a different shape from that of the full-scale column. Furthermore, the RSSCT did not predict the iron chromatographic effect observed in the full-scale columns. As for the NOM prediction, the RSSCT was only able to predict the NOM removals up to 2.5 L/g GAC. There was significant iron precipitation in the small-scale column. This caused additional iron removals which may have caused the overestimation of the iron breakthrough.

For the greensand treated waters, the batch kinetic tests indicated that the linear diffusivity assumption was more appropriate for the RSSCT tests, despite this both linear and constant diffusivity were evaluated for completeness. Both small scale columns predicted the NOM breakthrough very well up to $C/C_0 = 0.45$, that occurs at a throughput of 10 L/gGAC water treated. From then the full-scale column had a more gradual increasing breakthrough curve than that of the two RSSCT approaches. Of the two RSSCT approaches, the linear diffusivity RSSCT performed better but it was unable to mimic the full-scale column beyond that point of 10 L/gGAC water treated. In the long term, the linear diffusivity RSCCT had a breakthrough parallel to that of the full-scale with lower NOM removals of 15%. The additional removal in the full-scale column was presumably due to degradation by the

biofilm developed within the adsorber, the short duration of the RSSCT tests did not allow this biofilm to develop.

Given the fact that there is no iron in the greensand treated water, the large long-term NOM removal of 06% in the GAC full scale column (Figure 7-8) cannot be associated with any iron removal mechanism. Thus, the NOM removal is very likely to be due to biodegradation. Since the same type of organics were present in Vars raw water, the large long-term NOM removal of the GAC full scale column treating Vars raw water (Figure 7-5) is also likely to be due to biodegradation. A possible explanation for this large long-term removal is that the NOM in Vars raw water is mostly hydrophilic (i.e., 73 – 78% of the TOC). This hydrophilic fraction is expected to be biologically active due to the presence of biodegradable compounds such as carbohydrates, amino acids, and proteins (Croue *et al.*, 2000).

The use of RSSCT with iron-laden waters was proved to be troublesome due to the oxidation and precipitation of iron inside the small-scale column. Also, this method was not capable of capturing the NOM biodegradation observed in the full-scale column. Accordingly, pilot scale columns with larger GAC particles are recommended to be used at the treatment plant in order to capture the iron chromatographic effect. Additionally, the long operating times of the pilot scale column would also allow biofilms to be created with the GAC so NOM biodegradation can be incorporated into the simulation.

CHAPTER 8 CONCLUSIONS AND RECOMMENDATIONS

8.1 Conclusions

The main objective of this thesis was to gain an understanding of the interaction between NOM and iron in groundwater that may have caused the chromatographic effect in Vars GAC columns. The conclusions of this dissertation were presented based on the three main parts of the study: the Vars groundwater and treatment system characterization study, the competitive adsorption isotherm modeling, and the RSSCT performance predictions.

Vars groundwater and treatment system characterization study

1. The Vars groundwater characterization results indicated that the main species of iron in the groundwater was ferrous iron, and that NOM-iron complexes accounted for 15 – 35% of the iron.
2. The mini-column experiment conducted at the Vars facility showed that NOM-iron complexes were not the cause of the iron chromatographic displacement observed in Vars GAC columns. Hence, the first hypothesis was incorrect. The inability to reproduce the chromatographic effect did not permit the characterization of the chromatographic peak and thus it was not possible to determine if the phenomenon was associated with any of the iron or NOM fractions other than the NOM-iron complexes.
3. The greensand treatment only removed 9 to 13% of the NOM in Vars groundwater, and the NOM removed had low molecular weights (less than 1 kDal).
4. The full removal of iron during the greensand treatment indicated that NOM-iron complexes in the groundwater were either broken by the potassium permanganate oxidation or adsorbed by the greensand filter.

Competitive adsorption isotherm of iron and natural organic matter

1. In spite of numerous precautions that were taken in order to minimize the exposure of iron to oxygen during the preparation of the experiments, conducting the adsorption isotherms with iron-laden waters proved to be very challenging because of iron oxidation and precipitation.

2. The single adsorption isotherms of Vars groundwater's NOM was well described by the Freundlich, Summers-Roberts and Qi-Schideman models. The ferrous iron single solute isotherm was modeled well using the Freundlich, Langmuir and Summers-Roberts isotherm models. Among all these models, the Summers-Roberts model yielded the best simulation for both components.
3. The competitive adsorption of iron (an inorganic contaminant) with NOM was similar to the competitive adsorption of trace organic compounds with NOM in that the NOM greatly depressed the adsorption capacity of the target solute, ferrous iron, due to competition over GAC adsorption sites. The ferrous iron adsorption capacity was decreased by approximately a factor of 7. On the other hand, the presence of ferrous iron did not significantly decrease the adsorption capacity of NOM in Vars groundwater.
4. The adsorption isotherm of iron in competition with NOM in Vars groundwater was well simulated by several versions of the IAST models in combination with Freundlich and Summers-Roberts single solute isotherm models. Accordingly, the second hypothesis was correct. The IAST-SR models performed better than their IAST-FR counterparts, and the best fit was achieved using the IAST-SR model with one NOM pseudocomponent.
5. None of the IAST models were capable of simulating the NOM and ferrous iron competitive adsorption isotherm simultaneously; previous literature has revealed that this is also the case for the simulation of the competitive adsorption between NOM and organic target compounds. Given that the presence of iron did not significantly decrease the adsorption capacity of NOM, a simplified approach is to use the single-solute NOM isotherm to represent the competitive NOM isotherm.
6. Column simulations using the PSDM model could not predict the iron breakthrough at Vars. The most likely reason for this is that the competitive isotherms performed and modeled in this study did not incorporate NOM preloading while the Vars GAC columns experience preloading given their long EBCT. In addition, the discharge of the precipitated iron from the GAC column may also have had a significant role in the observed behavior at Vars.

Breakthrough prediction of NOM and iron removal by GAC using RSSCT

1. The use of RSSCT with Vars groundwater did not predict the iron chromatographic effect observed in the full-scale columns. This was at least in part because of the extensive iron oxidation and precipitation within the small voids in between the RSSCT column's small GAC particles. Thus, the third hypothesis was incorrect and it was concluded that the RSSCT are not recommended for the assessment of iron-laden waters. Alternatively, pilot scale tests with conventional size GAC particles are suggested.
2. For greensand treated waters, the RSSCT model predicted the initial part of the NOM breakthrough well. Although the batch kinetics tests showed that the surface diffusion coefficient was linearly related to the particle diameter, both the constant and linear diffusivity were used for completeness. The RSSCTs using both diffusivities predicted the initial part of the NOM's full-scale breakthrough. However, the constant diffusivity RSSCT greatly underestimated the full-scale column performance beyond 10-L water treated/g GAC, which is over 250 days of operation for the full-scale column. On the other hand, the linear diffusivity RSSCT slightly underestimated the performance beyond that point and its NOM breakthrough was quite parallel to the full-scale performance with lower NOM removals of approximately 15%. The increased NOM removal in the full-scale column was presumably due to degradation by the biofilm developed within the GAC; the short duration of the RSSCT did not allow this biofilm to develop.
3. A possible explanation for the large long-term NOM removal of 60% observed in the full scale columns treating Vars raw water and the greensand treated water is NOM biodegradation. The magnitude of this removal is extremely high, so other unidentified mechanisms may have been involved. However, the Vars NOM was expected to be fairly biodegradable given that the Vars NOM contains a very high hydrophilic fraction (i.e., 73 – 78% of the TOC) and that the hydrophilic fraction is expected to be more biodegradable because it consists of carbohydrates, amino acids, and proteins (Croue *et al.*, 2000).

8.2 Recommendations for Future Research

Based on the observations and limitations found throughout the present work, multiple research pathways are recommended for future work as follows:

1. As the present research stands alone as a study of NOM and iron competitive adsorption, and their interaction in groundwater, similar studies should be conducted on different iron-laden groundwater sources in order to investigate any possible correlations between the results.
2. This study and that of Narbaitz and Benedek (1994) reported that competing species did not significantly alter the NOM adsorption capacity. The universality of these results needs to be tested.
3. In order to further investigate the NOM preloading effect on the prediction of the iron breakthrough, it is recommended that isotherms with GAC preloaded with Vars NOM be conducted, model these isotherms and use these new isotherms to re-simulate the column performance for the prediction of the iron chromatographic effect.
4. The use of RSSCT with iron laden waters was proved to be troublesome due to the oxidation and precipitation of iron inside the small-scale column. Accordingly, pilot scale columns are recommended to be used at the treatment plant in order to capture the iron chromatographic effect. Additionally, the long operating times of the pilot scale column would also allow biofilms to be created with the GAC so NOM biodegradation can simulated.

REFERENCES

Adams, C.D., and Watson, T.L. (1996). "Treatability of s-triazine herbicide metabolites using powdered activated carbon." Journal of Environmental Engineering-ASCE, 122(4), 327-330.

Aiello, R., Nastro, A., and Colella, C. (1978). "Chemical aspects of one iron removal process." Effluent & Water Treatment Journal, 18(12), 611-617.

Aiken, G.R. (1985). "Humic Substances in Soil, Sediment, and Water: Geochemistry, Isolation, and Characterization." Wiley & Sons, New York, NY.

Alberti, G., D'Agostino, G., Palazzo, G., Biesuz, R., and Pesavento, M. (2005). "Aluminium speciation in natural water by sorption on a complexing resin." Journal of Inorganic Biochemistry, 99(9), 1779-1787.

Amy, G.L., Chadik, P.A., Sierka, R.A., and Cooper, W.J. (1986). "Ozonation of aquatic organic-matter and humic substances - an analysis of surrogate parameters for predicting effects on trihalomethane formation potential." Environmental Technology Letters, 7(2), 99-108.

Andrews, R.C. (1990). "Removal of low concentrations of chlorination by-products using activated carbon." PhD Thesis, University of Alberta, AB.

APHA/AWWA/WPCF (1998). "Standard Methods for the Examination of Water and Wastewater." 20th Edition. American Public Health Association, Washington, DC.

Bean, E.L. (1974). "Potable water-quality goals." Journal of the American Water Works Association, 66(4), 221-230.

Biesuz, R., Alberti, G., D'Agostino, G., Magi, E., and Pesavento, M. (2006). "Determination of cadmium(II), copper(II), manganese(II) and nickel(II) species in Antarctic seawater with complexing resins." Marine Chemistry, 101(3-4), 180-189.

Bond, R.G., and Digiano, F.A. (2004). "Evaluating GAC performance using the ICR database." Journal of the American Water Works Association, 96(6), 96-104.

Brookins, D.G. (1988). "Eh-pH Diagrams for Geochemistry." Springer-Verlag, Berlin-Heidelberg-New York.

Brown, G.K., Cabaniss, S.E., MacCarthy, P., and Leenheer, J.A. (1999). "Cu(II) binding by a pH-fractionated fulvic acid." Analytica Chimica Acta, 402(1-2), 183-193.

Bryant, E.A., Fulton, G.P., and Budd, G.C. (1992). "Disinfection Alternatives for Safe Drinking Water." Van Nostrand Reinhold, New York, NY.

Carberry, J.J. (1964). "Designing laboratory catalytic reactors." Industrial and Engineering Chemistry, 56(11), 39-46.

Carlson, K.H., Knocke, W.R., and Gertig, K.R. (1997). "Optimizing treatment through Fe and Mn fractionation." Journal of the American Water Works Association, 89(4), 162-171.

Carslaw, H.S., and Jaeger, J.C. (1986). "Conduction of Heat in Solids." Clarendon Press, Gloucestershire, England.

Carter, M.C., and Weber, W.J., Jr. (1994). "Modelling adsorption of TCE by activated carbon preloaded by background organic matter." Environmental Science & Technology, 28(4), 614-623.

Cerminara, P.J., Sorial, G.A., Papadimas, S.P., Suidan, M.T., Moteleb, M.A., and Speth, T.F. (1995). "Effect of influent oxygen concentration on the GAC adsorption of VOCs in the presence of BOM." Water Research, 29(2), 409-419.

Christman, R.F., Norwood, D.L., Seo, Y., and Frimmel, F.H. (1989). "Oxidative Degradation of Humic Substances from Freshwater Environments." Humic Subtances II, John Wiley & Sons, New York, NY.

City of Ottawa (1996). "1996 Annual Report for Vars Communal Well System." Ottawa, ON.

Corwin, C.J., and Summers, R.S. (2010). "Scaling trace organic contaminant adsorption capacity by granular activated carbon." Environmental Science & Technology, 44(14), 5403-5408.

Crittenden, J.C., Berrigan, J.K., and Hand, D.W. (1986a). "Design of rapid small-scale adsorption tests for a constant diffusivity." Journal Water Pollution Control Federation, 58(4), 312-319.

Crittenden, J.C., Hutzler, N.J., Geyer, D.G., Oravitz, J.L., Friedman, G. (1986b). "Transport of organic compounds with saturated groundwater flow: Model development and parameter sensitivity." Water Resources Research, 22(3), 271-284.

Crittenden, J.C., Berrigan, J.K., Hand, D.W., and Lykins, B. (1987a). "Design of rapid fixed-bed adsorption tests for nonconstant diffusivities." Journal of Environmental Engineering-ASCE, 113(2), 243-259.

Crittenden, J.C., Hand, D.W., Arora, H., and Lykins, B.W.J. (1987b). "Design considerations for GAC treatment of organic chemicals." Journal of the American Water Works Association, 79(1), 74-82.

Crittenden, J.C., Luft, P., and Hand, D.W. (1985a). "Prediction of multicomponent adsorption equilibria in background mixtures of unknown composition." Water Research, 19(12), 1537-1548.

Crittenden, J.C., Luft, P., Hand, D.W., Oravitz, J.L., Loper, S.W., and Arl, M. (1985b). "Prediction of multicomponent adsorption equilibria using ideal adsorbed solution theory." Environmental Science & Technology, 19(11), 1037-1043.

Crittenden, J.C., Reddy, P.S., Arora, H., Trynoski, J., Hand, D.W., Perram, D.L., and Summers, R.S. (1991). "Predicting GAC performance with rapid small-scale column tests." Journal of the American Water Works Association, 83(1), 77-87.

Crittenden, J.C., Reddy, P.S., Hand, D.W., and Arora, H. (1989). "Prediction of GAC performance using rapid small-scale column tests." AWWA Research Foundation report #90549, American Water Works Association, Denver, CO.

Crittenden, J.C., Vaitheeswaran, K., Hand, D.W., Howe, E.W., Aieta, E.M., Tate, C.H., McGuire, M.J., and Davis, M.K. (1993). "Removal of dissolved organic-carbon using granular activated carbon." Water Research, 27(4), 715-721.

Croue, J.P., Korshin, G.V., Benjamin, M.M. (2000). "Characterization of Natural Organic Matter in Drinking Water." AWWA Research Foundation, American Water Works Association, Denver, CO.

Cummings, L., and Summers, R.S. (1994). "Using RSSCTs to predict field-scale GAC control of DBP formation." Journal of the American Water Works Association, 86(6), 88-97.

Cussler, E.L. (2009). "Diffusion: Mass Transfer in Fluid Systems." Cambridge University Press, UK.

Dastgheib, S.A., Karanfil, T., and Cheng, W. (2004). "Tailoring activated carbons for enhanced removal of natural organic matter from natural waters." Carbon, 42(3), 547-557.

Ding, L. (2010). "Mechanisms of competitive adsorption between trace organic contaminants and natural organic matter on activated carbon." PhD Thesis, University of Illinois, Urbana, IL.

Ding, L., Marinas, B.J., Schideman, L.C., and Snoeyink, V.L. (2006). "Competitive effects of natural organic matter: Parametrization and verification of the three-component adsorption model COMPSORB." Environmental Science & Technology, 40(1), 350-356.

Draper, N.R., and Smith, H. (1998). "Applied Regression Analysis." Wiley & Sons, New York, NY.

Drever, J.I. (1997). "The Geochemistry of Natural Waters: Surface and Groundwater Environments." Prentice Hall, Upper Saddle River, NJ.

Dvorak, B.I., and Maher, M.K. (1999). "GAC contactor design for NOM removal: Implications of EBCT and blending." Journal of Environmental Engineering-ASCE, 125(2), 161-165.

Ebie, K., Li, F.S., Azuma, Y., Yuasa, A., and Hagishita, T. (2001). "Pore distribution effect of activated carbon in adsorbing organic micropollutants from natural water." Water Research, 35(1), 167-179.

Edzwald, J.K., and Tobiason, J.E. (1999). "Enhanced coagulation: US requirements and a broader view." Water Science and Technology, 40(9), 63-70.

Emmenegger, L., Schonenberger, R.R., Sigg, L., and Sulzberger, B. (2001). "Light-induced redox cycling of iron in circumneutral lakes." Limnology and Oceanography, 46(1), 49-61.

Environment Canada (1990). "Groundwater-Nature's Hidden Treasure." Water Fact Sheet #5, Environment Canada, Ottawa, ON.

Faust, S.D., and Aly, O.M. (1987). "Adsorption Processes for Water Treatment." Butterworths, Boston, MA.

Frick, B., and Sontheimer, H. (1983). "Adsorption equilibria in multisolute mixtures of known and unknown compositions." In: Treatment of Water by Granular Activated Carbon, Advances in Chemistry Series 202, Edited by M.J McGuire and I.H. Suffet, American Chemistry Society, Washington, DC.

Frick, B. (1980). "Adsorptionsgleichgewichte zwischen Aktivkohle und organischen Wasserinhaltsstoffen in Mehrstoffgemischen bekannter und unbekannter Zusammensetzung." (Adsorption equilibria between activated carbon and known as well as unknown mixtures of organic matter in water). PhD Thesis, University of Karlsruhe, Karlsruhe, Germany.

Fritz, W., and Schlunder, E.U. (1981). "Competitive adsorption of 2 dissolved organics onto activated carbon .1. adsorption equilibria." Chemical Engineering Science, 36(4), 721-730.

Gnielinski, V. (1978). "Gleichungen zur berechnung des warmeund stoffaustausches in durchstromten ruhenden kugelschuttungen bei mitteren und grossen pecletzahlen." Fortschritte der Verfahrenstechnik, 12 (6), 363-366.

Gillogly, T.E.T., Snoeyink, V.L., Elarde, J.R., Wilson, C.M., and Royal, E.P. (1998). "14-C-MIB adsorption: on PAC in natural water." Journal of the American Water Works Association, 90(1), 98-108.

Gjessing, E.T. (1976). "Physical and Chemical Characteristics of Aquatic Humus." Ann Arbor Science Publishers, Ann Arbor, MI.

Gu, B., Schmitt, J., Chen, Z., Liang L., and McCarthy, J.F. (1995). "Adsorption and desorption of different organic matter fractions on iron oxide." Geochimica Et Cosmochimica Acta, 59(2), 219-229.

Gurzau, E.S., Neagu, C., and Gurzau, A.E. (2003). "Essential metals - case study on iron." Ecotoxicology and Environmental Safety, 56(1), 190-200.

Hand, D.W., Crittenden, J.C., and Thacker, W.E. (1983). "User-oriented batch reactor solutions to the homogeneous surface-diffusion model." Journal of Environmental Engineering-ASCE, 109(1), 82-101.

Hand, D.W., Crittenden, J.C., Arora, H., Miller, J.M., and Lykins, B.W. (1989). "Designing fixed-bed adsorbers to remove mixtures of organics." Journal of the American Water Works Association, 81(1), 67-77.

Hansen, S., Jensen, N.E., and Nielsen, N. (1990), "Daisy – A Soil Plant Atmosphere System Model." NPO Research from the Environmental Protection Agency, Washington, DC.

Hand, D.W., Crittenden, J.C., Hokanson, D.R., and Bulloch, J.L. (1997). "Predicting the performance of fixed-bed granular activated carbon adsorbers." Water Science and Technology, 35, 235–241.

Harrington, G.W., and Digiano, F.A. (1989). "Adsorption equilibria of natural organic matter after ozonation." Journal of the American Water Works Association, 81(6), 93-101.

Hayduk, W., Laudie, H. (1974). "Prediction of diffusion coefficients for nonelecrolytes in dilute aqueous solutions." American Institute of Chemical Engineers Journal, 20(3), 611-615.

Hayes, M.H.B., MacCarthy, P., Malcolm, R.L., and Swift, R.S. (1989). "Structures of humic substances, the emergence of forms." In: Humic Substances II. In Search of Structures, Edited by M.H.B Hayes, P. MacCarthy, R.L. Malcolm, and R.S. Swift, Wiley, Chichester, 689-733.

Hem, J.D. (1989). "Study and Interpretation of the Chemical Characteristics of Natural Water." U.S. Geological Survey Water-Supply Paper 2254, Reston, VA.

Hepplewhite, C., Newcombe, G., and Knappe, D.R.U. (2004). "NOM and MIB, who wins in the competition for activated carbon adsorption sites?" Water Science and Technology, 49(9), 257-265.

Hineline, D., Crittenden, J.C., and Hand, D.W. (1987). "Use of the rapid small-scale column tests to predict full-scale adsorption capacity and performance." In the Proceedings of AWWA Annual Conference, Kansas City, MI.

Hooper, S. M., Summers, R. S., Solarik, G., and Hong, S. (1996). "GAC performance for DPB control: effect of influent concentration, seasonal variation, and pretreatment." In the Proceedings of AWWA Annual Conference, Toronto, ON.

Hsieh, C.T., and Teng, H.S. (2000). "Influence of mesopore volume and adsorbate size on adsorption capacities of activated carbons in aqueous solutions." Carbon, 38(6), 863-869.

Huang, C.P., and Blankenship, D.W. (1984). "The removal of mercury(ii) from dilute aqueous-solution by activated carbon." Water Research, 18(1), 37-46.

Hutzler, N.J., Crittenden, J.C., Gierke, J.S., Johnson, A.S. (1986) "Transport of organic compounds with saturated groundwater flow: Experimental results." Water Resources Research, 22(3), 285-295.

Jain, J.S., and Snoeyink, V.L. (1973). "Adsorption from bisolute systems on active carbon." Journal of the Water Pollution Control Federation, 45(12), 2463-2479.

Jarvie, M.E., Hand, D.W., Bhuvendralingam, S., Crittenden, J.C., and Hokanson, D.R. (2005). "Simulating the performance of fixed-bed granular activated carbon adsorbers: Removal of synthetic organic chemicals in the presence of background organic matter." Water Research, 39(11), 2407-2421.

Jensen, D.L., Boddum, J.K., Redemann, S., and Christensen, T.H. (1998). "Speciation of dissolved iron(II) and manganese(II) in a groundwater pollution plume." Environmental Science & Technology, 32(18), 2657-2664.

Jobin, R., and Ghosh, M.M. (1972). "Effect of buffer intensity and organic-matter on oxygenation of ferrous iron." Journal of the American Water Works Association, 64(9), 590-595.

Jones, L., and Atkins, P.W. (2000). "Chemistry: Molecules, Matter, and Change." W.H. Freeman, New York, NY.

Junk, G.A., Spalding, R.F., and Richard, J.J. (1980). "Areal, vertical, and temporal differences in groundwater chemistry: 2. Organic-constituents." Journal of Environmental Quality, 9(3), 479-483.

Jusoh, A., Cheng, W.H., Low, W.M., Nora'aini, A., and Noor, M. (2005). "Study on the removal of iron and manganese in groundwater by granular activated carbon." Desalination, 182(1-3), 347-353.

Karanfil, T., Kilduff, J.E., Schlautman, M.A., and Weber, W.J. (1996). "Adsorption of organic macromolecules by granular activated carbon: 1. Influence of molecular properties under anoxic solution conditions." Environmental Science & Technology, 30(7), 2187-2194.

Karanfil, T., Kitis, M., Kilduff, J.E., and Wigton, A. (1999). "Role of granular activated carbon surface chemistry on the adsorption of organic compounds: 2. Natural organic matter." Environmental Science & Technology, 33(18), 3225-3233.

Kilduff, J.E., Karanfil, T., and Weber, W.J. (1996). "Competitive interactions among components of humic acids in granular activated carbon adsorption systems: Effects of solution chemistry." Environmental Science & Technology, 30(4), 1344-1351.

Kilduff, J.E., Karanfil, T., Chin, Y.P., and Weber, W.J. (1996). "Adsorption of natural organic polyelectrolytes by activated carbon: a size-exclusion chromatography study." Environmental Science & Technology, 30(4), 1336-1343.

Kilduff, J.E., and Wigton, A. (1999). "Sorption of TCE by humic-preloaded activated carbon: Incorporating size-exclusion and pore blockage phenomena in a competitive adsorption model." Environmental Science & Technology, 33(2), 250-256.

Kim, D.S. (2004). "Adsorption characteristics of Fe(III) and Fe(III)-NTA complex on granular activated carbon." Journal of Hazardous Materials, 106(1), 45-54.

Kitis, M., Karanfil, T., Wigton, A., and Kilduff, J.E. (2002). "Probing reactivity of dissolved organic matter for disinfection by-product formation using XAD-8 resin adsorption and ultrafiltration fractionation." Water Research, 36(15), 3834-3848.

Knappe, D.R.U. (1996). "Predicting the removal of atrazine by powdered and granulated activated carbon." PhD Thesis, University of Illinois, Urbana, IL.

Knappe, D.R.U., and AWWA Research Foundation. (2003). "Effects of activated carbon characteristics on organic contaminant removal." AWWA Research Foundation, Denver, CO.

Knappe, D.R.U., Matsui, Y., Snoeyink, V.L., Roche, P., Prados, M.J., and Bourbigot, M.M. (1998). "Predicting the capacity of powdered activated carbon for trace organic compounds in natural waters." Environmental Science & Technology, 32(11), 1694-1698.

Knappe, D.R.U., Snoeyink, V.L., Roche, P., Prados, M.J., and Bourbigot, M.M. (1997). "The effect of preloading on rapid small-scale column test predictions of atrazine removal by GAC adsorbers." Water Research, 31(11), 2899-2909.

Knappe, D.R.U., Snoeyink, V.L., Roche, P., Prados, M.J., and Bourbigot, M.M. (1999). "Atrazine removal by preloaded GAC." Journal of the American Water Works Association, 91(10), 97-109.

Knocke, W.R., Occiano, S.C., and Hungate, R. (1991). "Removal of soluble manganese by oxide-coated filter media sorption rate and removal mechanism issues." Journal of the American Water Works Association, 83(8), 64-69.

Knocke, W.R., Van Benschoten, J.E., Kearney, M.J., Soborski, A.W., and Reckhow, D.A. (1991). "Kinetics of manganese and iron oxidation by potassium permanganate and chlorine dioxide." Journal of the American Water Works Association, 83(6), 80-87.

Knocke, W.R., McKinney, J.D., Golden, R.J., Ohanian, E.V., Schnell, R.C., Askenaizer, D., Neukrug, H., and Paris, D.B. (1993). "Research agenda for inorganic compounds." Journal of the American Water Works Association, 85(3), 62-67.

Knocke, W.R., Shorney, H.L., and Bellamy, J.D. (1994). "Examining the reactions between soluble iron, DOC, and alternative oxidants during conventional treatment: Speciation of iron is necessary in assessing whether oxidant addition will prove advantageous during treatment." Journal of the American Water Works Association, 86(1), 117-127.

Lalezary, S., Pirbazari, M., and McGuire, M.J. (1986). "Oxidation of five earthy-musty taste and odor compounds." Journal of the American Water Works Association, 78(3), 62-69.

Lead, J.R., Balnois, E., Hosse, M., Menghetti, R., and Wilkinson, K.J. (1999). "Characterization of Norwegian natural organic matter: size, diffusion coefficients, and electrophoretic mobilities." Environment International, 25(2-3), 245-258.

Lee, M.C., Snoeyink, V.L., and Crittenden, J.C. (1981). "Activated carbon adsorption of humic substances." Journal of the American Water Works Association, 73(8), 440-446.

Lee, T.Y., Park, J.W., and Lee, J.H. (2004). "Waste green sands as reactive media for the removal of zinc from water." Chemosphere, 56(6), 571-581.

Leenheer, J.A. (2007). "Progression from model structures to molecular structures of natural organic matter components." Annals of Environmental Science, 1, 57-68.

Leenheer, J.A., and Croue, J.P. (2003). "Characterizing aquatic dissolved organic matter." Environmental Science & Technology, 37(1), 18A-26A.

Leenheer, J.A., Malcolm, R.L., McKinley, P.W., and Eccles, L.A. (1974). "Occurrence of dissolved organic carbon in selected groundwater samples in the United States." Journal of Research of the U.S. Geological Survey, 2, 361-369.

Letterman, R.D., Quon, J.E., and Gemmell, R.S. (1974). "Film transport coefficient in agitated suspensions of activated carbon." Journal of the Water Pollution Control Federation, 46(11), 2536-2546.

Li , Q., Snoeyink, V.L., Mariãas, B.J., and Campos, C. (2003). "Elucidating competitive adsorption mechanisms of atrazine and NOM using model compounds." Water Research, 37, 773-784.

Li, F.S., Yuasa, A., Chiharada, H., and Matsui, Y. (2003). "Polydisperse adsorbability composition of several natural and synthetic organic matrices." Journal of Colloid and Interface Science, 265(2), 265-275.

Li, F.S., Yuasa, A., Chiharada, H., and Matsui, Y. (2003). "Storm impacts upon the composition of organic matrices in Nagara River - A study based on molecular weight and activated carbon adsorbability." Water Research, 37(16), 4027-4037.

Li, F.S., Yuasa, A., Ebie, K., Azuma, Y., Hagishita, T., and Matsui, Y. (2002). "Factors affecting the adsorption capacity of dissolved organic matter onto activated carbon: modified isotherm analysis." Water Research, 36(18), 4592-4604.

Li, L., Quinlivan, P.A., and Knappe, D.R.U. (2005). "Predicting adsorption isotherms for aqueous organic micropollutants from activated carbon and pollutant properties." Environmental Science & Technology, 39(9), 3393-3400.

Li, Q.L., Marinas, B.J., Snoeyink, V.L., and Campos, C. (2003a). "Three-component competitive adsorption model for flow-through PAC systems. 1. Model Application to a PAC/membrane system." Environmental Science & Technology, 37(13), 3005-3011.

Li, Q.L., Snoeyink, V.L., Mariaas, B.J., and Campos, C. (2003b). "Elucidating competitive adsorption mechanisms of atrazine and NOM using model compounds." Water Research, 37(4), 773-784.

Li, Q.L., Snoeyink, V.L., Marinas, B.J., and Campos, C. (2003c). "Pore blockage effect of NOM on atrazine adsorption kinetics of PAC: the roles of PAC pore size distribution and NOM molecular weight." Water Research, 37(20), 4863-4872.

MacCraith, B., Grattan, K.T.V., Connolly, D., Briggs, R., Boyle, W.J.O., and Avis, M. (1993). "Cross comparison of techniques for the monitoring of total organic-carbon (TOC) in water sources and supplies." Water Science and Technology, 28(11-12), 457-463.

Marhaba, T. (2000). "Examining bromate ion removal by GAC through RSSCT and pilot-scale columns." Environmental Engineering and Policy, 2, 59-64.

Martin, H. (1978). "Low peclet number particle-to-fluid heat and mass-transfer in packed-beds." Chemical Engineering Science, 33(7), 913-919.

Matsubara, H., and Nakayama, S. (1992). "Stability of premethylated aromatic model compounds of constituents of humic substances toward $KMnO_4$ oxidation." Water Research, 26, 1471–1478.

Matsuda, K., and Schnitzer, M. (1971). "The permanganate oxidation of humic acids extracted from acid soils." Soil Science, 114, 185–193.

Matsui, Y., Fukuda, Y., Inoue, T., and Matsushita, T. (2003). "Effect of natural organic matter on powdered activated carbon adsorption of trace contaminants: characteristics and mechanism of competitive adsorption." Water Research, 37(18), 4413-4424.

Matsui, Y., Kamei, T., Kawase, E., Snoeyink, V.L., and Tambo, N. (1994). "GAC adsorption of intermittently loaded pesticides." Journal of the American Water Works Association, 86(9), 91-102.

Matsui, Y., Knappe, D.R.U., and Takagi, R. (2002). "Pesticide adsorption by granular activated carbon adsorbers. 1. Effect of natural organic matter preloading on removal rates and model simplification." Environmental Science & Technology, 36(15), 3426-3431.

Matsui, Y., Yuasa, A., and Ariga, K. (2001). "Removal of a synthetic organic chemical by PAC-UF systems - I: Theory and modeling." Water Research, 35(2), 455-463.

Matsui, Y., Yuasa, A., and Li, F.S. (1998). "Overall adsorption isotherm of natural organic matter." Journal of Environmental Engineering-ASCE, 124(11), 1099-1107.

McCreary, J.J., and Snoeyink, V.L. (1980). "Characterization and activated carbon adsorption of several humic substances." Water Research, 14(2), 151-160.

McKay, G. (2001). "Solution to the homogeneous surface diffusion model for batch adsorption systems using orthogonal collocation." Chemical Engineering Journal, 81(1-3), 213-221.

Mertz, K.A., Gobin, F., Hand, D.W., Hokanson, D.R., Crittenden, J.C. (1999). "Manual: Adsorption Design Software for Windows (AdDesignS)." Michigan Technological University, Houghton, MI.

Mohan, D., and Chander, S. (2001). "Single component and multi-component adsorption of metal ions by activated carbons." Colloids and Surfaces a-Physicochemical and Engineering Aspects, 177(2-3), 183-196.

Moore, B.C., Cannon, F.S., Westrick, J.A., Metz, D.H., Shrive, C.A., DeMarco, J., and Hartman, D.J. (2001). "Changes in GAC pore structure during full-scale water treatment at Cincinnati: a comparison between virgin and thermally reactivated GAC." Carbon, 39(6), 789-807.

Morgan, J.J., and Stumm, W. (1964). "Colloid-chemical properties of manganese dioxide." Journal of Colloid Science, 19(4), 347-359.

MWH (2005). "Water Treatment: Principles and Design." John Wiley, Hoboken, NJ.

Myers, A.L., and Prausnitz, J.M. (1965). "Thermodynamics of mixed-gas adsorption." American Institute of Chemical Engineers Journal, 11(1), 121-127.

Najm, I.N., Snoeyink, V.L., Suidan, M.T., Lee, C.H., and Richard, Y. (1990). "Effect of particle-size and background natural organics on the adsorption efficiency of PAC." Journal of the American Water Works Association, 82(1), 65-72.

Najm, I.N., Snoeyink, V.L., and Richard, Y. (1991). "Effect of initial concentration of a SOC in natural water on its adsorption by activated carbon." Journal of the American Water Works Association, 83(8), 57-63.

Narbaitz, R.M. (1985). "Modeling the competitive adsorption of 1,1,2-trichloroethane with naturally occurring background organics onto activated carbon." PhD Thesis, McMaster University, Hamilton, ON.

Narbaitz, R.M. (1997). "Vars Water Quality and GAC Treatment." Report to the Regional Municipality of Ottawa-Carleton, Ottawa, ON.

Narbaitz, R.M., and Benedek, A. (1994). "Adsorption of 1,1,2-trichloroethane from river water." Journal of Environmental Engineering-ASCE, 120(6), 1400-1415.

Newcombe, G., and Drikas, M. (1997). "Adsorption of NOM onto activated carbon: Electrostatic and non-electrostatic effects." Carbon, 35(9), 1239-1250.

Newcombe, G., Drikas, M., Assemi, S., and Beckett, R. (1997). "Influence of characterised natural organic material on activated carbon adsorption: 1. characterisation of concentrated reservoir water." Water Research, 31(5), 965-972.

Newcombe, G., Drikas, M., and Hayes, R. (1997). "Influence of characterised natural organic material on activated carbon adsorption: 2. effect on pore volume distribution and adsorption of 2-methylisoborneol." Water Research, 31(5), 1065-1073.

Newcombe, G., Morrison, J., and Hepplewhite, C. (2002). "Simultaneous adsorption of MIB and NOM onto activated carbon: I. Characterisation of the system and NOM adsorption." Carbon, 40(12), 2135-2146.

Newcombe, G., Morrison, J., Hepplewhite, C., and Knappe, D.R.U. (2002). "Simultaneous adsorption of MIB and NOM onto activated carbon: II. Competitive effects." Carbon, 40(12), 2147-2156.

Nissinen, T.K., Miettinen, I.T., Martikainen, P.J., and Vartiainen, T. (2001). "Molecular size distribution of natural organic matter in raw and drinking waters." Chemosphere, 45(6-7), 865-873.

Noroozi, B., Sorial, G.A., Bahrami, H., and Arami, M. (2008). "Adsorption of binary mixtures of cationic dyes." Dyes and Pigments, 76(3), 784-791.

O'Connor, J.T. (1971). "Iron and Manganese." In: Water Quality and Treatment: A Handbook of Public Water Supplies, 3rd Edition. The American Water Works Association, Edited by M.E. Flentje, and R.J. Faust, McGraw-Hill Book Co., New York, NY.

Onganer, Y., and Temur, C. (1998). "Adsorption dynamics of Fe(III) from aqueous solutions onto activated carbon." Journal of Colloid and Interface Science, 205(2), 241-244.

Owen, D.M., Amy, G.L., Chowdhury, Z.K., Paode, R., McCoy, G., and Viscosil, K. (1995). "NOM characterization and treatability." Journal of the American Water Works Association, 87(1), 46-63.

Oxenford, J.L., and Lykins, B.W. (1991). "Conference summary - practical aspects of the design and use of GAC." Journal of the American Water Works Association, 83(1), 58-64.

Patrick, W.H., and Verloo, M. (1998). "Distribution of soluble heavy metals between ionic and complexed forms in a saturated sediment as affected by pH and redox conditions." Water Science and Technology, 37(6-7), 165-171.

Peel, R.G., and Benedek, A. (1980). "Attainment of equilibrium in activated carbon isotherm studies." Environmental Science & Technology, 14(1), 66-71.

Pelekani, C., and Snoeyink, V.L. (1999). "Competitive adsorption in natural water: Role of activated carbon pore size." Water Research, 33(5), 1209-1219.

Perdue, E.M. (1985). "Humic Substances in Soil, Sediments, and Water Geochemistry, Isolation, and Characterization: Acidic Functional Groups of Humic Substances." John Wiley & Sons, New York, NY.

Perdue, E.M. (1985). "Acidic Functional Groups of Humic Substances." Humic Substances in Soil, Sediments, and Water Geochemistry, Isolation, and Characterization, John Wiley & Sons, New York, NY.

Pesavento, M., Biesuz, R., Gnecco, C., and Magi, E. (2001). "Investigation of the metal species in seawater by sorption of the metal ion on complexing resins with different sorbing properties." Analytica Chimica Acta, 449(1-2), 23-33.

Pham, A.N., Rose, A.L., Feltz, A.J., and Waite, T.D. (2004). "The effect of dissolved natural organic matter on the rate of removal of ferrous iron in fresh waters." Natural Organic Material Research: Innovations and Applications for Drinking Water, 4(4), 213-219.

Potgieter, J.H., Potgieter-Vermaak, S.S., Modise, J., and Basson, N. (2005). "Removal of iron and manganese from water with a high organic carbon loading. Part II: The effect of various adsorbents and nanofiltration membranes." Water Air and Soil Pollution, 162(1-4), 61-70.

Qi, S.Y., Adham, S.S., Snoeyink, V.L., and Lykins, B.W. (1994). "Prediction and verification of atrazine adsorption by PAC." Journal of Environmental Engineering-ASCE, 120(1), 202-218.

Qi, S., and Schideman, L.C. (2008). "An overall isotherm for activated carbon adsorption of dissolved natural organic matter in water." Water Research, 42(13), 3353-3360.

Quinlivan, P.A., Li, L., and Knappe, D.R.U. (2005). "Effects of activated carbon characteristics on the simultaneous adsorption of aqueous organic micropollutants and natural organic matter." Water Research, 39(8), 1663-1673.

Radke, C.J., and Prausnitz, J.M. (1972). "Adsorption of organic solutes from dilute aqueous-solution on activated carbon." Industrial & Engineering Chemistry Fundamentals, 11(4), 445-&.

Radke, C.J., and Prausnitz, J.M. (1972). "Thermodynamics of multi-solute adsorption from dilute liquid solutions." American Institute of Chemical Engineers Journal, 18(4), 761-768.

Randtke, S.J., and Snoeyink, V.L. (1983). "Evaluating GAC adsorptive capacity." Journal of the American Water Works Association, 75(8), 406-413.

Razzaghi, M. (1976). "The competitive adsorption of carbohydrates, proteins, and lignosulfonates on activated carbon." MSc Thesis, McMaster University, Hamilton, ON.

Rose, A.L., and Waite, T.D. (2003). "Kinetics of iron complexation by dissolved natural organic matter in coastal waters." Marine Chemistry, 84(1-2), 85-103.

Rosen, J.B. (1952). "Kinetics of a fixed bed system for solid diffusion into spherical particles." Journal of Chemical Physics, 20(3), 387-394.

Satoh, K., Chang, H.T., Hattori, H., Tajima, K., and Furuya, E. (2005). "Simultaneous determination of multi-component isotherm parameters from single sample of liquid." Adsorption, 11, 79-83.

Schmitt, D., Saravia, F., Frimmel, F.H., and Schuessler, W. (2003). "NOM-facilitated transport of metal ions in aquifers: importance of complex-dissociation kinetics and colloid formation." Water Research, 37(15), 3541-3550.

Schnitzer, M., and Khan, S.U. (1972). "Humic Substances in the Environment." Marcel Dekker, New York, NY.

Siegrist, R.L. (2001). "Principles and Practices of In Situ Chemical Oxidation using Permanganate." Battelle Press, Columbus, OH.

Simpson, R. (1995). "Modeling competitive adsorption equilibria of synthetic organic chemicals in the presence of background organic matter." MEng Thesis, Univeristy of Ottawa, Ottawa, ON.

Simpson, R.K.D., and Narbaitz, R.M. (1997). "An evaluation of multicomponent adsorption equilibria models." Canadian Journal of Civil Engineering, 24(5), 828-839.

Singer, P.C. and Yen, C.Y. (1980). "Adsorption of alkyl phenols by activated carbon." In: Activated Carbon Adsorption of Organics from the Aqueous Phase, volume 1, Edited by I.H. Suffet, and M.J. McGuire, Ann Arbor Science Publishers, MI.

Sirichote, O., Innajitara, W., Chuenchom, L., Chunchit, D., and Naweekan, K. (2002). "Adsorption of iron (III) ion on activated carbons obtained from bagasse, pericarp of rubber fruit and coconut shell." Songklanakarin Journal of Science and Technology, 24(2), 235-242.

Smith, E.H., and Weber, W.J. (1988). "Modeling activated carbon adsorption of target organic-compounds from leachate-contaminated groundwaters." Environmental Science & Technology, 22(3), 313-321.

Snoeyink, V.L., and Summers, S.R. (1999). "Adsorption of Organic Compounds." In: Water Quality & Treatment - 5th edition, Edited by R. Letterman, McGraw Hill, , Washington, DC.

Snoeyink,V.L. (1990). "Adsorption of Organic Compounds." In: Water Quality and Treatment." 4th edition, Edited by F.W. Pontius, McGraw-Hill, New York, NY.

Sommerfeld E.O. (1999). "Iron and Manganese Removal Handbook." American Water Works, Denver, CO.

Sontheimer, H., Crittenden, J., and Summers, R. (1988). "Activated Carbon for Water Treatment." American Water Works Research Foundation Denver, CO.

Sorial, G.A., Suidan, M.T., Vidic, R.D., and Maloney, S.W. (1993). "Competitive adsorption of phenols on GAC: 1. Adsorption equilibrium." Journal of Environmental Engineering-ASCE, 119(6), 1026-1043.

Soylak, M. (2004). "Solid phase extraction of Cu(II), Pb(H), Fe(III), Co(II), and Cr(III) on Chelex-100 column prior to their flame atomic absorption spectrometric determinations." Analytical Letters, 37(6), 1203-1217.

Speth, T.F. (1991). "Evaluating capacities of GAC preloaded with natural-water." Journal of Environmental Engineering-ASCE, 117(1), 66-79.

Speth, T.F., and Miltner, R.J. (1989). "Effect of preloading on the scale-up of GAC microcolumns." Journal of the American Water Works Association, 81(4), 141-148.

Speth, T.F., and Miltner, R.J. (1990). "Technical note - adsorption capacity of GAC for synthetic organics." Journal of the American Water Works Association, 82(2), 72-75.

Statistics Canada (1996). "Quarterly Estimates of the Population of Canada, the Provinces and the Territories." Catalogue No. 91-001, Ottawa, ON.

Stevenson, F.J. (1982) "Methods of Soil Analysis: Nitrogen – Organic forms." American Society of Agronomy and Soil Science Society of America, Madison, WI.

Stevenson, F.J. (1983). "Nitrogen organic forms." In: Agronomy: A Series of Monographs, Volume 9, Methods of Soil Analysis, Part 2, Chemical and Microbiological Properties, 2nd Edition, Edited by A.L. Page, American Society of Agronomy, Soil Science Society of America, Inc. Publishers: Madison, WI.

Storrar, M. (2006). "Adsorption and desorption characteristics of natural organic matter in natural waters on granular activated carbon." MSc Thesis, Univeristy of Ottawa, Ottawa, ON.

Stover, E.L., and Thomas, J.A. (1992). "Carbon adsorption: A primer." The National Environmental Journal, 2(6), 28-32.

Stumm, W., and Lee, G.F. (1961). "Oxygenation of ferrous iron." Industrial and Engineering Chemistry, 53(2), 143-146.

Stumm, W., and Morgan, J.J. (1996). "Aquatic Chemistry: Chemical Equilibria and Rates in Natural Waters." Wiley & Sons, New York, NY.

Suffet, I.H., and MacCarthy, P. (1989). "Aquatic humic substances: Influence on fate and treatment of pollutants." In: Advances in Chemistry Series, volume 219, American Chemical Society, Washington, DC.

Summers, R.S., and Roberts, P.V. (1988). "Activated carbon adsorption of humic substances: 1. heterodisperse mixtures and desorption." Journal of Colloid and Interface Science, 122(2), 367-381.

Summers, R.S., and Roberts, P.V. (1988). "Activated carbon adsorption of humic substances: 2. size exclusion and electrostatic interactions." Journal of Colloid and Interface Science, 122(2), 382-397.

Summers, R.S., Haist, B., Koehler, J., Ritz, J., Zimmer, G., and Sontheimer, H. (1989). "The influence of background organic-matter on GAC adsorption." Journal of the American Water Works Association, 81(5), 66-74.

Summers, R.S., Hooper, S.M., Solarik, G., Owen, D.M., and Hong, S.H. (1995). "Bench-scale evaluation of GAC for NOM control." Journal of the American Water Works Association, 87(8), 69-80.

Summers, R.S., Hooper, S., and Hong, S. (1994). "The use of RSSCTs to predict GAC field-scale performance." In the Proccedings of the American Water Works Association Annual Conference, New York, NY.

Summers, R.S., and Roberts, P.V. (1987). "Rate of humic substance uptake during activated carbon adsorption." Journal of Environmental Engineering-ASCE, 113 (6): 1333-1349.

Sung, W., and Forbes, E.J. (1984). "Some considerations on iron removal." Journal of Environmental Engineering-ASCE, 110(6), 1048-1061.

Tadanier, C.J., Berry, D.F., and Knocke, W.R. (2000). "Dissolved organic matter apparent molecular weight distribution and number-average apparent molecular weight by batch ultrafiltration." Environmental Science & Technology, 34(11), 2348-2353.

Thacker, W.E., Snoeyink, V.L., and Crittenden, J.C. (1981). "Modeling of activated carbon and coal gasification char adsorbents in single solute and bi solute systems." University of Illinois at Urbana-Champaign Water Resources Center Research Report (161), 1-166.

Theis, T.L., and Singer, P.C. (1974). "Complexation of iron(II) by organic-matter and its effect on iron(II) oxygenation." Environmental Science & Technology, 8(6), 569-573.

Thurman, E.M. (1985). "Organic Geochemistry of Natural Waters." M. Nijhoff, Distributors for the U.S. and Canada, Kluwer Academic, Dordrecht, Boston Hingham, MA.

Thurman, E.M., and Malcolm, R.L. (1981). "Preparative isolation of aquatic humic substances." Environmental Science & Technology, 15(4), 463-466.

Tien, C. (1994). "Adsorption Calculation and Modeling." In: Series in Chemical Engineering, Butterworth–Heinemann, London, England.

To, P.C., Marinas, B.J., Snoeyink, V.L., and Ng, W.J. (2008). "Effect of pore-blocking background compounds on the kinetics of trace organic contaminant desorption from activated carbon." Environmental Science & Technology, 42(13), 4825-4830.

To, P.C., Marinas, B.J., Snoeyink, V.L., and Ng, W.J. (2008). "Effect of strongly competing background compounds on the kinetics of trace organic contaminant desorption from activated carbon." Environmental Science & Technology, 42(7), 2606-2611.

Ucer, A., Uyanik, A., and Aygun, S.F. (2006). "Adsorption of Cu(II), Cd(II), Zn(II), Mn(II) and Fe(III) ions by tannic acid immobilised activated carbon." Separation and Purification Technology, 47(3), 113-118.

Ucer, A., Uyanik, A., Cay, S., and Ozkan, Y. (2005). "Immobilisation of tannic acid onto activated carbon to improve Fe(III) adsorption." Separation and Purification Technology, 44(1), 11-17.

Uchida, M., Ito, S., Kawasaki, N., Nakamura, T., and Tanada, S. (1999). "Competitive adsorption of chloroform and iron ion onto activated carbon fiber." Journal of Colloid and Interface Science, 220(2), 406-409.

Uchida, M., Shinohara, O., Ito, S., Kawasaki, N., Nakamura, T., and Tanada, S. (2000). "Reduction of iron(III) ion by activated carbon fiber." Journal of Colloid and Interface Science, 224(2), 347-350.

Urynowicz, M. A., Balu, B., and Udayasankar, U. (2008). "Kinetics of natural oxidant demand by permanganate in aquifer solids." Journal of Contaminant Hydrology, 96(1-4), 187-194.

USEPA (1973). "Water Quality Criteria 1972." National Academy of Sciences, USEPA, Research series, Washington, DC.

USEPA (1991). "Granular Activated Carbon Treatment." Engineering Bulletin. USEPA, Office of emergency and remedial response, Washington, DC.

USEPA (1992). "Manual of Small Public Water Supply Systems." C.K. Smoley, Boca Raton, FL.

USEPA (1997). "1996 Clean Water Needs Survey Report to Congress." Office of Water, Washington, DC.

Uzun, I., and Guzel, F. (2002). "Adsorption of some heavy metal ions from aqueous solution by activated carbon and comparison of percent adsorption results of activated carbon with those of some other adsorbents." Turkish Journal of Chemistry, 24, 291-297.

Van der Aa, L., Rietveld, L.C., and Van Dijk, J.C. (2011). "Effects of ozonation and temperature on the biodegradation of natural organic matter in biological granular activated carbon filters." Drinking Water Engineering and Science, 4, 25-35.

VanLoon, G.W., and Duffy, S.J. (2005). "Environmental Chemistry: A Global Perspective." Oxford University Press, Oxford; New York, NY.

Vidic, R. D., and Suidan, M. T. (1991). "Role of dissolved-oxygen on the adsorptive capacity of activated carbon for synthetic and natural organic-matter." Environmental Science & Technology, 25(9), 1612-1618.

Vidic, R.D., Sorial, G.A., Papadimas, S.P., Suidan, M.T., and Speth, T.F. (1992). "Effect of molecular oxygen on the scaleup of GAC adsorbers." Journal of the American Water Works Association, 84(8), 98-105.

Wassenaar, L., Aravena, R., Fritz, P., and Barker, J. (1990). "Isotopic composition (C-13, C-14, H-2) and geochemistry of aquatic humic substances from groundwater." Organic Geochemistry, 15(4), 383-396.

Weber, W.J., and Smith, E.H. (1989). "Effects of humic background on granular activated carbon treatment efficiency." ACS Symposium Series, 219, 501-532.

Weber, W.J., Voice, T.C., and Jodellah, A. (1983). "Adsorption of humic substances - the effects of heterogeneity and system characteristics." Journal of the American Water Works Association, 75(12), 612-619.

Weber, W.J. (1972). "Physicochemical Processes for Water Quality Control." Wiley-Interscience, New York, NY.

WHO (1996). "Guidelines for Drinking-Water Quality." World Health Organization, Geneva, Switzerland.

WHO (2004). "Guidelines for Drinking Water Quality." 3rd edition, Volume 1, Geneva, Switzerland.

WHO (2011). "Guidelines for Drinking-Water Quality." World Health Organization, Geneva, Switzerland.

Willey, B. and Jennings, H. (1963). "Iron and manganese removal with potassium permanganate." Journal of the American Water Works Association, 65, 729-735.

Yoon, Y.M., Amy, G., Cho, J.W., and Her, N. (2005). "Effects of retained natural organic matter (NOM) on NOM rejection and membrane flux decline with nanofiltration and ultrafiltration." Desalination, 173(3), 209-221.

Yuasa, A., Li, F., Matsui, Y., and Ebie, K. (1996). "Adsorption equilibria of multicomponent organic mixtures of unknown composition." In the Proceedings of the Environmental Engineering Research, 33, 123-132.

Yuasa, A., Li, F.S., Matsui, Y., and Ebie, K. (1997). "Characteristics of competitive adsorption of aquatic humic substances onto activated carbon." Water Science and Technology, 36(12), 231-238.

Zogorski, J.S., Faust, S.D., and Haas, J.H. (1976). "Kinetics of adsorption of phenols by granular activated carbon." Journal of Colloid and Interface Science, 55(2), 329-341.

APPENDIX A CHARACTERISTICS OF VARS RAW WATER USED FOR ISOTHERM EXPERIMENTS

Table A-1: Characteristics of Vars groundwater performed on different dates

Parameters	Unit	(August 25th, 2008)	(September 20th, 2011)
pH	-	7.8	7.5
Temperature	°C	8.2	8.9
Turbidity	N.T.U	0.21	0.24
Total Alkalinity	mg/L (as CaCO3)	223	198
Total Hardness	mg/L (as CaCO3)	221	216
Total Fe	mg/L	1.13	1.07
Fe (II)	mg/L	1.10	1.05
Fe (III)	mg/L	0.03	0.02
TOC	mgTOC/L	4.22	4.15

A.1 Ferric Iron Isotherm Modeling

The initial concentration of ferric iron used for the isotherm experiment was 1.5 mg/L but it dropped to 1.30 mg/L by the end of the of the isotherm experiment due to ferric iron precipitation, indicating that 13.3% of the iron was precipitated. Figure A-1 shows the isotherm data of ferric iron compared to the adsorption isotherm of ferrous iron. It is clear from the figure that ferric iron has a lower adsorption capacity than ferrous iron over the concentration range (e.g., 2.1 mg/gGAC for ferric iron versus 6.5 mg/gGAC for ferrous iron at equilibrium concentration (C_e) of 0.2 mg/L). Also, as shown in Table A-2, the lower ferric iron adsorbing capacity agrees with the findings of Uchida *et al.* (2000) who studied ferrous and ferric iron ion adsorption onto activated carbon fibers. Using an equilibrium concentration of 0.2 mg/L for ferric iron, the solid phase concentrations (q_e) of ferric iron obtained in this study and by Uchida *et al.* (2000) were 2.1 and 1.8 mg/gGAC, respectively. One of the main problems associated with the adsorption experiments of ferric iron was the sorption/precipitation of iron hydroxide on the surface of activated carbon particles, as

shown in Figure A-2. The observed surface coverage may block the entrance to adsorption sites and limit the capacity of GAC when used for the adsorption of ferric iron.

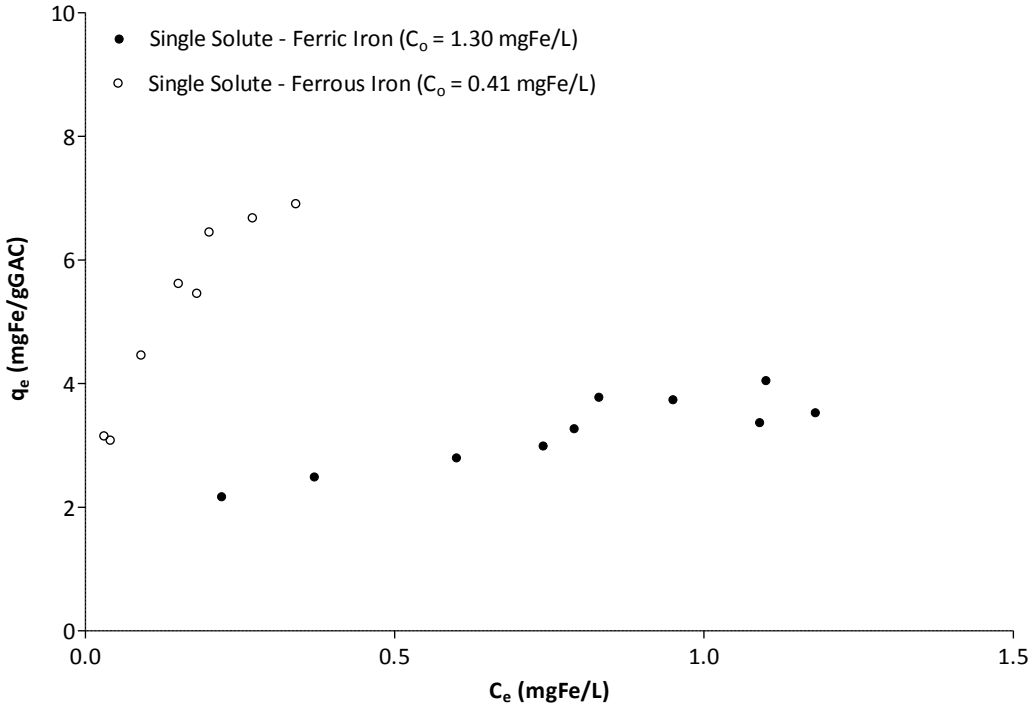

Figure A-1: Adsorption isotherms for ferric and ferrous iron in organic free water

Table A-2: Comparison of isotherm results of ferric iron between this study and a study by Uchida *et al.* (2000)

	Equilibrium Concentration Range (mg/L)	Amount of Ferric Iron Adsorbed Range (mg/gGAC)
This Study	0.22 – 1.18	2.08 – 3.53
Uchida *et al.*, (2000)	0.20 – 1.05	1.80 – 3.00

Figure A-2: Ferric iron hydroxide precipitates on the surface of GAC particles (mesh size 40×50) used in the isotherm experiment of ferric iron

The ferric iron single isotherm data were modeled using the same models used for ferrous iron. The isotherm data were modeled using Freundlich (Figure A-3.a), Langmuir (Figure A-3.b) and Summers-Roberts isotherm (Figure A-4) models. All models fit the ferric isotherm data well with most of the isotherm data. However, Freundlich and Langmuir fits were somewhat better than the Summers-Roberts model. Based on the fit indicators, the Freundlich model described the data best, and had the lowest values of the CV(RMSE) and AAPE (8.6% and 6.2%, respectively).

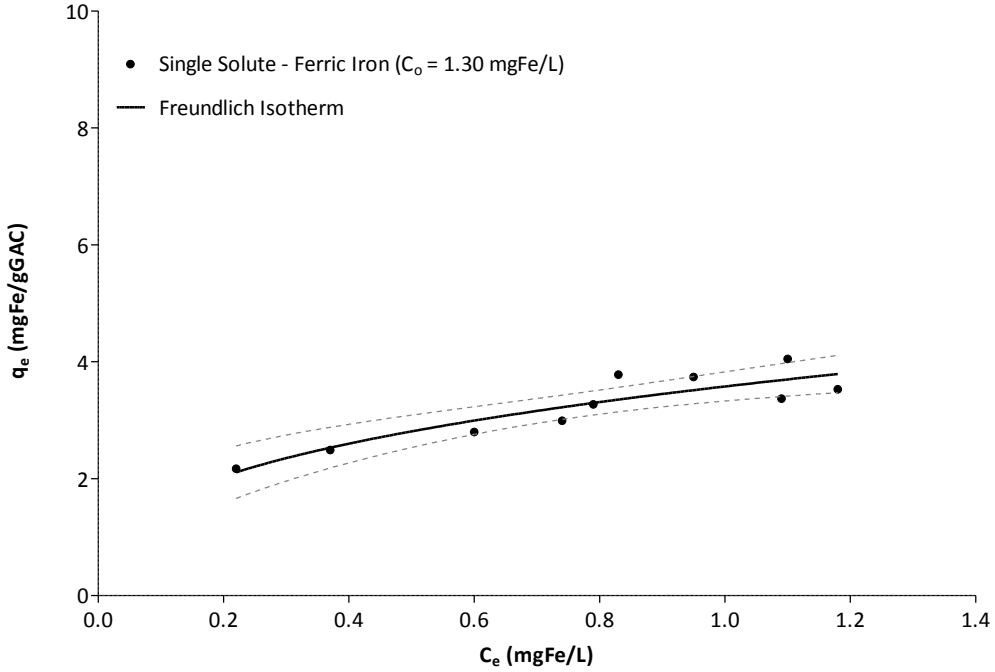

(a)

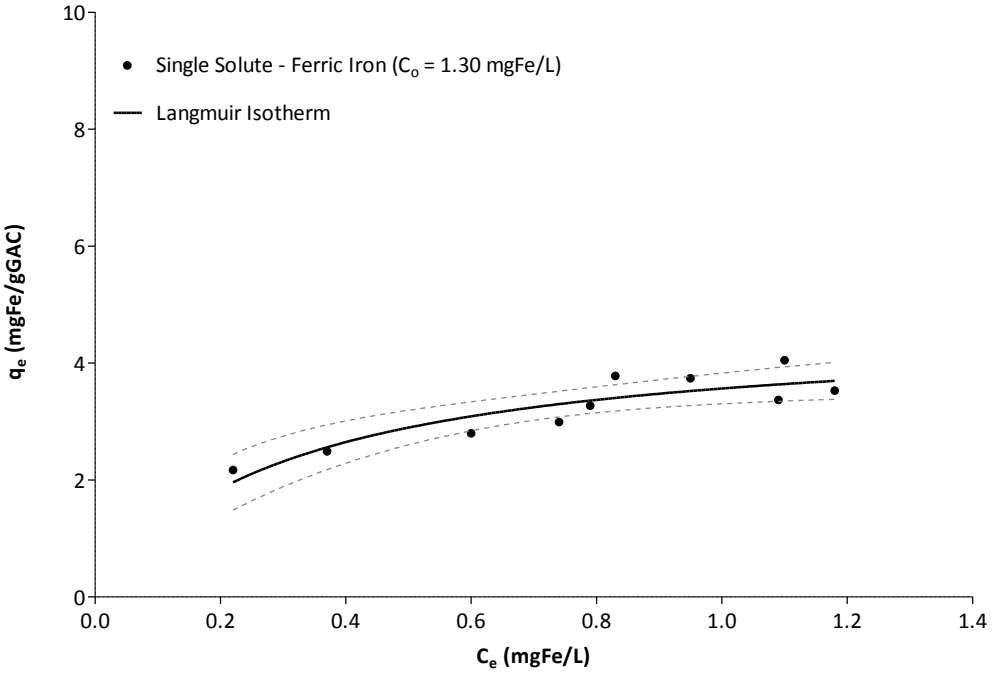

(b)

Figure A-3: Single solute isotherms for ferric iron using: (a) Freundlich and (b) Langmuir models within the 95% confidence interval (F-400 GAC (40×50 mesh size), C_o = 1.30 mg/L, pH= 6, Temperature = 25 ^oC)

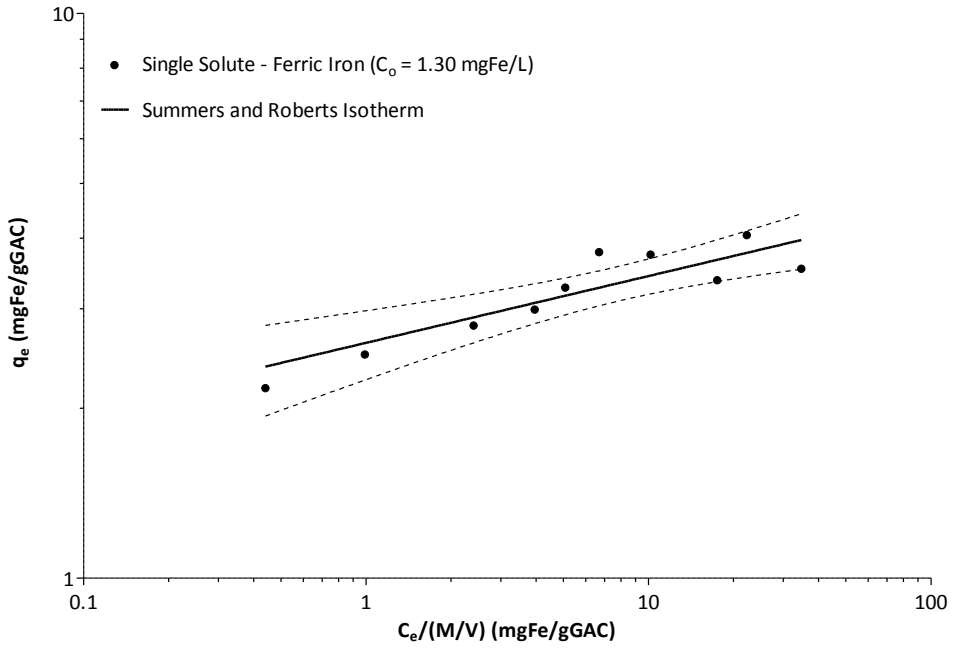

Figure A-4: Single solute isotherms of ferric iron using Summers-Roberts model within the 95% confidence interval (F-400 GAC (40×50 mesh size), C_o = 1.30 mg/L, pH= 6, Temperature = 25 ^oC)

Table A-3: Fitted parameter for Langmuir, Freundlich and Summers-Roberts models used to model ferric iron as single solute in organic free water

Model	Parameter	Parameter Value	95% Confidence Interval	Model Fit Indicators	
				CV(RMSE), %	AAE, %
Langmuir Isotherm	q_s (mg/g)	4.64	3.61 – 5.67	9.1	7.4
	b (L/mg)	3.33	0.75 – 5.90		
Freundlich Isotherm	K_F (mg/g)·(L/mg)^n	3.58	3.33 – 3.83	8.6	6.2
	n_F	0.35	0.19 – 0.51		
Summers-Roberts Isotherm	K_{SR} (mg/g)·(g/mg)^n	2.61	2.25 – 2.97	9.8	7.3
	n_{SR}	0.12	0.06 – 0.18		

Number of data points = 10

Number of regressed parameters (Langmuir Model) = 2 (q_s and b)

Number of regressed parameters (Freundlich Model) = 2 (K_F and n_F)

Number of regressed parameters (Summers-Roberts Model) = 2 (K_{SR} and n_{SR})

APPENDIX B ADDITIONAL VARIATION OF THE IAST MODELS

B.1 IAST-FR-EBC Model

IAST-FR-EBC is the equivalent background compound (EBC) model which incorporates the IAST competitive adsorption model and uses the Freundlich isotherm to describe the single solute isotherms. The IAST-FR-EBC model regressions search for the optimal value of the following four parameters: $C_{o\text{-}NOM}$, $K_{NOM,}$ n_{NOM}, and the NOM's molecular weight. It is essentially the same as the one pseudocomponent IAST model in which C_o is regressed, not fixed like in the standard one pseudocomponent IAST model. The ferrous iron simulation using IAST EBC model (Figure B-1.b) shows a good fit for the ferrous iron data. However, the EBC isotherm was very poor simulation of the NOM adsorption data (Figure B-1.a). The IAST EBC characteristics are summarized in Table B-1. The regressed value of the NOM initial concentration based on the IAST EBC model was 7.10 mgTOC/L which is higher than the actual Vars TOC concentration of 4.24 mgTOC/L. Thus, the regressed initial EBC concentration of NOM is unrealistic and the simulation result of IAST EBC was rejected as a reasonable simulation of Vars raw water isotherm data. Even though, it was thought that adding one more parameter (i.e., Co) to be regressed in the IAST-FR-EBC compared to the IAST-FR one pseudocomponent, the simulations results were almost the same. The difference in the fit indicators (CV(RMSE) and AAPE) for the ferrous iron solid-phase concentration between IAST-FR-EBC and IAST-FR one pseudocomponent were found to be 0.3% and 0.4%, respectively. The difference in the fit indicators (CV(RMSE) and AAPE) for the NOM solid phase concentration were 4.3% and 1.7%, respectively (Table B-2).

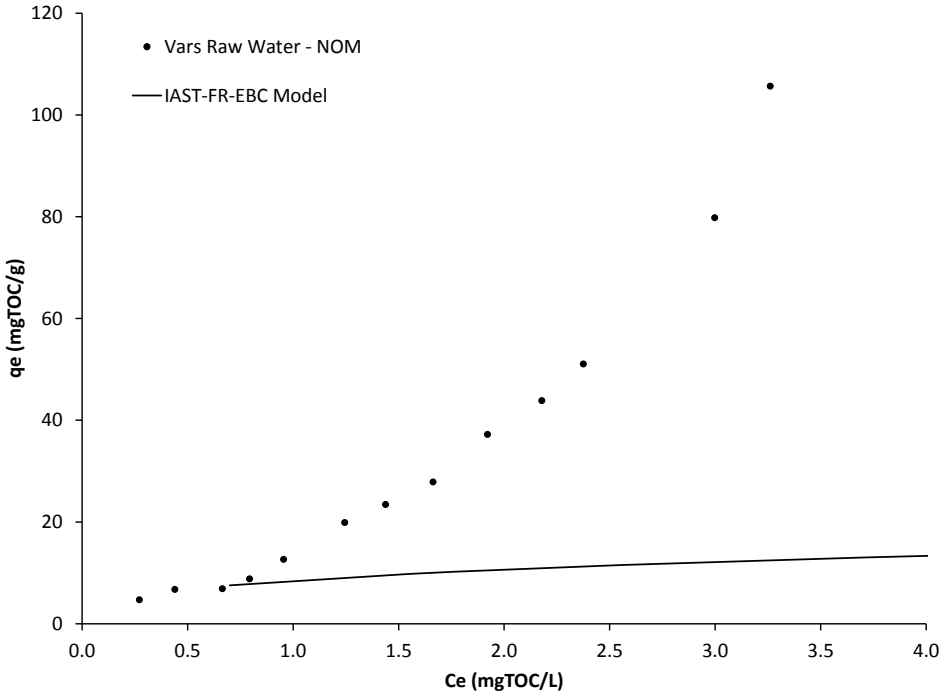

(a)

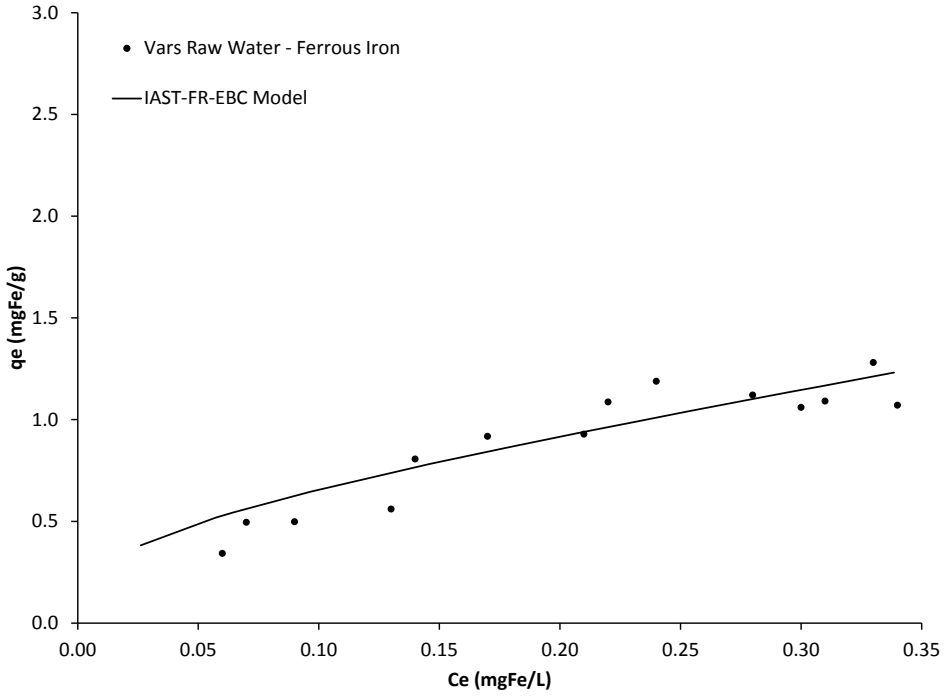

(b)

Figure B-1: IAST-FR-EBC model simulation of: (a) NOM and (b) ferrous iron

Table B-1: Regressed parameters for IAST-FR-EBC model

Model	Component	Initial Concentration (mg/L)	Initial Concentration (μmol/L)	Molecular Weight (g/mol)	K_F $(\mu mol/g)\cdot(L/\mu mol)^n$	n_F
IAST-FR-EBC	NOM	7.10	127.24	111.6	60.50	0.33
	Ferrous Iron	0.35	6.27	55.8	67.98	0.35

Note: Organic carbon was assumed to account for 50% of the NOM molecular weight

Table B-2: Comparison between fit indicators for IAST-FR-EBC and IAST-FR one pseudocomponent models

Model	Fit Indicator	Ferrous Iron q	NOM q
IAST-FR-EBC	**CV(RMSE) (%)**	10.5	122.2
	AAPE (%)	7.6	48.2
IAST-FR One Pseudocomponent	**CV(RMSE) (%)**	10.2	126.5
	AAPE (%)	8.0	46.5

Number of data points = 14

Number of regressed parameters (IAST EBC) = 4 ($C_{o\text{-}NOM}$, MW_{NOM}, K_{NOM}, n_{NOM})

Number of regressed parameters (IAST-FR One Pseudocomponent) : 3 (MW_{NOM}, K_{NOM}, n_{NOM})

APPENDIX C LANGMUIR SINGLE ISOTHERM MODEL FOR NOM

The NOM isotherm data was modeled by the Langmuir model using the nonlinear regression method (Figure C-1.a). The model simulation was not particularly good. It has a straight line shape over the whole range of the data points, whereas the NOM isotherm data was curved. Furthermore, Table C-1 shows that the average absolute error is approximately 50% and the regressed q_s value is extremely large (q_s = 29422.21 mgTOC/gGAC). The value of q_s obtained is abnormally high as it implies that GAC can adsorb NOM up to 29 times its own weight. For this reason, the Langmuir model was regressed using a linear regression method, leading to a transformation that gives more weight to the lower concentration range of the isotherm. To obtain the parameters of the Langmuir isotherm (q_s and b), a manipulated linear form of the Langmuir isotherm equation is used:

$$\frac{1}{q_e} = \frac{1}{q_s} + \frac{1}{q_s . b} . \frac{1}{C_e} \qquad \text{(C-1)}$$

Plotting the isotherm data in a suitable manner ($1/q_e$ (gGAC/mgTOC) versus $1/C_e$ (L/mgTOC)) will yield a straight line with a slope of $1/q_s$ and an intercept of $1/(q_s \cdot b)$. Figure C-1.b shows the results of the Langmuir model using the linear regression method. The model was capable of modeling the NOM isotherm data with liquid phase concentration (C_e) up to 1.75 mgTOC/L. However, the model was not capable of simulating the curvature of the NOM isotherm data which led to the underestimation of the isotherm data with higher equilibrium liquid phase concentrations (i.e., C_e higher than 2.0 mgTOC/L). The value of q_s obtained by the linear regression was found to be 388.35 mgTOC/gGAC. Even though the value of q_s obtained is 3.7 times more than the isotherm data point with the highest adsorption capacity (C_e = 3.26 mgTOC/L and q_e = 105.63 mgTOC/gGAC), it is more reasonable than the value obtained by the nonlinear regression method (i.e., q_s = 29422.21 mgTOC/gGAC). Accordingly, for competitive adsorption models based on Langmuir single solute isotherms, the linear-regression based Langmuir isotherm model parameter values will be used. As for the quality of the Langmuir model fit, the high value of the fit indicators CV(RMSE) and AAPE summarized in Table C-1 imply that the Langmuir model simulations

of the NOM isotherm data are rather poor and the models do not describe the data well for both types of regression, linear and nonlinear.

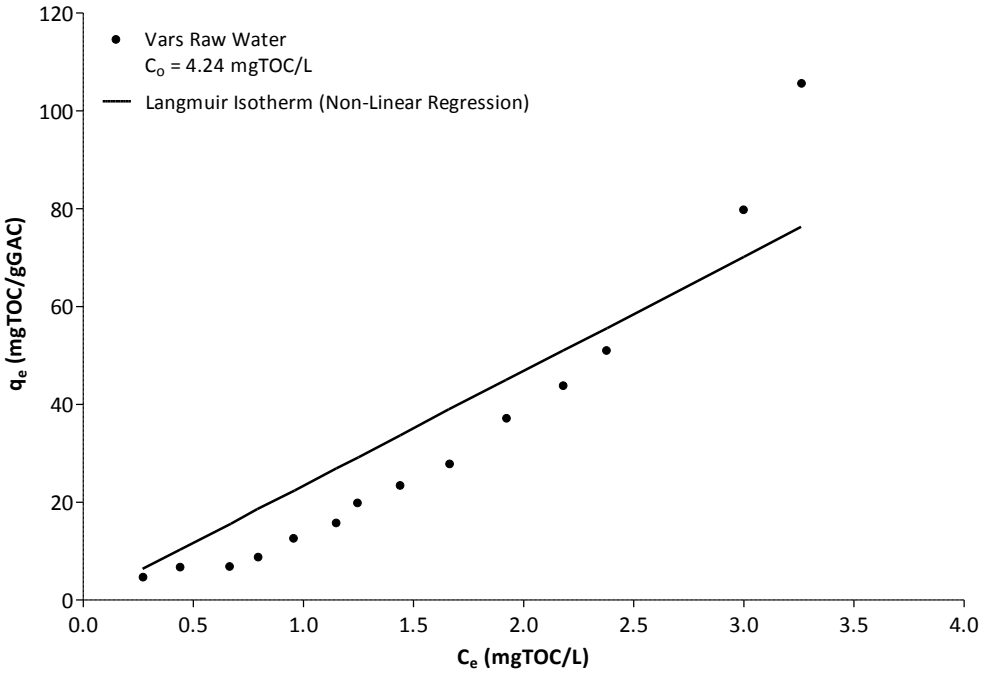

(a)

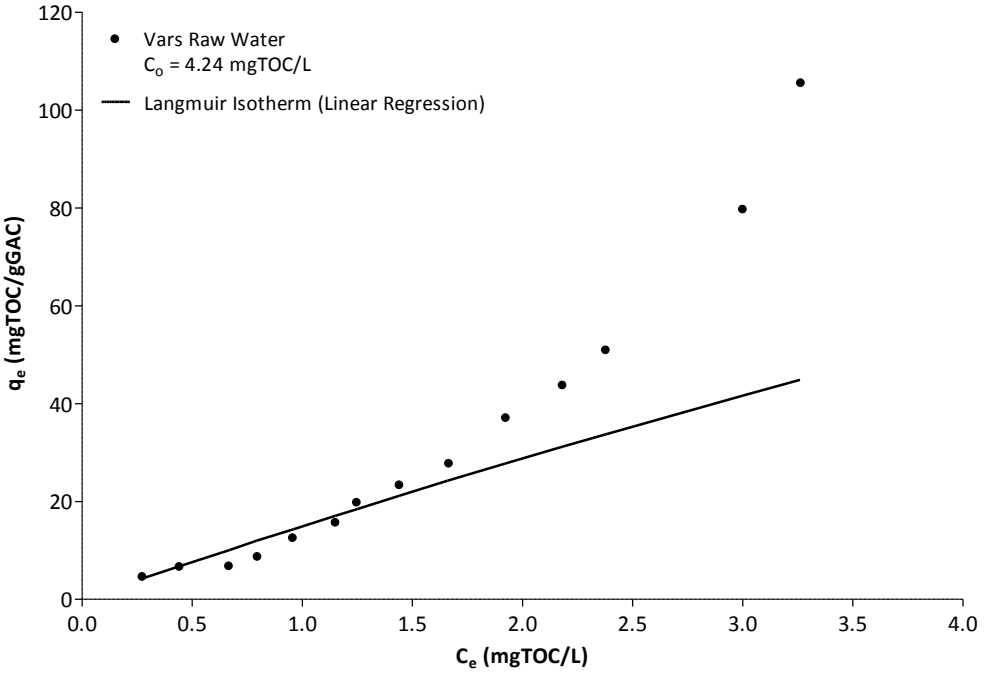

(b)

Figure C-1: Single solute isotherms of NOM in Vars raw water using Langmuir models obtained by: (a) nonlinear regression and (b) linear regression (F-400 GAC (40×50 mesh size), C_o = 4.24 mg/L, pH = 7.5, Temperature = 25 ^oC)

Table C-1: Fitted parameter for Langmuir model used to model the NOM in Vars raw water

Model	Parameter	Parameter Value	Parameter 95% Confidence Interval	Model Fit Indicators	
				CV(RMSE) (%)	AAPE (%)
Langmuir Isotherm (Nonlinear Regression)	q_s (mg/g)	29422.21	Very Wide	39.1	49.7
	b (L/mg)	0.001			
Langmuir Isotherm (Linear Regression)	q_s (mg/g)	388.35	Very Wide	56.4	30.0
	b (L/mg)	0.04			

Number of data points = 14

Number of regressed parameters (Langmuir Model) = 2 (q_s and b)

APPENDIX D ALTERNATIVE MULTISOLUTE MODELING TECHNIQUES

The alternative competitive adsorption isotherm models that are covered in this appendix are Jain and Snoeyink, Razzaghi and Fritz and Schlunder models.

D.1 Jain and Snoeyink Model

Butler and Ockrent (1930) developed one of the first competitive adsorption models derived from the Langmuir model for bi-solute solutions (Sontheimer *et al.*,1988). The Butler and Ockrent model led to unsatisfactory results when some parts of the adsorption were non-competitive. Accordingly, the model proposed by Jain and Snoeyink attempted to overcome this difficulty after taking into consideration the non-competitive adsorption on the adsorbent surface (Jain and Snoeyink, 1973). For a bisolute system, Jain and Snoeyink (1973) model can be written as:

$$q_1 = \frac{(q_{S1}-q_{S2})\, b_1 C_1}{1+b_1 C_1} + \frac{q_{S2}\, b_1 C_1}{1+b_1 C_1+b_2 C_2} \qquad \text{(D-1)}$$

$$q_2 = \frac{q_{S2}\, b_2 C_2}{1+b_1 C_1+b_2 C_2} \qquad \text{(D-2)}$$

Where: q_1 and q_2 = the solid phase concentration of components 1 and 2 in equilibrium with C_1 and C_2 (mol/gGAC); C_1 and C_2 = the liquid phase at equilibrium of components 1 and 2 within the bisolute mixture (mol/L); q_{s1} and q_{s2} = the monolayer adsorption capacity of components 1 and 2 from the corresponding Langmuir single solute isotherms (mol/gGAC); b_1 and b_2 = the energy constant of components 1 and 2 from the corresponding Langmuir single solute isotherms (L/mol). The model is molar based and the molecular weight of each component would impact the values of q_s and b. The values of q_{s1}, q_{s2}, b_1 and b_2 used in the model were determined in section 5.2.1.1 from the Langmuir single isotherm of both components, the first term ($q_{s1} - q_{s2}$) of Equation (D-1) includes the quantity of what adsorbs without competition. This quantity is based on the assumption that the difference is only

available for the component with the higher maximum solid phase capacity. The choice of which component is component 1 is based on the values of q_{s1} and q_{s2} in which $q_{s1} > q_{s2}$.

Jain and Snoeyink extended Langmuir model was used to predict the competitive adsorption in Vars raw water. Since the molecular size of NOM is considered to be one of the main factors influencing the competition over the adsorbing sites, the Jain and Snoeyink model was tested using a range of molecular weights of NOM. The molecular weights ranged from 111.6 and 10,000 g/mol. Table D-1 show the parameters used for Jain and Snoeyink extended Langmuir model. The comparison between experimental data and simulations based on the Jain and Snoeyink model for both NOM and ferrous iron in Vars raw water is shown in Figure D-1. The correlations between the simulations and the experimental data were very poor for both iron and different molecular weights of NOM. The Jain and Snoeyink model underpredicted the NOM adsorption, and overpredicted the ferrous iron multisolute isotherm by a factor of six. Overall, the Jain and Snoeyink extended Langmuir model does not predict well the competitive adsorption of NOM and iron in Vars raw water.

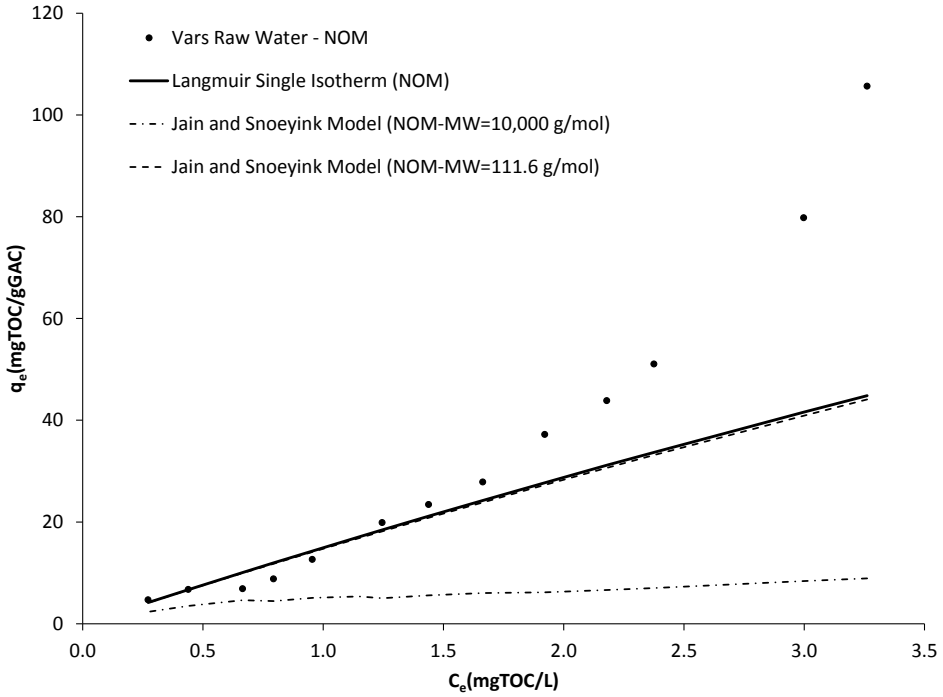

(a)

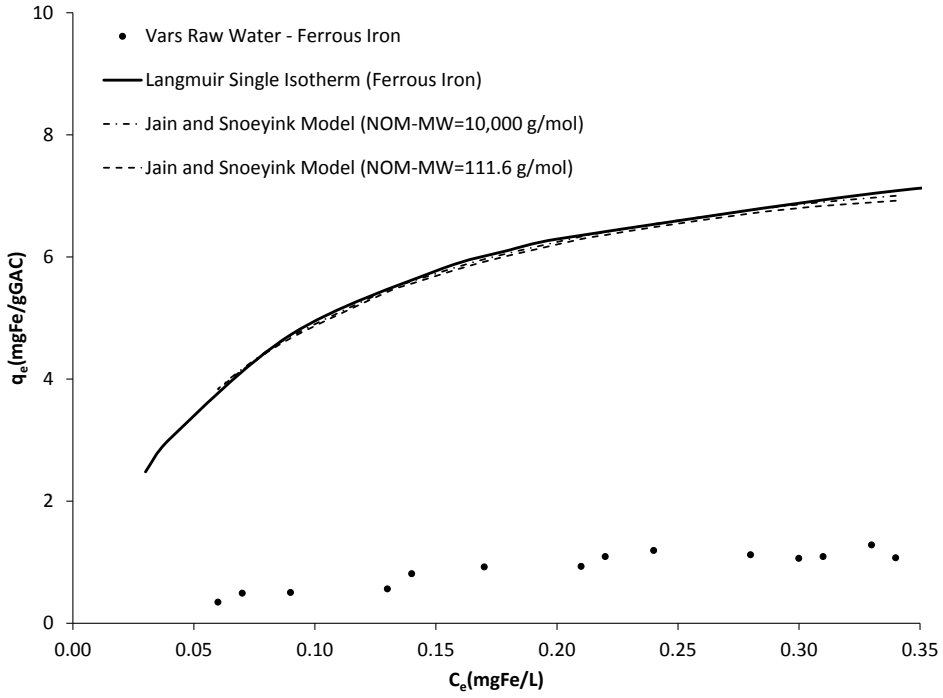

(b)

Figure D-1: Jain and Snoeyink model for: (a) NOM and (b) ferrous iron

Table D-1: Parameters for Jain and Snoeyink model

	Ferrous Iron	NOM	
MW (g/mol)	55.8	10,000	111.6
Equilibrium Concentration Range (µmol/L)	0.54 – 8.06	0.05 – 0.65	4.88 – 58.46
q_s (µmol/g)	154.73	77.67	6959.62
b (L/µmol)	0.75	0.20	0.002

Note: Organic carbon was assumed to account for 50% of the NOM molecular weight

D.2 Razzaghi Model

Multicomponent models with non-competitive terms are seen as good candidates given that the NOM adsorption shows little or no competition. Another multicomponent model with a non-competitive term is the Freundlich-based model developed by Razzaghi (1976). Narbaitz and Benedek (1994) found that this model yielded reasonable simulations for NOM and 1,1,2-Trichloroethane isotherms, in which the NOM was also not significantly affected by competition. The general form of the model used to calculate q_i, the equilibrium solid phase concentrations in the multisolute mixture, is:

$$q_i = (1-w_i) K_{F-i} C_i^{n_{F-i}} + w_i \left(\frac{C_i}{\sum_{j=1}^{N} C_j} \right)^{n_{F-i}} K_{F-i} C_i^{n_{F-i}} \qquad \text{(D-3)}$$

Where: K_{F-i} = The Freundlich single isotherm regressed parameter of component i in the mixture $((mol/g)\cdot(L/mol)^n)$; and n_{F-i} = The Freundlich single isotherm regressed exponent of component i in the mixture; C_i is the equilibrium liquid phase concentration of component i within the multisolute mixture in (mol/L); w_i is the fraction of the total capacity of component i within the mixture that is involved in competition.

Modeling the competitive adsorption of NOM and ferrous iron data using the Razzaghi model requires the regression of three parameters (w_1, w_2, NOM's Freundlich parameters and NOM's molecular weight). The parameters w_1 and w_2 represent the fraction of the adsorptive capacity of ferrous iron and NOM, respectively. The Freundlich parameters of ferrous iron were obtained from the Freundlich single solute isotherms and they were not regressed. Figure D-2 shows Razzaghi model simulations for the data of both components and the regressed parameters are summarized in Table D-2. Using an average molecular weight of 1000 g/mol to represent the competing fraction of NOM in Vars raw water, the model appears to describe the NOM data very well but not the ferrous iron isotherm data. A sensitivity analysis was conducted by varying the NOM's molecular weight and changing the values of w_1 and w_2 between 0 and 1. It was found that choosing a higher molecular weight for the NOM did not improve the modeling of ferrous iron. The only way to improve the modeling of ferrous iron was by equating the molecular weights of NOM to 100 g/mol and fixing the values of w_1 and w_2 to 1. Even though, the NOM simulation using NOM molecular weight of 1000 g/mol (represented by the dotted line in Figure D-2) improved compared to the 100 g NOM/mol simulation; the Razzaghi model greatly over predicted the ferrous iron adsorption. The simulations of ferrous iron could presumably be improved using even smaller NOM molecular weights; however these molecular weights would be unrealistically small. Accordingly, it was concluded that Razzaghi model could not simulate well the competitive adsorption isotherm of NOM and iron in Vars raw water. However, the Razzaghi model was only capable of simulating the NOM in Vars raw water as can be seen in Figure D-2.a.

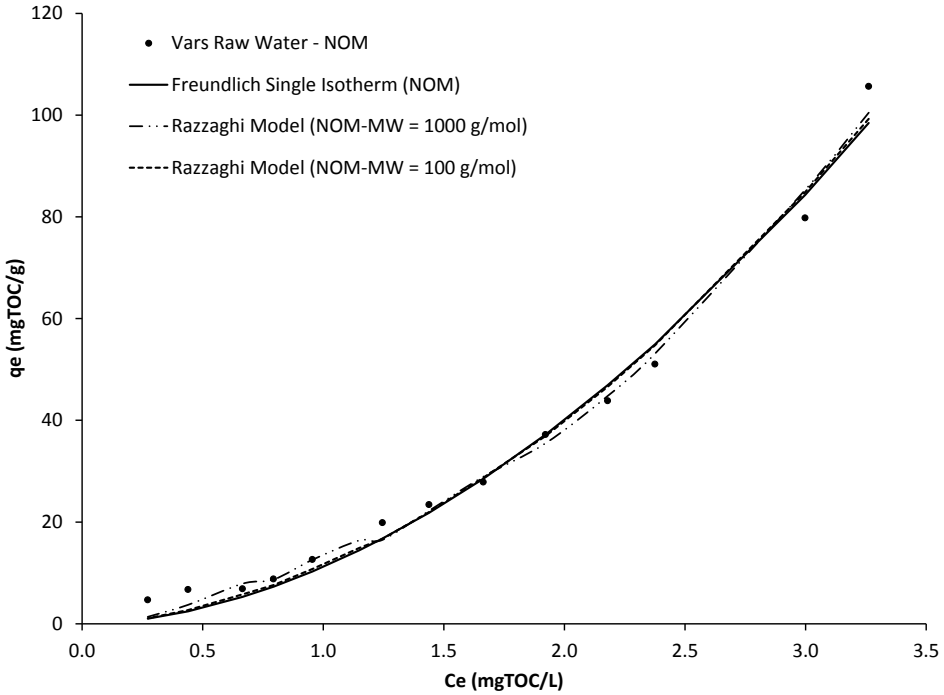

(a)

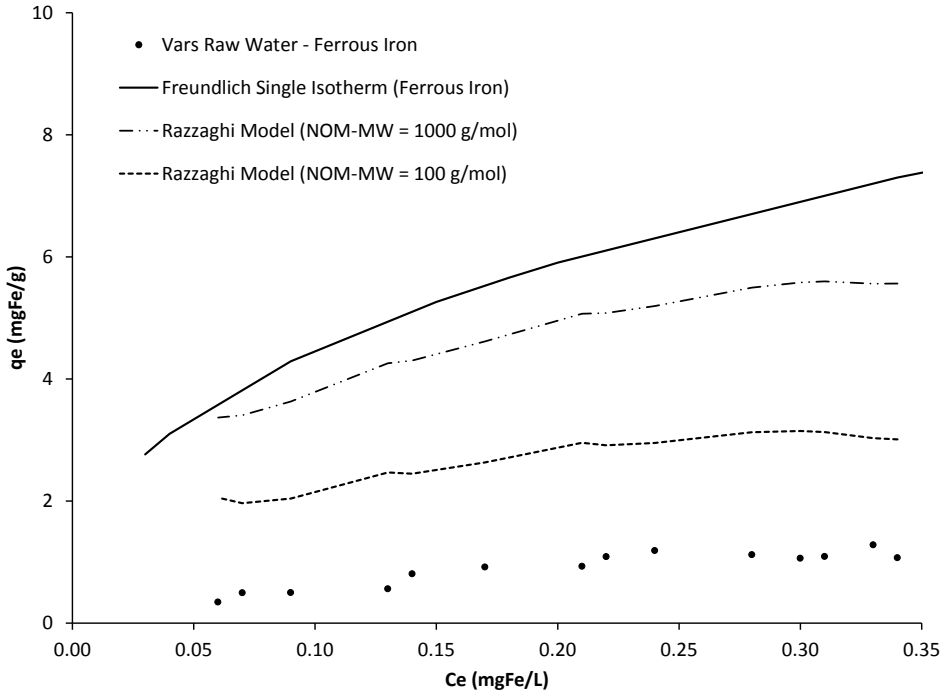

(b)

Figure D-2: Razzaghi model of: (a) NOM and (b) ferrous iron

Table D-2: Regressed parameters used in Razzaghi model

Trial	Component	MW (g/mol)	K_F (µmol/g)·(L/µmol)^n	n_F	w_1	w_2	CV(RMSE) (%)	AAPE (%)
(1)	Ferrous Iron	55.8	67.98	0.35	1	-	475.3	480.7
	NOM	1000	33.37	1.48	-	1	10.0	13.2
(2)	Ferrous Iron	55.8	67.98	0.35	1	-	221.6	232.3
	NOM	100	1.50	1.76	-	1	11.7	17.0

Note: Organic carbon was assumed to account for 50% of the NOM molecular weight
Number of data points = 14
Number of regressed parameters (NOM) = 4 (MW_{NOM}, w_1, K_{NOM}, n_{NOM})
Number of regressed parameters (Ferrous Iron) = 2 (MW_{NOM}, w_2)

D.3 Fritz and Schlunder Model

A very flexible regression model for competitive adsorption in multicomponent systems was developed by Fritz and Schlunder (1981) as an extension of the Freundlich isotherm. The general empirical equations for a bisolute system are:

$$q_1 = \frac{K_{F\text{-}1} C_1^{(n_{F\text{-}1}+n_{11})}}{k_{12} C_2^{n_{12}} + C_1^{n_{11}}} \qquad \text{(D-4)}$$

$$q_2 = \frac{K_{F\text{-}2} C_2^{(n_{F\text{-}2}+n_{22})}}{k_{21} C_1^{n_{21}} + C_2^{n_{22}}} \qquad \text{(D-5)}$$

Where: q_1 and q_2 = the solid phase concentration of components 1 and 2 in equilibrium with C_1 and C_2 (mg/gGAC); C_1 and C_2 = the liquid phase at equilibrium of components 1 and 2 within the bisolute mixture (mg/L); $K_{F\text{-}1}$, $K_{F\text{-}2}$, $n_{F\text{-}1}$ and $n_{F\text{-}2}$ = the regressed parameters of the Freundlich single isotherm of components 1 and 2. The two equations contain ten parameters. Four of these coefficients (k_1, k_2, n_1 and n_2) are obtained from Freundlich isotherm model of the single solute isotherms of the two solutes. The other six parameters (n_{11}, n_{22}, n_{12}, n_{21}, k_{12} and k_{21}) are obtained by non-linear regression using the competitive

isotherm data of both components to help describing the competitive interactions. The values of C_1 and C_2 represent the equilibrium liquid phase concentration of components 1 and 2 within the bisolute mixture.

When the six parameters (n_{11}, k_{12}, n_{12}, n_{22}, k_{21} and n_{21}) were regressed, the model gave a satisfactory fit for both NOM and ferrous iron data (Figure D-3). The reason for the good fit is the fact that the equations of each component have three adjustable parameters that helps in quantifying the interactions between the NOM and ferrous iron in Vars raw water. A sensitivity analysis was performed on the model in order to investigate the correlation between these six regressed parameters and their impact on modeling both components. Four out of the six parameters (n_{22}, k_{21}, n_{21} and n_{12}) had no impact on the goodness of the models fit even when their values were set to zero as shown in Table D-3. Setting the values of n_{22} = k_{21} = n_{21} = 0, makes the equation of q_{NOM} becomes the Freundlich single isotherm of NOM. The parameter (n_{12}) is linked to the NOM's part of the equation that calculates q_{Fe} and setting the value of (n_{12}) to zero would detach the competitive effect of NOM from modeling the competitive isotherm data of ferrous iron. Accordingly, the Fritz and Schlunder model that describes ferrous iron in Vars raw water would change to the following form:

$$q_{Fe} = \frac{k_{Fe} C_{Fe}^{(n_{Fe}+n_{11})}}{k_{12} + C_{Fe}^{n_{11}}} \qquad \text{(D-6)}$$

The best fit for both NOM and ferrous iron was obtained with regressed values of k_{12} and n_{11} equal to 3.59 $(mg/g)\cdot(L/mg)^n$ and 0.28, respectively (Table D-3). The fit indicators (CV(RMSE) and AAPE) for the solid-phase concentration of ferrous iron are 13.0% and 11.0%, respectively. The fit indicator (CV(RMSE) and AAPE) for the solid-phase concentration of NOM are 11.7% and 18.7%, respectively. Thus, Fritz and Schlunder model gave good simulations for both NOM and ferrous iron. The Fritz and Schlunder model was the only competitive isotherm model among the other tested models that was capable to model both NOM and ferrous iron in Vars raw water at the same time. According to the results of the model, the NOM did not seem to be impacted much by the ferrous iron.

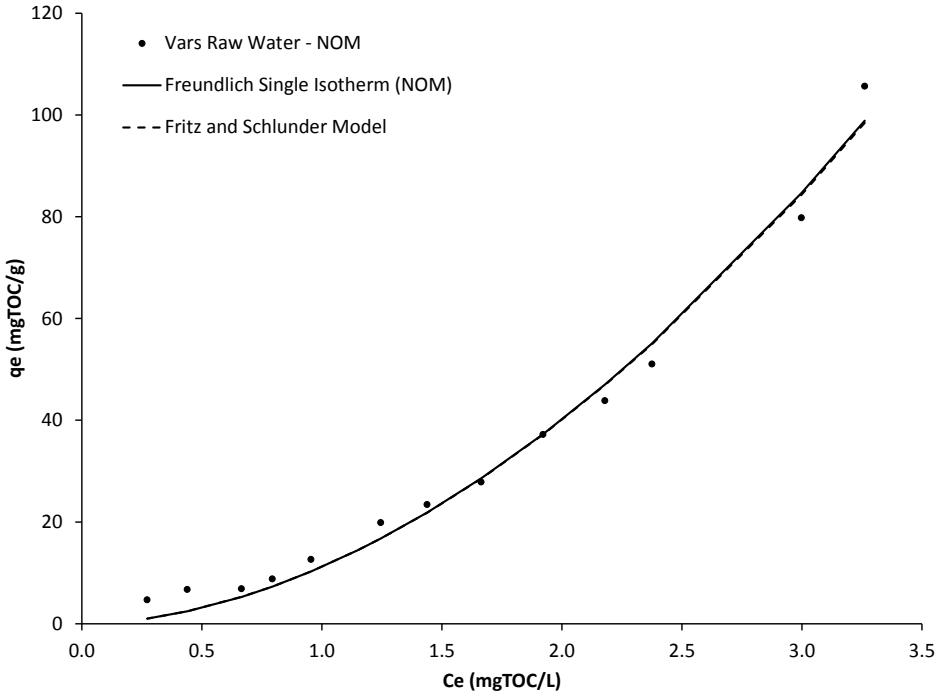

(a)

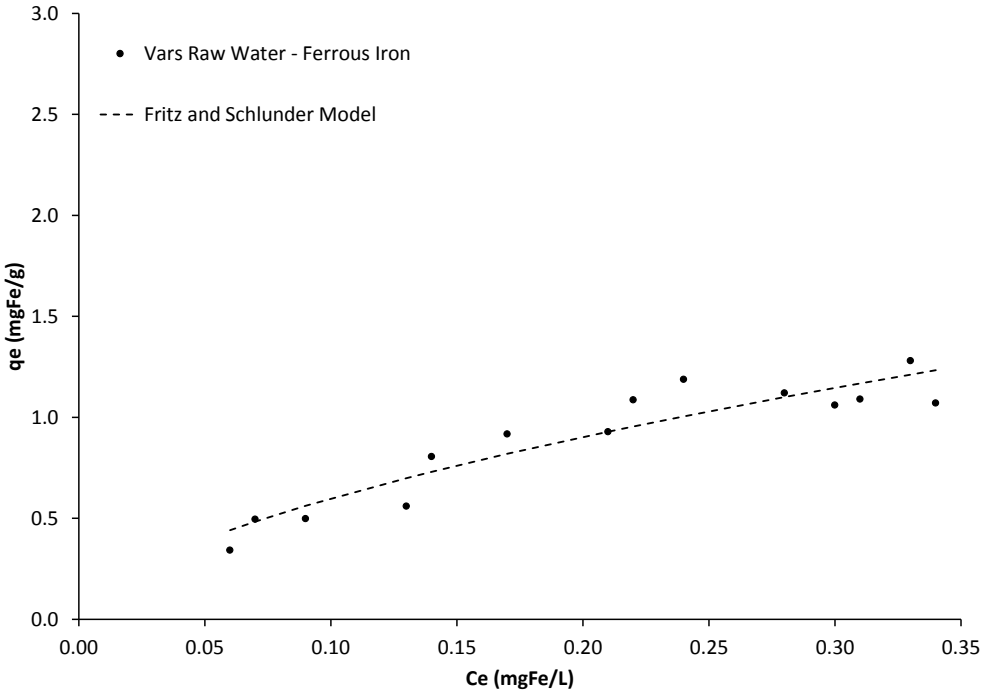

(b)

Figure D-3: Fritz and Schlunder model of: (a) NOM and (b) ferrous iron

Table D-3: Regressed parameters used for Fritz and Schlunder model

	K_F (mg/g).(L/mg)^n	n_F	k_{12} (mg/g).(L/mg)^n	k_{21} (mg/g).(L/mg)^n	n_{11}	n_{12}	n_{21}	n_{22}	CV(RMSE) (%)	AAPE (%)
NOM	11.18	1.84	3.59 (2.52 – 4.66)	0.0	0.28 (0.08 – 0.48)	0.0	0.0	0.0	11.7	18.7
Ferrous Iron	10.56	0.35							13.0	11.0

Number of data points = 14

Number of regressed parameters (NOM) = 3 (n_{11}, n_{12}, k_{12})

Number of regressed parameters (Ferrous Iron) = 3 (n_{22}, n_{21}, k_{21})

APPENDIX E THE FORTRAN CODE: IAST-FR

```
C ************************************************************
C     PROGRAM IAST-FR SIMULATES COMPETITIVE ADSORPTION OF A
C     MULTISOLUTE MIXTURE ACCORDING TO THE PSEUDOCOMPONENTS
C     APPROACH USING IAST WITH FREUNDLICH MODEL
C     THE PROGRAM WAS WRITTEN BY ROBERT K.D. SIMPSON
C     MODIFIED BY OMAR AL-ATTAS
C     ENGINEERING DEPARTMENT, UNIVERSITY OF OTTAWA,
C     THANKS TO DR. ROBERTO NARBAITZ
C ************************************************

      PROGRAM IAST-FR
      REAL KMG,KMOL,MW,NF,KMG2,NF2,MW2
      REAL  WK(621),FNORM,MASS,BETA(25)
      REAL X(10), XGUESS(10)
            REAL A(10,40),A1(10,40),PW(10,40,40),P(10,40),Z(10,40)
      INTEGER NDATA,NPAR,PC1,PC2,PC3,PC4,PC5,PC6
            EXTERNAL MODEL,COEFF,SUDO
            COMMON /DATA/CPRED(40,10),QPRED(40,10),CEXP(40,10),QEXP(40,10)
      COMMON/POW/NSIG,NC,NKC,ITMAX,NPSUD
      COMMON/SOC1/KMOL(10),NF(10),MW(10),CINMOL(10),CINMG(10)
      COMMON/SOC2/KMG(10),SUMC,NRES
      COMMON/SOC3/NERR,RESP,TRACE
      COMMON/SOC4/CINM2(10),KMG2(10),NF2(10),MW2(10)
      COMMON/SOC5/PC1,PC2,PC3,PC4,PC5,PC6
      COMMON/SOC6/ITIMEC,ITIMEK,ITIMEN,ITIMEM,STEPC,STEPK,STEPN,STEPM
      COMMON/LAST/NFIG,NDATA,MAXITR,NI,NO
      COMMON/LAST2/DEL,RLAM,FACT,RLMAX,RLMIN,Y(10,40),
     1  U(2,40),RLAMI
      COMMON/HAPPY/MASS(40),VOL(40)
      COMMON/WHAT/CNON,CAPP
      COMMON/NEW/PAR(32)
            CHARACTER*30 TEST,COMP
      CHARACTER*1 RESP,TRACE

            OPEN (unit=5,file ="C:\\FORTRAN\\ALATTAS IAST\\IASTOMAR.DAT")
      OPEN (unit=6,file ="C:\\FORTRAN\\ALATTAS IAST\\IASTOMAROUT.DAT")
      OPEN (unit=7,file ="C:\\FORTRAN\\ALATTAS IAST\\IASTCLEANOUT.DAT")

C **** READ IN THE CONTROLS FOR THE SOLVER
      READ(5,*) ITMAX,NSIG,NDATA,NC,NKC
C ******  READ IN THE INITIAL CONCENTRATIONS ************
      READ(5,*)  (CINMG(I),I=1,NC+1)
C ******  READ IN THE MOLECULAR WEIGHTS
      READ(5,*) (MW(I),I=1,NC)
C  ******** READ IN THE FREUNDLICH PARAMETERS
      READ(5,*)  (KMG(I), I=1,NC), (NF(I),I=1,NC)
C *****  READ IN THE EXPERIMENTAL VALUES OF IRON ISOTHERM
      DO 35 I=1,NDATA
      READ(5,*) (CEXP(I,J),J=1,NKC),(QEXP(I,J),J=1,NKC),
     1  MASS(I),VOL(I)
   35 CONTINUE
C *******  READ IN THE VALUES OF NOM ISOTHERM CONC. *******
       DO 65 I=1,NDATA
       READ(5,*)  CEXP(I,NC+1),QEXP(I,NC+1)
   65  CONTINUE
C **** READ IN THE COMPONENT OF THE BACKGROUND ORGANICS(NOM FREUNDLICH SINGLE SOLUTE ISOTHERM)
      READ(5,*) CNON,CAPP,KMG(NC+1),KMG(NC+2),NF(NC+1),NF(NC+2)
NFIG,'NO=',NO
               NI=2
       NRES=NO
       RLAMI=RLAM
C *******  CHANGE THE INITIAL CONCENTRATIONS AND K's TO VALUES ON
C         ON MOLAR BASIS FOR KNOWN COMPONENTS ( IRON = IRON)
```

```
      DO 30 I=1,NKC
      CINMOL(I)=1000*(CINMG(I)/MW(I))
      KMOL(I)=(KMG(I)*((1000*MW(I))**NF(I))/(1000*MW(I)))
      KMOL(I)=KMOL(I)/(1000000**NF(I))*1000000
   30 CONTINUE
C **** REDUCE THE INITIAL CONCENTRATION OF THE BACKGROUND ORGANICS
C      BY THE NON-ADSORBABLE COMPONENT
       CINMG(NC+1)=CINMG(NC+1)-CNON
C ****  REDUCE THE EXPERIMENTAL CONCENTRATION OF THE BACKGROUND ORGANICS BY THE NON ADSORBABLE
COMPONENT
        DO 10 IC1=1,NDATA
        CEXP(IC1,NC+1)=CEXP(IC1,NC+1)-CNON
   10   CONTINUE
C *** COMPUTE THE NUMBER OF PSEUDOCOMPONENTS
      NPSUD=NC-NKC
C ****  PUT THE VALUES INTO ANOTHER ARRAY *******
       DO 11 KNOW=NKC+1,NC
       CINM2(KNOW)=CINMG(KNOW)
       KMG2(KNOW)=KMG(KNOW)
       NF2(KNOW)=NF(KNOW)
       MW2(KNOW)=MW(KNOW)
   11  CONTINUE
C **  COMPUTE THE NUMBER OF PARAMETERS TO BE REGRESSED
      NPAR=4*NPSUD-1
C *** SET THE EXPERIMENTAL VALUES OF THE LIQUID-PHASE CONCENTRATIONS
C **** FOR THE KNOWN COMPONENTS (IRON)
      DO 501 ISAY1=1,NKC
      DO 502 ISAY2=1,NDATA
      Y(ISAY1,ISAY2)=CEXP(ISAY2,ISAY1)
  502 CONTINUE
  501 CONTINUE
C **** DO THE SAME FOR THE BACKGROUND ORGANICS
      IF(NRES .GT. NKC) THEN
      DO 504 ISAY2=1,NDATA
      Y(NKC+1,ISAY2)=CEXP(ISAY2,NC+1)
  504 CONTINUE
      ENDIF
C **** ASSIGN THE VOL/MASS FOR EACH DATA POINT
      DO 165 IC3=1,NDATA
      U(1,IC3)=VOL(IC3)
  165 CONTINUE
      DO 159 IC3=1,NDATA
      U(2,IC3)=MASS(IC3)
  159 CONTINUE
C **** DEFINE THE STEP SIZES FOR SEARCHING FOR THE OPTIMAL
C ****  INITIAL GUESSES
      STEPC =CINMG(NC+1)/10.0
      STEPK=10.0
      STEPN=0.10
      STEPM=100.00
C *** DEFINE THE NO. OF TIMES THE INITIAL GUESSES SHOULD BE CHANGED
C *** FOR EACH OF THE PARAMETERS
      ITIMEC=10
      ITIMEK=20
      ITIMEN=10
      ITIMEM=25
      CALL SUDO
            STOP
            END

C *** SUBROUTINE FOR COMBINING THE INITIAL GUESSES
      SUBROUTINE SUDO

      REAL KMG,MW,NF,KMG2,MW2,NF2
      INTEGER PC1,PC2,PC3,PC4,PC5,PC6
      COMMON/POW/NSIG,NC,NKC,ITMAX,NPSUD
      COMMON/SOC1/KMOL(10),NF(10),MW(10),CINMOL(10),CINMG(10)
      COMMON/SOC2/KMG(10),SUMC,NRES
      COMMON/SOC3/NERR,RESP,TRACE
```

```
      COMMON/SOC4/CINM2(10),KMG2(10),NF2(10),MW2(10)
      COMMON/SOC5/PC1,PC2,PC3,PC4,PC5,PC6
      COMMON/SOC6/ITIMEC,ITIMEK,ITIMEN,ITIMEM,STEPC,STEPK,STEPN,STEPM
      COMMON/LAST3/SERMIN,BMIN(25),MINC,DMIN,DMINC
      COMMON/DONT/ISEL
      REAL BETA(25)
      CHARACTER*1 RESP,TRACE

      OPEN (unit=5,file ="C:\\FORTRAN\\ALATTAS IAST\\IASTOMAR.DAT")
      OPEN (unit=6,file ="C:\\FORTRAN\\ALATTAS IAST\\IASTOMAROUT.DAT")
      OPEN (unit=7,file ="C:\\FORTRAN\\ALATTAS IAST\\IASTCLEANOUT.DAT")
      NPAR=4*NPSUD-1
C *** TRY TO GET SOME FIRST SET OF INITIAL GUESSES *****
C *** FIRST SET SOME ARBITRARY VALUES FOR THE C,MW,K,N
      CINMG(2) = 0.2
            CINMG(3)= CINMG(4)-CINMG(2)
            MW(2) = 100.0
            MW(3) = 100.0
            NF(3) = 0.1
            NF(3) = 0.1
            KMG(2) = 0.5
            KMG(3) = 0.5

            DO 100 IWENT01=1,8
            CINMG(2) = CINMG(2) + 0.5
            CINMG(3)= CINMG(4)-CINMG(2)

            MW(2) = 100.0
            MW(3) = 100.0

            NF(2)= 0.1
            NF(3)= 0.1

            KMG(2) = 0.5
            KMG(3) = 0.5

      DO 200 IWENT02=1,20
      MW(3)=MW(3)+50.0

      MW(2) = 100.0
            DO 300 IWENT03=1,20
      MW(2)=MW(2)+50.0

            NF(3)= 0.01
            DO 400 IWENT04=1,20
            NF(3)=NF(3)+0.1
C           NF(3)=NF(2)

            NF(2)= 0.01
            DO 500 IWENT05=1,20
            NF(2)=NF(2)+0.1
C           NF(2)=NF(3)

            KMG(2)= 0.5
            DO 600 IWENT06=1,5
      KMG(2)=KMG(2)+5

            KMG(3)= 0.5
      DO 700 IWENT07=1,1
      KMG(3)=KMG(3)+5

            CALL COEFF(BETA,NPAR)

  700 CONTINUE
  600 CONTINUE
  500 CONTINUE
  400 CONTINUE
  300 CONTINUE
  200 CONTINUE
```

```
 100 CONTINUE
  70 RETURN
           END
     SUBROUTINE COEFF(BETA,NPAR)

     DIMENSION AERR1(10),AERR2(10)
     REAL KMG,KMOL,MW,NF,KMG2,NF2,MW2,MASS
     REAL WK(621),FNORM,BINIT(25),BETA(25)
     REAL X(10)
           REAL A(10,40),A1(10,40),PW(10,40,40),P(10,40)
     INTEGER NDATA,NPAR,PC1,PC2,PC3,PC4,PC5,PC6
     COMMON/DATA/CPRED(40,10),QPRED(40,10),CEXP(40,10),QEXP(40,10)
     COMMON/POW/NSIG,NC,NKC,ITMAX,NPSUD
     COMMON/SOC1/KMOL(10),NF(10),MW(10),CINMOL(10),CINMG(10)
     COMMON/SOC2/KMG(10),SUMC,NRES
     COMMON/SOC3/NERR,RESP,TRACE
     COMMON/SOC4/CINM2(10),KMG2(10),NF2(10),MW2(10)
     COMMON/LAST/NFIG,NDATA,MAXITR,NI,NO
     COMMON/LAST2/DEL,RLAM,FACT,RLMAX,RLMIN,Y(10,40),
    1 U(2,40),RLAMI
     COMMON/LAST3/SERMIN,BMIN(25),MINC,DMIN,DMINC
     COMMON/HAPPY/MASS(40),VOL(40)
     COMMON/WHAT/CNON,CAPP
     COMMON/DONT/ISEL
     CHARACTER*30 TEST,COMP
     CHARACTER*1,RESP,TRACE

           OPEN (unit=5,file ="C:\\FORTRAN\\ALATTAS IAST\\IASTOMAR.DAT")
     OPEN (unit=6,file ="C:\\FORTRAN\\ALATTAS IAST\\IASTOMAROUT.DAT")
     OPEN (unit=7,file ="C:\\FORTRAN\\ALATTAS IAST\\IASTCLEANOUT.DAT")
     OPEN (unit=8,file = "C:\\FORTRAN\\ALATTAS IAST\\IASTPRINT.DAT")

C  *** FIRST DETERMINE THE NUMBER OF PARAMETERS(COEFFICIENTS) TO BE
C **** ESTIMATED
            NPAR=4*NPSUD-1
C **** SET THE FIRST SET OF BETA'S(COEFFICIENTS) TO THE INITIAL
C **** CONCENTRATIONS (THIS IS FOR THE BACKGROUND ORGANICS)
           DO 166 IC4=1,NPSUD-1
     BINIT(IC4)=CINMG(NKC+IC4)
     BETA(IC4) =CINMG(NKC+IC4)
     WRITE(6,*) 'BETA (',IC4,') =',BETA(IC4)
  166 CONTINUE
C ****  SET THE SECOND SET OF BETA'S(COEFFICIENTS) TO THE  FREUNDLICH K
     DO 167 IC4=NPSUD,2*NPSUD-1
     BINIT(IC4)=KMG(2*NKC+IC4-NC+1)
     BETA(IC4)=KMG(2*NKC+IC4-NC+1)
           WRITE(6,*) 'BETA (',IC4,') =',BETA(IC4)
  167 CONTINUE
C ****  SET THE THIRD SET OF BETA'S(COEFFICIENTS) TO THE FREUNDLICH N
           DO 168 IC4=2*NPSUD,3*NPSUD-1
     BINIT(IC4)=NF(3*NKC+IC4-2*NC+1)
     BETA(IC4)=NF(3*NKC+IC4-2*NC+1)
           WRITE(6,*) 'BETA (',IC4,') =',BETA(IC4)
  168 CONTINUE
C ****  SET  THE LAST SET OF BETA'S(COEFFICIENTS) TO THE MOLECULAR WEIGH
           DO 169 IC4=3*NPSUD,NPAR
     BINIT(IC4)=0.5*MW(4*NKC+IC4-3*NC+1)
     BETA(IC4)=0.5*MW(4*NKC+IC4-3*NC+1)
     WRITE(6,*) 'BETA (',IC4,') =',BETA(IC4)
  169 CONTINUE
C ********************    CALL MODEL  ************************
     CALL MODEL(Y,U,BETA,NPAR,A,NDATA)
C *****  COMPUTE AVERAGE PERCENT ERRORS IN C *****************
     DO 172 ITINK=1,NC+1
     AERR1(ITINK)=0.0
     AERR2(ITINK)=0.0
  172 CONTINUE
C *** ADD THE NON-ADSORBABLE COMPONENT TO THE EXPERIMENTAL AND
C     PREDICTED LIQUID PHASE CONCENTRATIONS FOR THE HUMICS
```

```
C     FOR PLOTTING
      DO 5000 IGO=1,NDATA
      CEXP(IGO,NC+1)=CEXP(IGO,NC+1)+CNON
      CPRED(IGO,NC+1)=CPRED(IGO,NC+1)+CNON
 5000 CONTINUE
C **** FOR IRON *******
      DO 171 ISAY2=1,NKC
      DO 171 ISAY1=1,NDATA
              CPRED(ISAY1,ISAY2)= CPRED(ISAY1,ISAY2) * 0.001 * MW(ISAY2)
              AERR1(ISAY2)=AERR1(ISAY2)+ ABS(CEXP(ISAY1,ISAY2)-
     1 CPRED(ISAY1,ISAY2))/CEXP(ISAY1,ISAY2)
  171 CONTINUE
C **** FOR NOM
      DO 800 ISAY1=1,NDATA
      AERR1(NC+1)=AERR1(NC+1)+ABS(CEXP(ISAY1,NC+1)-CPRED(ISAY1,NC+1))
     1/CEXP(ISAY1,NC+1)
  800 CONTINUE
      DO 173 ISAY1=1,NKC
      AERR1(ISAY1)=AERR1(ISAY1)*100/NDATA
  173 CONTINUE
      AERR1(NC+1)=AERR1(NC+1)*100/NDATA

C**** COMPUTE AVERAGE PERCENT ERRORS IN Q  ********

C **** FOR IRON
      DO 174 ISAY2=1,NKC
      DO 174 ISAY1=1,NDATA
      AERR2(ISAY2)=AERR2(ISAY2)+ABS(QEXP(ISAY1,ISAY2)-
     1 QPRED(ISAY1,ISAY2))/QEXP(ISAY1,ISAY2)
  174 CONTINUE
C *** FOR NOM
C **** FIRST SUM ALL Q'S
      DO 936 ISAY2=1,NDATA
      QPRED(ISAY2,NC+1)=0.
  936 CONTINUE
      DO 937 ISAY1=1,NDATA
      DO 937 ISAY2=NKC+1,NC
      QPRED(ISAY1,NC+1)=QPRED(ISAY1,NC+1)+QPRED(ISAY1,ISAY2)
  937 CONTINUE
      DO 810 ISAY1=1,NDATA
      AERR2(NC+1)=AERR2(NC+1)+ABS(QEXP(ISAY1,NC+1)
     1 - QPRED(ISAY1,NC+1))/QEXP(ISAY1,NC+1)
  810 CONTINUE
      DO 175 ISAY1=1,NKC
      AERR2(ISAY1)=AERR2(ISAY1)*100/NDATA
  175 CONTINUE
      AERR2(NC+1)=AERR2(NC+1)*100/NDATA
C *** DETERMINE WHETHER RESULTS ARE FEASIBLE *****
      DO 222 IC9 = 1,NKC
              WRITE(6,*) 'AERR1', AERR1(IC9)
              WRITE(6,*) 'AERR2', AERR2(IC9)
  222 CONTINUE
              IF(AERR1(1) .GT. 40.0 .OR. AERR2(1) .GT. 10.) THEN
              WRITE(6,*) 'NO FEASIBLE SOLUTION - GOING BACK TO SUDO'
      GOTO 911
      ELSE
      WRITE(6,*) 'SMILE - A SOLUTION WAS FOUND'
      ENDIF
C **** WRITE OUT VALUES FOR PLOTTING FILE   ************************
C **** FOR KNOWN COMPONENTS ( IRON) *********
      WRITE(8,*) NDATA
              DO 176 ISHOT=1,NKC
      DO 176 ISAY1=1,NDATA
      CPRED(ISAY1,ISHOT)= CPRED(ISAY1,ISHOT)
              WRITE(8,177) CEXP(ISAY1,ISHOT),CPRED(ISAY1,ISHOT),
     1 KMG(ISHOT)*CEXP(ISAY1,ISHOT)**NF(ISHOT),
     2 QEXP(ISAY1,ISHOT),QPRED(ISAY1,ISHOT)
  177  FORMAT(1X,6(3X,F15.6))
  176 CONTINUE
```

```
C **** FOR BACKGROUND ORGANICS ****************************
              DO 178 ISAY1=1,NDATA
     IF(CEXP(ISAY1,NC+1) .GT. CAPP) THEN
       KMG(NC+1)=KMG(NC+2)
       NF(NC+1)=NF(NC+2)
     ENDIF
     SSOL=KMG(NC+1)*(CEXP(ISAY1,NC+1)-CNON)**NF(NC+1)
     WRITE(8,177) CEXP(ISAY1,NC+1),CPRED(ISAY1,NC+1),
    1 SSOL,
    2  QEXP(ISAY1,NC+1),QPRED(ISAY1,NC+1)
  178 CONTINUE

**************************************************************************
C ****  WRITE OUT THE VALUES FOR KNOWN COMPONENT(S) **********
C      WRITE OUT VALUES FOR KNOWN COMPONENTS (SYNTHETIC ORGANICS)
       WRITE(7,1000)
 1000  FORMAT(1X,///,30X,'KNOWN SYNTHETIC ORGANIC COMPOUNDS',//)
       WRITE(7,1010)

 1010  FORMAT(1X,30X,12X,'PARAMETERS',/1X,25X,'CO',15X,'K',15X,'N',15X,
    1 'MW',/1X,22X,'(MG/L)',5X,'(MG/L)/(MG/G)**N',24X,'(G)',/)

       DO 1020 IC10=1,NKC
       WRITE(7,1030) IC10,CINMG(IC10),KMG(IC10),NF(IC10),MW(IC10)
 1030  FORMAT(1X,'COMPONENT #',I3,4(5X,F12.5))
 1020  CONTINUE
       WRITE(7,1040)
 1040  FORMAT(1X,///)

       WRITE(7,1060)
 1060  FORMAT(1X,30X,'BACKGROUND ORGANIC COMPOUNDS',//)

       WRITE(7,1050) NPSUD
 1050  FORMAT(1X,3X,'REGRESSED PARAMETERS FOR',I3,' PSEUDOCOMPONENTS')
       WRITE(7,1070)
 1070  FORMAT(1X,/1X,25X,'CO',15X,'K',15X,'N',15X,
    1 'MW',/1X,22X,'(MG/L)',5X,'(MG/G)/(MG/L)**N',24X,'(G)',/)

C **  WRITE OUT NON-ADSORBABLE COMPONENT

       WRITE(7,5001) CNON
 5001   FORMAT(1X,'NON-ADSORBABLE ',F16.5)

      DO 1080 IC10=NKC+1,NC
      IF (IC10 .LT. NC) THEN
      WRITE(7,1090) IC10,BETA(IC10-NKC),BETA(IC10-NKC+NPSUD-1),
     1 BETA(IC10-NKC+2*NPSUD-1),BETA(IC10-NKC+3*NPSUD-1)

      ELSE
      WRITE(7,1090) IC10,CINMG(NC+1)-SUMC,BETA(IC10-NKC+NPSUD-1),
     1 BETA(IC10-NKC+2*NPSUD-1),BETA(IC10-NKC+3*NPSUD-1)
      ENDIF
 1090  FORMAT(1X,'COMPONENT #',I3,4(5X,F12.5))
 1080  CONTINUE

      WRITE(7,1100)
 1100   FORMAT(1X,///,40X,'S I M U L A T I O N S ',//)

C **** FOR IRON ****

       DO 200 IC5=1,NKC

       WRITE(7,33) IC5
   33  FORMAT(//,'COMPONENT # ',I3,//,7X,'V',7X,'M',15X,'CEXP',11X,
     1'CPRED',10X,'QEXP',12X,'QPRED',/,6X,'(L)',5X,'(G)',21X,'MG/L',27X,
     2'MG/G')
       DO 210 IC6=1,NDATA
              WRITE(7,31) VOL(IC6),MASS(IC6),CEXP(IC6,IC5),CPRED(IC6,IC5)
    1  ,QEXP(IC6,IC5),QPRED(IC6,IC5)
```

```
 31  FORMAT(2(2X,F8.4),4(4X,F12.4))
210  CONTINUE

      WRITE(7,890) AERR1(IC5),AERR2(IC5)
890  FORMAT(1X,/,'ABSOLUTE AVERAGE PERCENT ERROR IN C =',F8.2,/
   1 'ABSOLUTE AVERAGE PERCENT ERROR IN Q =',F8.2)

200  CONTINUE
     WRITE(7,900)
900  FORMAT(1X,//)
     DO 910 IC6=1,NDATA
     WRITE(7,31) VOL(IC6),MASS(IC6),CEXP(IC6,NC+1),CPRED(IC6,NC+1),
   1  QEXP(IC6,NC+1),QPRED(IC6,NC+1)
910  CONTINUE

**********************************************************************
              WRITE(7,890) AERR1(NC+1),AERR2(NC+1)
              GOTO 950
911 CONTINUE
950 RETURN
              END

     SUBROUTINE MODEL(Y,U,BETA,NPAR,A,NDATA)
     REAL WK(621),FNORM,A(10,40),Y(10,40),U(2,40)
     REAL KMOL,MW,NF,ERRREL
              COMMON /POW/ NSIG,NC,NKC,ITMAX,NPSUD
     REAL XSTO(40),XGUESS(40),X(10)
     EXTERNAL FCN,NEQNF
     COMMON /DATA/CPRED(40,10),QPRED(40,10),CEXP(40,10),QEXP(40,10)
     COMMON/SOC1/KMOL(10),NF(10),MW(10),CINMOL(10),CINMG(10)
     COMMON/SOC2/KMG(10),SUMC,NRES
     COMMON/NEW/PAR(32)
              REAL BETA(25)
              INTEGER N

     OPEN (unit=5,file ="C:\\FORTRAN\\ALATTAS IAST\\IASTOMAR.DAT")
     OPEN (unit=6,file ="C:\\FORTRAN\\ALATTAS IAST\\IASTOMAROUT.DAT")
     OPEN (unit=7,file ="C:\\FORTRAN\\ALATTAS IAST\\IASTCLEANOUT.DAT")

C ******* DEFINE PARAMETERS FOR USE IN NEQNF SUBROUTINE **********
C ***** 3 FIXED PARAMETERS ARE TO BE ASSIGNED FOR EACH COMPONENT,
C      I.E. CINMOL, NF AND THE KMOL.  THE TOTAL NUMBER OF FIXED
C      PARAMETERS FOR NC COMPONENTS = 6+3*(NC-2), AND THEN
C      THE VARIABLE PARAMETERS, THE CARBON MASS AND
C      THE LIQUID VOLUME

     NPARM=6+3*(NC-2)
C **** TEST THE VALUE OF THE REGRESSED PARAMETERS
C ***  FIRST DETERMINE THE INITIAL CONCENTRATION OF THE LAST
C ***  PSEUDOCOMPONENT

     SUMC=0.0

              DO 93 IC2=NKC+1,NC-1
     SUMC=SUMC+BETA(IC2-NKC)
 93  CONTINUE

     PAR(NC)=1000*((CINMG(NC+1)-SUMC)/(BETA(NPAR)))
     WRITE(6,*) 'PAR(',NC,')',PAR(NC)

     DO 120 IC1=1,NPAR
     IF(BETA(IC1) .LE. 0.0 .OR. PAR(NC) .LE. 0.0) THEN
     WRITE(6,*)  '********NEGATIVE********'
     WRITE(6,*) 'BETA ',BETA(IC1),' PAR(NC)  ',PAR(NC)

158  DO 156 IPUT=1,NDATA

              DO 130 IC5=1,NKC
     WRITE(6,*)  '**********EXITING FROM HERE'
```

```
      A(IC5,IPUT)=A(IC5,IPUT)*1000.0
  130  CONTINUE

               IF(NRES .GT. NKC) THEN
      A(NKC+1,IPUT)=A(NKC+1,IPUT)*1000.0
      ENDIF

  156  CONTINUE
               GOTO 155

               ENDIF

  120  CONTINUE

C **** SET THE INITIAL CONCENTRATIONS AS THE FIRST SET OF
C      PARAMETERS

C *** SET THE PARAMETERS (INITITAL CONCENTRATIONS) FOR THE  IRON***

      DO 90 IC2=1,NKC
      PAR(IC2)=CINMOL(IC2)
      WRITE(6,*) 'PAR(',IC2,')',PAR(IC2)
   90  CONTINUE

C **** SET THE PARAMETERS(INITIAL CONCENTRATIONS) FOR THE
C*******BACKGROUND ORGANICS ****

      DO 91 IC2=NKC+1,NC-1
               PAR(IC2)=1000* (BETA(IC2-NKC)/(BETA(IC2-NKC+3*NPSUD-1)))
      WRITE(6,*) 'PAR(',IC2,')',PAR(IC2)
   91  CONTINUE

C SET THE PARAMETERS (INITIAL CONCENTRATIONS) FOR THE LAST
C PSEUDOCOMPONENT, BUT FIRST SUM UP ALL INITIAL CONCS
C OF THE NC-1 PSEUDOCOMPONENTS

C ****  SET THE K's AS THE SECOND SET OF PARAMETERS FOR THE  IRON

      DO 92  IC2=NC+1,NC+NKC
      PAR(IC2)=KMOL(IC2-NC)
  92   CONTINUE

C **** SET THE K'S AS THE SECOND SET OF PARAMETERS FOR THE BACKGROUND
C  ****  ORGANICS BY FIRST CHANGING THE K'S TO VALUES ON MOLAR BASIS
C      CARBON WAS ASSUMED TO ACCOUNT FOR 50% OF THE NOM MOLECULAR WEIGHT
      DO 30 IPRAY=NKC+1,NC
      KMOL(IPRAY)=(BETA(IPRAY-NKC+NPSUD-1)
               1*(1000*BETA(IPRAY-NKC+3*NPSUD-1))
     2 **(BETA(IPRAY-NKC+2*NPSUD-1))) /
     3(1000*BETA(IPRAY-NKC+3*NPSUD-1))
               KMOL(IPRAY)=KMOL(IPRAY)/(1000000**(BETA(IPRAY-NKC+2*NPSUD-1)))
     4 * (1000000)
   30  CONTINUE

C*** NOW SET THE K'S AS THE SECOND SET OF PARAMETERS FOR THE BACKGROUND
C*****ORGANICS
               DO 31 IC2=NC+NKC+1,2*NPARM/3
      PAR(IC2)=KMOL(IC2-NC)
      WRITE(6,*) 'PAR(',IC2,')',PAR(IC2)
   31   CONTINUE

C ****  SET THE N's AS THE THIRD SET OF PARAMETERS FOR THE  IRON
C ****  FIRST SET THE N's FOR THE  IRON

      DO 110 IC2=(2*NPARM/3)+1,(2*NPARM/3+NKC)
      PAR(IC2)=NF(IC2-2*NC)
      WRITE(6,*) 'PAR(',IC2,')',PAR(IC2)
  110  CONTINUE
```

```
C ***  SET THE (N'S) AS THE THIRD SET OF PARAMETERS FOR
C **** THE BACKGROUND ORGANICS

      DO 111 IC2=(2*NPARM/3+NKC+1),NPARM
      PAR(IC2)=BETA(IC2-3*NKC-1)
      WRITE(6,*) 'PAR(',IC2,')',PAR(IC2)
 111  CONTINUE

C**** SOLVE THE RESULTING EQUATIONS AND THEN REGRESS THE RESULTS
C***  TO FIND THE BEST FIT
      DO 100 I=1,NDATA

C *** SET COUNTER FOR CONTROL OF NO. OF TIMES OF CALLS TO NEQNF
C ***  WITH DIFFERENT INITIAL GUESSES FOR EACH DATA POINT

      ICNT=0
      PRINT*,  '******** POINT NO *********',I

C ***  SET THE CARBON VOLUME AND MASS AS THE LAST TWO PARAMETERS FOR
C ****  NEQNF (SOLVER)

      PAR(NPARM+1)=U(2,I)
      PAR(NPARM+2)=U(1,I)

C  *** MAKE YOUR INITIAL GUESSES OF Q FOR THE SOLVER
C  ***  FOR THE  IRON

      DO 40 J=1,NKC
      IF (I .EQ. 1) THEN
      X(J)=0.1*CINMOL(J)*PAR(NPARM+2)/PAR(NPARM+1)
      XSTO(J)=0.1*CINMOL(J)*PAR(NPARM+2)/PAR(NPARM+1)
              ELSE
       X(J)=1000*1.0*QPRED(I-1,J)/MW(J)
       XSTO(J)=1000*1.0*QPRED(I-1,J)/MW(J)
      ENDIF
 40   CONTINUE

C ***  FOR THE NC-1 PSEUDOCOMPONENTS
      DO 41 J=NKC+1,NC-1
      IF (I .EQ. 1) THEN
      X(J)=0.1*1000*BETA(J-NKC)/(BETA(J-NKC+3*NPSUD-1))*PAR(NPARM+2)
              1 /PAR(NPARM+1)
      XSTO(J)=0.1*1000*BETA(J-NKC)/(BETA(J-NKC+3*NPSUD-1))
     1  *PAR(NPARM+2)/PAR(NPARM+1)
      WRITE(6,*) 'FIRST X(',J,')',X(J)
      ELSE
       X(J)=1000*1.0*QPRED(I-1,J)/(BETA(J-NKC+3*NPSUD-1))
       XSTO(J)=1000*1.0*QPRED(I-1,J)/(BETA(J-NKC+3*NPSUD-1))
      ENDIF
 41   CONTINUE

C ***  FOR THE LAST PSEUDOCOMPONENT
      IF(I .EQ. 1) THEN
      X(NC)=0.1*PAR(NC)*PAR(NPARM+2)/PAR(NPARM+1)
      XSTO(NC)=0.1*PAR(NC)*PAR(NPARM+2)/PAR(NPARM+1)
      ELSE
      X(NC)=1000*1.0*QPRED(I-1,NC)/BETA(NPAR)
      XSTO(NC)=1000*1.0*QPRED(I-1,NC)/BETA(NPAR)
      ENDIF

              GOTO 175

C *** REDEFINE THE INITIAL GUESSES IF THE FIRST SET DID NOT WORK
170  DO 171 J=1,NKC
      IF(I .EQ. 1) THEN
      X(J)=XSTO(J)+0.1*XSTO(J)
      XSTO(J)=X(J)
      ELSE
      X(J)=XSTO(J)-0.1*XSTO(J)
```

```
      XSTO(J)=X(J)
      ENDIF
  171 CONTINUE

C *** FOR THE NC-1 COMPONENTS
      DO 172 J=NKC+1,NC-1
      IF(I .EQ. 1) THEN
      X(J)=XSTO(J)+0.1*XSTO(J)
      XSTO(J)=X(J)
      ELSE
      X(J)=XSTO(J)-0.1*XSTO(J)
      XSTO(J)=X(J)
      ENDIF
  172  CONTINUE

C **** FOR THE LAST PSEUDOCOMPONENT
      IF(I .EQ. 1) THEN
      X(NC)=XSTO(NC)+0.1*XSTO(NC)
      XSTO(NC)=X(NC)
      ELSE
      X(NC)=XSTO(NC)-0.1*XSTO(NC)
      XSTO(NC)=X(NC)
      ENDIF

C **** CALL NEQNF FOR EACH DATA POINT TO COMPUTE Q's
  175 N=NC

      ERRREL = 0.001
            DO 12121 OMAR=1,N
      XGUESS(OMAR) = X(OMAR)
12121 CONTINUE

            CALL NEQNF (FCN,ERRREL,N,ITMAX,XGUESS,X,FNORM)


C     SET THE X'S TO THEIR RESPECTIVE Q'S
C *** FOR KNOWN COMPONENTS (IRON)

      DO 21 IC8=1,NKC
      QPRED(I,IC8)=X(IC8)
21   CONTINUE

C **** FOR BACKGROUND ORGANICS

            DO 22 IC8=NKC+1,NC
      QPRED(I,IC8)=X(IC8)
22   CONTINUE

C **** CALCULATE C's FOR EACH COMPONENT **********
C *** FOR  IRON
            DO 150 IC4=1,NKC
      CPRED(I,IC4)=CINMOL(IC4)-(QPRED(I,IC4)*U(2,I)/U(1,I))
150  CONTINUE

C ************AND FOR BACKGROUND ORGANICS ***************
C  FOR THE NC-1 COMPONENTS
            DO 151 IC4=NKC+1,NC-1
      CPRED(I,IC4)=1000*(BETA(IC4-NKC)/BETA(IC4-NKC+3*NPSUD-1))
     1  -QPRED(I,IC4)*U(2,I)/U(1,I)
151  CONTINUE

C  FOR THE LAST PSEUDOCOMPONENT
            CPRED(I,NC)=PAR(NC)-QPRED(I,NC)*U(2,I)/U(1,I)

C  CHANGE THE PREDICTED VALUES OF Q INTO THOSE ON MASS
C  BASIS FOR KNOWN COMPONENTS
            DO 160 IC4=1,NKC
      QPRED(I,IC4)=QPRED(I,IC4)*MW(IC4)*0.001
160  CONTINUE
```

```
C FOR BACKGROUND ORGANICS
            DO 161 IC4=NKC+1,NC
     QPRED(I,IC4)=QPRED(I,IC4)*BETA(IC4-NKC+3*NPSUD-1)*0.001
161  CONTINUE

C **** COMPUTE RESIDUALS  AS Y's (CEXP-CPRED) FOR  IRON *****
            DO 101 IC5=1,NKC
     A(IC5,I)=Y(IC5,I)-CPRED(I,IC5)*MW(IC5)*0.001
101  CONTINUE

C ***  COMPUTE RESIDUALS AS Y'S (CEXP-CPRED) FOR BACKGROUND ORGANICS
C **   FIRST SUM UP ALL LIQUID-PHASE CONCENTRATIONS OF THE
C ***  PSEUDOCOMPONENTS
     CPRED(I,NC+1)=0
     DO 102 IC5=NKC+1,NC
     CPRED(I,NC+1)=CPRED(I,NC+1)+CPRED(I,IC5)
            1*BETA(IC5-NKC+3*NPSUD-1)*0.001
 102 CONTINUE

 100 CONTINUE

155  RETURN
     END

C **** SUBROUTINE FCN FOR CALCULATING THE F FUNCTIONS THAT ARE *******
C **************   TO BE  ZEROED  **************************

     SUBROUTINE FCN(X,F,N)
     INTEGER N
     REAL F(N),X(N)
     COMMON/NEW/PAR(32)

     OPEN (unit=5,file = "C:\\FORTRAN\\ALATTAS IAST\\IASTOMAR.DAT")
     OPEN (unit=6,file = "C:\\FORTRAN\\ALATTAS IAST\\IASTOMAROUT.DAT")
     OPEN (unit=7,file = "C:\\FORTRAN\\ALATTAS IAST\\IASTCLEANOUT.DAT")

     NPARM = 6 + 3 * (N-2)
     SUMXI = 0.0
     SUMXON = 0.0

     DO 130 IC3=1,N
     SUMXI = SUMXI + X(IC3)
     SUMXON = SUMXON + X(IC3) / PAR (2 * NPARM / 3 + IC3)
 130 CONTINUE

            IF(SUMXON .LT. 0) THEN
 132 DO 135 IC4=1,N
    F(IC4)=100.0
 135 CONTINUE
    GOTO 150
    ENDIF

    DO 140 IC3=1,N
            TTERM = ( PAR(2*NPARM/3+IC3) * SUMXON)/PAR(N+IC3)
            FTERM=1/PAR(2*NPARM/3+IC3)

            IF(LOG(TTERM)*FTERM .LT. -99.9999 .OR. LOG(TTERM)*FTERM.GT.10.0)
   1 GOTO 132

    F(IC3)=PAR(IC3)-(PAR(NPARM+1)/PAR(NPARM+2))*X(IC3)-(X(IC3)
   2 /SUMXI)*((PAR(2*NPARM/3+IC3)*SUMXON)/PAR(N+IC3))**
   3  (1/PAR(2*NPARM/3+IC3))

 140 CONTINUE

 150 RETURN

            END
```

Input File for the FORTRAN Code: IAST-FR

```
200   3  14   3   1
0.35  0.1 0.1 4.24
55.8  200.00 200.00
10.56 5.00 5.00  0.35  0.05 0.05
0.06     0.34     0.1357 0.160
0.07     0.49     0.0911 0.161
0.09     0.50     0.0841 0.161
0.13     0.56     0.0632 0.161
0.14     0.81     0.0420 0.161
0.17     0.92     0.0316 0.161
0.21     0.93     0.0243 0.161
0.22     1.09     0.0193 0.161
0.24     1.19     0.0149 0.161
0.28     1.12     0.0100 0.161
0.30     1.06     0.0076 0.161
0.31     1.09     0.0059 0.162
0.33     1.28     0.0025 0.161
0.34     1.07     0.0015 0.161
0.27     4.68
0.44     6.72
0.67     6.85
0.79     8.78
0.96     12.61
1.15     15.76
1.25     19.87
1.44     23.42
1.66     27.84
1.92     37.18
2.18     43.82
2.38     51.03
3.00     79.79
3.26     105.63
0.000 2.12 11.18 11.18 1.84 1.84
```

APPENDIX F THE FORTRAN CODE: IAST-SR

```
C ************************************************************
C     PROGRAM IAST-SR SIMULATES COMPETITIVE ADSORPTION OF A
C     MULTISOLUTE MIXTURE ACCORDING TO THE PSEUDOCOMPONENTS
C     APPROACH USING IAST WITH SUMMERS-ROBERTS MODEL
C     THE PROGRAM WAS WRITTEN BY ROBERT K.D. SIMPSON
C     MODIFIED BY OMAR AL-ATTAS
C     ENGINEERING DEPARTMENT, UNIVERSITY OF OTTAWA,
C     THANKS TO DR. ROBERTO NARBAITZ
C ************************************************

      PROGRAM IAST-SR
      REAL KMG,KMOL,MW,NF,KMG2,NF2,MW2
      REAL  WK(621),FNORM,MASS,BETA(25)
      REAL X(10), XGUESS(10)
            REAL A(10,40),A1(10,40),PW(10,40,40),P(10,40),Z(10,40)
      INTEGER NDATA,NPAR,PC1,PC2,PC3,PC4,PC5,PC6
            EXTERNAL MODEL,COEFF,SUDO
            COMMON /DATA/CPRED(40,10),QPRED(40,10),CEXP(40,10),QEXP(40,10)
      COMMON/POW/NSIG,NC,NKC,ITMAX,NPSUD
      COMMON/SOC1/KMOL(10),NF(10),MW(10),CINMOL(10),CINMG(10)
      COMMON/SOC2/KMG(10),SUMC,NRES
      COMMON/SOC3/NERR,RESP,TRACE
      COMMON/SOC4/CINM2(10),KMG2(10),NF2(10),MW2(10)
      COMMON/SOC5/PC1,PC2,PC3,PC4,PC5,PC6
      COMMON/SOC6/ITIMEC,ITIMEK,ITIMEN,ITIMEM,STEPC,STEPK,STEPN,STEPM
      COMMON/LAST/NFIG,NDATA,MAXITR,NI,NO
      COMMON/LAST2/DEL,RLAM,FACT,RLMAX,RLMIN,Y(10,40),U(2,40),RLAMI
      COMMON/HAPPY/MASS(40),VOL(40)
      COMMON/WHAT/CNON,CAPP
      COMMON/NEW/PAR(32)
            CHARACTER*30 TEST,COMP
      CHARACTER*1 RESP,TRACE

      OPEN(unit=5,file = "C:\\FORTRAN\\ALATTAS IAST\\IAST-SROMAR.DAT")
      OPEN(unit=6,file ="C:\\FORTRAN\\ALATTAS IAST\\IAST-SROMAROUT.DAT")
      OPEN(unit=7,file ="C:\\FORTRAN\\ALATTAS IAST\\IAST-SRCLEANOUT.DAT")

C **** READ IN THE CONTROLS FOR THE SOLVER
      READ(5,*) ITMAX,NSIG,NDATA,NC,NKC
      WRITE(6,*) 'ITMAX =',ITMAX,'  NSIG ',NSIG,' NDATA ',NDATA,' NC ',
     1 NC

C ******  READ IN THE INITIAL CONCENTRATIONS ************
      READ(5,*)  (CINMG(I),I=1,NC+1)
      WRITE(6,*) 'CINMG =', (CINMG(I),I=1,NC+1)

C ******  READ IN THE MOLECULAR WEIGHTS
      READ(5,*) (MW(I),I=1,NC)
      WRITE(6,*) 'MW =',(MW(I),I=1,NC)

C  ******** READ IN THE FREUNDLICH PARAMETERS
      READ(5,*)  (KMG(I), I=1,NC), (NF(I),I=1,NC)
      WRITE(6,*) 'K =',(KMG(I), I=1,NC)
      WRITE(6,*) 'N =',(NF(I),I=1,NC)

C *****  READ IN THE EXPERIMENTAL VALUES OF IRON ISOTHERM
      DO 35 I=1,NDATA
      READ(5,*) (CEXP(I,J),J=1,NKC),(QEXP(I,J),J=1,NKC),
     1  MASS(I),VOL(I)
   35 CONTINUE

C *******  READ IN THE VALUES OF NOM ISOTHERM CONC. *******
       DO 65 I=1,NDATA
       READ(5,*)  CEXP(I,NC+1),QEXP(I,NC+1)
```

```
 65  CONTINUE

C **** READ IN THE NON-ADSORBABLE COMPONENT OF THE BACKGROUND ORGANICS (NOM SUMMERS-ROBERTS
C **** SINGLE SOLUTE ISOTHERM)
      READ(5,*) CNON,CAPP,KMG(NC+1),KMG(NC+2),NF(NC+1),NF(NC+2)
       NI=2
       NRES=NO
       RLAMI=RLAM

C *******  CHANGE THE INITIAL CONCENTRATIONS AND K's TO VALUES ON
C         ON MOLAR BASIS FOR KNOWN COMPONENTS (IRON = IRON) **********
      DO 30 I=1,NKC
      CINMOL(I)=1000*(CINMG(I)/MW(I))
               KMOL(I)=(KMG(I)*((1000*MW(I))**NF(I))/(1000*MW(I)))
               KMOL(I)=KMOL(I)/(1000000**NF(I))*1000000
               WRITE(6,*) (KMG(I)), (NF(I)), (MW(I))
               WRITE(6,*) 'CINMOL=', CINMOL(I),'KMOL=', KMOL(I)
  30 CONTINUE

C **** REDUCE THE INITIAL CONCENTRATION OF THE BACKGROUND ORGANICS
C      BY THE NON-ADSORBABLE COMPONENT
       CINMG(NC+1)=CINMG(NC+1)-CNON

C ****  REDUCE THE EXPERIMENTAL CONCENTRATION OF THE BACKGROUND ORGANICS
C       BY THE NON ADSORBABLE COMPONENT
        DO 10 IC1=1,NDATA
        CEXP(IC1,NC+1)=CEXP(IC1,NC+1)-CNON
  10   CONTINUE

C *** COMPUTE THE NUMBER OF PSEUDOCOMPONENTS
      NPSUD=NC-NKC

C ****  PUT THE VALUES INTO ANOTHER ARRAY *******
       DO 11 KNOW=NKC+1,NC
       CINM2(KNOW)=CINMG(KNOW)
       KMG2(KNOW)=KMG(KNOW)
       NF2(KNOW)=NF(KNOW)
       MW2(KNOW)=MW(KNOW)
  11  CONTINUE

C **  COMPUTE THE NUMBER OF PARAMETERS TO BE REGRESSED
      NPAR=4*NPSUD-1

C *** SET THE EXPERIMENTAL VALUES OF THE LIQUID-PHASE CONCENTRATIONS
C **** FOR THE KNOWN COMPONENTS (SYNTHETHICS)
      DO 501 ISAY1=1,NKC
      DO 502 ISAY2=1,NDATA
      Y(ISAY1,ISAY2)=CEXP(ISAY2,ISAY1)
  502 CONTINUE
  501 CONTINUE

C **** DO THE SAME FOR THE BACKGROUND ORGANICS
      IF(NRES .GT. NKC) THEN
      DO 504 ISAY2=1,NDATA
      Y(NKC+1,ISAY2)=CEXP(ISAY2,NC+1)
  504 CONTINUE
      ENDIF

C **** ASSIGN THE VOL/MASS FOR EACH DATA POINT
      DO 165 IC3=1,NDATA
      U(1,IC3)=VOL(IC3)
  165 CONTINUE
      DO 159 IC3=1,NDATA
      U(2,IC3)=MASS(IC3)
  159 CONTINUE

C **** DEFINE THE STEP SIZES FOR SEARCHING FOR THE OPTIMAL
C ****  INITIAL GUESSES
      STEPC =CINMG(NC+1)/10.0
```

```
      STEPK=10.0
      STEPN=0.10
      STEPM=100.00

C *** DEFINE THE NO. OF TIMES THE INITIAL GUESSES SHOULD BE CHANGED
C *** FOR EACH OF THE PARAMETERS
      ITIMEC=10
      ITIMEK=20
      ITIMEN=10
      ITIMEM=25

      CALL SUDO

            STOP

            END

C *** SUBROUTINE FOR COMBINING THE INITIAL GUESSES
      SUBROUTINE SUDO

      REAL KMG,MW,NF,KMG2,MW2,NF2
      INTEGER PC1,PC2,PC3,PC4,PC5,PC6
      COMMON/POW/NSIG,NC,NKC,ITMAX,NPSUD
      COMMON/SOC1/KMOL(10),NF(10),MW(10),CINMOL(10),CINMG(10)
      COMMON/SOC2/KMG(10),SUMC,NRES
      COMMON/SOC3/NERR,RESP,TRACE
      COMMON/SOC4/CINM2(10),KMG2(10),NF2(10),MW2(10)
      COMMON/SOC5/PC1,PC2,PC3,PC4,PC5,PC6
      COMMON/SOC6/ITIMEC,ITIMEK,ITIMEN,ITIMEM,STEPC,STEPK,STEPN,STEPM
      COMMON/LAST3/SERMIN,BMIN(25),MINC,DMIN,DMINC
      COMMON/DONT/ISEL
      REAL BETA(25)
      CHARACTER*1 RESP,TRACE


      OPEN(unit=5,file ="C:\\FORTRAN\\ALATTAS IAST\\IAST-SROMAR.DAT")
      OPEN(unit=6,file ="C:\\FORTRAN\\ALATTAS IAST\\IAST-SROMAROUT.DAT")
      OPEN(unit=7,file ="C:\\FORTRAN\\ALATTAS IAST\\          IAST-SRCLEANOUT.DAT")

      NPAR=4*NPSUD-1
C *** TRY TO GET SOME FIRST SET OF INITIAL GUESSES *****
C *** FIRST SET SOME ARBITRARY VALUES FOR THE C,K,N

       CINMG(2) = 1.0
       CINMG(3)= CINMG(4)-CINMG(2)

            MW(2) = 200.0
            MW(3) = 100.0

            NF(2) = 0.10
            NF(3) = 0.10

            KMG(2) = 4.0
            KMG(3) = 4.0

            DO 100 IWENT01=1,2

            CINMG(2) = CINMG(2) + 0.5
            CINMG(3)= CINMG(4)-CINMG(2)

            MW(2) = 200.0
            MW(3) = 100.0

            NF(2)= 0.10
            NF(3)= 0.10

            KMG(2) = 4.0
            KMG(3) = 4.0
```

```
      DO 200 IWENT02=1,10
      MW(2)=MW(2)+50

      MW(3) = 100.0
            DO 300 IWENT03=1,10
      MW(3)=MW(3)+50

            NF(2)= 0.10
            DO 400 IWENT04=1,10
            NF(2)=NF(2)+0.05
C           NF(3)=NF(2)

            NF(3)= 0.10
            DO 500 IWENT05=1,10
            NF(3)=NF(3)+0.05
C           NF(2)=NF(3)

            KMG(2)= 4.0
            DO 600 IWENT06=1,10
      KMG(2)=KMG(2)+0.5

            KMG(3)= 4.0
      DO 700 IWENT07=1,10
      KMG(3)=KMG(3)+0.5

            CALL COEFF(BETA,NPAR)

  700 CONTINUE
  600 CONTINUE
  500 CONTINUE
  400 CONTINUE
  300 CONTINUE
  200 CONTINUE
  100 CONTINUE
   70 RETURN

            END

      SUBROUTINE COEFF(BETA,NPAR)

      DIMENSION AERR1(10),AERR2(10)
      REAL KMG,KMOL,MW,NF,KMG2,NF2,MW2,MASS
      REAL WK(621),FNORM,BINIT(25),BETA(25)
      REAL X(10)
      REAL A(10,40),A1(10,40),PW(10,40,40),P(10,40)
      INTEGER NDATA,NPAR,PC1,PC2,PC3,PC4,PC5,PC6
      COMMON/DATA/CPRED(40,10),QPRED(40,10),CEXP(40,10),QEXP(40,10)
      COMMON/POW/NSIG,NC,NKC,ITMAX,NPSUD
      COMMON/SOC1/KMOL(10),NF(10),MW(10),CINMOL(10),CINMG(10)
      COMMON/SOC2/KMG(10),SUMC,NRES
      COMMON/SOC3/NERR,RESP,TRACE
      COMMON/SOC4/CINM2(10),KMG2(10),NF2(10),MW2(10)
      COMMON/LAST/NFIG,NDATA,MAXITR,NI,NO
      COMMON/LAST2/DEL,RLAM,FACT,RLMAX,RLMIN,Y(10,40),
     1 U(2,40),RLAMI
      COMMON/LAST3/SERMIN,BMIN(25),MINC,DMIN,DMINC
      COMMON/HAPPY/MASS(40),VOL(40)
      COMMON/WHAT/CNON,CAPP
      COMMON/DONT/ISEL
      CHARACTER*30 TEST,COMP
      CHARACTER*1,RESP,TRACE


      OPEN(unit=5,file = "C:\\FORTRAN\\ALATTAS IAST\\IAST-SROMAR.DAT")
      OPEN(unit=6,file ="C:\\FORTRAN\\ALATTAS IAST\\IAST-SROMAROUT.DAT")
      OPEN(unit=7,file ="C:\\FORTRAN\\ALATTAS IAST\\          IAST-SRCLEANOUT.DAT")
      OPEN (unit=8,file = "C:\\FORTRAN\\ALATTAS IAST\\IAST-SRPRINT.DAT")
```

```
C  *** FIRST DETERMINE THE NUMBER OF PARAMETERS(COEFFICIENTS) TO BE
C **** ESTIMATED
              NPAR=4*NPSUD-1

C **** SET THE FIRST SET OF BETA'S(COEFFICIENTS) TO THE INITIAL
C **** CONCENTRATIONS (THIS IS FOR THE BACKGROUND ORGANICS)
     DO 166 IC4=1,NPSUD-1
     BINIT(IC4)=CINMG(NKC+IC4)
     BETA(IC4) =CINMG(NKC+IC4)
     WRITE(6,*) 'BETA (',IC4,') =',BETA(IC4)
  166 CONTINUE

C ****  SET THE SECOND SET OF BETA'S(COEFFICIENTS) TO THE  FREUNDLICH K
     DO 167 IC4=NPSUD,2*NPSUD-1
     BINIT(IC4)=KMG(2*NKC+IC4-NC+1)
     BETA(IC4)=KMG(2*NKC+IC4-NC+1)
              WRITE(6,*) 'BETA (',IC4,') =',BETA(IC4)
  167 CONTINUE

C ****  SET THE THIRD SET OF BETA'S(COEFFICIENTS) TO THE FREUNDLICH N
              DO 168 IC4=2*NPSUD,3*NPSUD-1
     BINIT(IC4)=NF(3*NKC+IC4-2*NC+1)
     BETA(IC4)=NF(3*NKC+IC4-2*NC+1)
              WRITE(6,*) 'BETA (',IC4,') =',BETA(IC4)
  168 CONTINUE

C ****  SET  THE LAST SET OF BETA'S(COEFFICIENTS) TO THE MOLECULAR WEIGH
              DO 169 IC4=3*NPSUD,NPAR
     BINIT(IC4)=0.5*MW(4*NKC+IC4-3*NC+1)
     BETA(IC4)=0.5*MW(4*NKC+IC4-3*NC+1)
     WRITE(6,*) 'BETA (',IC4,') =',BETA(IC4)
  169 CONTINUE

C *********************    CALL MODEL  ************************
     CALL MODEL(Y,U,BETA,NPAR,A,NDATA)

C *****  COMPUTE AVERAGE PERCENT ERRORS IN C ******************

     DO 172 ITINK=1,NC+1
     AERR1(ITINK)=0.0
     AERR2(ITINK)=0.0
  172 CONTINUE


C *** ADD THE NON-ADSORBABLE COMPONENT TO THE EXPERIMENTAL AND
C     PREDICTED LIQUID PHASE CONCENTRATIONS FOR THE HUMICS
C     FOR PLOTTING
     DO 5000 IGO=1,NDATA
     CEXP(IGO,NC+1)=CEXP(IGO,NC+1)+CNON
     CPRED(IGO,NC+1)=CPRED(IGO,NC+1)+CNON
 5000 CONTINUE

C **** FOR IRON *******
     DO 171 ISAY2=1,NKC
     DO 171 ISAY1=1,NDATA
              CPRED(ISAY1,ISAY2)= CPRED(ISAY1,ISAY2) * 0.001 * MW(ISAY2)
              AERR1(ISAY2)=AERR1(ISAY2)+ ABS(CEXP(ISAY1,ISAY2)-
    1 CPRED(ISAY1,ISAY2))/CEXP(ISAY1,ISAY2)
  171 CONTINUE

C **** FOR NOM
     DO 800 ISAY1=1,NDATA
     AERR1(NC+1)=AERR1(NC+1)+ABS(CEXP(ISAY1,NC+1)-CPRED(ISAY1,NC+1))
    1/CEXP(ISAY1,NC+1)
  800 CONTINUE

     DO 173 ISAY1=1,NKC
     AERR1(ISAY1)=AERR1(ISAY1)*100/NDATA
  173 CONTINUE
```

```
      AERR1(NC+1)=AERR1(NC+1)*100/NDATA

C**** COMPUTE AVERAGE PERCENT ERRORS IN Q  ********

C **** FOR IRON
      DO 174 ISAY2=1,NKC
      DO 174 ISAY1=1,NDATA
      AERR2(ISAY2)=AERR2(ISAY2)+ABS(QEXP(ISAY1,ISAY2)-
     1 QPRED(ISAY1,ISAY2))/QEXP(ISAY1,ISAY2)
  174 CONTINUE

C *** FOR NOM
C **** FIRST SUM ALL Q'S
      DO 936 ISAY2=1,NDATA
      QPRED(ISAY2,NC+1)=0.
  936 CONTINUE

      DO 937 ISAY1=1,NDATA
      DO 937 ISAY2=NKC+1,NC
      QPRED(ISAY1,NC+1)=QPRED(ISAY1,NC+1)+QPRED(ISAY1,ISAY2)
  937 CONTINUE

      DO 810 ISAY1=1,NDATA
      AERR2(NC+1)=AERR2(NC+1)+ABS(QEXP(ISAY1,NC+1)
     1 - QPRED(ISAY1,NC+1))/QEXP(ISAY1,NC+1)
  810 CONTINUE

      DO 175 ISAY1=1,NKC
      AERR2(ISAY1)=AERR2(ISAY1)*100/NDATA
  175 CONTINUE

      AERR2(NC+1)=AERR2(NC+1)*100/NDATA

C *** DETERMINE WHETHER RESULTS ARE FEASIBLE *****
      DO 222 IC9 = 1,NKC
            WRITE(6,*) 'AERR1', AERR1(IC9)
            WRITE(6,*) 'AERR2', AERR2(IC9)
  222 CONTINUE

            IF(AERR1(1) .GT. 40.0 .OR. AERR2(1) .GT. 8.0) THEN
            WRITE(6,*) 'NO FEASIBLE SOLUTION - GOING BACK TO SUDO'
      GOTO 911
      ELSE
      WRITE(6,*) 'SMILE - A SOLUTION WAS FOUND'
      ENDIF


C **** WRITE OUT VALUES FOR PLOTTING FILE   ************************

C **** FOR KNOWN COMPONENTS (IRON) *********
      WRITE(8,*) NDATA
            DO 176 ISHOT=1,NKC
      DO 176 ISAY1=1,NDATA
      CPRED(ISAY1,ISHOT)= CPRED(ISAY1,ISHOT)
            WRITE(8,177) CEXP(ISAY1,ISHOT),CPRED(ISAY1,ISHOT),
     1 KMG(ISHOT)*CEXP(ISAY1,ISHOT)**NF(ISHOT),
     2 QEXP(ISAY1,ISHOT),QPRED(ISAY1,ISHOT)
  177  FORMAT(1X,6(3X,F15.6))
  176 CONTINUE

C **** FOR BACKGROUND ORGANICS  ****************************
            DO 178 ISAY1=1,NDATA
      IF(CEXP(ISAY1,NC+1) .GT. CAPP) THEN
        KMG(NC+1)=KMG(NC+2)
        NF(NC+1)=NF(NC+2)
      ENDIF
      SSOL=KMG(NC+1)*(CEXP(ISAY1,NC+1)-CNON)**NF(NC+1)
      WRITE(8,177) CEXP(ISAY1,NC+1),CPRED(ISAY1,NC+1),
     1 SSOL,
```

```
     2  QEXP(ISAY1,NC+1),QPRED(ISAY1,NC+1)
   178 CONTINUE

C **********************************************************************
C ****  WRITE OUT THE VALUES FOR KNOWN COMPONENT(S) **********
C      WRITE OUT VALUES FOR KNOWN COMPONENTS (SYNTHETIC ORGANICS)
       WRITE(7,1000)
  1000  FORMAT(1X,///,30X,'KNOWN SYNTHETIC ORGANIC COMPOUNDS',//)
       WRITE(7,1010)
  1010  FORMAT(1X,30X,12X,'PARAMETERS',/1X,25X,'CO',15X,'K',15X,'N',15X,
     1 'MW',/1X,22X,'(MG/L)',5X,'(MG/L)/(MG/G)**N',24X,'(G)',/)

       DO 1020 IC10=1,NKC
       WRITE(7,1030) IC10,CINMG(IC10),KMG(IC10),NF(IC10),MW(IC10)
  1030  FORMAT(1X,'COMPONENT #',I3,4(5X,F12.5))
  1020  CONTINUE
       WRITE(7,1040)
  1040  FORMAT(1X,///)

       WRITE(7,1060)
  1060  FORMAT(1X,30X,'BACKGROUND ORGANIC COMPOUNDS',//)

       WRITE(7,1050) NPSUD
  1050  FORMAT(1X,3X,'REGRESSED PARAMETERS FOR',I3,' PSEUDOCOMPONENTS')
       WRITE(7,1070)
  1070  FORMAT(1X,/1X,25X,'CO',15X,'K',15X,'N',15X,
     1 'MW',/1X,22X,'(MG/L)',5X,'(MG/G)/(MG/L)**N',24X,'(G)',/)

C **  WRITE OUT NON-ADSORBABLE COMPONENT
       WRITE(7,5001) CNON
 5001   FORMAT(1X,'NON-ADSORBABLE ',F16.5)

      DO 1080 IC10=NKC+1,NC
      IF (IC10 .LT. NC) THEN
      WRITE(7,1090) IC10,BETA(IC10-NKC),BETA(IC10-NKC+NPSUD-1),
     1 BETA(IC10-NKC+2*NPSUD-1),BETA(IC10-NKC+3*NPSUD-1)
      ELSE
      WRITE(7,1090) IC10,CINMG(NC+1)-SUMC,BETA(IC10-NKC+NPSUD-1),
     1 BETA(IC10-NKC+2*NPSUD-1),BETA(IC10-NKC+3*NPSUD-1)
      ENDIF
  1090  FORMAT(1X,'COMPONENT #',I3,4(5X,F12.5))
  1080  CONTINUE

      WRITE(7,1100)
  1100   FORMAT(1X,///,40X,'S I M U L A T I O N S ',//)

C **** FOR IRON ****
       DO 200 IC5=1,NKC
       WRITE(7,33) IC5
   33  FORMAT(//,'COMPONENT # ',I3,//,7X,'V',7X,'M',15X,'CEXP',11X,
     1'CPRED',10X,'QEXP',12X,'QPRED',/,6X,'(L)',5X,'(G)',21X,'MG/L',27X,
     2'MG/G')
        DO 210 IC6=1,NDATA
                WRITE(7,31) VOL(IC6),MASS(IC6),CEXP(IC6,IC5),CPRED(IC6,IC5)
     1  ,QEXP(IC6,IC5),QPRED(IC6,IC5)
   31  FORMAT(2(2X,F8.4),4(4X,F12.4))
  210  CONTINUE

       WRITE(7,890) AERR1(IC5),AERR2(IC5)
  890  FORMAT(1X,/,'ABSOLUTE AVERAGE PERCENT ERROR IN C =',F8.2,/
     1 'ABSOLUTE AVERAGE PERCENT ERROR IN Q =',F8.2)
  200  CONTINUE

      WRITE(7,900)
  900  FORMAT(1X,//)
      DO 910 IC6=1,NDATA
      WRITE(7,31) VOL(IC6),MASS(IC6),CEXP(IC6,NC+1),CPRED(IC6,NC+1),
     1  QEXP(IC6,NC+1),QPRED(IC6,NC+1)
  910  CONTINUE
```

```
            WRITE(7,890) AERR1(NC+1),AERR2(NC+1)

            GOTO 950

 911 CONTINUE

 950 RETURN

            END



      SUBROUTINE MODEL(Y,U,BETA,NPAR,A,NDATA)

       REAL WK(621),FNORM,A(10,40),Y(10,40),U(2,40)
       REAL KMOL,MW,NF,ERRREL
            COMMON /POW/ NSIG,NC,NKC,ITMAX,NPSUD
      REAL XSTO(40),XGUESS(40),X(10)
      EXTERNAL FCN,NEQNF
      COMMON /DATA/CPRED(40,10),QPRED(40,10),CEXP(40,10),QEXP(40,10)
      COMMON/SOC1/KMOL(10),NF(10),MW(10),CINMOL(10),CINMG(10)
      COMMON/SOC2/KMG(10),SUMC,NRES
      COMMON/NEW/PAR(32)
            REAL BETA(25)
            INTEGER N


      OPEN(unit=5,file = "C:\\FORTRAN\\ALATTAS IAST\\IAST-SROMAR.DAT")
      OPEN(unit=6,file ="C:\\FORTRAN\\ALATTAS IAST\\IAST-SROMAROUT.DAT")
      OPEN(unit=7,file ="C:\\FORTRAN\\ALATTAS IAST\\          IAST-SRCLEANOUT.DAT")

C ******* DEFINE PARAMETERS FOR USE IN NEQNF SUBROUTINE **********
C ***** 3 FIXED PARAMETERS ARE TO BE ASSIGNED FOR EACH COMPONENT,
C      I.E. CINMOL, NF AND THE KMOL.  THE TOTAL NUMBER OF FIXED
C      PARAMETERS FOR NC COMPONENTS = 6+3*(NC-2), AND THEN
C      THE VARIABLE PARAMETERS, THE CARBON MASS AND
C      THE LIQUID VOLUME
      NPARM=6+3*(NC-2)

C **** TEST THE VALUE OF THE REGRESSED PARAMETERS
C ***  FIRST DETERMINE THE INITIAL CONCENTRATION OF THE LAST
C ***  PSEUDOCOMPONENT
      SUMC=0.0

            DO 93 IC2=NKC+1,NC-1
      SUMC=SUMC+BETA(IC2-NKC)
  93  CONTINUE

      PAR(NC)=1000*((CINMG(NC+1)-SUMC)/(BETA(NPAR)))
      DO 120 IC1=1,NPAR
      IF(BETA(IC1) .LE. 0.0 .OR. PAR(NC) .LE. 0.0) THEN
      WRITE(6,*)  '*********NEGATIVE*********'
      WRITE(6,*) 'BETA ',BETA(IC1),' PAR(NC)  ',PAR(NC)

 158  DO 156 IPUT=1,NDATA
            DO 130 IC5=1,NKC
      WRITE(6,*)  '**********EXITING FROM HERE'
      A(IC5,IPUT)=A(IC5,IPUT)*1000.0
 130  CONTINUE
            IF(NRES .GT. NKC) THEN
      A(NKC+1,IPUT)=A(NKC+1,IPUT)*1000.0
      ENDIF
 156  CONTINUE
            GOTO 155
            ENDIF
 120  CONTINUE

C **** SET THE INITIAL CONCENTRATIONS AS THE FIRST SET OF
```

```
C     PARAMETERS

C *** SET THE PARAMETERS (INITITAL CONCENTRATIONS) FOR THE IRON***

      DO 90 IC2=1,NKC
      PAR(IC2)=CINMOL(IC2)
 90  CONTINUE

C **** SET THE PARAMETERS(INITIAL CONCENTRATIONS) FOR THE
C*******BACKGROUND ORGANICS ****

      DO 91 IC2=NKC+1,NC-1
            PAR(IC2)=1000* (BETA(IC2-NKC)/(BETA(IC2-NKC+3*NPSUD-1)))
 91  CONTINUE

C SET THE PARAMETERS (INITIAL CONCENTRATIONS) FOR THE LAST
C PSEUDOCOMPONENT, BUT FIRST SUM UP ALL INITIAL CONCS
C OF THE NC-1 PSEUDOCOMPONENTS


C ****  SET THE K's AS THE SECOND SET OF PARAMETERS FOR THE IRON
      DO 92  IC2=NC+1,NC+NKC
      PAR(IC2)=KMOL(IC2-NC)
92   CONTINUE


C **** SET THE K'S AS THE SECOND SET OF PARAMETERS FOR THE BACKGROUND
C  ****  ORGANICS BY FIRST CHANGING THE K'S TO VALUES ON MOLAR BASIS
C      CARBON WAS ASSUMED TO ACCOUNT FOR 50% OF THE NOM MOLECULAR WEIGHT
      DO 30 IPRAY=NKC+1,NC
      KMOL(IPRAY)=(BETA(IPRAY-NKC+NPSUD-1)
            1*(1000*BETA(IPRAY-NKC+3*NPSUD-1))
     2 **(BETA(IPRAY-NKC+2*NPSUD-1))) /
     3(1000*BETA(IPRAY-NKC+3*NPSUD-1))
            KMOL(IPRAY)=KMOL(IPRAY)/(1000000**(BETA(IPRAY-NKC+2*NPSUD-1)))
     4 * (1000000)
 30  CONTINUE

C*** NOW SET THE K'S AS THE SECOND SET OF PARAMETERS FOR THE BACKGROUND
C*****ORGANICS

            DO 31 IC2=NC+NKC+1,2*NPARM/3
      PAR(IC2)=KMOL(IC2-NC)
31   CONTINUE

C ****  SET THE N's AS THE THIRD SET OF PARAMETERS FOR THE IRON
C ****  FIRST SET THE N's FOR THE IRON
      DO 110 IC2=(2*NPARM/3)+1,(2*NPARM/3+NKC)
      PAR(IC2)=NF(IC2-2*NC)
110  CONTINUE

C ***  SET THE (N'S) AS THE THIRD SET OF PARAMETERS FOR
C **** THE BACKGROUND ORGANICS
      DO 111 IC2=(2*NPARM/3+NKC+1),NPARM
      PAR(IC2)=BETA(IC2-3*NKC-1)
111  CONTINUE

C**** SOLVE THE RESULTING EQUATIONS AND THEN REGRESS THE RESULTS
C***  TO FIND THE BEST FIT
      DO 100 I=1,NDATA

C *** SET COUNTER FOR CONTROL OF NO. OF TIMES OF CALLS TO NEQNF
C ***  WITH DIFFERENT INITIAL GUESSES FOR EACH DATA POINT
      ICNT=0
      PRINT*,  '******** POINT NO *********',I

C ***  SET THE CARBON VOLUME AND MASS AS THE LAST TWO PARAMETERS FOR
C ****  NEQNF (SOLVER)
      PAR(NPARM+1)=U(2,I)
```

```
      PAR(NPARM+2)=U(1,I)

C  *** MAKE YOUR INITIAL GUESSES OF Q FOR THE SOLVER
C  ***  FOR THE IRON
      DO 40 J=1,NKC
      IF (I .EQ. 1) THEN
      X(J)=CINMOL(J)*PAR(NPARM+2)/PAR(NPARM+1)
      XSTO(J)=CINMOL(J)*PAR(NPARM+2)/PAR(NPARM+1)
               ELSE
       X(J)=1000*1.0*QPRED(I-1,J)/MW(J)
       XSTO(J)=1000*1.0*QPRED(I-1,J)/MW(J)
      ENDIF
 40   CONTINUE

C ***  FOR THE NC-1 PSEUDOCOMPONENTS
      DO 41 J=NKC+1,NC-1
      IF (I .EQ. 1) THEN
      X(J)=1000*BETA(J-NKC)/(BETA(J-NKC+3*NPSUD-1))*PAR(NPARM+2)
             1 /PAR(NPARM+1)
      XSTO(J)=1000*BETA(J-NKC)/(BETA(J-NKC+3*NPSUD-1))
     1  *PAR(NPARM+2)/PAR(NPARM+1)
      ELSE
       X(J)=1000*1.0*QPRED(I-1,J)/(BETA(J-NKC+3*NPSUD-1))
       XSTO(J)=1000*1.0*QPRED(I-1,J)/(BETA(J-NKC+3*NPSUD-1))
      ENDIF
 41   CONTINUE

C ***  FOR THE LAST PSEUDOCOMPONENT

      IF(I .EQ. 1) THEN
      X(NC)=PAR(NC)*PAR(NPARM+2)/PAR(NPARM+1)
      XSTO(NC)=PAR(NC)*PAR(NPARM+2)/PAR(NPARM+1)
      ELSE
      X(NC)=1000*1.0*QPRED(I-1,NC)/BETA(NPAR)
      XSTO(NC)=1000*1.0*QPRED(I-1,NC)/BETA(NPAR)
      ENDIF
               GOTO 175

C *** REDEFINE THE INITIAL GUESSES IF THE FIRST SET DID NOT WORK
 170  DO 171 J=1,NKC
      IF(I .EQ. 1) THEN
      X(J)=XSTO(J)+0.1*XSTO(J)
      XSTO(J)=X(J)
      ELSE
      X(J)=XSTO(J)-0.1*XSTO(J)
      XSTO(J)=X(J)
      ENDIF
  171 CONTINUE

C *** FOR THE NC-1 COMPONENTS
      DO 172 J=NKC+1,NC-1
      IF(I .EQ. 1) THEN
      X(J)=XSTO(J)+0.1*XSTO(J)
      XSTO(J)=X(J)
      ELSE
      X(J)=XSTO(J)-0.1*XSTO(J)
      XSTO(J)=X(J)
      ENDIF
 172  CONTINUE

C **** FOR THE LAST PSEUDOCOMPONENT
      IF(I .EQ. 1) THEN
      X(NC)=XSTO(NC)+0.1*XSTO(NC)
      XSTO(NC)=X(NC)
      ELSE
      X(NC)=XSTO(NC)-0.1*XSTO(NC)
      XSTO(NC)=X(NC)
      ENDIF
```

```
C **** CALL NEQNF FOR EACH DATA POINT TO COMPUTE Q's
  175 N=NC

      ERRREL = 0.0001
              DO 12121 OMAR=1,N
      XGUESS(OMAR) = X(OMAR)
12121 CONTINUE

              CALL NEQNF (FCN,ERRREL,N,ITMAX,XGUESS,X,FNORM)


C     SET THE X'S TO THEIR RESPECTIVE Q'S
C *** FOR KNOWN COMPONENTS (IRON)
      DO 21 IC8=1,NKC
      QPRED(I,IC8)=X(IC8)
21    CONTINUE

C **** FOR BACKGROUND ORGANICS
              DO 22 IC8=NKC+1,NC
      QPRED(I,IC8)=X(IC8)
22    CONTINUE

C **** CALCULATE C's FOR EACH COMPONENT **********
C *** FOR IRON
              DO 150 IC4=1,NKC
      CPRED(I,IC4)=CINMOL(IC4)-(QPRED(I,IC4)*U(2,I)/U(1,I))
150   CONTINUE

C ***********AND FOR BACKGROUND ORGANICS ***************
C  FOR THE NC-1 COMPONENTS
              DO 151 IC4=NKC+1,NC-1
      CPRED(I,IC4)=1000*(BETA(IC4-NKC)/BETA(IC4-NKC+3*NPSUD-1))
     1  -QPRED(I,IC4)*U(2,I)/U(1,I)
151   CONTINUE

C  FOR THE LAST PSEUDOCOMPONENT
              CPRED(I,NC)=PAR(NC)-QPRED(I,NC)*U(2,I)/U(1,I)

C  CHANGE THE PREDICTED VALUES OF Q INTO THOSE ON MASS
C  BASIS FOR KNOWN COMPONENTS
              DO 160 IC4=1,NKC
      QPRED(I,IC4)=QPRED(I,IC4)*MW(IC4)*0.001
 160  CONTINUE

C FOR BACKGROUND ORGANICS
              DO 161 IC4=NKC+1,NC
      QPRED(I,IC4)=QPRED(I,IC4)*BETA(IC4-NKC+3*NPSUD-1)*0.001
161   CONTINUE

C **** COMPUTE RESIDUALS  AS Y's (CEXP-CPRED) FOR IRON *****
              DO 101 IC5=1,NKC
      A(IC5,I)=Y(IC5,I)-CPRED(I,IC5)*MW(IC5)*0.001
101   CONTINUE

C ***  COMPUTE RESIDUALS AS Y'S (CEXP-CPRED) FOR BACKGROUND ORGANICS
C **   FIRST SUM UP ALL LIQUID-PHASE CONCENTRATIONS OF THE
C ***  PSEUDOCOMPONENTS
      CPRED(I,NC+1)=0
      DO 102 IC5=NKC+1,NC
      CPRED(I,NC+1)=CPRED(I,NC+1)+CPRED(I,IC5)
              1*BETA(IC5-NKC+3*NPSUD-1)*0.001
 102 CONTINUE

C      IF(NRES .GT. NKC) THEN
C  **** COMPUTE RESIDUALS FOR BACKGROUND ORGANICS
 100  CONTINUE
 155  RETURN
      END
```

```
C **** SUBROUTINE FCN FOR CALCULATING THE F FUNCTIONS THAT ARE *******
C ***************   TO BE  ZEROED  ************************

      SUBROUTINE FCN(X,F,N)
      INTEGER N
      REAL F(N),X(N)
      COMMON/NEW/PAR(32)

      OPEN(unit=5,file = "C:\\FORTRAN\\ALATTAS IAST\\IAST-SROMAR.DAT")
      OPEN(unit=6,file ="C:\\FORTRAN\\ALATTAS IAST\\IAST-SROMAROUT.DAT")
      OPEN(unit=7,file ="C:\\FORTRAN\\ALATTAS IAST\\IAST-SRCLEANOUT.DAT")

            NPARM = 6 + 3 * (N-2)
      SUMXI = 0.0
      SUMXON = 0.0
      DO 130 IC3=1,N
      SUMXI = SUMXI + X(IC3)
            SUMXON = SUMXON + X(IC3) / PAR (2 * NPARM / 3 + IC3)
  130 CONTINUE
            IF(SUMXON .LT. 0) THEN
  132 DO 135 IC4=1,N
     F(IC4)=100.0
  135 CONTINUE
     GOTO 150
     ENDIF
     DO 140 IC3=1,N
            TTERM = ( PAR(2*NPARM/3+IC3) * SUMXON)/PAR(N+IC3)
            FTERM=1/PAR(2*NPARM/3+IC3)
     F(IC3)=PAR(IC3)-(PAR(NPARM+1)/PAR(NPARM+2))*X(IC3)-(X(IC3)
    2 /SUMXI)*(PAR(NPARM+1)/PAR(NPARM+2))
    3*((PAR(2*NPARM/3+IC3)*SUMXON)/PAR(N+IC3))**
    4  (1/PAR(2*NPARM/3+IC3))
  140 CONTINUE
  150 RETURN

            END
```

Input File for the FORTRAN Code: IAST-SR

```
200   3  14   3   1
0.35  0.1 0.1 4.24
55.8  200.00 200.00
4.20 5.00 5.00  0.20  0.1 0.1
0.06     0.34     0.1357 0.160
0.07     0.49     0.0911 0.161
0.09     0.50     0.0841 0.161
0.13     0.56     0.0632 0.161
0.14     0.81     0.0420 0.161
0.17     0.92     0.0316 0.161
0.21     0.93     0.0243 0.161
0.22     1.09     0.0193 0.161
0.24     1.19     0.0149 0.161
0.28     1.12     0.0100 0.161
0.30     1.06     0.0076 0.161
0.31     1.09     0.0059 0.162
0.33     1.28     0.0025 0.161
0.34     1.07     0.0015 0.161
0.27     4.68
0.44     6.72
0.67     6.85
0.79     8.78
0.96     12.61
1.15     15.76
1.25     19.87
1.44     23.42
1.66     27.84
1.92     37.18
2.18     43.82
2.38     51.03
3.00     79.79
3.26     105.63
0.000 2.12 7.65 7.65 0.45 0.45
```